Research Reactor Application for Materials under High Neutron Fluence

IAEA
International Atomic Energy Agency

RESEARCH REACTOR APPLICATION FOR MATERIALS UNDER HIGH NEUTRON FLUENCE

The following States are Members of the International Atomic Energy Agency:

AFGHANISTAN	GHANA	NORWAY
ALBANIA	GREECE	OMAN
ALGERIA	GUATEMALA	PAKISTAN
ANGOLA	HAITI	PALAU
ARGENTINA	HOLY SEE	PANAMA
ARMENIA	HONDURAS	PARAGUAY
AUSTRALIA	HUNGARY	PERU
AUSTRIA	ICELAND	PHILIPPINES
AZERBAIJAN	INDIA	POLAND
BAHRAIN	INDONESIA	PORTUGAL
BANGLADESH	IRAN, ISLAMIC REPUBLIC OF	QATAR
BELARUS	IRAQ	REPUBLIC OF MOLDOVA
BELGIUM	IRELAND	ROMANIA
BELIZE	ISRAEL	RUSSIAN FEDERATION
BENIN	ITALY	SAUDI ARABIA
BOLIVIA	JAMAICA	SENEGAL
BOSNIA AND HERZEGOVINA	JAPAN	SERBIA
BOTSWANA	JORDAN	SEYCHELLES
BRAZIL	KAZAKHSTAN	SIERRA LEONE
BULGARIA	KENYA	SINGAPORE
BURKINA FASO	KOREA, REPUBLIC OF	SLOVAKIA
BURUNDI	KUWAIT	SLOVENIA
CAMBODIA	KYRGYZSTAN	SOUTH AFRICA
CAMEROON	LATVIA	SPAIN
CANADA	LEBANON	SRI LANKA
CENTRAL AFRICAN	LESOTHO	SUDAN
REPUBLIC	LIBERIA	SWEDEN
CHAD	LIBYAN ARAB JAMAHIRIYA	SWITZERLAND
CHILE	LIECHTENSTEIN	SYRIAN ARAB REPUBLIC
CHINA	LITHUANIA	TAJIKISTAN
COLOMBIA	LUXEMBOURG	THAILAND
CONGO	MADAGASCAR	THE FORMER YUGOSLAV
COSTA RICA	MALAWI	REPUBLIC OF MACEDONIA
CÔTE D'IVOIRE	MALAYSIA	TUNISIA
CROATIA	MALI	TURKEY
CUBA	MALTA	UGANDA
CYPRUS	MARSHALL ISLANDS	UKRAINE
CZECH REPUBLIC	MAURITANIA	UNITED ARAB EMIRATES
DEMOCRATIC REPUBLIC	MAURITIUS	UNITED KINGDOM OF
OF THE CONGO	MEXICO	GREAT BRITAIN AND
DENMARK	MONACO	NORTHERN IRELAND
DOMINICAN REPUBLIC	MONGOLIA	UNITED REPUBLIC
ECUADOR	MONTENEGRO	OF TANZANIA
EGYPT	MOROCCO	UNITED STATES OF AMERICA
EL SALVADOR	MOZAMBIQUE	URUGUAY
ERITREA	MYANMAR	UZBEKISTAN
ESTONIA	NAMIBIA	VENEZUELA
ETHIOPIA	NEPAL	VIETNAM
FINLAND	NETHERLANDS	YEMEN
FRANCE	NEW ZEALAND	ZAMBIA
GABON	NICARAGUA	ZIMBABWE
GEORGIA	NIGER	
GERMANY	NIGERIA	

The Agency's Statute was approved on 23 October 1956 by the Conference on the Statute of the IAEA held at United Nations Headquarters, New York; it entered into force on 29 July 1957. The Headquarters of the Agency are situated in Vienna. Its principal objective is "to accelerate and enlarge the contribution of atomic energy to peace, health and prosperity throughout the world''.

IAEA-TECDOC-1659

RESEARCH REACTOR APPLICATION FOR MATERIALS UNDER HIGH NEUTRON FLUENCE

Proceedings of an
IAEA Technical Meeting
(TM -34779)

INTERNATIONAL ATOMIC ENERGY AGENCY
VIENNA, 2011

FOREWORD

Research reactors (RRs) have played, and continue to play, a key role in the development of the peaceful uses of nuclear energy and technology. The role of the IAEA is to assist Member States in the effective utilization of these technologies in various domains of research such as fundamental and applied science, industry, human health care and environmental studies, as well as nuclear energy applications. In particular, material testing reactors (MTRs), serve as unique tools in scientific and technological development and they have quite a wide variety of applications. Today, a large range of different RR designs exist when compared with power reactors and they also have different operating modes, producing high neutron fluxes, which may be steady or pulsed. Recently, an urgent need has arisen for the development of new advanced materials, for example in the nuclear industry, where RRs offer capacities for irradiation programmes. Besides the scientific and research activities and commercial applications, RRs are also used extensively for educational training activities for scientists and engineers.

This report is a compilation of outputs of an IAEA Technical Meeting (TM-34779) held on Research Reactor Application for Materials under High Neutron Fluence. The overall objective of the meeting was to review typical applications of small and medium size RRs, such as material characterization and testing, neutron physics and beam research, neutron radiography and imaging as well as isotope production and other types of non-nuclear applications. Several issues were discussed during the meeting, in particular: (1) recent development of irradiation facilities, specific irradiation programmes and their implementation; (2) effective and optimal RR operation regimes for irradiation purposes; (3) sharing of best practices and existing technical knowledge; and (4) fostering of advanced or innovative technologies, e.g. information exchange and effective collaboration.

This publication summarizes all individual reports presented by participants during the TM, and presents the overall conclusions and main findings identified and agreed during the meeting. The IAEA acknowledges the valuable contributions of individual participants as well as experts who reviewed and finalized this report, particularly L. Debarberis (Netherlands) and V. Kryukov. The IAEA officers responsible for this publication were A. Zeman and P. Salame of the Division of Physical and Chemical Sciences.

EDITORIAL NOTE

CONTENTS

Chapter 1

INTRODUCTION

Research Reactors (RR) have played and continue to play a key role in the development of the peaceful uses of atomic energy. Moreover these facilities are used intensively for education and training purposes of scientists and engineers. At present, a larger scale of designs is in use and they also have different operating modes, producing energy which may be steady or pulsed. Due to this, RR are very unique tools in the scientific and technological development area and they have a fairly wide spectra of applications. In principle, there is a common approach for design which is the pool type reactor in which the core is a cluster of fuel elements sitting in a large pool of water. Such adapted design allows for the reach of higher neutron fluence due to higher power density and therefore these facilities are primarily used for irradiation purposes. This offers various studies of irradiation damage for a broad-range of structural materials and their properties. Existing RR facilities, especially in developing countries, are often under-utilized and could be used more effectively (e.g. for material testing, radioisotope production, beam line applications, nuclear transmutation doping and analytical services), with new initiatives on a national, regional and inter-regional level. The sharing of resources can increase the utilization on one hand and pave the way for the decommissioning of under-utilized ageing reactors on the other, without depleting knowledge base and human resources.

1.1. Objectives

The overall objective of this publication is to overview the activities in the area of RR applications for studies of materials under high neutron fluence. It is expected that this technical document will help to stimulate new activities by using of RRs as well as strengthening of the expertise, know-how and best practise .

The report is also focused on the specific RRs applications in irradiation of materials at high neutron flux and fluence, as well as integration issues, including:

− Available irradiation facilities and recent development of irradiation facilities,
− New material irradiation programmes and their implementation,
− Contribution to the better understanding of radiation damage at high doses and dose rates,
− Effective and optimal operation procedures for irradiation purposes,
− Fostering the advanced or innovative technologies by promotion of information exchange, collaboration and networking,
− Sharing of information and know-how.

1.2. Scope

The scope of this report is to summarise available information in the area, presented by participating IAEA Member States in order to enhance research reactors utilization for practical applications. Today's multipurpose research reactors are used for various applications with respect of individual needs of particular countries, such as irradiation services, isotope production, neutron radiography and beam research as well as material characterization and testing. This document gives brief overview of such practical applications and basic information about related infrastructure.

1.3. Material irradiation programme

(i) Structural materials of present nuclear reactors

Typically, neutron-based irradiation programmes are carried out at RRs for several purposes, in particular irradiation of materials of conventional nuclear power plants, where the RRs can be used effectively for the monitoring of irradiation embrittlement of Nuclear Power Plant (NPP) structural materials. The aim of such an experiment is the determination of the dose and dose rate effects, resulting in the change of mechanical behaviour of irradiated materials. Recommended lead factor for surveillance programmes of water cooled pressure vessels is in the range of 1 to 3. Some RRs, however, also offer tests which can be carried out until much higher factors are reached (50-500). This of course does not guarantee that the irradiation damage is similar to the one suffered by the structural materials in service. Proper maintenance, manipulation and positioning of the irradiated materials ensure that the probes can be evaluated in a proper manner from a fracture toughness point of view. Irradiation temperature, as one of the key parameters, must be maintained with respect to the operational conditions of a particular type of structural material in a real NPP. A further area is the study of new advanced nuclear reactor systems where even higher operational parameters are foreseen. Many new materials have to be tested at extremely high doses for long-term radiation stability.

(ii) R&D of new materials

Today only research reactors are able to simulate the operational conditions for the testing of such new materials; neutron radiation damage rates are sufficient for the majority of the R&D of new materials and components for the new generation fission reactors, like Generation IV and INPRO initiatives. In addition, irradiation of materials for fusion energy devices (ITER) involves very specific testing. Significant progress has been achieved in the development of so called Reduced Activation Ferritic-Martensitic (RAFM) steels, like EUROFER'97, where RRs have played a dominant role in the development, testing and optimization of properties for such structural steel. For the End-Of-Life (EOL) conditions of fast reactors and fusion power plants, additional materials testing devices are necessary for new irradiation tests.

The following table specifies the overview of required material irradiation and testing programmes needed to support the development of nuclear industry:

TABLE 1. OVERVIEW OF REQUIRED MATERIAL IRRADIATION AND TESTING PROGRAMMES NEEDED TO SUPPORT THE DEVELOPMENT OF NUCLEAR INDUSTRY

Country	Structural Material	Testing Conditions
Bangladesh	SS	No irradiation, SANS, NAA chemical composition analysis
Brazil	Al	40-100ºC
China	ODS (Chinese), F/M, insulator	HFETR, MJTR
Czech Republic	SS, Ferritic, High-Nickel alloys, Ceramics	Porosity, microstructure deformation, phase transformation SCWR, VHTR, Pb-Li
EC	ODS, SiC/SiC, FM, RAFM steels	Range: 500ºC, 1.5 dpa LFR, SFR, SCWR
Egypt	Al, Zircalloy, SS	Range: 35-70ºC, 0.1 dpa RR surveillance program
Hungary	SiN/CNT, VVER-440, ODS	SCWR range: 500ºC, 0.3-1dpa PWR surveillance program (RPV)
India	SS (D9, D9I), ferritic steels, ODS alloy	SFR cladding and wrapper tube materials, 380 – 700ºC, up to 200 dpa
Israel	Accelerator window material (ADS)	-
Japan	SiC/SiC, RAFM, ODS steel Ferritic/Austenitic steels	SFR range: 500ºC, 200 dpa VHTR
Kazakhstan	SS, nano-structured materials, materials with fine grain	Range 0.5-5 dpa Availability of several high dpa irradiated materials
Korea	Zr, ODS, SS, high Cr alloys	SMART project, VHTR, SFR, ITER
Ukraine	VVER-1000 RPV steel	PWR surveillance program (RPV), fracture toughness
Uzbekistan	Al alloys, Nano-structured materials	Range: 0.5-2 dpa per year Research reactor materials

1.4. Fundamental physics and modelling

Another very important topic is fundamental physics and modelling of radiation damage and its prediction. However, this is still a pending issue since mechanisms of radiation damage involve a very high recombination rate of radiation-induced point defects or a very difficult formation of dislocation loops. At any rate, it seems to be related to an exceptional tolerance of this material toward a high concentration of intrinsic defects even in the absence of radiation and there are several world-wide initiatives on this subject, however, further understanding can only be achieved by the strengthening of interlink between theoretical and experimental studies. Almost all initiatives in this area involves dealing with specific irradiation of model alloys and steels and, only by fully understanding the basic processes and their relations, can further progress be reached in the area of multi-component systems like steels. Furthermore, nuclear based non-destructive techniques can provide complex information on evolution of microstructure changes and the residual stress level as a function

of time and neutron fluence. This plays a key role for assessment of the component integrity and for an estimation of the operational life. Studies of structure defects as well as the residual stresses in as-manufactured and used components are thus of great importance. By this way, neutron-based techniques accommodated at RRs provide unique possibilities of nondestructive evaluation microstructural changes and/or residual stresses. The nondestructive neutron diffraction and scattering methods for scanning of the internal stresses in polycrystalline materials as well as small-angle neutron scattering (SANS) for studies of inhomogeneities in surrounding homogeneous bulk material have become widely applied. The utilization of such techniques for material characterization is theus very important.

1.5. R&D of nuclear fuel

The RR remains the critical tool for the development, testing and licensing of nuclear fuel. In particular, dedicated irradiation rigs with the possibility to in-situ fission gas analysis (also in case of simulated accidental conditions) are extremely important. Various rigs are used by different Member States for such fuel qualification together with out-of-pile facilities. Especially, the irradiation rigs which allow ramp-testing of fuel assemblies at different power rates are desirable in fuel development process and safety assessment.

1.6. Radioisotope production and other applications

The production of radioisotope is also an important area of RRs applications. Present developments in cancer treatment are making use of RRs competences and facilities and represent an essential contribution to health care. A wide-range of radioisotopes for nuclear medicine, radiotherapy and radiation diagnostics is produced. Finally, there are also non-nuclear applications of RRs under this specific subject, such as Neutron Transmutation Doping (NTD) of silicon or development of materials for fuel cell membranes which are typical examples of the effective application of irradiation services of research reactors.

1.7. On-going issues in utilization of RR irradiation facilities

The specific overview of expected demand on the utilization of RRs in the area of material testing for nuclear industry is shortly summarised as following:

- R&D process of new advanced materials for innovative nuclear reactor systems requires their qualification by out-of-pile tests like mechanical property evaluation tests, corrosion tests, etc. This also includes an investigation of the irradiation performance under different experimental conditions.
- Evaluation of performance for highly irradiated materials under long-term storage conditions.
- Testing of present class structural materials (surveillance programme) in the current reactors concepts for their qualification under new conditions and life-time extension programme.
- Examination of new conditions and capacity of present irradiation facilities available for material testing with the emphasis on wide range of design parameters required for qualification of new structural materials.
- Closer collaboration and technical knowledge exchange between Member States in the area of reactor/testing facilities. This could help to improve the existing concepts of irradiation rigs.
- Coordination of future efforts on development of new/advanced instrumented irradiation capsule. Based on the Member States request, the IAEA should take the role of the coordinator in this area.

(i) Complementary applied methods

Participating representatives of the Member States identified that following test techniques play an important role in the testing and/or characterisation of the structural materials at the national or regional level, in particular:

- Mechanical tests: tensile, charpy, hardness, C-T, shear punch, creep, creep-fatigue, fracture mechanics, deformation microcalorymetry, optical extensometry (laser),
- NDT: Visual inspection, gamma scanning, dimensional verification, ultrasonic testing,
- Neutron probing: SANS, HRPD, Neutron radiography, NAA, Tomography,
- Micro analysis: XRD, XRF, 3D-AP, optical microscopy, electron microscopy (SEM/ TEM), PAS, EPMA, Ion probing (RBS, PIXE, PIGE),
- In-pile testing: stress corrosion cracking (SCC), electro chemical potential (ECP), fuel performance, in-situ measurements of some physical and chemical properties,
- Physical properties: Electrical conductivity, thermal properties, optical properties, density measurement,
- Tools: theoretical calculation technology for neutron fluence rate spectrum, gamma fluence rate spectrum, gamma heating, burn-up, lead factor, shield, cross section, thermal-hydraulics and so on, test measurement technology for neutron fluence rate spectrum, gamma fluence rate spectrum, gamma heating, burn-up, energy spectrum adjustment, activity, cross section, temperature, pressure, velocity, and so on.

(ii) Identified materials for future investigation

It is suggested to focus further experimental studies on the following steels, compounds and/or alloys, recognised to be important structural materials in nuclear industry and nuclear technology, in particular:

- ODS steels.
- SiC/SiC materials.
- Advanced ceramics and compounds (Si_3N_4 based compound, etc.),
- FM and RAFM steels.
- Austenitic stainless steel.

Any activity should be driven by real national or regional need for investigation of such materials. Besides new materials, some present material concepts could be included in the testing roadmap, especially linked with the surveillance programme of the RR.

(iii) Challenges for future studies

The following areas have been pointed out as subjects of common interest and it is suggested for future studies, in particular:

- Implementation of new test techniques which may be applied to investigate the un-irradiated and irradiated materials. Special focus should be given to the proposal for round-robin testing of selected materials and continuous improvement of neutron dosimetry (e.g. Nb-alloys for high temperatures). Moreover, continuous development of new irradiation experiments for development of fuel cladding and wrapper tube materials for fast reactors which can withstand a temperature range of 400-700°C and a radiation damage level up to 200 dpa is desired.
- Development of instrumented/non-instrumented irradiation capsules for structural material testing of advanced materials as well as implementation of theoretical code calculations for neutronics, gamma scanning and shielding.

- Fundamental and applied research in the field of irradiation ageing of structural materials for present and new reactor concepts is on-going activity in several Member States. However, further development of new reactor materials and the design of experiments should be supported by modeling of the relevant physical phenomena (e.g. synergy between the alloying elements).
- Combination of mechanical testing and microstructural investigation, as well as continuous improvement of quality and implementation of instrumented methods for testing of the materials irradiated at high dpa, especially for the new classes of the NPP structural materials is essential. Enhancement of understanding of microstructural processes in radiation damage phemeomenon, as well as miniaturisation of the samples (e.g. mini CV, etc.) and validation issue for such studies are needed.
- Establishing new international research programmes for materials irradiation (including advanced material irradiation and RR surveillance), in particular, the sharing of the facilities are highly desired.
- Exchange of expertise for irradiation testing devices (medium and high fluence) for effective sharing of the knowledge in the irradiation programmes is needed e.g. through the support of the technical meetings/conferences in the subject.
- Continuous improvement of the irradiation programmes, communication and coordination between the irradiation groups can be foreseen as part of existing RR Technical Working Group (RR-TWG). This will help to improve and harmonize QA/QC requirements and procedures for materials irradiation.
- Testing of new structural materials (e.g. HTR/VHTR, SFR, SCWR and LFR) should be supported by irradiation at RRs and accelerators. Also, the techniques related to such materials are of crucial interest, including development of neutron monitors compatible with different environmental conditions. Knowledge transfer in the field of irradiation technology (workshops, visit to assembly sites, etc.) is needed to train new professionals.
- In view of effective utilization of RR's, their categorization in the irradiation capabilities is important. In this way, a small size RR can complement MTR and contribute to the post-irradiation experiments with available Hot-cells facilities.
- It is critical that in the future, IAEA will continue to cooperate between the RR centres in particular to enhance the transfer of appropriate knowledge.

<div align="center">**Chapter 2**</div>

CURRENT STATUS AND PERSPECTIVES OF NUCLEAR REACTOR BASED RESEARCH IN BANGLADESH

S.M. HOSSAIN[1], M.A. ZULQUARNAIN[2], I. KAMAL[1] AND M.N. ISLAM[1]
[1]Institute of Nuclear Science & Technology, Atomic Energy Research Establishment
G.P.O. Box No.-3787, Savar, Dhaka-1000, E-Mail: Syed9495@Yahoo.Com

[2]. Reactor Operation and Maintenance Unit, Atomic Energy Research Establishment
G.P.O. Box No.-3787, Savar, Dhaka-1000

Abstract: The Bangladesh Atomic Energy Commission (BAEC) has been operating the country's only research reactor, a 3 MW TRIGA Mark-II, for the last 22 years. The reactor is equipped with a number of irradiation facilities: dry central thimble (DCT), neutron beam tubes (tangential, radial piercing, radial-1 and radial-2), pneumatic transfer system, rotary specimen rack (Lazy Suzan), thermal column, etc. Since its establishment, the BAEC TRIGA reactor has been playing pioneering role in scientific research and in providing services to the people. For example, the radioisotopes produced in this reactor are being used in different nuclear medicine centers of the country for both diagnostic and therapeutic purposes. On the other hand, with a view to opening a new avenue of fundamental and applied research in the country, a number of different experimental facilities were installed around the reactor in early nineties of the last century. With the aim of socio economic development of the country, these facilities are being used in various fields of research and utilization, such as, isotope production, material research using neutron scattering, materials characterization by neutron radiography, qualitative and quantitative assessment of elements in variety of sample matrices and nuclear data measurements using neutron activation analysis as well as training and service as centers of excellence in Science & Technology. The aim of this article is to explore the current status of nuclear reactor based research in Bangladesh with special emphasis on neutron activation analysis and future plan of enhancing its utilization.

2.1. Brief history of BAEC TRIGA reactor

The Atomic Energy Research Establishment, the biggest research wing of BAEC is blessed by the presence of only nuclear research reactor in the country. It was established about two decades back with the aim of peaceful use of atomic energy in the country. It is a tank type research reactor. It has achieved its first criticality in the morning of September 14, 1986. This may be identified as a memorial event in the scientific annals of the country. It was tested and commissioned fully at the end of October 1986. The technical, operational and utilization data is quoted in Table 1 and the core configuration with irradiation channels of BAEC TRIGA reactor is shown in Fig.1.

TABLE 1. SALIENT FEATURES OF BAEC TRIGA REACTOR [1]

Technical data	
Power output	3 MW (thermal)
Fuel moderator material	Uranium Zirconium Hydride (U-ZrH$_{1.6}$)
^{235}U enrichment	19.7 wt%
Cooling	Natural/Forced
Number of fuel element	100
Coolant	Demineralized water
Core loading	Fuel elements = 93; IFE = 02; FFCR = 05
Control rod	6 rods of Boron Carbide (B$_4$C)
Reflector	Graphite
Operation and utilization data 14 September 1986 to 30 October 2008 [2]	
Hours operated per day	6
Total hours operated	7412
Hours at full power operated	2444
Total burn—up	15017 MWh
Number of irradiation request catered	1274
Radioisotope produced	> 87.01 Ci (^{131}I, ^{99m}Tc, ^{46}Sc)

Position	Thermal flux, n.cm^{-2}s^{-1}	Epithermal flux, n.cm^{-2}.s^{-1}
DCT	7.53×10^{13}	3.81×10^{12}
RSR (Lazy Suzan)	1.39×10^{13}	6.59×10^{11}
Pneumatic Transfer System	2.64×10^{13}	1.23×10^{12}
Tangential beam port	1.32×10^{7}	2.18×10^{5}
Radial piercing beam port	1.2×10^{5}	-

2.2. Utilization status

Utilization of BAEC TRIGA reactor includes isotope production, material research using neutron scattering, materials characterization by neutron radiography, and the use of NAA for the qualitative and quantitative assessment of elements in variety of sample matrices and Nuclear Data measurements, manpower training, education, etc.
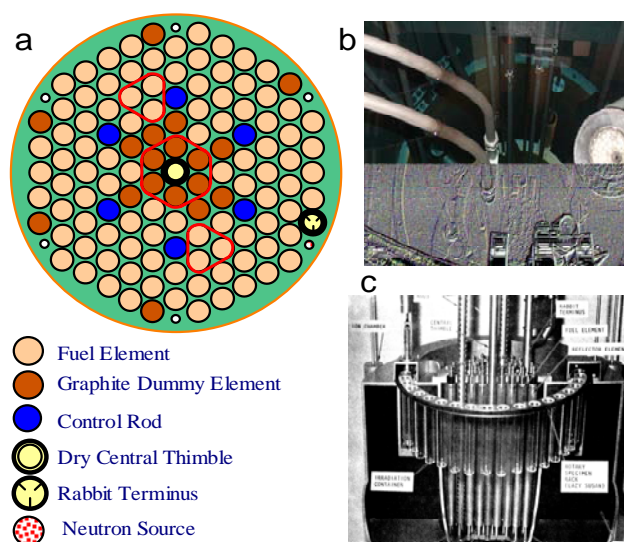
FIG.1. (a) BAEC TRIGA Reactor core configuration; (b) Pneumatic transfer pipes entered into the Rabbit Terminus of the reactor core; (c) Rotary specimen rack surrounding the reactor core.

Isotope production

In Bangladesh, 12 nuclear medicine centers and two Institutes of Nuclear Medicine run by BAEC are serving millions of people and performing research to extend its application. The aim of radioisotope production using BAEC TRIGA reactor is to fulfil the local demand of short-lived medical radioisotopes and radiopharmaceuticals both for diagnosis and therapeutic purposes. The major facilities of radioisotope production include: ^{99m}Tc generator production plant, ^{131}I production plant, ^{131}I Capsule production facility, QA/QC facility, etc.

Neutron scattering

With a view to utilize the reactor for materials research, a Triple Axis Neutron Spectrometer (TAS) has been set up in the radial piercing beam port of the TRIGA MARK-II research reactor. The spectrometer is being effectively used for the studies of structural and characteristic properties of materials for their potential applications. The present scope of research using TAS facilities include: neutron powder diffraction studies for structural characterization of materials such as metals, metallic oxides, alloys, ceramics, superconductors and various types of magnetic materials; small angle neutron scattering for determining shape, size and molecular weights of particles in various kinds of biological aggregates and polymers; and texture studies for identification of texture in industrial and structural materials. Various types of materials are studied by the diffraction and Small Angle Neutron Scattering (SANS) techniques using the TAS. For instance, the crystal and magnetic structures of a variety of ferrites, superconducting materials, alloys, amorphous materials, etc., have been studied in the diffraction method [3].

Neutron radiography

Neutron Radiography (NR) facility has been installed at the tangential beam port of the TRIGA research reactor with a view to create opportunity for nondestructive testing of materials using the neutron beam. This beam port has been chosen in order to get a thermal neutron beam with minimum gamma content. The NR facility is being used for research on various materials and quality control of some industrial products. In the existing NR facility

only direct film neutron radiography method is being used and has already characterized various types of materials. For example, detection of corrosion in aluminum, study of the quality of some industrial products (leather, rubber, ceramics, etc.), determination of defects in some shielding materials, determination of defects and water absorption behavior in some building materials, study of defects and water absorption behaviour in various wood plastic composites and jute reinforced polymer composites [4].

Neutron activation analysis

In spite of advanced nuclear analytical methods developed (PIXE, XRF, etc.) in Bangladesh, the (n,γ) reactor neutron activation analysis (NAA) is still preserving its role as a "workhorse" for the diversity of analytical work [5-12]. Combined with computerized high resolution gamma-ray spectrometry, NAA offers mostly nondestructive, simultaneous multi-element analysis needed in many areas. In using NAA, the relative standardization method is being used in BAEC by employing multi-element standards and certified reference materials. However, the k_0-standardization approach will be implemented in the near future. The NAA Group is also involved in nuclear data measurements. The activity of NAA lab of BAEC can be categorized into four dimensions, such as Research & Development work (R&D), service, project and academic collaboration.

R&D activities

In the frame of R&D work, NAA Group helps other research groups to characterize different irradiation channels of TRIGA reactor. For instance recently, the Radiation Safety and Control Committee (RSCC) and Research Reactor Operation and Utilization Committee (RROUC) have decided to enhance ^{131}I production using the same amount of TeO_2 and irradiation time by filling up the CT with water instead of dry condition. The feasibility study in terms radioactivity, temperature and production rate has been performed by the NAA Group.

In order to investigate the possible pathways of arsenic and heavy metals exposure and their effects on population health and to define the contaminated area, samples of soil, foodstuffs, tube well water, human hair, etc. were collected from different regions of Bangladesh and were analyzed under R&D work [8,9]. Environmental pollution due to discharge of industrial effluents from tannery, dying and textile industry has been investigated in the NAA lab and cost effective mitigation approaches of pollutants have been suggested [7]. Assessment of environmental pollution due to ship breaking and their effects on occupational workers are in progress.

Since the installation of Triple Axis Spectrometer (TAS) in the radial piercing beam port of the reactor, it has been utilized for material research using the neutron scattering technique. Recently, a new arena has been opened up to utilize the radial piercing beam port for determination of neutron capture cross sections at a rare thermal energy region using NAA technique. So far, three experiments in determining the neutron capture cross section for reactions ^{186}W(n,γ)^{187}W, ^{71}Ga(n,γ)^{72}Ga, ^{152}Sm(n,γ)^{153}Sm and ^{154}Sm(n,γ)^{155}Sm relative to the ^{197}Au(n,γ)^{198}Au monitor reaction at the thermal energy of 0.0536 eV have been carried out successfully [13-15]. The measured cross sections for the first two reactions are shown in Fig. 2-3.
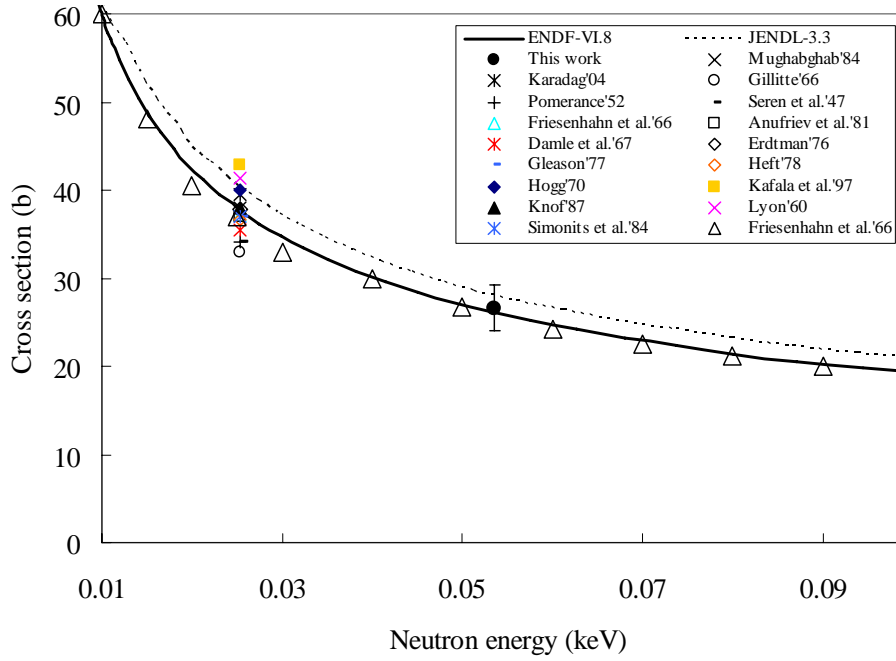
FIG.2. Neutron capture cross sections for the $^{186}W(n,\gamma)^{187}W$ reaction.
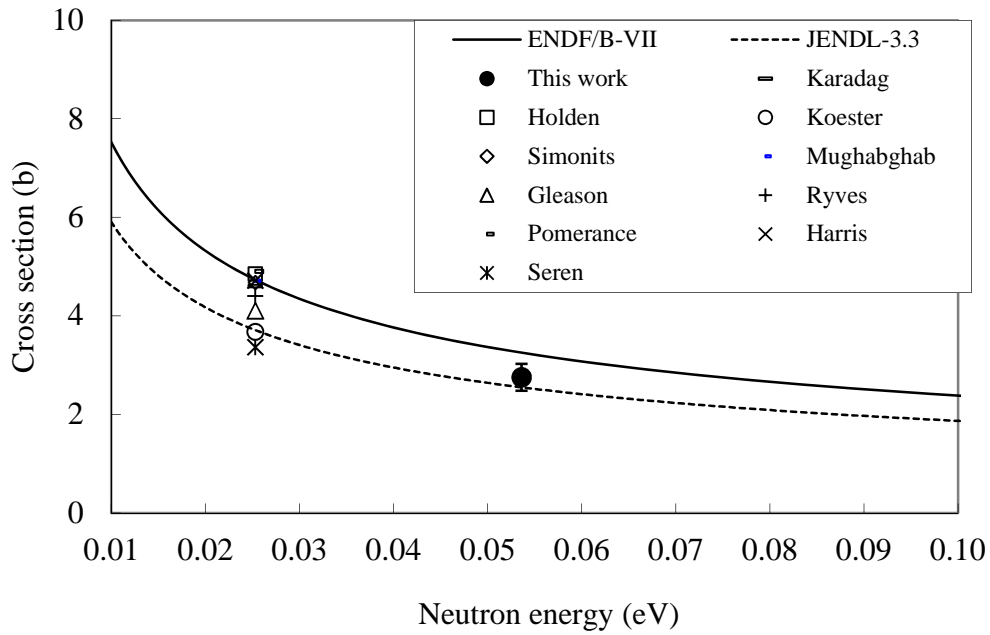
FIG.3. Neutron capture cross sections for the $^{71}Ga(n,\gamma)^{72}Ga$ reaction.

Service

In order to pursue and stimulate NAA activities in Bangladesh in a strategic way, the Group is trying to make an effort to connect the unique features of NAA to the country's social needs. For instance, Bangladesh is confronting the crisis of arsenic contamination in drinking water. The epidemic of arsenic related diseases has begun. Arsenic patients from different areas of Bangladesh are visiting doctors with complain. Before giving treatment, doctors need to know

11

the arsenic level in their body. Most of the time doctors fall in embarrassing situation when patients want to know where the arsenic level can be examined in their body. For doing so, the scope is very limited in Bangladesh. Under this circumstance, some Hospitals/Clinics send samples in abroad for analysis, which is very costly and most of the people cannot afford it. For helping these helpless people, NAA Group has taken initiative to estimate arsenic level (on payment, low cost and even in some cases free of cost) in human body by analyzing hair. A number of patients are being referred from different hospitals of the country to NAA lab. Mention can be made with some examples:

Case 1: Female married patient; age: 26 years, P.S.: Bhanga, District: Faridpur; referred by: Dr. Mir Nazrul Islam, Consultant Dermatologist, BIRDEM Hospital, Dhaka. The total arsenic concentration measured on her scalp via INAA was 36.4 ± 1.5 µg/g, whereas the normal level of arsenic in human hair is less than 1 µg/g;

Case 2: Female married patient, age: 34 years, P.S. and District: Gopalganj; referred by Professor Dr. A.Z.M. Maidul Islam, Head of Skin & V. D. Department, Bangabandhu Sheikh Mujib Medical College (BSMM) University, Dhaka. The arsenic level on her scalp determined amounted to 25.5 ± 5.1 µg/g;

Case 3: Male married patient, age: 35 years, P.S.: Brahman Para, District: Comilla; referred by Dr. Mansurul Alam, Department of Dermatology & STDs, Chittagong Medical College & Hospital, Chittagong. The total arsenic concentration on his scalp was found to be 5.31 ± 0.32 µg/g.

NAA laboratory received a number of married and unmarried male and female patients. The names of the patients are avoided in this article due to their social problem. The devastating physical condition of some arsenic contaminated patients who visited the NAA laboratory is shown in Fig.4.
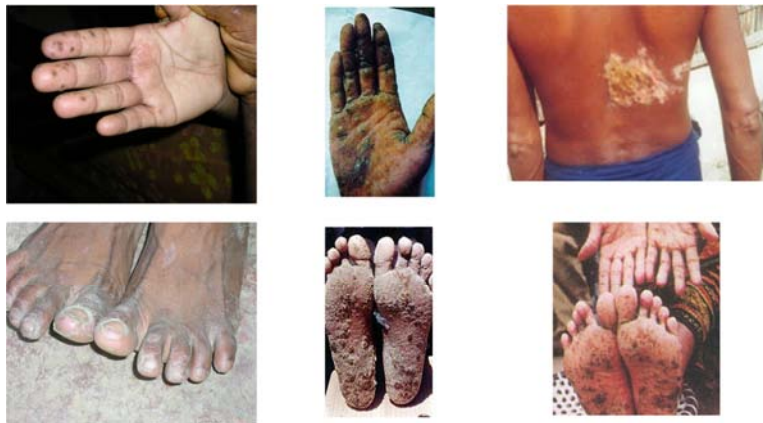
FIG.4. Arsenic affected patients who visited the NAA laboratory.

In addition to arsenocosis patients, NAA laboratory is involved in giving analytical services to the government, non-government organizations, universities, etc.

Projects

The NAA Group successfully completed several IAEA Technical Cooperation Projects. Recently, the IAEA TC Project BGD/8/018 entitled "Isotope techniques for mitigating arsenic contamination in groundwater (NAA component)" was completed. At present, the group is working on the following projects:

(1) Forum of Nuclear Cooperation in Asia (FNCA) on Research Reactor Utilization-NAA.

(2) Annual Development Program of Bangladesh Government Project on "Strengthening the Utilization of 3MW TRIGA Mark-II Research Reactor".

Academic Collaboration

Throughout the world, the decline of nuclear education has become an issue of great concern. It is therefore essential to take all necessary action so as to develop competent nuclear professionals by stimulating and supporting enrolments in the study of Nuclear Science and Technology and related disciplines. To address the problem, all the laboratories around TRIGA reactor are very keen to collaborate with almost every University of the country. Students from different universities and other scientific organizations of the country carry out their research work at various laboratories around TRIGA reactor to obtain academic degrees under the guidance of the relevant experts. At present 4 Ph.D., 2 M.Phil., and 6 M.Sc. students from different universities of Bangladesh are working at the NAA laboratory for preparing their theses.

Future trend

Although the BAEC TRIGA reactor has been operating since 1986, because of several limitations its optimum utilization could not be achieved yet. The radial beam ports 1 & 2 and thermal column are still lying unutilized. However, in order to optimize its utilization, several initiatives have been taken. For instance, a high resolution powder diffractometer (HRPD) and a digital neutron radiography setup are being installed at the radial beamport-1 and tangential beam port, respectively under an ADP (Annual Development) Project financed by the Government of Bangladesh. A project has also been submitted under the ADP program for installation of PGNAA. The present analog console of the reactor will be replaced by a digital one under an ongoing ADP project. The establishment of ^{99m}Tc kit production laboratory is also in process in the framework of a separate ADP project.

2.3. Conclusions

Since its establishment, the reactor has been utilized without any major incident. However, a few minor incidents sometimes hampered the operation of the reactor. For instance, the N-16 decay tank (DT) leakage problem that arised due to pitting corrosion at several areas of the DT caused by rainwater suspended the operation of the reactor at high power level for about 4 years (from 1997 to 2001). With limited facilities, different utilization groups have been trying for proper utilization of BAEC TRIGA reactor in both fundamental research and service purposes. However, in reality, the neutrons generated in the reactor core cannot be exploited efficiently using the present experimental facilities and, as a result, the optimum utilization of the BAEC TRIGA reactor is not being possible. Under these circumstances, it is strongly felt that measures have to be taken so as to update and extend the laboratory facilities with the help of national and international strategic partners.

REFERENCES

[1]   HAQUE, M.M., Operation and Maintenance Status of the 3 MW TRIGA Mark-II Research Reactor of Bangladesh, International Seminar on Nuclear Safety (2005), Operation and Maintenance of Nuclear Facilities Course, International Nuclear Technology Cooperation Centre and Radiation Application Development Association (RADA), Japan (2005).

[2]   Operational Log Book of Reactor Operation and Maintenance Unit.

[3]   ZAKARIA, A.K.M., et al., Studies of $Mn_{0.5}Cr_{0.5}Fe_2O_4$ ferrite by neutron diffraction at different temperatures in the range $768k \geq T \geq 13k$, Indian Journal of Pure and Applied Physics, 40 (2002) 46.

[4]   ISLAM, M.N, KHAN, M.A., ZAMAN, M.A., Study of the defects and water absorption behaviour in Jute-reinforced polymer composites using film neutron radiography, Journal of Reinforced plastics and composites, 24 No.16 (2005) 1697.

[5]   HOSSAIN, S.M., et al., Analysis of Mymensingh sand for traces of gold using instrumental neutron activation analysis, INST Internal Report, INST-116/RNPD-28 (2008).

[6]   HOSSAIN, S.M., et al., Utilization of radial piercing beam port of TRIGA reactor for nuclear cross section measurements, INST Internal Report, INST–115/RNPD-27 (2008).

[7]   HOSSAIN, S.M., et al., Environmental Pollution Assessment due to Discharge of Industrial Effluents using NAA technique, 6th International Conference on Isotopes, Seoul, Korea (2008).

[8]   RAHMAN, M.M., et al., Estimation of arsenic toxicity in human hair and water by NAA method, Bangladesh Journal of Nuclear Medicine, 10 No.1 (2007) 58.

[9]   HOSSAIN, S.M., et al., Estimation of arsenic level in patients by analyzing hair using instrumental neutron activation analysis, NAMLS8, 8th International Conference on Nuclear Analytical Methods in the Life Sciences, Conference Proceedings Log 115 (2005), 98.

[10]   HOSSAIN, S.M., DE CORTE, F., VANDENBERGHE, D., VAN DEN HAUTE, P., The role of k_0-NAA in the assessment of the annual radiation dose for use in TL/OSL dating of sediments, J. Radioanalytical and Nuclear Chemistry, 257 No.3 (2003) 639.

[11]   HOSSAIN, S.M., DE CORTE, F., VANDENBERGHE, D., VAN DEN HAUTE, P., A comparison of methods for the annual radiation dose determination in the luminescence dating of sediment, Nuclear Instruments and Methods in Physics Research A, 490/3 (2002) 598.

[12]   MOLLA, N.I., et al., M.I. Elemental analysis in bed sediment samples of Karnafuli estuarine zone in the Bay of Bengal by Instrumental Neutron Activation Analysis, J. Radioanal. Nucl. Chem., Articles, 216 No.2 (1997) 213.

[13]   UDDIN, M.S., et al., S.M., Neutron capture cross-section measurement for the $^{186}W(n,\gamma)^{187}W$ reaction at 0.0536 eV energy, Applied Radiation and Isotopes, 66 (2008) 1235.

[14]   UDDIN, M.S., et al., Measurement of neutron capture cross section of the $^{171}Ga(n,\gamma)^{172}Ga$ reaction at 0.0536 eV energy, Nuclear Instruments and Methods in Physics Research B, 266 (2008) 3341.

[15]   DDIN, M.S., et al., Thermal neutron capture cross sections for the $^{152}Sm(n,\gamma)^{153}Sm$ and $^{154}Sm(n,\gamma)^{155}Sm$ reactions at 0.0536 eV energy, Nuclear Instruments and Methods in Physics Research B, 266 (2008) 4855.

UTILIZATION OF EGYPTIAN RESEARCH REACTOR AND MODES OF COLLABORATION

M.A. GAHEEN, M.K. SHAAT
Egyptian Research Reactor (Etrr-2), Egyptian Atomic Energy Authority, 13759
Abou Zabal, Egypt
Email: mgahen@etrr2-aea.org.eg

Abstract: The new Egyptian Research Reactor (ETRR-2) is a Material Testing Reactor (MTR) commissioned in 1997. It is an open pool Research Reactor (RR) using low enriched MTR fuel elements (less than 20% enrichment), cooled and moderated with light water and reflected by beryllium. The reactor power is 22 MW with high neutron flux irradiation positions (flux $> 10^{14}$ n/cm^2.s) and can be operated up to 19 days providing high neutron fluence. Also, the reactor has two fast irradiation positions, two silicon irradiation positions, three radial and one tangential beam tubes, and thermal column. ETRR-2 is a multipurpose reactor, several experimental and production facilities have been installed for Radio Isotope (RI) production (I-131, I-125, Cr-51, Ir-192, and Co-60), Neutron Activation Analysis (NAA) applications, Neutron Transmutation Doping (NTD), neutron radiography experiments, and training of personnel. A special hot cell for irradiated material testing has been installed where the impact tests, tensile tests, and other material characterization can be applied for irradiated samples of materials used in Nuclear Power Plant (NPP) and advanced reactors. In this paper, the utilization of ETRR-2 and future plans for development of some of existing and new facilities are presented as well as modes of collaboration with regional countries for sharing RR services.

3.1. Introduction

Applications of research reactor include irradiations, neutron beam work and training of personnel. Every research reactor is capable of being used for training purposes, but RRs with higher neutron flux have more capabilities for irradiation and neutron beam applications and should have effective utilization plans [1].

The ETRR-2 plan for utilization has been updated to achieve an effective use of its irradiation and beam tube facilities. Modifications to some irradiation facilities have been proposed to increase the utilization and improve the provided services. The proposed modifications will achieve and maintain an increase of the utilization through enhancement of the existing facilities or installation of new facilities. In view of increasing and improving the provided service, collaboration with other RR institutes will help to share available services and encourage the better utilization.

In section 2, the current utilization of ETRR-2 and potential capabilities is described. The proposed modifications and new facilities are presented in section 3. The services and modes of collaboration with other RR institutes are summarized in section 4 and the conclusions are presented in section 5.
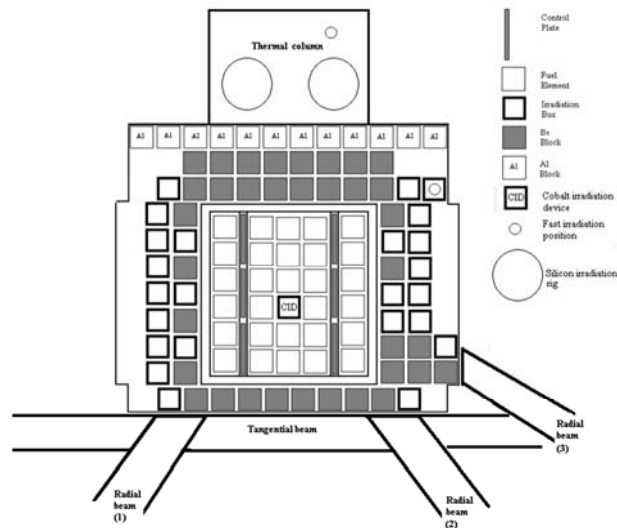
FIG.1. ETRR-2 existing irradiation facilities and beam tubes.

3.2. Current utilization of ETRR-2 and potential capabilities

An important element in RR utilization is the evaluation current utilization and potential capabilities of the reactor. ETRR-2 existing irradiation facilities and beam tubes are shown in Fig.1.

Sample irradiation and radio-isotopes production

Irradiation positions in core and in reflector area are dedicated for sample irradiation and RI production. High thermal flux positions (flux > 10^{14} n/cm^2.s) [2] meets the requirements of radioisotope production of Cr-2, Ir-192, Co-60 and other isotopes produced in low and medium thermal flux reactors.

The isotopes I-131, I-125, Cr-51, and Ir-192 can be produced using irradiation facilities at ETRR-2. Target samples are prepared and placed inside of aluminum can (23.5 mm x 70 mm) and loaded in can holder. Loading operation is performed inside of transfer cell, and then can holder are transferred to the main pool using sample carrier to be placed in irradiation box at irradiation grid. Once irradiation time is reached the can holder will be handled and transferred to the transfer cell using sample carrier. Once cooled, irradiated cans will be unloaded and transferred to the universal cell using interconnection conduit and be loaded in the shielded container and send to RI Production Facilities, Fig.2.

As shown in Fig.1, core center position is dedicated for ^{60}Co production (up to 50.000 Ci can be produced per year) [2]. Loading operation of cobalt irradiation device in shielded container is performed under water. Cobalt hot cell is installed for ^{60}Co engineering processing and sealed source production.

16
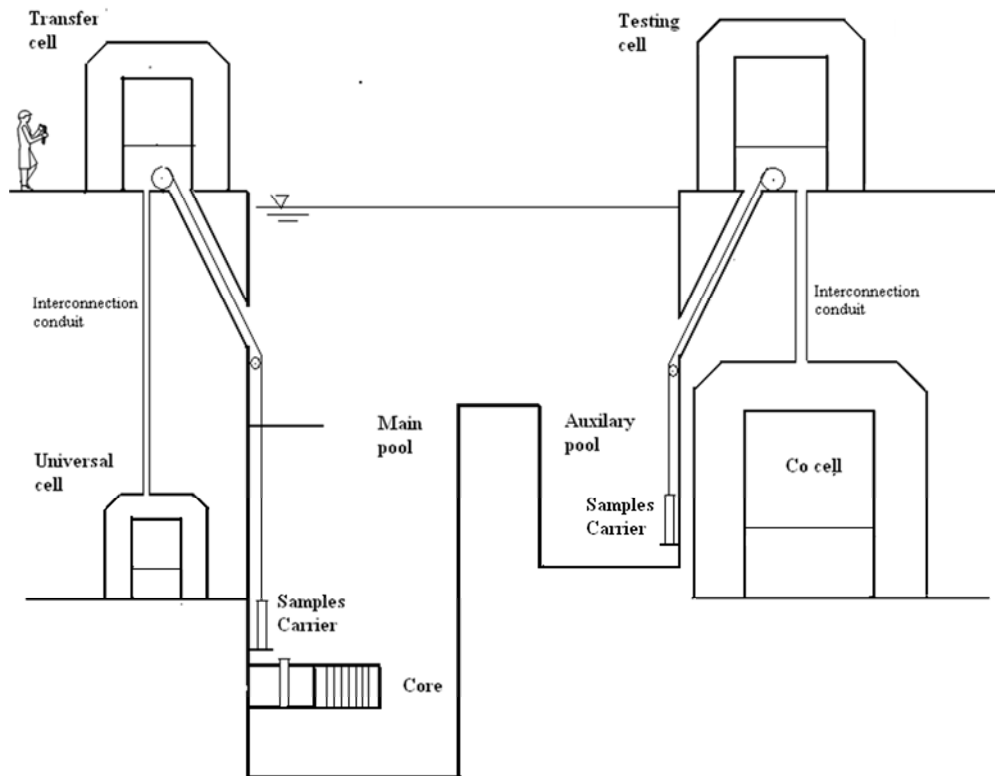
FIG.2. Hot cells interconnections and connections to main and auxiliary pools.

Material testing cell

A material testing hot cell is installed for performing destructive tests on irradiated samples (standard specimens). The cell is provided with impact machine, micro-hardness tester, and tensile machine. Irradiated samples are transported under water from main pool to the auxiliary pool using proper operational tools. The cell is connected to the auxiliary pool, sample carrier is used to transport irradiated samples from the lower part of the auxiliary pool into the testing cell where mechanical tests can be carried out, Fig. 2.

Neutron activation analysis

Two fast transport pneumatic tubes are available for fast irradiation samples for the use in NAA applications. The system has two positions of irradiation. One position in the reflector area with thermal flux of 9×10^{13} n/cm^2.s and the other position being in the thermal column with thermal flux of 2×10^{11} n/cm^2.s, Fig.1.

The NAA laboratory is provided with high efficiency detection systems for elemental analysis of irradiated samples. Environmental, geological, and biological samples could be analyzed for different applications at the NAA laboratories with the provided detection systems. The laboratory contributes to the reactor routine measurements of pools water samples, etc.

Neutron transmutation doping

Neutron transmutation doping facilities at ETRR-2 consist of two irradiation rigs located in the thermal column for silicon irradiation, Fig. 1. Theses rigs are capable of irradiating up to 28 cm long five-inch diameter ingot (127 mm) with axial resistively variation in the product

less than 5%. Labs of post irradiation tests and measurements are also included. The existing silicon irradiation rigs should be modified to meet the customer requirements for larger size ingots.

Neutron radiography facilities

Radiography facility mounted in front of a beam radial tube (tube1 in Fig.1) with proper shielding and samples handling mechanisms.

- Beam port flux about 3.0×107 n/cm^2.s;
- L= 3315 mm;
- D= 30 mm.

Underwater neutron radiography facility for irradiated samples non-destructive tests is installed at radial beam tube (tube 3 in Fig 1) housed at the main pool.

- Beam port thermal flux bout $1.8 \ 10^9$ n/cm^2.s;
- L= 1377 mm;
- D= 40 mm.

Thermal Column

Thermal column and connected shielded room with access control are dedicated for BNCT application.
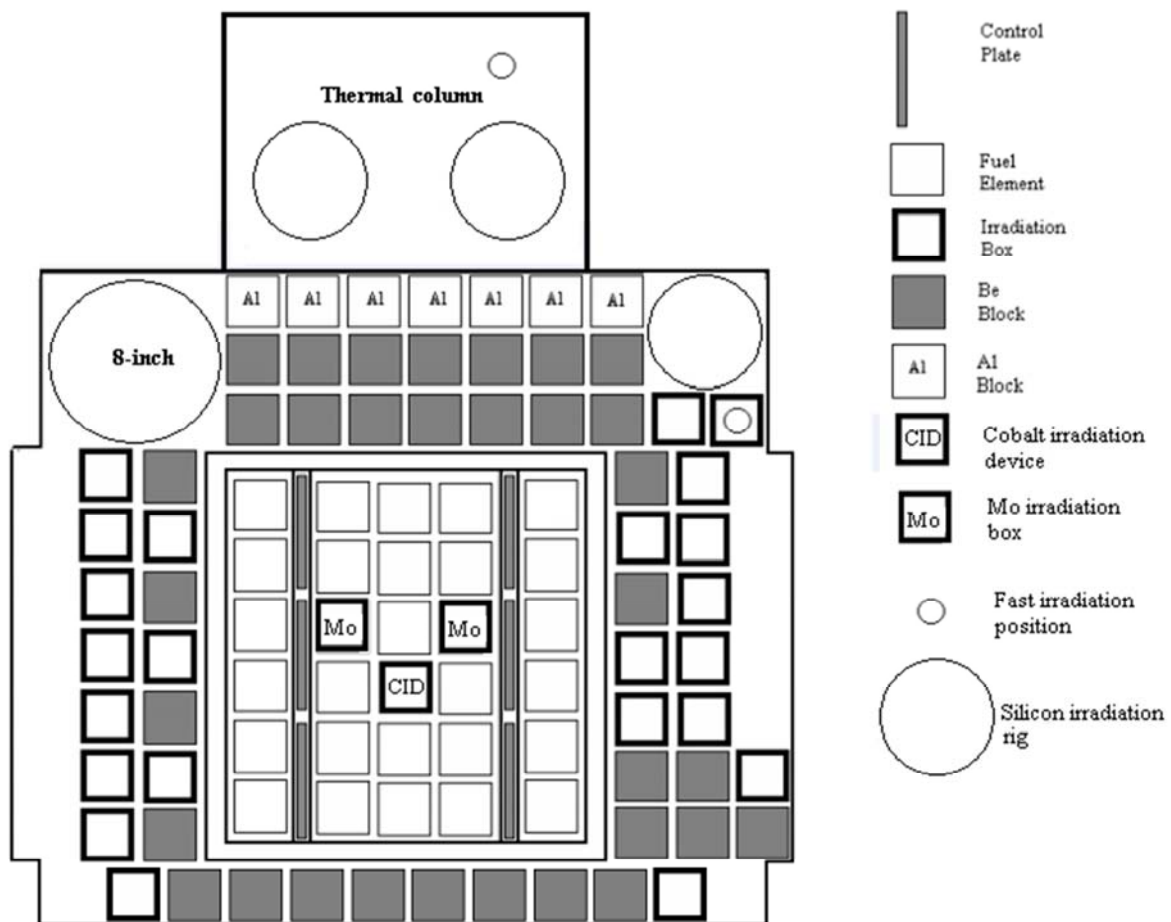
FIG.3. ETRR-2 irradiation facilities with modifications.

Upgrading of silicon transmutation doping facilities

It is possible to introduce modifications to the existing silicon irradiation rig to irradiate six–inch diameter silicon ingots instead of dismantling it and constructing a new rig in the same place. The existing aluminum container (about 15 mm thick) in the irradiation rig can be substituted with another one of appropriate thickness (3 mm) and inner diameter sufficient to accommodate six-inch diameter. A simple design of new aluminum container has been completed as well as manufacturing of one new container for the purpose of irradiation tests and commissioning. The new container can irradiate two six-inch ingot instead of one 5-inch ingot in old five-inch container. Irradiation tests and commissioning of the upgraded facility are in progress.

The outer positions in the irradiation grid could be made available for irradiation of 8-inch ingots and more six-inch diameter. An example of new proposed silicon irradiation positions is shown in Fig 3. Should there not be a big for 8-inch size the same rig can also be used to irradiate more six-inch diameter. A simple irradiation rig design similar to the one used in IEA-R1 research reactor is suggested to be adapted in ETRR-2 [3].

In-core ^{99}Mo productions

Low Enriched Uranium-aluminum plates will be irradiated in the reactor core in special dedicated irradiation boxes to produce 1000 Ci of ^{99}Mo per week. The existing in-core irradiation box for ^{60}Co production will remain in the new core design. Two irradiation boxes will be placed inside the core for the purpose of ^{99}Mo production replacing two fuel elements as shown in Fig.3.

Each irradiation box contains two target holders where the targets are loaded. The loading operation is performed inside the testing cell, and then target holders are transferred to the auxiliary pool to be assembled in the irradiation box. Irradiation boxes are transferred from auxiliary pool to the reactor core for irradiation. The in core irradiation has the advantage that no special cooling or irradiation loop is required. The irradiation boxes will be loaded into or removed from the core while the reactor is shut down. In-core irradiation for ^{99}Mo production is performed in RA3 research reactor [4].

Once the irradiation time is reached, each irradiation box is removed with the operational tool from the core. Once cooled, the irradiation box is transferred to the auxiliary pool where it is disassembled under water. Targets holders are transported from the auxiliary pool to the testing cell using the sample carrier. Inside the testing cell, plates are transferred to the target containers and sent to the cobalt cell using the correspondent interconnection conduit. The target containers are loaded in the shielded container previously entered into the cobalt cell and sent to RI Production Facilities, Fig.2.

Installation of SANS

Etrr-2 has appropriate design of the beam tubes and optimal conditions for installation of 2 or 3 scattering instruments. It is possible to start with an instrument of intermediate level. The IAEA will support a first SANS for applications in materials science and engineering.

3.3. Services and collaboration

Better utilization can also be achieved by collaborating with countries which have no RR and with other RR institutes. The modes of collaboration are to maximize the use of ETRR-2 for regional benefit and improve the reactor products and services and exchange experience.

Services which can be provided

- Neutron radiography;
- Irradiation of silicon ingots with diameters five and 6-inch diameter and length of 28 cm;
- Irradiation services to produces, ^{131}I, ^{125}I, ^{60}Co, etc.;
- NAA for geological, foodstuff, biological, and environmental samples.
- On the job training;
- Training on calculation codes (e.g. MCNP code, MTR- Package, etc.);
- Training and workshops activities in the field of radiation protection, core calculations and isotope production.

Modes of Collaboration

- Networking and bilateral co-operation;
- Technical cooperation projects;
- Conferences and forum;
- Meetings , training activates , workshops, expert mission and scientific visits;
- Experimental facilities sharing;
- Common research and scientific publications;
- Participation in Research Projects.

3.4. Conclusions

The main utilization aspect of ETRR-2 design is its flexible irradiation positions and potential for modification to harmonize with the requirements of the utilization. Effective utilization of ETRR-2 facilities can be achieved through (i) development of an effective and updated utilization plan, (ii) manpower development to support longer operation, (iii) implementation of necessary modifications, which incorporate experience of similar research reactor designs and utilization and indicant simple design, (iv) IAEA Technical cooperation activities, and (v) collaboration with other RR centers and sharing services.

REFERENCES

[1] INTERNATIONAL ATOMIC ENERGY AGENCY, The Applications of Research Reactors, IAEA-TECDOC-1234, IAEA, Vienna (1999).
[2] Safety Analysis Report (SAR) of ETRR-2, Egyptian Atomic Energy Authority, Cairo, Egypt (2003).
[3] CABONARI, A.W., PENDL, W., SEBASTIÃO, J.R., SAXENA, R.N., DIAS, M.S., An irradiation rig for neutron transmutation doping of silicon in the IEA-R1 research reactor, Nuclear Instruments and Methods in Physics Research B83, North-Holland (1993) 157.
[4] CALABRESE, R., GRANT, C., MARAJOFSKY, A., PARKANSKY, D.G., Analysis of Mo99 Production Irradiating 20 %U Targets, International Meeting on Reduced Enrichment for Research and Test Reactors, Sao Paulo, Brazil (1998).

Chapter 4

STATUS OF RESEARCH REACTOR UTILIZATION IN BRAZIL

J.A. PERROTTA
Instituto De Pesquisas Energéticas E Nucleares
Ipen/Cnen-Sp. Brazil
Email: perrotta@ipen.br

Abstract: Brazil has four research reactors in operation: the IEA-R1, a pool type research reactor of 5 MW; the IPR-R1, a TRIGA Mark I type research reactor of 100 kW; the ARGONAUTA, an Argonaut type research reactor of 500 W; and the IPEN/MB-01 a critical facility of 100 W.

Research reactor utilization has more than fifty years in Brazil. The first three reactors, constructed in the late 50´s and early 60´s at university campus in Sao Paulo, Belo Horizonte and Rio de Janeiro, had their utilization for training, teaching and nuclear research. The IPEN/MB-01, designed and constructed in IPEN in the late 80´s, is utilized for the development and qualification of reactor physics calculation for PWR core application.

The IEA-R1 has had its application and utilization increased through the years and it is presently used for radioisotope production, neutron beam application, neutrongraphy, neutron activation analysis, and limited fuel and material irradiation tests, besides the regular use for training and teaching. The low power of the reactor and the lack of hot cells for post irradiation analysis limits its technical application for the nuclear fuel industry.

Brazil has two nuclear power plants in operation, one unit starting construction and four more units planned for the next two decades. Brazil has significant quantities of uranium ore and has expertise in all the fuel cycle steps, including uranium enrichment, and produces the fuel assemblies for the nuclear power plants. These industrial activities demand the need of material and fuel irradiation tests.

IPEN produces radiopharmaceutical kits for the treatment of more than three million patients each year. The majority of the radiopharmaceutical kits is produced from imported radioisotopes. The increasing price and shortage of world supply of ^{99m}Tc leads also to the need of increasing the radioisotope production in Brazil. Due to these new demands, the Brazilian Nuclear Energy Commission is analyzing the costs and benefits of developing and constructing a new Research Reactor in Brazil, which besides radioisotope production and material testing can be a new tool for neutron beam application to the scientific community as well.

This paper presents the actual research reactor utilization in Brazil, and the perspectives of developing and constructing a new multipurpose research reactor.

4.1. ARGONAUTA Research Reactor

The ARGONAUTA Reactor is an Argonaut type reactor (Argonne National Laboratory Nuclear Assembly for University Training) installed in 1965 at the Nuclear Engineering Institute (IEN) of the Brazilian Nuclear Energy Commission located at the Rio de Janeiro University Campus. It has 500 W of maximum power, and uses U_3O_8-Al MTR dispersion fuel type with 20% uranium enrichment. The main use of the reactor is for teaching and training in reactor physics, neutrongraphy and neutron activation analysis. Nuclear engineering post-graduate courses at the University of Rio de Janeiro use the reactor for practical laboratory classes in reactor physics [1-4].
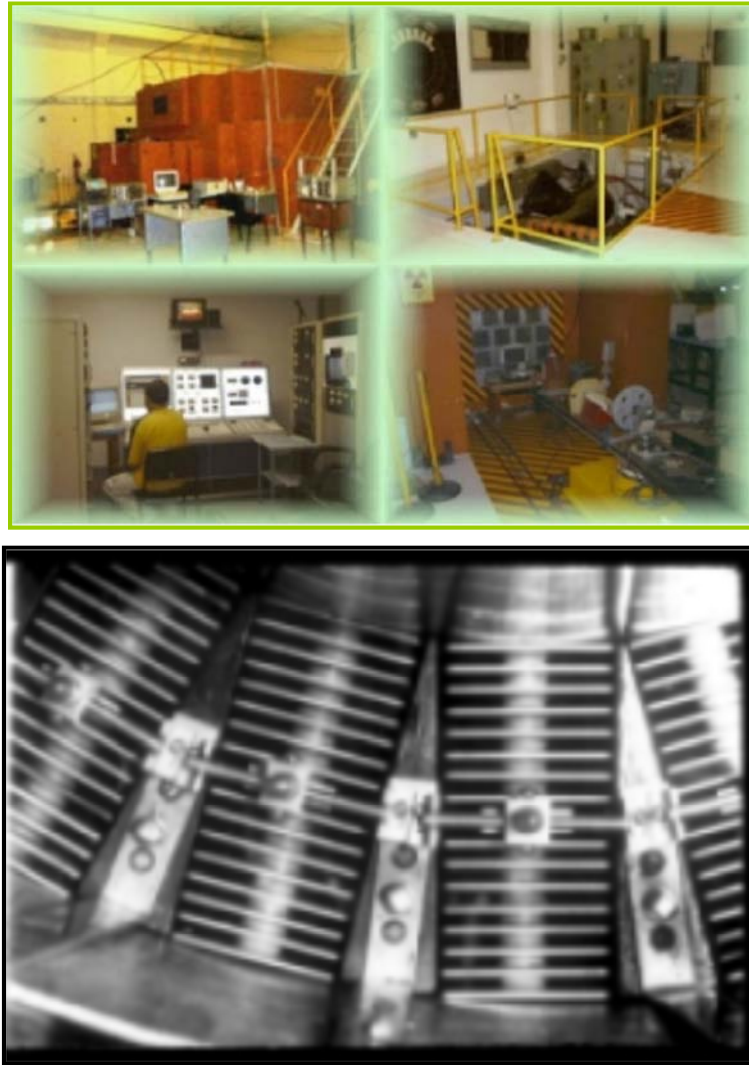
FIG.1. Argonauta research reactor.

4.2. IPR-R1 research reactor

The IPR-R1 research reactor is a TRIGA MarkI type reactor, constructed by General Atomic Company, USA, and installed in 1960 at the previous Radioactive Research Institute (IPR), today the Nuclear Technology Developing Center (CDTN) of the Brazilian Nuclear Energy Commission, located at Belo Horizonte, Minas Gerais Federal University Campus. It has 100 kW of maximum power for continuous operation, and uses U-Zr-H TRIGA pin type fuel with 20% uranium enrichment. The main use of the reactor is for the production of specific radioisotope for applications in industry, medicine, agriculture and engineering, neutron activation analysis and teaching and training in reactor physics. The reactor is one of the training tools for licensing the Brazilian nuclear power reactor operators. The reactor has been refurbished along the operating years and now will have its maximum power license increased to 250 kW for improving its application [5-11].
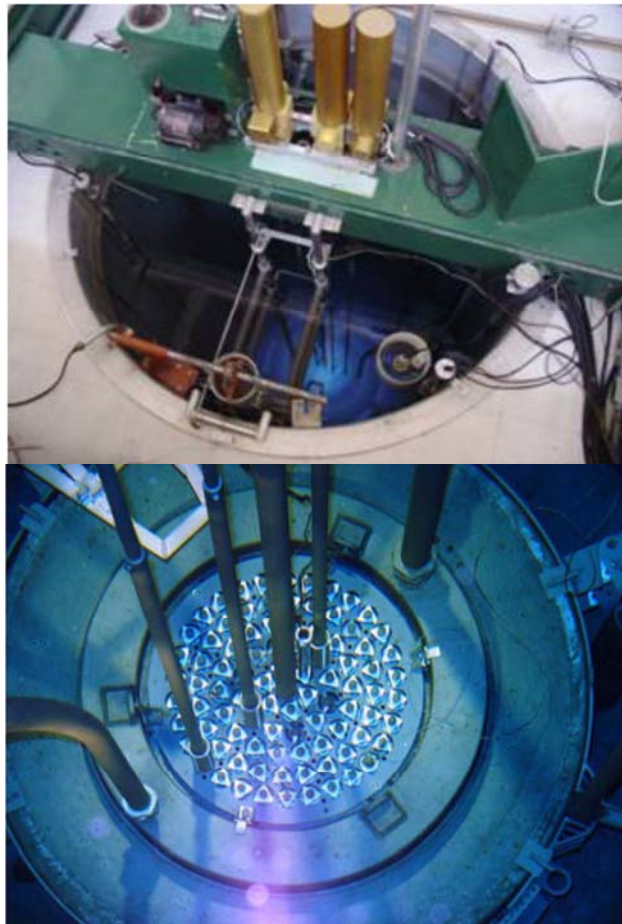
FIG.2. IPR-R1 Research Reactor.

4.3. IPEN/MB-01 research reactor

The IPEN/MB-01 is the first reactor designed and constructed with Brazilian technology. Installed at the Nuclear and Energy Research Institute (IPEN) of the Brazilian Nuclear Energy Commission site, in Sao Paulo, inside the Sao Paulo University Campus, had its first criticality in 1988. The reactor is a critical facility, with a maximum power of 100 W, and has the objective of validating reactor physics methodology and nuclear data associated for PWR core analysis. UO_2 fuel pins with 4.3% uranium enrichment, arranged in a rectangular array, compose the reactor core. The international community recognizes some experiments performed at this reactor as benchmarking data. The experimental data obtained at the reactor are: integral and differential reactivity worth of control rods; power calibration by foils activation and noise analysis; temperature and void reactivity coefficients; spatial and energetic flux distribution by foils activation and fission chambers detectors; reaction rates and spectral index measurement inside fuel rods; buckling measurement with different "baffle" material and thickness; and criticality tests with different burnable poison among other tests. The reactor is also used for teaching post-graduated students at IPEN, and for nuclear power reactor operators training as well. The reactor has recently obtained authorization to increase its maximum operation power to 1 kW in order to improve the quality of the measurements in experimental tests [12-15].
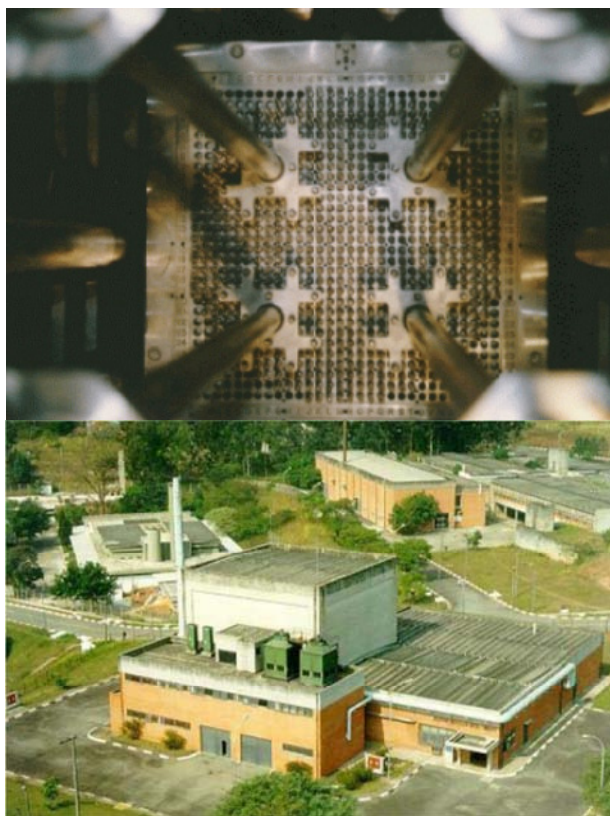
FIG.3. IPEN/MB-01 Research Reactor.

4.4. IEA-R1 research reactor

IEA-R1 is the largest research reactor in Brazil, with a maximum power rating of 5 MW. Installed at the previous Atomic Energy Institute (IEA), nowadays the Nuclear and Energy Research Institute (IPEN) of the Brazilian Nuclear Energy Commission site, in Sao Paulo, inside the Sao Paulo University Campus, the reactor achieved its first criticality on September 16, 1957. The reactor originally used 93% enriched U-Al fuel elements, but now it uses 20% enriched uranium U_3Si_2-Al fuel produced at IPEN.

The IEA-R1 reactor is a multidisciplinary facility used extensively for basic and applied research in nuclear and neutron related sciences and engineering. The reactor produces some radioisotopes with applications in industry and nuclear medicine, performs miscellaneous irradiation services, and has been used for training as well. Several departments of IPEN routinely use the reactor for their research and development work. Many scientists and students at universities and other research institutions in Brazil also use it quite often for academic and technological research. However, the main user of the reactor is the staff of the IEA-R1 Research Reactor Center (CRPq) with interest in basic and applied research in the areas of nuclear and neutron physics, nuclear metrology, and nuclear analytical techniques [15, 16].

Besides the main radioisotope production for the IPEN Radiopharmacy Center, some of the products and services offered by the CRPq find their application in the petroleum industry, aeronautical and space industry, medical clinics and hospitals, semiconductor industry, environmental agencies, universities and research institutions.

The reactor produces ^{131}I routinely for radiopharmaceutical kits manufactured at IPEN, produces also special radioisotopes such as ^{41}Ar and ^{82}Br for industrial process inspection, ^{192}Ir and ^{198}Au radiation sources for brachytherapy, and ^{153}Sm for EDTMP used in pain palliation in bone metastases. The reactor also produces ^{99}Mo by activation under demand

from the IPEN Radiopharmacy Center, as they can produce ^{99m}Tc generator kits by the gel process (with lower specific activity compared to the fission route).

The reactor has a neutron diffractometer that includes nine position sensitive detectors (PSD), a rotating oscillating collimator and an elastically bent silicon single crystal focusing monochromator. The PSD stack permits simultaneous measurement of neutron intensity in an angular interval of 30 degrees. The monochromator permits the choice of three different neutron wavelengths.

The CRPq offers regular services of non-destructive testing by real-time neutron radiography installed in a beam hole of the reactor. Multi-element trace analysis by neutron activation analysis supported by a radiochemical laboratory is an important activity developed by CRPq. Neutron irradiation of silicon single crystals for doping with phosphorus was developed at IPEN in the early 1990's. A simple device for irradiating silicon crystals with up to 12.7 cm diameter and 50 cm long, located in the graphite reflector, was installed in the reactor for commercial irradiation [17, 18].

The CRPq offers miscellaneous neutron irradiation of samples for research applications. The reactor permits irradiation tests of fuel for research and power reactor. An irradiation rig is used for testing MTR fuel type mini plates. A pressurized loop for testing mini rods of PWR fuel rod type was manufactured and is planned to be installed in the reactor in the near future. An irradiation rig for structural material test is also available for specific tests at temperatures up to 300°C. As the IEA-R1 installation does not have any hot cell, the post irradiation analysis are only non-destructive tests (NDT) performed inside the reactor pool. These tests are: visual inspection, dimensional inspection, gamma scanning and sipping test.

During the last several years, many changes in the reactor systems and components have been made in an effort to extend the lifetime of the reactor and guarantee its safe and sustainable operation. IEA-R1 is one of the oldest reactors of its kind in the world and has been operating for nearly 51 years with excellent safety records. Some of the important improvements made in the reactor systems during the last decades are: (a) modification of the reactor core from 6x5 to 5x5 using LEU fuel elements; (b) installation of a central beryllium element for samples irradiation; (c) replacement of 10 graphite reflectors with beryllium reflectors; (d) installation of four isolation valves in the primary cooling system; (e) repairs in the cooling tower and pipelines; (f) installation of a new ventilation and air conditioning system; (g) improvement in the control instrumentation; (h) replacement of the old radiation monitoring system; (i) and installation of an emergency core cooling system. With these modifications introduced, an authorization from the Brazilian regulatory body was obtained in September 1997 for continuous operation of the reactor at 5 MW.

The aging management and refurbishment program for the IEA-R1 reactor components and systems is a continuous and on-going activity of the Research Reactor Center. For example, the reactor pool water treatment and purification system was replaced in 2004. The older control and safety elements of the reactor began to show signs of aging and were replaced in 2004 with identical elements, (fork type Ag-In-Cd) fabricated at IPEN. The infrastructure modernization efforts include the Technical Cooperation (TC) project BRA/04/056: "Modernization of the IEA-R1 research reactor to secure safe and sustainable operation for radioisotope production," supported by the IAEA during 2005-2006. The project contemplated several training programs for the reactor operation and maintenance personnel as well as improving the technical infrastructure of the reactor. Some of the goals achieved through the TC project were: (a) replacement of some electrical and refrigeration systems; (b) radiometric analysis system for water and air samples; (c) reactor control instrumentation; (d) radiation monitoring equipment; (e) neutron flux mapping facility using self-powered neutron detectors; (f) improved computational facility for neutronic calculations; (g) a highly

radioactive sample handling facility; (h) training of personnel engaged in electrical and mechanical maintenance, water chemistry, and irradiation services; (i) and installation of a continuous vibration monitoring system for rotating machinery. Today, on-going new projects are the instrumentation and control room modernization and building maintenance. The current phase of the reactor modernization program is estimated to be completed by 2009 [18, 19].

In 1999 all the spent fuel elements stored in the reactor pool since its first criticality (a total of 127 elements) were transferred to the USA under a bilateral agreement (DOE-IPEN/CNEN). A transfer of an additional batch of 40 spent fuel elements to the USA took place in 2007 under the same agreement. The reactor pool at present has storage space for more than 130 spent fuel elements. The available pool storage space should be sufficient for about 7-8 years of reactor operation at 5 MW, 120h/week. A new project for spent fuel management and storage was initiated in 2001 at IPEN to verify the possibility of an alternate dry storage space. This project received active support from the IAEA in the form of a regional project. A prototype of a dry storage cask for 21 spent fuel elements is under qualification testing.

The reactor modernization program, introduced several years ago at IPEN, and its effective implementation during all these years with solid investments, guarantees safe and continuous operation of the reactor. The improved operational regime of the reactor has stimulated renewed interests in other applications, which are currently in experimental stages, such as boron neutron capture therapy (BNCT) and coloration of topaz. Neutron beam research will benefit due to availability of more intense neutron beams. A viability study has recently been made for the possibility of installing a small angle neutron scattering (SANS) facility at the reactor. It should be emphasized that academic research and postgraduate teaching at the Reactor Center are very important programs in the effective utilization of the reactor. Research scientists, students, and professors from universities and other research institutions and their students have free access to the research facilities at the CRPq.

4.5. Future perspective

In 2006 the Brazilian government created a working group, composed by the top managers of the nuclear area sectors, for reviewing the Brazilian nuclear program (NP). The working group proposed some guidelines and projects for the development of the NP. An Advisory Group of 11 Ministers analyzes the actions proposed for the NP before addressing them to the Brazilian President for decision making. This program is based on the fundamental principle of pacific and non-proliferation use of nuclear energy consonant with the Brazilian Constitution and International Treaties and Agreements. The NP identifies that nuclear energy will continue to be used in Brazil for the production of electricity and for several applications to the benefit of the Brazilian society.
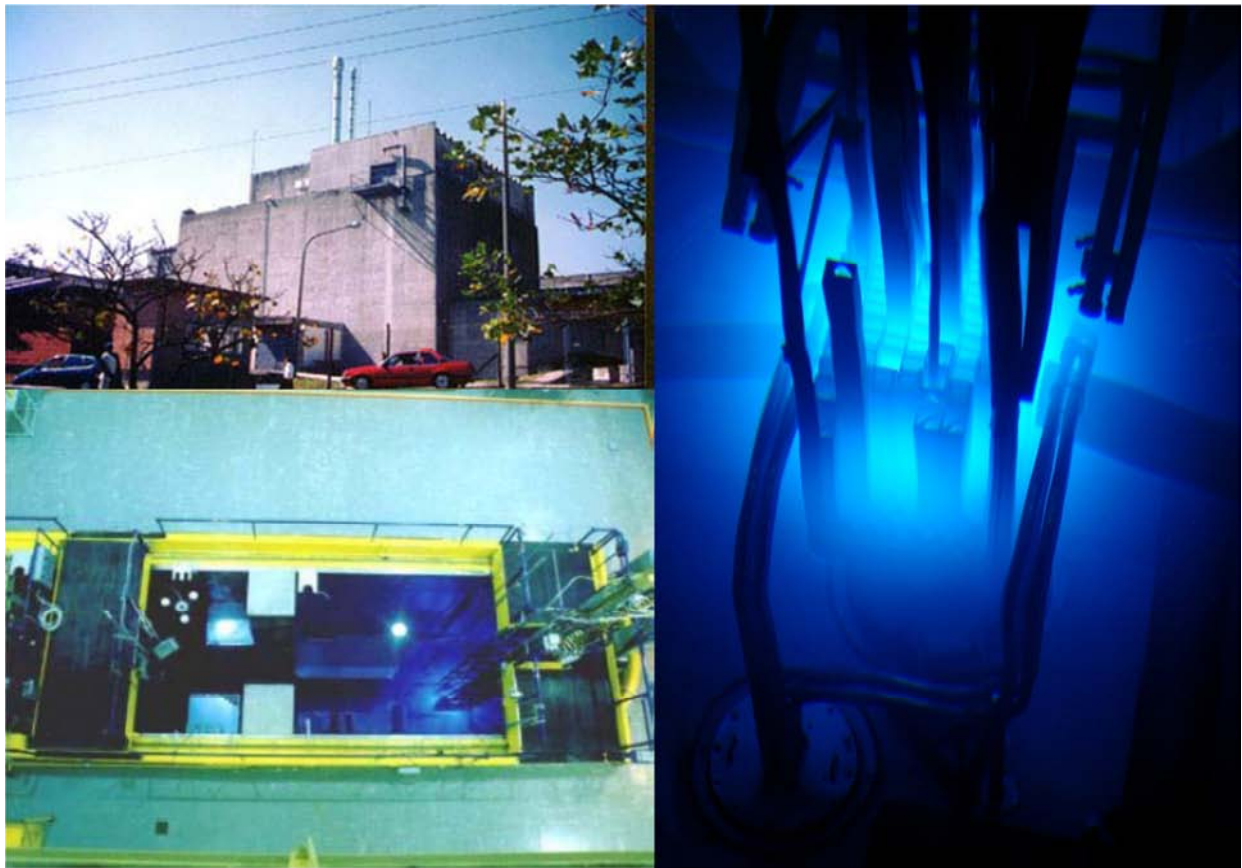
FIG.4. IEA-R1 research reactor.

Brazil has around 90 GW of electricity production installed capacity and of this, 70 GW is of hydraulic origin, and only 2 GW comes from nuclear power plants. The 2030 Brazilian energy plan envisages a total of 216 GW of electricity production installed, from which 164 GW of the total is from hydraulic origin and only 7.3 GW from nuclear power plants. Today Brazil has two nuclear power plants in operation, Angra I and Angra II, with a total of 2 GW electrical power. A new nuclear power plant, Angra III, 1.3 GW, is resuming construction, and four more nuclear power units are planned up to the year 2030. The new four units will certainly be from the generation 3+ PWR reactor type, as the ones that are being designed and licensed around the world. Seven nuclear power plants is a significant number for a nuclear program of any country, but it still represents a very modest participation in the electricity production matrix (3.3%) in the case of Brazil.

Brazil has the sixth known reserve of uranium ore in the world. This reserve may increase considerably by detailed soil prospecting along the country. There are two mines being exploited nowadays, and produces enough uranium quantities for all the Brazilian nuclear program needs. Brazil dominates the fuel cycle technologic steps, being one of the few countries that have the autonomous technology for uranium enrichment. INB (Industrias Nucleares do Brasil) is the company in charge of producing the fuel assemblies for the Brazilian nuclear power plants. Nowadays INB imports some of the fuel manufacturing steps (UF_6 conversion and enrichment steps), but the NP proposes that all nuclear fuel manufacturing steps for the 2030 energy plan shall be made by INB.

The two industrial activities shown before, nuclear power plants construction/operation and nuclear fuel manufacture, lead to the necessity of technological development in the area of reactor and fuel engineering. In this autonomous development there is the technical need of fuel and material testing under irradiation and post irradiation analysis as well.

IPEN produces the majority of the radiopharmaceuticals used in Brazil. The radiopharmaceuticals produced in IPEN are distributed to more than 300 hospital and clinics attending more than 3 million patients per year. The base radioisotopes used are imported or produced at IEA-R1 research reactor. The ^{99m}Tc generator kits have activities varying from 250 mCi to 2,000 mCi and are produced from the fission of ^{99}Mo isotope imported from Canada, due to the low flux of the IEA-R1 reactor for the desired activity. The ^{99m}Tc generator kits production is continuously increasing, with the current production of about 20.000 Ci of ^{99m}Tc per year. Historically the ^{99m}Tc generator kits application is increasing 10% per year in Brazil and there is the perspective of continuing this figure in the near future. Different from ^{99}Mo, the ^{131}I radioisotope is partially imported from Canada and partially produced at IPEN. The one from Canada is produced from fission and the one from IPEN is produced by activation. An amount of 2,000 Ci of ^{131}I is distributed by IPEN per year. The potential increase to the ^{131}I radiopharmaceutical utilization is higher than the ^{99m}Tc kits.

A huge cause for concern is the future prospects of radioisotope availability for medical use. The main radioisotope commercial producers in the world have their reactor facilities getting older, and in the second semester of 2008 there were a shortage of these products on the market. There is an increase in prices and future prospects depend on the construction of new reactors. In the case of IPEN, increase in the radioisotope production depends on the power scale up of the IEA-R1 research reactor. However, due to limitations on the reactor design and the site licensing, the reactor cannot increase its power beyond 5 MW or IPEN cannot construct any hot cell for ^{99}Mo processing from fission. These limitations lead to the need of a cost-benefit study concerning the construction of a new reactor [10-15].

As pointed out before, either the industrial application of power reactor and nuclear fuel technology or the radioisotope production for radiopharmaceuticals application requires, for an autonomous development, a new research reactor. Besides this, the actual utilization of neutron beams in Brazil, for fundamental and technological research, also requires a higher powered research reactor with appropriate installations as neutron guides using cold and hot neutron sources.
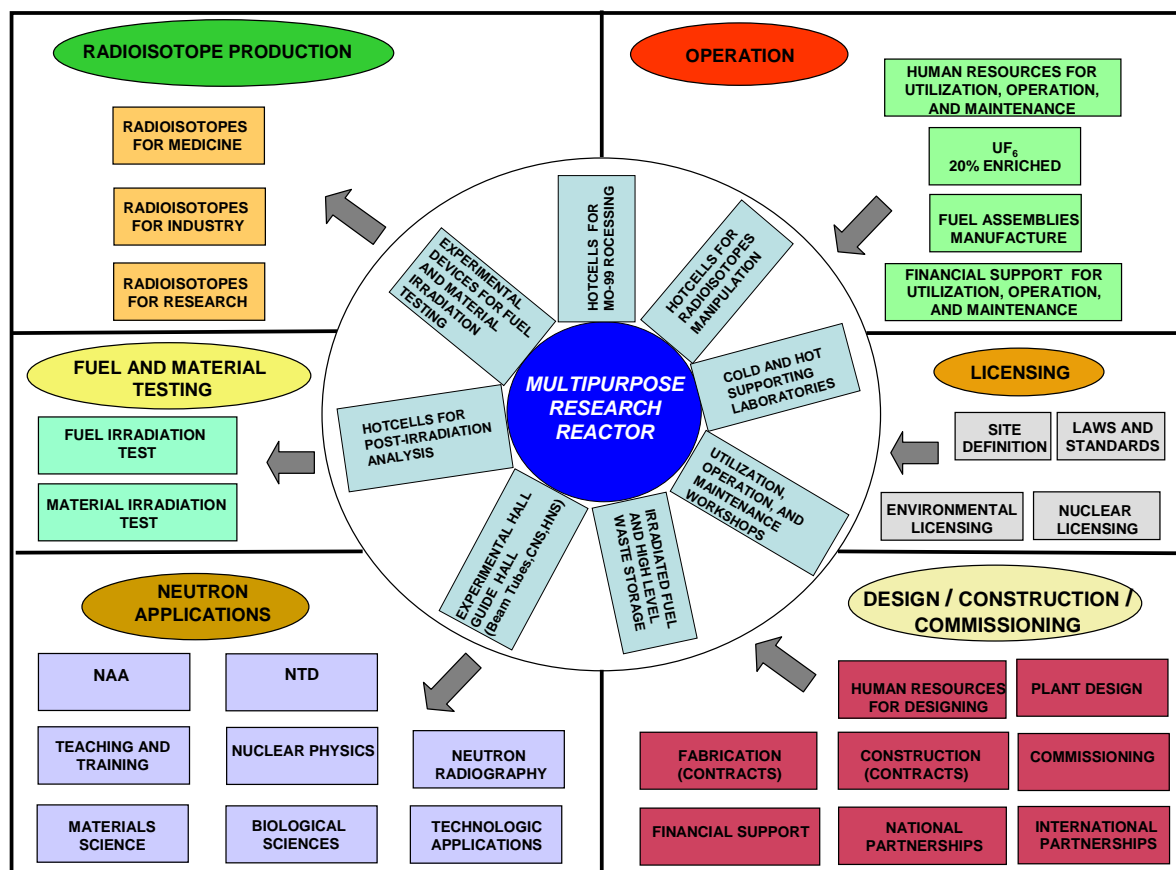
FIG.5. Multipurpose research reactor scope.

Based on these facts, the CNEN (Brazilian Nuclear Energy Commission) started to analyze the costs and benefits of developing and constructing a new research reactor in Brazil. The study has to take into account all the aspects involved in the design and construction of a research reactor as well as the supporting installations needed for its application and operation. The figure below summarizes the points that have to be addressed in the scope of the reactor. One important point in the case of the Brazilian project decision is the aspect of multipurpose utilization. The neutron flux of the reactor has to be compatible with the needs described above. The studies will finish in 2009 for submission to the NP advisory group [17-20].

ACKNOWLEDGMENTS

REFERENCES

[1]   SILVANI, M.I., LOPES, R. T., ALMEIDA, G. L., GONÇALVES, M. J. FURIERI, R. C. A. A., On The Impact Of Neutron Beam Divergence And Scattering On The Quality Of Transmission Acquired Tomographic Images, Nuclear Instruments and Methods in Physics Research, B 263 (2007) 253.

[2]   ALMEIDA, G.L., SILVANI, M.I., FURIERI, R.A.A., GONÇALVES, M.J., LOPES, R.T., Forecasting the Effect of Neutron Beam Divergence on the Quality of

Tomographic Images, Nuclear Instruments and Methods in Physics Research, A 579 (2007) 231.

[3] SILVANI, M.I., et al., Conversion of a X-ray Position Sensitive Detector for Use in a Thermal Neutron Tomographic System, Nuclear Instruments and Methods in Physics Research, B 213(2004) 294.

[4] SILVANI, M.I., LOPES, R.T., JESUS, E.F.O., ALMEIDA, G.L., BARBOSA, A.F., Evaluation of a Computer Aided Neutron Tomographic System Incorporating a Gaseous Position Sensitive Detector, Nuclear Instruments and Methods in Physics Research, A 505 (2003) 568.

[5] STASIULEVICIUS, R. Irradiação de diamantes com capas no reator TRIGA-IPR-R1. Belo Horizonte, CDTN-2001. (CDTN-881)

[6] PAIANO SOBRINHO, S., The experience of CDTN/CNEN, Centro de Desenvolvimento da Tecnologia Nuclear: a medium size nuclear research centre in Brazil, Nuclear Research Centres in the 21st Century, Final report IAEA Vienna (2001) 39.

[7] MESQUITA, A.Z., REZENDE, H. C., Thermal behaviour of the IPR-R1 TRIGA nuclear reactor, International Journal of Nuclear Energy Science and Technology - IJNEST, 3 (2007) 160.

[8] MESQUITA, A.Z., REZENDE, H.C., TAMBOURGI, E.B., Power Calibration of the TRIGA Mark I Nuclear Research Reactor, Journal of the Brazilian Society of Mechanical Sciences and Engineering, v. XXIX, No.3 (2007) 240.

[9] ZANGIROLAMI, D.M. , VIDAL FERREIRA A. , DE OLIVEIRA A.H., Specific Induced Activity Profile at the Rotary Specimen Rack of IPR-R1 TRIGA Reactor , Brazilian journal of physics ISSN 0103-9733 , 39 (2009), 260.

[10] LEAL, A.S., SEBASTIÃO, R.C.O., RODRIGUES, R.R., MENEZES, M.A.B.C., New Perspectives for the TRIGA IPR-R1 Research Reactor, International Conference on Research Reactors Safe Management and Effective Utilization, Sydney, Australia (2007).

[11] LEAL, A.S., MENEZES, M.A.B.C., VERMAERCKE, P., SNEYERS, L., JENSEN, C.E.M., Investigation of chemical impurities in formulations, phytotherapics and polyvitaminic medicines by k0-instrumental neutron activation analysis, Nuclear Instrumetns and Methods A, 564 (2006) 729.

[12] ULYSSES D.B., FERNANDO, P.G.M., ROGÉRIO, J., Measurements of the Neutron Spectrum Energy in the IPEN/MB-01 Reactor Core, Brazilian Journal of Physics, 39, No.1 (2009) 39.

[13] ULYSSES, D'U.B., ADIMIR, D.S., Experimental Determination of the Spectral Indices $^{28}\rho$ and $^{25}\delta$ of the IPEN/MB-01 Reactor, Journal of Nuclear Science and Technology, 2 (2002) 932 .

[14] SANTOS, A., et al., The experimental determination of the relative abundantes and decay constants of delayed neutrons of the IPEN/MB-01 reactor, The Physics of Fuel Cycle and Advanced Nuclear Systems: Global Developments, Chicago, Ill., USA, Proceedings ANS (2004) (PHYSOR2004).

[15] RAJENDRA, N.S., The IEA-R1 Research reactor: 50 years of Operating Experience and Utilization for Research, Teaching and Radioisotopes Production, International Conference on Research Reactors Safe Management and Effective Utilization, Sydney, Australia (2007).

[16] ARMELIN, M.J.A., PIASENTIN, R.M., PRIMAVESI, O., Neutron Activation Analysis applied to determine zinc in forages used in intensive dairy cattle production systems, Journal of Radioanalytical and Nuclear Chemistry 252 No.3, (2002) 585.

[17] CAMPOS, L.C., PARENTE, C.B.R., MAZZOCCHI, V.L., HELENE, O., Determination of the beta quartz cell parameters using NMD azimuthal angular differences, Congress and General Assembly of the International Union of Crystallography, 19th, Geneva, Switzerland, Proceedings 2 (2002) 356.

[18] PARENTE, C.B.R., MAZZOCCHI, V.L, MASCARENHAS, Y.P., The new IPEN-CNEN/SP neutron powder diffraction, International Conference on research reactor Utilization, safety, decommissioning, fuel and waste management, Santiago, Chile, (2003).

[19] MENEZES,M.,O., PUGLIESI, R., ANDRADE, M.L.G., PEREIRA, M.S., Real-time neutron radiography at IPEN-CNEN/SP, Brazilian Journal of Physics, 33 No.2 (2003) 282.

[20] VASCONCELLOS, M.B.A., et al., Multielemental hair composition of Brazilian Indian populational groups by instrumental neutron activation analysis, Journal Radioanalytical Nuclear Chemistry, Budapest, 249 No.2 (2001) 491.

<div align="center">

Chapter 5

</div>

LVR-15 REACTOR APPLICATION FOR MATERIAL TESTING

M. MAREK, J. KYSELA, J. BURIAN
Nuclear Research Institute Řež plc
250 68 Czech Republic
Email: mam@nri.cz

Abstract: The LVR-15 research reactor was commenced in 1957 as a multipurpose source of neutrons for basic research at horizontal channels and user-oriented research at mostly vertical loop channels and rigs. The advantage of the reactor layout comes from flexible diameter of irradiation channels, good access to the upper part of the channels, and the fact that the core can be refueled without let-up of operation of the irradiation facility. The main fields of the reactor utilization are neutron beam research including BNCT, fuel and material irradiation tests, and radioisotope and silicon production. The reactor has joined the Russian Research Reactor Fuel Return (RRRFR) initiative to convert from HEU to LEU. At present the transportation of the spent fuel to Russia is being prepared. This paper covers the present status and future plans of LVR-15 utilization.

5.1. Introduction

The LVR-15 research reactor commenced operation in 1957 as a multipurpose source of neutrons for basic research at horizontal channels and user-oriented research at mostly vertical loop channels and rigs.

Since 1957 the reactor has undergone two reconstructions. During the last one in 1989 all the reactor components and systems were replaced, including the reactor vessel. The LVR-15 is a tank type reactor (Fig. 1) and currently uses IRT-2M fuel of 36 wt.% ^{235}U enrichment manufactured by the NZCHK Company in Novosibirsk, Russia. The fuel features limit the output reactor power to 10 MW. The thermal and fast neutron flux reach up to 1.5×10^{18} n/m^{2}s and 2.5×10^{18} n/m^{2}s, respectively. Due to the nature of the reactor use, the reactor working cycle is 21 days and the number of the cycles is 8-10 per year.

5.2. Reactor use for material research

The advantage of the reactor arrangement results from the flexible diameter of irradiation channels, good access to the upper parts of the channels, and the fact that the core can be refueled without outage of the irradiation facility. The main fields of the reactor utilization are neutron beam research including BNCT, fuel and material irradiation tests, and radioisotopes and silicon production. LVR-15 special reactor features in the field of material research can be summarized:

– Core and irradiation channel size flexibility.
– Irradiation rigs for irradiation of small (ring, tensile) to large (1CT, 2CT) specimens.
– Five big loops with specialized mechanically loaded or heated irradiation channels.
– Water chemistry and dosimetry control ensuring the conditions in testing facilities to be as close as to the conditions in power plants.

FIG.1. LVR-15 research reactor.
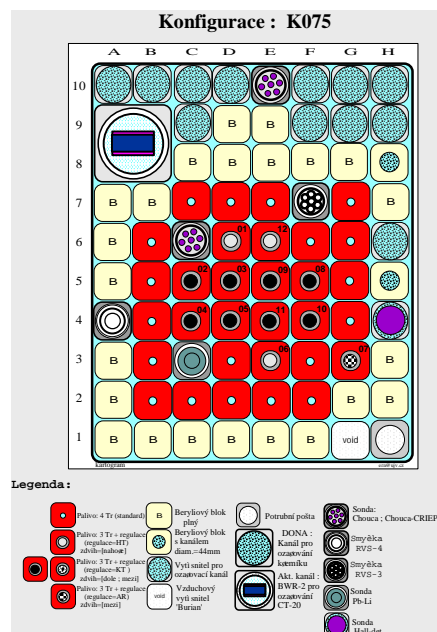
FIG.2. An example of LVR-15 core (axial cross section).

5.3. Material research

The advantage of the reactor arrangement results from the flexible diameter of irradiation channels, good access to the upper parts of the channels, and the fact that the core can be refueled without outage of the irradiation facility. The main fields of the reactor utilization are neutron beam research including BNCT, fuel and material irradiation tests, and radioisotopes and silicon production. LVR-15 special reactor features in the field of material research can be summarized:

- Core and irradiation channel size flexibility;
- Irradiation rigs for irradiation of small (ring, tensile) to large (1CT, 2CT) specimens;
- Five big loops with specialized mechanically loaded or heated irradiation channels;
- Water chemistry and dosimetry control ensuring the conditions in testing facilities to be as close as to the conditions in power plants.

Other, more limited uses are in the areas of medicinal and industrial radioisotope manufacturing, production of radiation doped silicon and development of boron neutron capture therapy.

The reactor is equipped with hot cells for a post-irradiation sample manipulation, disassembling and assembling core channels.

Location of loops and rigs in LVR-15 reactor
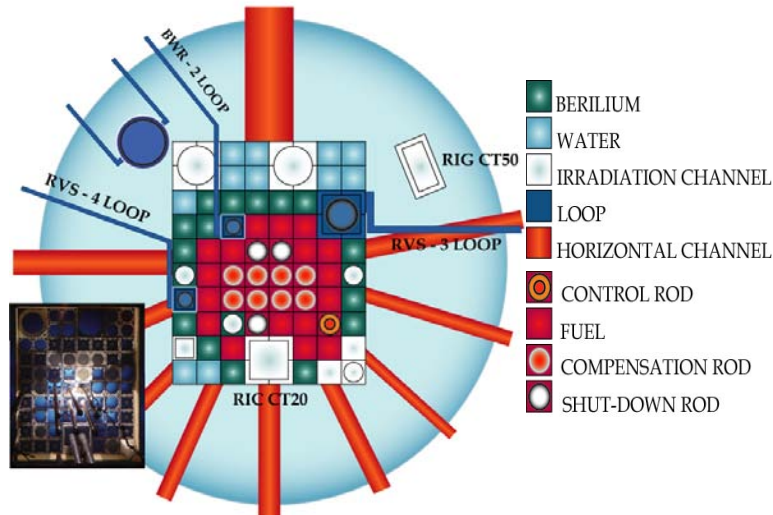
FIG.3. Location of loops and rigs in LVR-15 reactor.

Due to its output and achievable neutron fluxes the LVR-15 reactor specializes, in the study of combined effects of radiation and ambient media on materials. The reactor is equipped with experimental facilities such as loops and rigs, which permit an exposure under conditions corresponding to those in power reactors. The generally utilized procedure is that the material is pre-irradiated in rigs and then is further exposed in loops also enabling the simulation of the thermal flux or physical stresses.

FIG.4. Instrumentation of a side loop irradiation channel with CT samples.

The irradiation rigs permit the exposure starting from small samples (ring, tensile) up to very large samples (1CT, 2CT). Total five loops simulating either PWR or BWR conditions in various irradiation channels and other specialized facilities are in the operation at the reactor:

Reactor rigs:

- Chouca for Charpy V, tensile, 0.5 CT specimens, and
- flat rig for 1-2 CT specimens.

Reactor loops:
- BWR –1 for structural material testing.
- BWR-2 for reactor pressure vessel (RPV) and internals steels testing, Fig.5.
- Zinc loop for radioactive material transport and water chemistry testing.
- RVS-4 for testing of fuel cladding corrosion.
- Irradiation channels - in-pile channel for RPV steel, in-pile channel for austenitic steel, and in-pile channel for slow strain rate tests (SSRT), Fig.5.
- Pb-Li loop and primary first wall (PFW) materials of the fusion program.

Important experimental projects were/are aimed at:
- Material degradation studies (RPV and core internals for VGB, in-pile and out-of-pile studies for EPRI, irradiation of RPV steels for JAPEIC, studies of pre-irradiated austenitic specimens for Czech Electric Company).
- Study of Zr alloys cladding corrosion in PWR and VVER conditions, with electrically heated fuel rod imitators.
- Water chemistry influence on radioactivity transport and build-up in primary circuit, ammonia, hydrogen, zinc addition chemistry effects, high pH and hydrazine chemistry.
- Fusion reactors materials and technology (PFW and Test Blanket Module for ITER).
- Irradiation test certificates for RPV materials of VVER-440, VVER-1000 reactors.
- European projects - MTR-I3, RAPHAEL, EFDA, HPWLWR, ITSR, ELSY, FRAME, CASTOC, PISA, PERFECT, REDOS.

Experience based on long-term research in material, water chemistry and radiolysis tests for PWR, VVER and BWR is used in research supporting development of the new generation of reactors (GEN-IV). The following facilities has been designed at the reactor:

- Super Critical Water Reactor (SCWR) Loop for Water Chemistry and Radiolysis Study with parameters 600^oC, 30 MPa in the active core and 350-400 ^oC in the main pipelines with flow rate of 1000 kg/h for the study of in-core radiolysis for in-flux behavior of materials;
- High Temperature Reactor loop cooled with helium (Fig.6), the loop comprises of a irradiation part, an electric heating part, a regenerative heating exchanger, a cooler and a compressor. The irradiated part will have an outer diameter of 57 mm and core height of 580 mm. The irradiation temperature range is supposed at 500-1000^oC, with a flow rate of 20g/s and He pressure of 7 MPa;
- Fusion Reactor Structural Material – research and development and irradiation services for primary first wall and European test blanket module concepts (HCLL, HCPB).
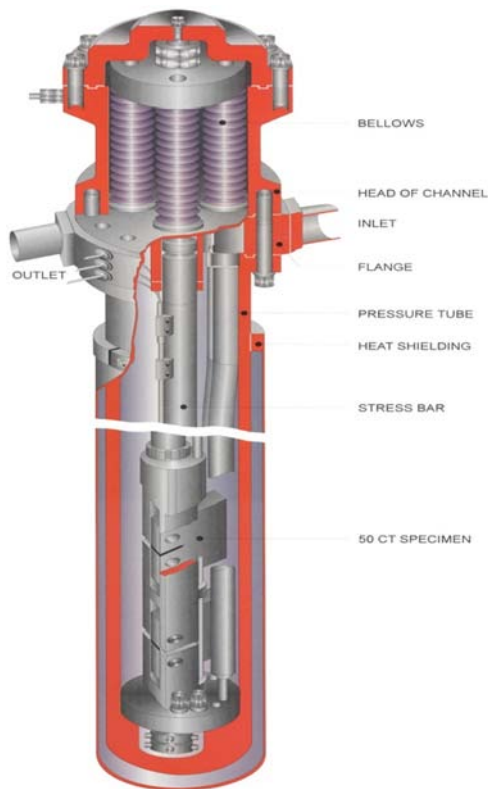
FIG.5. Active channel of the BWR-2 loop.
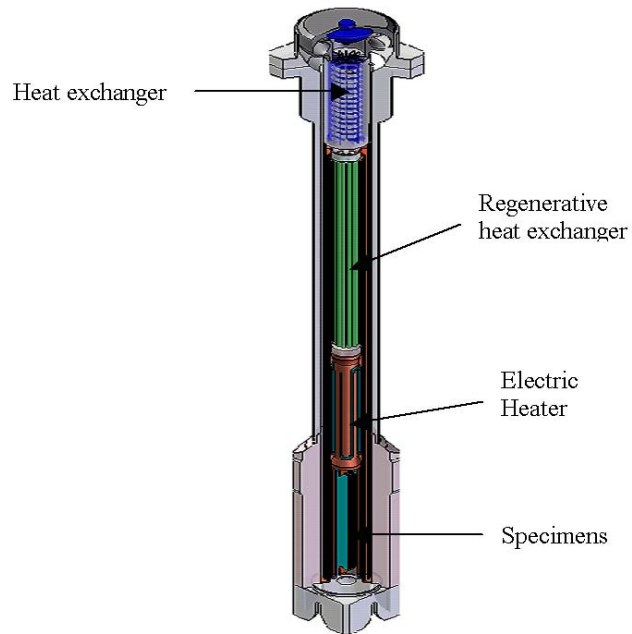
FIG.6. Design of a helium loop.

5.4. Post-radiation evaluation

At NRI Rez, there are several hot cells laboratories, which are used in the area of materials research. Hot cells on the reactor serve for the extraction of samples from rigs and loops, and their preparation before transport to hot cells outside the reactor building, where post-radiation work is carried out. In these hot cells the following procedures, among others, can be performed: static tensile tests, impact instrumented Charpy V-notch type tests on standard and sub size specimens, static fracture toughness tests on standard and sub size specimens, crack growth rate in air, vacuum and BWR/PWR environments, stress corrosion tests in BWR/PWR environments, slow rate stress corrosion tests.

5.5. HEU to LEU conversion

The LVR-15 reactor is operated with the IRT-2M 36% fuel and has sufficient fuel reserve until 2010. Nevertheless, first studies about the HEU to LEU conversion had started as was already reported. The prospective type of fuel assembly design that could be potentially used is IRT-4M with UO_2-Al fuel, which is compatible with the current LVR-15 core lattice and control rods system. This oxide fuel design is commercially available. However, the new FA type will require a more challenging licensing of mixed cores during gradual conversion for the LVR-15 reactor environment as ^{235}U content and the geometry of FAare substantially different. Basic advantage of the IRT-4M design is that the FA could be used at 15 MW. They have been tested in Uzbekistan and are used at the Vrabec VR-1 reactor at Prague Technical University. So far, performed analyses have been oriented to how the summary rods worth is bound to the total reactivity excess, fuel depletion, and neutron spectrum change assessment.
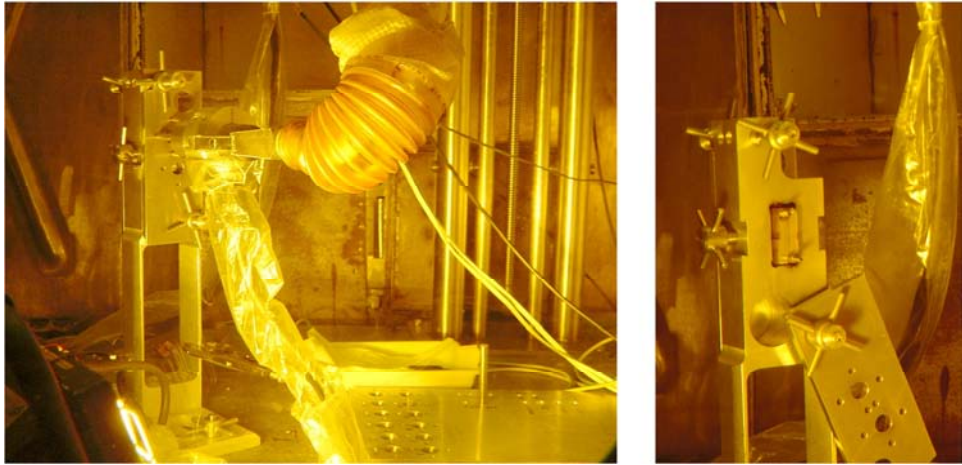
FIG.7. Equipment for samples welding in hot cells.

The value of ratio of the total rods worth and the total reactivity excess is a key parameter deciding if the given core pattern can be utilized. Based on the performed calculations and operational experience this criterion could be fulfilled only up to [235]U content of about 300 – 325 g in IRT-4M (8 tubes) fuel assembly. The exploitation of the proposed LEU fuel could reduce the annual consumption of FAs more than 30% comparing with the IRT-2M (36%) currently used.
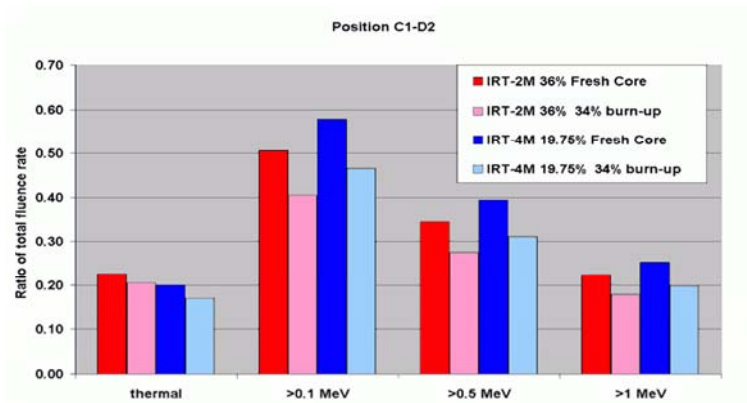
FIG.8. Ratio of total fluence rate by neutron energy averaged over the stainless steel samples irradiated in the large flat rig at the core periphery.
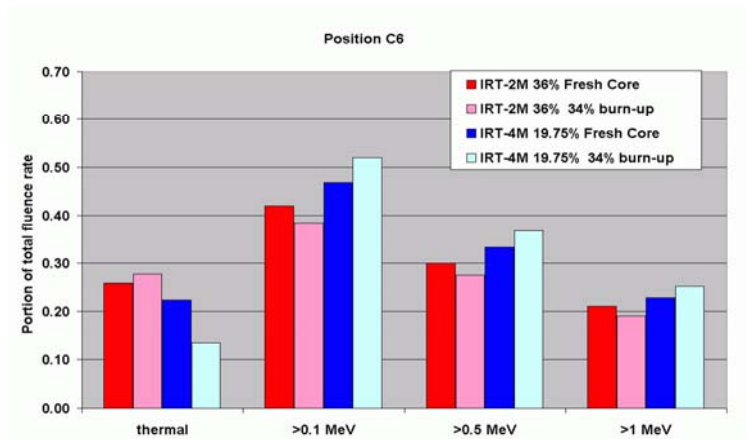
FIG.9. Ratio of total fluence rate by neutron energy averaged over the stainless steel samples irradiated in the core.

Results of calculations for in-core positions and close to the core periphery confirmed the known fact that neutron spectrum shifts towards higher energies when enrichment decreases, Fig. 8-9. The increase of the fast neutron fluxes varies from 32% to 35% for the half burnt fuel while the thermal neutron flux decreases up to –52% under the same conditions. The increase of the fast neutron fluxes is a beneficial consequence of the conversion regarding the prevalence of the commercially important irradiations based on material studies that are realized at the reactor. Next step should provide a complex conversion study of the transition from MEU to LEU core via mixed cores. Work will cover the assessment of neutronic and thermo-hydraulic aspects of the LVR-15 reactor. Decision what type of fuel is the most appropriate for the LVR-15 will be based on a detailed analysis of physical and economical aspects of the conversion.

5.6. Fuel cycle

The reactor has joined the Russian Research Reactor Fuel Return (RRRFR) initiative to be converted from HEU to LEU. Together 32 FAs are in the reactore core and the present fresh fuel stock consists of 73 fuel assemblies that are sufficient for the reactor operation untill the end of 2010 year. The spent fuel FAs are stored either at the reactor site in the reactor pools (28 FAs) or in the NRI HLWSF interim storage.
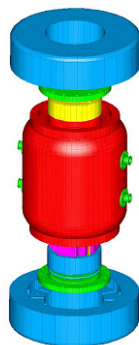
FIG.10. VPVR/M cask for storage and transport of SF from Russian origin research reactors.
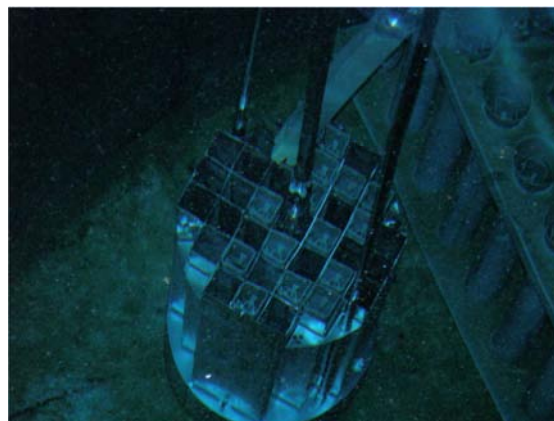
FIG.11. Loading the SNF from the HLWSF pool.

FIG.12. VPVR/M cask being moved into the storage area.

FIG.13. Interior of the ISO container with one VPVR/M cask.

Spent fuel was shipped to Russia in autumn 2007 in the VPVR casks (Fig.10-13) that were designed for all the Russian fuel types used in the LVR-15 similar research reactors of Russian origin around the world. The cask is licensed in the Czech Republic and Russia. Technical acceptability of the VPVR/M cask, handling and loading spent fuel at the research reactor facilities, as well as receipt and unloading at the Mayak facilities in Russia were demonstrated. Three demonstrations were organized at the SKODA manufacturer, at LVR-15 research reactor at NRI Rez, and in Mayak facilities in Russia.

At present the shipment of the spent fuel to Russia is being finalized. All the FAs have been loaded into 16 VPVR/M casks. At first, three casks were loaded at the LVR-15 reactor site with 91 IRT-2M (36%) FAs and 10 IRT-2M (80%) FAs in March and May 2007 and then transported to the HLWSF facility at NRI.

Between May-August 2007 six casks were loaded with 206 EK-10 FAs from the HLWSF hot cell by manual and robotic manipulators. Seven additional casks were loaded with 242 IRT-2M (80 %) (235 FAs from the HLWSF pool and 7 repacked FAs from hot cell). All the 16 casks were loaded into ISO containers. In autumn 2007 the containers were transported to a railroad station on trucks and then on railroad carriages to the Russian Federation.

5.7. Conclusions

The LVR-15 reactor is an important facility which supports and contributes to research of nuclear materials and water chemistry. Experience achieved operating the reactor during the last 50 years can be now transferred to the new irradiation facility designs including those which performs the research for Generation IV reactors, for example such as reactors cooled by high-temperature helium or water with supercritical parameters.

ACKNOWLEDGEMENTS

BIBLIOGRAPHY

[1] KYSELA, J., ZMÍTKO, M., VŠOLÁK, R., Loop capabilities at Řež for water chemistry and corrosion control of cladding and in-core components, Technical Committee Meeting on Water Chemistry and Corrosion Control of Cladding and Primary Circuit Components; Czech Republic (1998).
[2] KYSELA, J., et al., Overview of loop's facilities for in-core materials and water chemistry testing; JAIF International Conference on Water Chemistry in Nuclear Power Plants, Kashiwazaki, Japan (1998).
[3] KYSELA, J., ERNEST, J., MAREK, M., LVR-15 Reactor performance and transformation to low enriched fuel, International Meeting on Reduced Enrichment for Research and Test Reactors (RERTR), IAEA Vienna (2004).
[4] MAREK, M., NOVOSAD, P., KOTNOUR, P., PICEK, M., SKODA VPVR/M, Cask for Spent Nuclear Fuel from Research Reactors, TM on Specific Application of Research Reactor, IAEA, Vienna (2006).
[5] MAREK, M., KYSELA, J., ERNEST, J., FLIBOR, S., BROZ, V. Impact of the HEU/LEU Conversion on Experimental Facilities, The RERTR-2007: International Meeting on Reduced Enrichment for Research and Test Reactors, Praha (2007).
[6] SVITAK, F., et al., Present Experience of NRI Rez with Preparation of Spent Nuclear Fuel Shipment to Russian Federation, The RERTR-2007: International Meeting on Reduced Enrichment for Research and Test Reactors, Praha (2007).

Chapter 6

MATERIAL IRRADIATION AT HANARO, KOREA

K.N. CHOO, M.S. CHO, B.G. KIM, Y.H. KANG, Y.K. KIM
Korea Atomic Energy Research Institute
150 Deokjin-Dong, Yuseong-Gu, Daejeon 305-353, Korea
Email: Knchoo@Kaeri.Re.Kr

Abstract: The High-flux Advanced Neutron Application Reactor (HANARO: High flux Advanced Neutron Application Reactor) is an open-pool type multi-purposed research reactor located at KAERI, in Korea. It was designed to provide a peak thermal and fast flux of 5×10^{14} n/cm^2.s and 2.1×10^{14} n/cm^2.s (E >1.0MeV) respectively at a 30 MW maximum thermal power. A capsule system has been developed for irradiation tests of nuclear materials and fuels in the core region of the HANARO reactor. Extensive efforts have been made to establish the design and manufacturing technology for a capsule and temperature control system, which should be compatible with HANARO's characteristics. A material capsule system consisting of main capsule, fixing, control, cutting, and transport system were developed for an irradiation test of non-fissile materials. This capsule system has been actively utilized for the various material irradiation tests requested by users from research institutes, universities and the industries. More than 7000 specimens have been irradiated at dedicated vertical hole of HANARO by using the developed capsule system since 1995.
Based on the accumulated experience and the user's sophisticated requirements, new instrumented capsule technologies for a more precise control of the irradiation condition are being developed at HANARO. A strategic irradiation program at HANARO will place more emphasis on a special-purpose capsule system by focusing on the specific material or fuels for a next generation power reactor.

6.1. Material Irradiation at HANARO

In April 1995, the Korea Atomic Energy Research Institute (KAERI) completed the construction of high performance multipurpose research reactor named HANARO which means, in Korean, "uniqueness". The core features a combination of light-water cooled/moderated inner core and light-water cooled/heavy-water moderated outer core. The inner core has 28 fuel sites and 3 test sites. 3 test sites are hexagonal shapes and used for capsules, FTL (Fuel Test Loop), and RI (Radioisotope) production. The outer core consists of 4 fuel sites and 4 test sites, which are embedded in the reflector tank. There are several vertical test holes such as CT, IR1, IR2 (hexagonal type) and OR (cylindrical type) in the core of HANARO, and LH (Large Hole), HTS (Hydraulic Transfer System), NTD (Neutron Transmutation Doping) and IP (Irradiation Position) in the reflector region of the reactor for nuclear fuels/materials irradiation testing, RI production and Si-doping, as shown in Fig. 1. Table 1 shows the characteristics of the reactor test holes for a fuel/material irradiation at HANARO. The neutron flux of IP holes varies markedly depending upon the location in the reactor core. The 7 horizontal beam ports such as ST1, ST2, ST3, ST4, NR, CN and IR in the reflector region of the reactor are being actively applied for a scattering and diffraction of neutron, neutron radiography, and ex-core neutron irradiation facilities: BNCT (Boron Neutron Capture Therapy) and Dynamic NR.
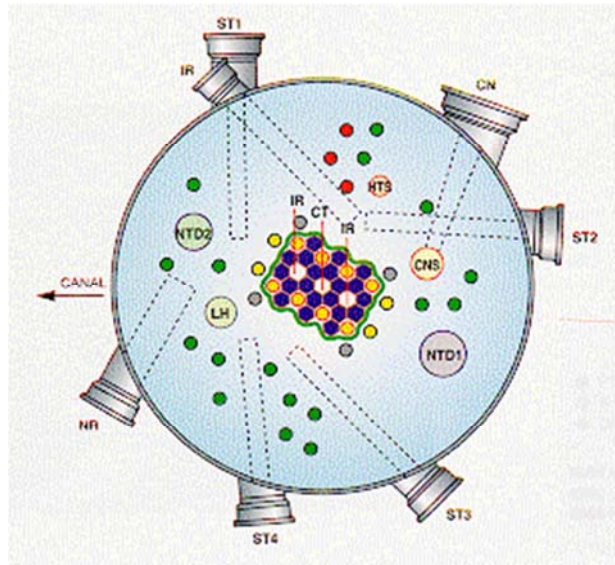
FIG.1. Core configuration of HANARO.

TABLE 1. CHARACTERISTICS OF TEST HOLES FOR MATERIAL IRRADIATION IN HANARO

Location	Hole		Inside ø(cm)	Neutron Flux (n/cm^2.s)		Remarks
	Name	N^o		Fast neutron (E>0.82 MeV)	Thermal neutron (E<0.625 eV)	
Core	CT	1	7.44	1.95×10^{14}	4.30×10^{14}	Fuel/material test
	IR	2	7.44	1.80×10^{14}	3.83×10^{14}	
	OR	4	6.00	2.01×10^{13}	3.30×10^{14}	Radioisotope production
Reflector	LH	1	15.0	7.35×10^{11}	9.72×10^{13}	Fuel/material and
	HTS	1	10.0	1.72×10^{11}	8.82×10^{13}	others test
	IP	17	6.0	1.43×10^9-2.17×10^{12}	2.16×10^{13}-1.81×10^{14}	Radioisotope production

6.2. Irradiation facilities

Various neutron irradiation facilities such as the rabbit (small non-instrumented capsule) irradiation facilities loop and capsule irradiation facilities for irradiation tests of nuclear materials, fuels, and radioisotope products have been developed at HANARO [1]. Among the irradiation facilities in HANARO, the capsule and rabbit systems have been used for the irradiation of nuclear materials and the FTL will be installed in IR1 by the end of 2008.

The rabbit was originally designed for an isotope production, but it can be used for the irradiation test of a fuel and a material. Fig. 2 shows the typical rabbit (20 mm in diameter and

30 mm in length for specimen) inserted into the HTS hole. It is very useful for numerous irradiation tests of small specimens at low temperature (below 200°C) and neutron flux condition.

The instrumented and non-instrumented capsules have been developed at HANARO for new alloy and fuel developments and the life time estimation of nuclear power plants. For the development of an instrumented capsule system, the capsule related systems such as a supporting, connecting, and controlling system were also developed as shown in Fig. 3. After a locking of the capsule in a test hole, the instrumented capsule is fixed by a chimney bracket and robotic arm supporting systems. Two sets of cantilever type robotic arm systems for the CT and IR2 test holes were installed at the location of the platform level of the reactor that is 5.5 m in height from the bottom of the capsule, but the in-chimney bracket is temporarily installed on the top of the reactor chimney for a capsule irradiation test. At the Junction Box system, heaters and thermocouples can be easily connected and separated to/from the capsule controlling system before/after an irradiation test. The capsule temperature control system consists of three subsystems: a vacuum control system, a multi-stage heater control system, and a man-machine interface system. After an irradiation test, the main body of the instrumented capsule is cut off at the bottom of the protection tube with the cutting system and it is transported to the IMEF (Irradiated Materials Examination Facility) by using a HANARO fuel cask.

The FTL is a facility which can conduct fuel and material irradiation tests at HANARO. It is composed of an In-Pile Test (IPT) section and an Out-Pile Test (OPT) system. The IPS in IR1 irradiation holes can accommodate up to 3 pins of PWR or CANDU type fuels and have instruments such as a thermocouple, LVDT and SPND to measure a fuel's performance during a test. The environment around the IPS is subjected to a high neutron flux (thermal flux : 1.2×10^{14} n/cm^{2}s, fast flux : 1.6×10^{14} n/cm^{2}s). The FTL simulates a commercial NPP's operating conditions such as its pressure, temperature, flow and neutron flux to conduct the irradiation tests. The application fields of the FTL are the nuclear fuel and material irradiation tests at the operating conditions of a commercial power plant, fuel burn-up and mechanical integrity verification tests, irradiation data generation for a performance analysis model (PWR fuel, CANDU fuel and metallic fuel), technical improvement of a design and fabrication process for an advanced fuel development, fuel rod irradiation test for a performance verification, etc. The typical design pressure and temperature of the in-pile section of the FTL is 17.5 MPa and 350°C, respectively. An irradiation test using the FTL will be possible from the beginning of 2009.

The HANARO has two irradiation holes for a Neutron Transmutation Doping to manufacture high quality semiconductors. High quality semiconductors are needed for an effective use of high power electricity such as for the KTX (Korea Train Express) or an electric train. A semiconductor doped with neutrons has the best quality among them for power devices. The demand for NTD-silicon is increasing rapidly accompanied with the increase of wind, solar and fuel cell energy systems, hybrid cars and hydrogen fuel cell engines, and devices to reduce an electricity loss. A commercial NTD service for 5 inch silicon ingots was started at NTD2 with the world best quality product. Additional 6 inch irradiation at this hole started in 2005. A new irradiation facility for 6 and 8 inch silicon ingots using the NTD1 hole is under testing. It will meet the demand for 8 inch wafers for hybrid cars in the near future.

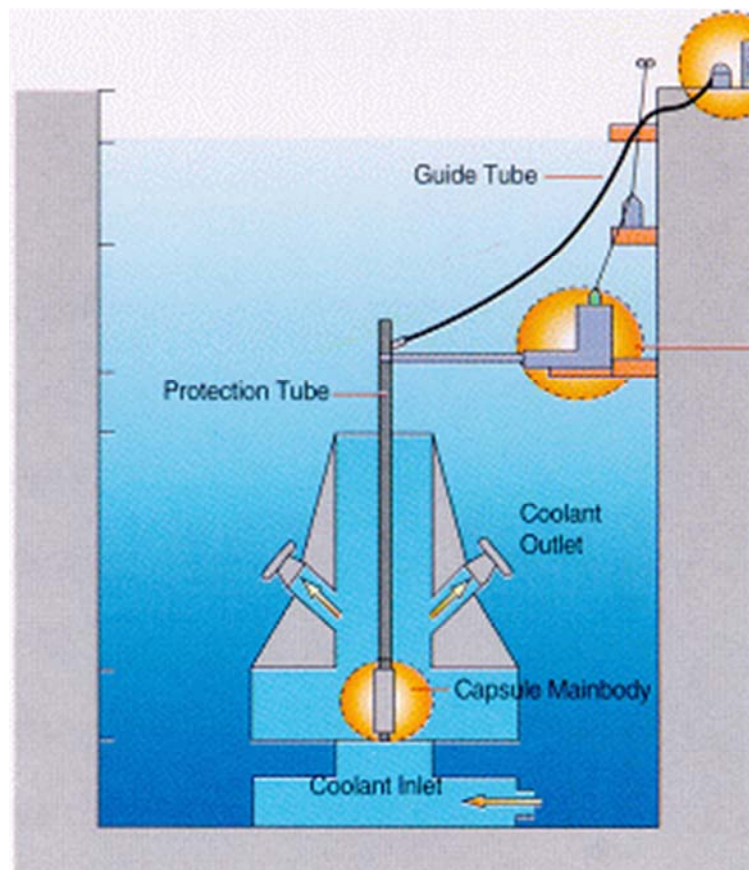*FIG.2. Irradiation rabbit, non-instrumented capsule and an instrumented capsule.*

FIG.3. Schematic view of the HANARO instrumented capsule system.

6.3. Capsule irradiation in HANARO

HANARO irradiation capsule

Among the irradiation facilities, a capsule is the most useful device to cope with the various test requirements. Instrumented and non-instrumented capsules have been developed at HANARO for a new alloy and fuel development and the life time estimation of nuclear power plants. Extensive efforts have been made to establish design and manufacturing technology for a capsule and temperature control system, which should be compatible with HANARO's characteristics [2, 3]. Up to now, material and fuel capsules have been developed and are being utilized for the irradiation test of materials and nuclear fuel at HANARO, and the creep and fatigue capsules are being developed to study the creep and fatigue behaviours of materials under irradiation.

The material capsule is one of the irradiation devices which can evaluate the irradiation performance of nuclear and high-technology materials at HANARO. The capsule has an important role for the integrity evaluation of reactor core materials and the development of new materials through precise irradiation tests of specimens such as a RPV, reactor core structural materials, parts of a fuel assembly and high technology materials.

The fuel capsule is applicable to research into the irradiation characteristics of a fuel pellet and to obtain the in-core performance and the design data of a nuclear fuel at HANARO. The fuel capsule has also been utilized for the irradiation characteristics test of a DUPIC (Direct Use of Spent PWR Fuel in CANDU Reactors) fuel and advanced PWR fuel pellets. The instrumented fuel capsule can be used to measure a fuel's temperature, internal pressure of a fuel rod, a fuel's deformation and a neutron flux during a fuel irradiation test.

The creep and fatigue capsules were developed to obtain the creep and fatigue characteristics of a nuclear material during an irradiation test. The loading stress needed for a test is applied on a specimen by a bellows system controlled by an external He gas pressure.

Design and analysis of material capsule

A typical HANARO irradiation material capsule consists of three main parts which are connected to each other: protection tube (5 m), guide tube (9.5 m) and a capsule's main body as shown in Fig. 3 main body including the specimens and instruments is a cylindrical shape tube of 60 mm in diameter and 1.170 mm in length. The main body has 5 stages with independent micro-electric heaters and contains 12 thermocouples and 5 sets of Fe-Ni-Ti neutron fluence monitors to measure the temperature of the specimens and the fast neutron fluences, respectively. Heaters and thermocouples are connected to a capsule temperature controlling system through a guide tube and connection box system. A friction welded tube using STS304 and Al1050 alloys is introduced to prevent a coolant leakage into a capsule during a capsule cutting process after an irradiation.

Based on a specimen's configuration and the basic design of a capsule, the reactivity effect, neutron flux, and gamma heating of specimens are calculated by the MCNP code [4]. To compare the neutron flux of the specimens that are calculated by using the MCNP computer program before an irradiation test, 2 kinds of F/M (Fluence Monitor) are installed in the Al thermal media near a specimen (one F/M per one stage) in a capsule. Monitoring wires such as Fe, Ni, Ti, Nb, Ag are inserted in an Al tube with an Al internal tube and spacers. Nb-Ag and Fe-Ni-Ti wires are inserted for the measurements of the thermal and fast neutron fluences of the specimens, respectively. After an irradiation, F/M is dismantled in a hot cell and the weight changes and gamma ray spectrum of the wires are measured to obtain a neutron spectrum. The obtained fast neutrons (E>1.0 MeV) by using the SANDII code are known to

be located within about a 20% error range of the theoretical values calculated by the MCNP code. The temperature of the specimens during an irradiation is initially increased by the gamma heating and then roughly adjusted to an optimum condition by a gas control system and then finally adjusted to a desired value by a micro-electric heater. After the irradiation tests, the dpa and activation of the irradiated specimens are also evaluated by using the SPECTOR [5] and ORIGEN2 codes [6], respectively.

The irradiation temperature of the specimens is preliminary analyzed by using the GENGTC [7] and ANSYS codes [8]. Because the gamma heating rate varies along the vertical position of the reactor core, a gap adjustment between the capsule parts is very important to maintain a uniform temperature of the specimens over the region. Because of the complicated configuration of a specimen, a gap adjustment between the capsule parts is performed based on the expected temperatures obtained by the GENGTC code.

Utilization of irradiation capsules

The national research and development program on nuclear reactors and nuclear fuel cycle technology in Korea requires numerous in-pile tests at HANARO. The main activities of the capsule development and utilization programs are focused on the in-reactor material tests, safety-related research and development for nuclear reactor materials and components, and basic research. 7,000 specimens from research institutes, nuclear industry companies and universities, have been irradiated at HANARO for 75,000 hours using the developed capsule and rabbit irradiation systems since 1995. 19 instrumented capsules and 2 non-instrumented capsules have been successfully irradiated in the HANARO CT, IR and OR test holes since 1995. The capsules were mainly designed for the irradiation of a RPV (Reactor Pressure Vessel), reactor core materials, and Zr-based alloys. Most capsules were made for KAERI material research projects, but some capsules were made as a part of national projects for a promotion of a HANARO utilization for universities and for the irradiation tests requested by international research projects.

Fig. 4 shows the increasing trends of the irradiation specimens and the time requested by users. Through this research, the nuclear characteristics of the HANARO capsules were also produced and stored in our database. The metallic material specimens were mainly irradiated at around 300°C up to a fast neutron fluence of 1.4×10^{21} n/cm^2 (E>1.0 MeV).

6.4. New capsule technology

Based on the accumulated experience and the user's sophisticated requirements, several advances in material capsule technologies were obtained recently for a more precise control and analysis of the neutron irradiation effect at HANARO. New instrumented capsule technologies for a more precise control of the irradiation temperature and fluence of a specimen, irrespective of the reactor operation, have been developed and out-pile tested. The OR/IP capsule technologies for an irradiation test in the HANARO OR and IP test holes with a relatively lower neutron flux than the CT and IR test holes have also been developed and in-pile tested, successfully. The development of advanced capsules including a high temperature irradiation technology up to 1000°C, re-instrumentation, and re-irradiation technology are under development. These development programs are closely connected with the national research and development program in Korea on nuclear reactors and nuclear fuel cycle technology.
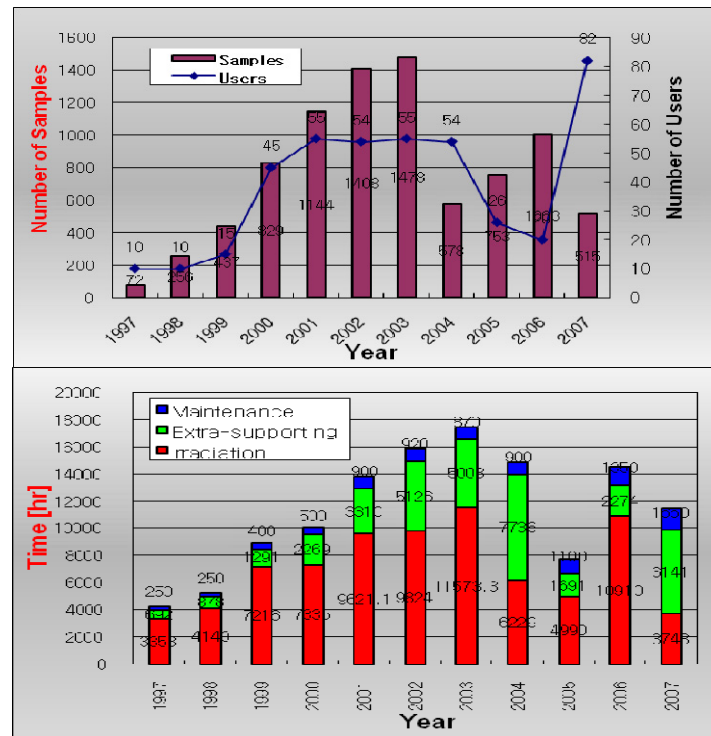
FIG.4. Annual trends of HANARO users, samples, irradiation times.

Development of a temperature control capsule

The irradiation temperature of a specimen is determined by the micro-heater output and helium gas pressure of the gap in a capsule as well as the neutron flux of a capsule itself. However, during a reactor power transient such as a start-up, an irradiated specimen is subjected to a change of the temperature as well as of the neutron flux. Such simultaneous changes of the temperature and neutron flux, both of which cause irradiation damage to a material, make it difficult to elucidate the radiation damage mechanism. The results of previous researches clearly show that temperature changes during a reactor start up and shutdown affect the microstructures of irradiated specimens [9, 10]. To avoid such undesirable effects, the temperature of the specimens during a reactor start-up and shut-down should be kept as uniform as possible with that of a specimen at a normal operation of a reactor. Thus it was necessary to maintain a sample at a specified temperature by heating the sample using auxiliary devices before a reactor power increase in order to eliminate the effect of a temperature transient during the recent irradiation tests. Fig. 5 shows a typical concept of a temperature control irradiation test at HANARO. The temperature control before a reactor start-up is done by an electric heater and by controlling the helium gas pressure in a capsule. The specimen temperature was successfully raised to the target temperature of 300°C before a reactor start-up.

Development of a fluence control capsule

In an irradiation test using a capsule, the neutron fluence of a specimen is mainly dependent on the reactor operation time. For the required specific fluence of the specimens, the reactor operation period has been controlled at HANARO. However it became difficult because of an increased number of reactor users and a stabilized reactor operation schedule. Therefore, short time irradiation tests such as RPV materials requiring only a 2 day-irradiation for a life time neutron fluence requires new capsule technology.
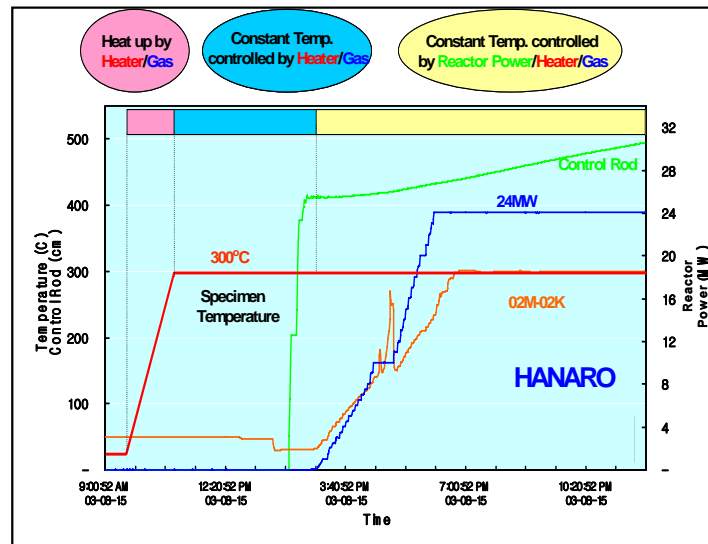
FIG.5. Design concept of the temperature control irradiation capsule in HANARO.

Based on the standard material capsule system, a fluence control capsule system was designed. The capsule system mainly consists of a main capsule and capsule related systems. Fig. 6 shows the conceptual design of a fluence control capsule. The system mainly consists of a main capsule, a protecting tube, a junction box, and a lifting device. The basic design and instruments are almost the same as that of a standard material capsule. A specimen can be lifted up by a withdrawal mechanism using a steel wire that is bolted to the specimen. After a desired neutron irradiation test, the specimen can be lifted up by a handling device, irrespective of a reactor operation.

Moreover, the fluence control capsule will make it possible to irradiate specimens at different temperatures and with different fluences. With this one capsule, five different total fluences at five different temperatures can be ideally realized. Usually, one capsule realizes only one irradiation fluence at one temperature. Thus, it takes several years and an expensive irradiation cost for several capsules to carry out a systematic irradiation at different temperatures with different neutron fluences. The new capsule system was successfully verified and evaluated to be applicable to HANARO.
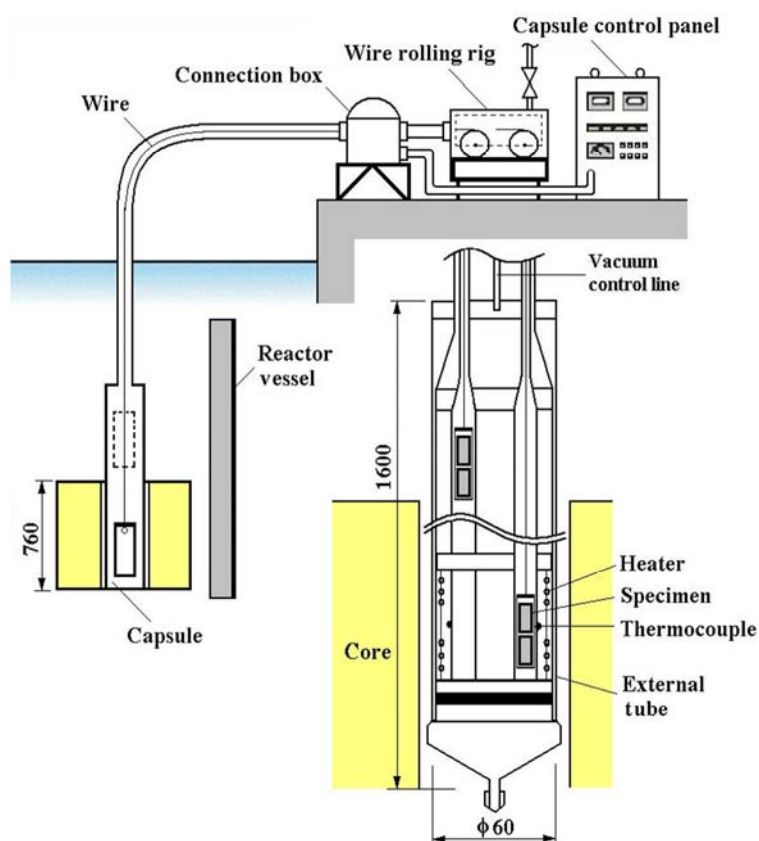
FIG.6. Schematic diagram of the fluence control capsule.

Development of a low flux irradiation capsule

Most material irradiation tests of nuclear materials at HANARO have been performed in the HANARO CT and IR test holes with a relatively higher neutron flux. Due to a fixed operation cycle for the HANARO (about 24 operation days and 11 maintenance days), the neutron fluence of a capsule specimen exceeds 1.0 x 10^{20} n/cm^2.s (E >1.0 MeV) after one cycle of irradiation tests in these holes. Therefore, new capsule technology was required to meet the user's requirements requiring a low neutron fluence. The OR/IP capsule technologies for an irradiation test in the HANARO OR and IP test holes with a relatively lower neutron flux than the CT and IR test holes as shown in Table 1 have been developed and in-pile tested, successfully.

6.5. Development program of other advanced irradiation facilities

A strategic irradiation program at HANARO will place more emphasis on a special-purpose capsule system by focusing on the specific material or fuels for a next generation power reactor. The development of advanced capsules including a high temperature irradiation technology up to 1000°C, re-instrumentation, and re-irradiation technology are under development. These development programs are closely connected with the national research and development (R&D) program in Korea on nuclear reactors and nuclear fuel cycle technology such as the Generation IV (GEN-IV) and Fusion reactor programs. Among the six GEN-IV systems, Korea has participated in the VHTR (Very-High-Temperature Reactor System) and SFR (Sodium-Cooled Fast Reactor System) R&D programs and provisionally participated in the SCWR (Super Critical Water Reactor) program. These new advanced nuclear reactor systems inevitably require higher irradiation test parameters than the conventional irradiation tests. Therefore, sharing of resources and information, networking

and close regional collaboration on research reactors are very important for the development of the other advanced irradiation facilities that are needed for the relevant national R&D programs.

6.6. Conclusions

A HANARO irradiation capsule system has been developed and actively utilized for the irradiation tests of fuels & materials of the commercially operating nuclear reactors in Korea. Based on experience and user's needs, new instrumented capsule technologies for a more precise control of the irradiation temperature and fluence of a specimen, and for an irradiation test in a wider neutron flux condition have been developed. The development programs of advanced capsules and the FTL are closely connected with the national research and development program in Korea on nuclear reactors and nuclear fuel cycle technology. A strategic irradiation program will place more emphasis on a special-purpose irradiation system for a next generation power reactor. HANARO is widely available for international research programs and cooperation.

REFERENCES

[1] KAERI, HANARO, KAERI Summarized Report, KAERI/PR-001/97 (1997).
[2] KANG, Y.H., et al., A study on the development of instrumented capsule for the material irradiation test, KAERI Research Report, KAERI/RR-1760/96 (1997).
[3] KANG, Y.H., et al., Safety analysis report (SAR) for the HANARO capsule and related systems, KAERI Technical Report, KAERI/TR-985/98 (1998).
[4] BRIESMEISTER, J., MCNP-A General Monte Carlo N-Particle Transfer Code, Version 4C, LA-13709-M (2000).
[5] SOMEYA, H., et al., A. Computer Program, JAERI Report, JAERI-M 87-148 (1987).
[6] CROFF, A.G., A User's Manual for The Orgen-2 Computer Code, ORNL/TM-7175 (1980).
[7] ANSYS IP Inc., ANSYS User's manual, Ver. 9.0, ANSYS IP Inc., USA (2005).
[8] GREENWOOD, L.R., SMITHER, R.K., Neutron damage calculations for materials irradiations, ANL/FPP/TM-197.
[9] KIRITANI, M., The Need for Improved Temperature Control during Reactor Irradiation, J. Nuclear Materials, 160 (1988) 135.
[10] GARNER, F.A., et al., Influence of details of reactor history on microstructural development during neutron irradiation, J. Nuclear Materials, 205-206 (1993).

ANGLE SOFTWARE FOR SEMICONDUCTOR DETECTOR GAMMA-EFFICIENCY CALCULATIONS: APPLICABILITY TO REACTOR NEUTRON FLUX CHARACTERIZATION

S. JOVANOVIC, A. DLABAC
University of Montenegro, Faculty of Sciences
P.O.Box 211, Cetinjski put bb, MNE-81000 Podgorica, Montenegro
Email: Bobojovanovic@yahoo.co.uk

Abstract: Angle software for semiconductor detector efficiency calculations in its various forms has been in use for 15 years now in numerous gamma-spectrometry based analytical laboratories all around. It goes about a semi-empirical approach, which combines advantages of both absolute and relative methods to determining sample activity by gamma-spectrometry, while conciliating and minimizing their drawbacks. Physical model behind is the concept of the effective solid angle – a parameter calculated upon the input data on geometrical, physical and chemical (composition) characteristics of (1) the source (incl. its container vessel), (2) the detector (incl. crystal housing and end-cap) and (3) counting arrangement (incl. intercepting layers between the latter two). It was shown earlier that only simultaneous differential treatment of gamma attenuation, counting geometry and detector response, as is the case with Angle, is essentially justified for this type of calculations. Attempting the other-way-round, i.e. to separately calculate these three phenomena, generally lead to (over)simplifications, which further require complex corrections with limited success.

The program can be applied to practically all situations encountered in gamma-laboratory practice: point, disc, cylindrical or Marinelli samples, small and large, of any matrix composition. No standards are required, but a start-up "reference efficiency curve" should be obtained ("once for ever") by measuring a set of calibrated point sources at a large source-to-detector distance (e.g. 20-30cm, to avoid true coincidence effects). Calibration sources are chosen to cover gamma-energy region of analytical interest (e.g. 50-3000 keV). This initial effort is largely paid back in future exploitation. Briefly, ANGLE is characterized by (1) a broad application range, (2) good accuracy for this type of calculations (of a few percent order), (3) comfortable data manipulation (Windows), (4) short computation times, (5) flexibility with respect to input parameters and output data, including easy communication with another software and (6) suitability for didactical/training purposes. ANGLE frame is also convenient for accommodating other efficiency calculation methods of semi-empirical or absolute type, Monte Carlo for instance.

In addition, it is a matter of little effort to extend its existing scope of applicability to further/particular user's needs and/or fields of interest (can be regarded as "open-ended" computer code). For reactor neutron flux characterization purposes, ANGLE applicability is related to flux monitor measurements. The emphasis is given to suitable metal foils and alloys which are being irradiated/ activated in characteristic reactor positions so as to give subsequently gamma spectrum information of flux density, shape, etc.

7.1. Introduction

In any gamma-spectrometric measurement with semiconductor detectors, the question of converting the number of counts (collected in a full energy peak) into the activity of the sample/source cannot be avoided. There are, in principle, three approaches to this issue:

(1) *Relative,* where one tries to imitate as accurately as possible the source by a standard (or vice versa), while keeping the same counting conditions for the two. If enough care is paid, the result is in general, so accurate that it cannot be surpassed by other methods. However, we all know what "enough care" means in practice. Combined with the inflexibility in respect of varying source & container parameters (shape, dimensions, material composition), this represents *raison d'être* of the other approaches, as follows.

(2) *Absolute calculations* (e.g. Monte Carlo methods) yield full energy peak efficiency (ε_p) for a given counting arrangement. It is essentially statistical treatment of the events which photons undergo - from being emitted by a source atom until the interaction with the detector active body - including the treatment of the so produced electrons, positrons and other subsequent energy carriers. This approach is very precise, under the following conditions: there are a sufficiently large number of incident photons, of which details are

known about (i) source, detector and intercepting layers' geometrical & compositional data, (ii) the corresponding photon attenuation coefficients, (iii) energy and angle dependent cross section for various photon interactions with the detector active body, and (iv) parameters characterizing electron/positron behavior in the latter. At present, inherent statistical uncertainty of Monte Carlo methods, unsatisfactory manufacturers' detector specifications and relatively poor knowledge of (some of) the above physical parameters are the limiting factors for its applicability. However, with the speeding up of computers, and with more accurate detector specifications and cross section data (the determination of which is, on its turn, related to more careful and sophisticated measurements), it is reasonable to assume that the time works for absolute methods, and that in future they might be the dominant ones.

(3) *Semiempirical models,* trying to conciliate the previous two. Semiempirical models commonly consist of two parts: (i) experimental (producing one kind or another of reference efficiency characteristic of the detector) and (ii) relative-to-this calculation of ε_p. Inflexibility of the relative method is avoided in this way, as well as the demand for some physical parameters needed in Monte Carlo calculations. Numerous variations exist within this approach, with emphases either to experimental or to computational part. Most of them simplify (or oversimplify) the physical model behind, i. e. the treatment of gamma-attenuation, geometry and detector response. Moens et al. [1-3] showed that only the simultaneous differential treatment of these three factors is essentially justified. This fact is transformed into the concept of the effective solid angle ($\overline{\Omega}$), a calculated value incorporating the three components, and closely related to the detection efficiency (see further).

Theoretical

Given a gamma-source (S) and a semiconductor detector (D) (Fig. 1.), the effective solid angle is defined as [1,2]:

$$\overline{\Omega} = \int_{V_S, S_D} d\overline{\Omega} \tag{1}$$

with V_S= source volume, S_D= detector surface exposed to the source ("visible" by the source) and

$$d\overline{\Omega} = \frac{F_{att} \cdot F_{eff} \cdot \mathbf{TP} \cdot \mathbf{n}_u}{|\mathbf{TP}|^3} d\sigma \tag{2}$$

Here T is point varying over V_S, P point varying over S_D, and n_u the external unit vector normal to infinitesimal area $d\sigma$ at S_D. Equation (1) is thus a five fold integral. Factor F_{eff} accounts for gamma attenuation of the photon following the direction TP out of the detector active zone, while F_{eff} describes the probability of an energy degradable photon interaction with the detector material (i.e. coherent scattering excluded), initiating the detector response.

The two factors include therefore geometrical and compositional parameters of the materials traversed by the photon.

With ε_p being proportional to $\overline{\Omega}$, the detection efficiency is then found as:

$$\varepsilon_p = \varepsilon_{p,ref} \frac{\overline{\Omega}}{\overline{\Omega}_{ref}} \tag{3}$$

where index "ref" denotes reference counting geometry to which the actual one is relative.
So as to apply this method the following should be known:

- reference efficiency curve, usually obtained by counting calibrated point sources at a reference distance (e. g. 15-20 cm), and covering gamma-energies (E_γ) in the region of interest (e. g. 50 -3000 keV); considerable effort should be put in this phase to reach accurate $\varepsilon_{p,ref}(E_\gamma)$ function, but it pays off in further exploitation.
- geometrical and compositional data about the source, detector and all intercepting layers (for the latter e.g. source container and holder, detector end cap and housing, dead layers, etc.).
- gamma-attenuation coefficients for all materials involved.

For a cylindrical source coaxially positioned with the detector, and with radius smaller than that of the detector ($r_o < R_o$, Fig. 2.). Equation (1) than gives

$$\overline{\Omega} = \frac{4}{r_o^2 L} \int_0^L (d+l)dl \int_0^{r_o} rdr \int_0^\pi d\phi \int_0^{R_o} \frac{F_{att} \cdot F_{eff} \cdot RdR}{\left[R^2 - 2Rr\cos\phi + r^2 + (d+l)^2\right]^{3/2}} \tag{4}$$

In the above, five fold integral is reduced to four fold due to axial symmetry. Disk and point sources are included in Equation (4) (for L=0, and L=0, r_o=0, respectively).
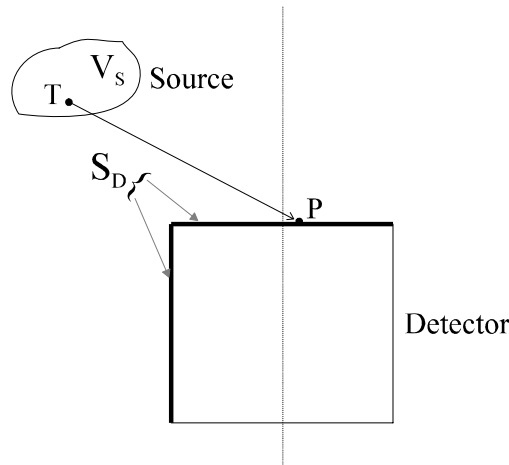

FIG.1. To the definition of the effective solid angle ($\overline{\Omega}$).
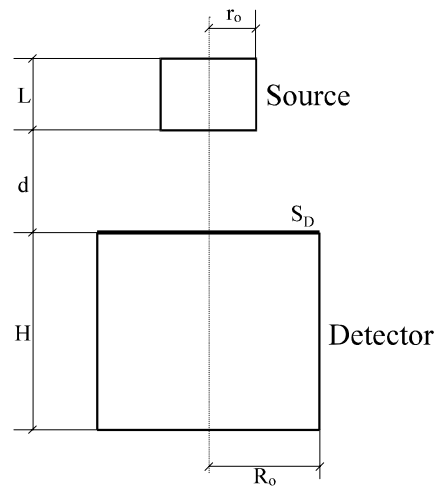

53

FIG. 2. Cylindrical source (ro < Ro).

For sources with radii larger than that of the detector ($r_O > R_O$, Fig. 3.):

$$\overline{\Omega} = \int\limits_{V_1,S_1} d\overline{\Omega} + \int\limits_{V_2,(S_1+S_2)} d\overline{\Omega} =$$

$$= \frac{4}{r_o^2 L} \int\limits_0^L (d+l)dl \int\limits_0^{r_o} rdr \int\limits_0^\pi d\phi \int\limits_0^{R_o} \frac{F_{att} \cdot F_{eff} \cdot RdR}{\left[R^2 - 2Rr\cos\phi + r^2 + (d+l)^2\right]^{3/2}} + \tag{5}$$

$$+ \frac{4R_o}{(r_o^2 - R_o^2)L} \int\limits_0^L dl \int\limits_{R_o}^{r_o} rdr \int\limits_0^{\phi_o} d\phi \int\limits_{-H}^0 \frac{F_{att} \cdot F_{eff} \cdot (r\cos\phi - R_o)dh}{\left[R_o^2 - 2R_o r\cos\phi + r^2 + (d+l-h)^2\right]^{3/2}}$$

with

$$\phi_o = \phi_o(r) = \operatorname{arctg} \frac{\sqrt{r^2 - R_o^2}}{R_o}$$

Marinelli geometry (Fig. 4.) can be described by:

$$\overline{\Omega} = \int\limits_{(V_1+V_2),S_1} d\overline{\Omega} + \int\limits_{V_2,S_2} d\overline{\Omega} + \int\limits_{V_3,S_1} d\overline{\Omega} + \int\limits_{(V_3+V_4),S_2} d\overline{\Omega} + \int\limits_{V_5,(S_2+S_3)} d\overline{\Omega} =$$

$$= \frac{4}{r_o^2 L + (r_o^2 - r_\varphi^2)L_\varphi} \int\limits_0^L (d+l)dl \int\limits_0^{r_o} rdr \int\limits_0^\pi d\phi \int\limits_0^{R_o} \frac{F_{att} \cdot F_{eff} \cdot RdR}{\left[R^2 - 2Rr\cos\phi + r^2 + (d+l)^2\right]^{3/2}} +$$

$$+ \frac{4R_o}{r_o^2 L + (r_o^2 - r_\varphi^2)L_\varphi} \int\limits_0^L dl \int\limits_{R_o}^{r_o} rdr \int\limits_0^{\phi_o} d\phi \int\limits_{-H}^0 \frac{F_{att} \cdot F_{eff} \cdot (r\cos\phi - R_o)dh}{\left[R_o^2 - 2R_o r\cos\phi + r^2 + (d+l-h)^2\right]^{3/2}} +$$

$$+ \frac{4}{r_o^2 L + (r_o^2 - r_\varphi^2)L_\varphi} \int\limits_0^d ldl \int\limits_{r_\varphi}^{r_o} rdr \int\limits_0^\pi d\phi \int\limits_0^{R_o} \frac{F_{att} \cdot F_{eff} \cdot RdR}{\left(R^2 - 2Rr\cos\phi + r^2 + l^2\right)^{3/2}} +$$

$$+ \frac{4R_o}{r_o^2 L + (r_o^2 - r_\varphi^2)L_\varphi} \int\limits_{d-L\varphi}^d dl \int\limits_{r_\varphi}^{r_o} rdr \int\limits_0^{\phi_o} d\phi \int\limits_{-H}^0 \frac{F_{att} \cdot F_{eff} \cdot (r\cos\phi - R_o)dh}{\left[R_o^2 - 2R_o r\cos\phi + r^2 + (l-h)^2\right]^{3/2}} +$$

$$+ \frac{-4}{r_o^2 L + (r_o^2 - r_\varphi^2)L_\varphi} \int\limits_{d-L\varphi}^{-H} (l+H)dl \int\limits_{r_\varphi}^{r_o} rdr \int\limits_0^\pi d\phi \int\limits_0^{R_o} \frac{F_{att} \cdot F_{eff} \cdot RdR}{\left[R^2 - 2Rr\cos\phi + r^2 + (l+H)^2\right]^{3/2}} \tag{6}$$
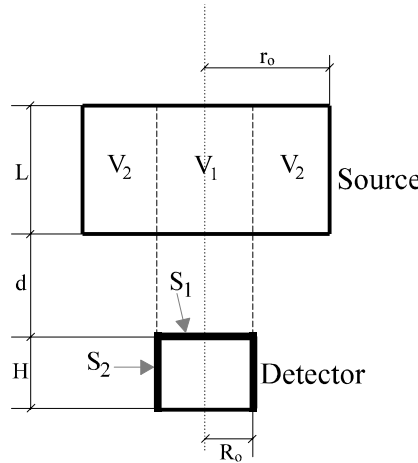
FIG.3. Cylindrical source ($r_O > R_O$).
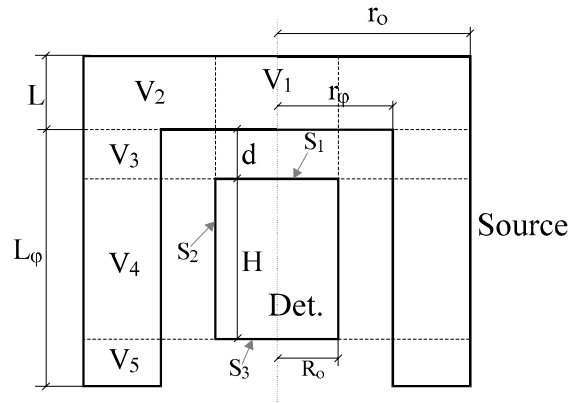
FIG.4. Marinelli geometry.

Computer code description

The above effective described solid angles and corresponding detector efficiencies are calculated by our ANGLE software [4-6]. Its main screen is shown in Fig. 5, with input data being entered within five main sections (Detector, Container, Geometry, Source and 'Other').

Detector, container and geometry windows are organized in the same way: at the left-hand side names of previously created detector (or container, or geometry) files are listed. Each of them contains all necessary data characterizing the detector (or container, or geometry).

When, for instance, a new detector is being introduced, one first chooses its type: closed end coaxial HPGe (high purity Ge detector), true coaxial HPGe, closed- or open-end coaxial Ge(Li), planar LEPD (explain) or well type. Program then asks for numerical values of the parameters characterizing the type chosen (crystal dimensions, including core or hole, dead and contact layers, end cap, inner housing, beryllium window, antimicrophonic shield, etc.). Entering these data is facilitated by multicolor illustrations at which current parameter is visually emphasized, Fig. 6. For the source container the procedure is similar. We firstly choose between cylinder or Marinelli type. The following refers to geometrical and compositional data characterization of the container, Fig. 7.
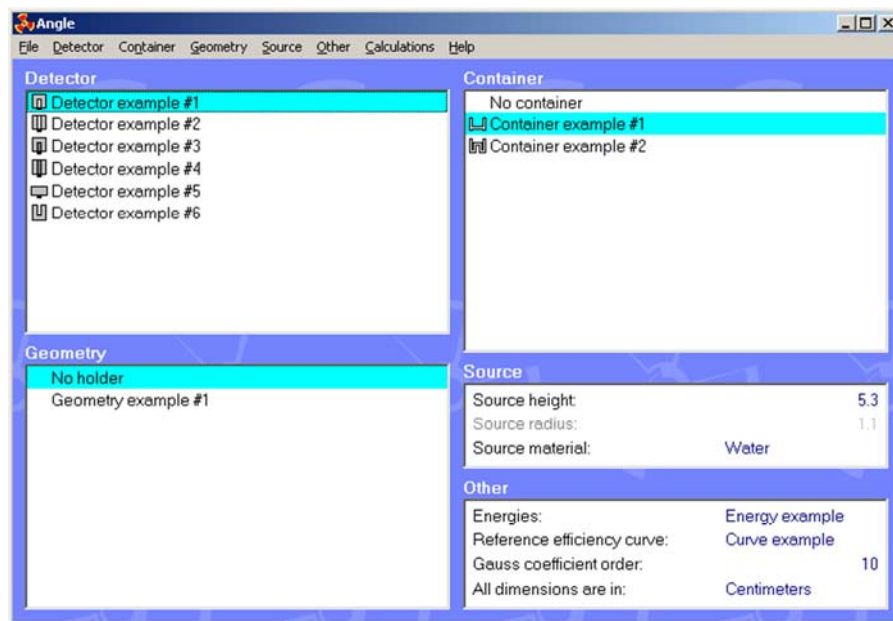
FIG.5. ANGLE main window.
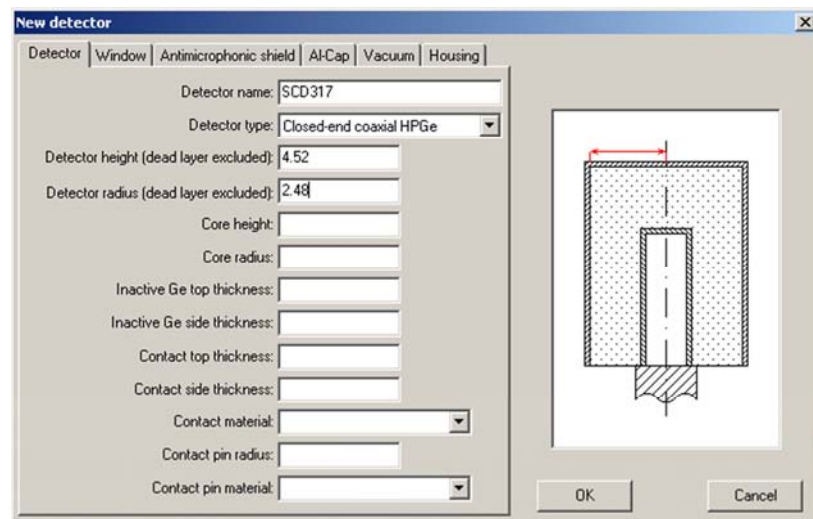
FIG.6. Entering the data for a detector.
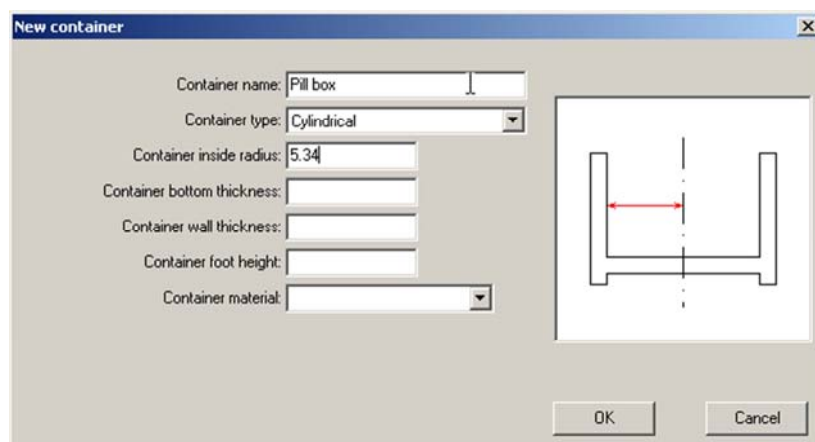
FIG.7. Entering the data for a container.

When material composition is being entered - not only for the source itself, but also for any material of the source container, holder, intercepting layer or detector, the same subroutine is activated: one can choose between a few most encountered ones (air, water, plastic, aluminum), or introduce a new one. In the latter case, any composition is acceptable (pure element, or compound, or mixtures). It is assumed that percentages of the major constituents are known (at least roughly), as well as their chemical formulae. These data, together with gamma attenuation coefficients, are used to calculate attenuation factors. Attenuation coefficients are found in an extensive (per element and per energy) data file.
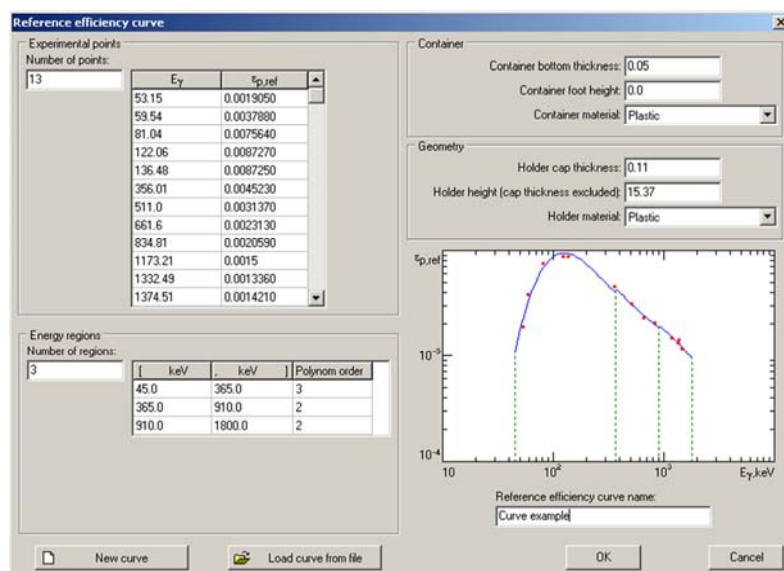
FIG.8. Creating a reference efficiency curve.
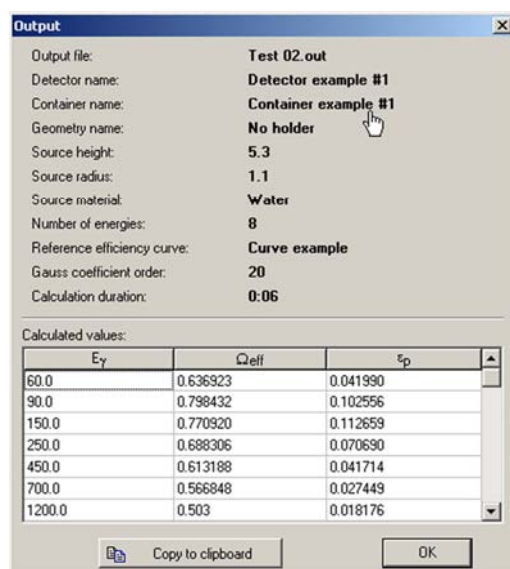
FIG.9. ANGLE output file.

In the 'Other' window there are:

  − Gamma energies of interest. We can give a set of energies from a previously created file, or create a new one.

- Gauss coefficient order for numerical integration procedure (see Theoretical). The higher the order, the more precise is the result, but the computation time is longer.
- Language: English as the program communication language can be replaced by any other one, simply by translating message-by-message.
- Reference efficiency curve, as in Fig. 8.

At the output, calculated effective solid angles and full energy peak efficiencies are found per gamma energy given, Fig. 9. Output files can be handled in the standard way and are suitable for further programming.

7.2. Practical verification and applicability to research reactor neutron flux characterization

In routine applications accuracies of 3-4% are obtained, and not worse than 7% for the most unfavourable geometries (bulky samples at the detector top) [5,6]. These uncertainties originate for the most part from (i) the reference efficiency curve and (ii) poor detector specifications [2,5-8], while (iii) contribution of computation error is negligible.

For reactor neutron flux characterization purposes, ANGLE applicability is related to flux monitor measurements. The emphasis is given to suitable metal foils and alloys which are being irradiated/ activated in characteristic reactor positions so as to give subsequently gamma spectrum information of flux density, shape, etc. Examples of these practices are given in e.g. Refs. [9-17].

7.3. Conclusions

We can summarize the main features of the here presented ANGLE code for calculation of semiconductor detector full energy peak efficiencies as: (i) broad application range, covering the vast majority of gamma-counting situations, including reactor neutron flux measurements/characterization; (ii) good accuracy (uncertainties of the order of a few percent), based upon the concept of the effective solid angle; (iii) easy data manipulation with windows menus; (iv) flexibility in respect with changing input parameters, and (v) didactical suitability (e.g. in gamma-spectrometry courses), since practically all parameters characterizing the detection process are found therein, systematically grouped and easy to follow and understand. It is also important to note that ANGLE frame can be readily adjusted to accommodating some other semi-empirical or Monte Carlo methods for efficiency calculations.

General applicability of ANGLE in gamma spectrometry with semiconductor detector makes it suitable for reactor neutron flux characterization with any flux monitor based on (n, gamma) activation. This methodology can help to improve the characterization of the neutron field parameters, especially for material irradiation programmes.

REFERENCES

[1]   MOENS, L., Ph.D. Thesis, University of Gent, Belgium (1981).
[2]   MOENS, L., et al., Nuclear Instruments and Methods in Physics Research, 187 (1981) 451.
[3]   MOENS, L., HOSTE, J., Int.J.App.Radiat.Isotop., 34 (1983) 1085.
[4]   JOVANOVIC, S., DLABAC, A., MIHALJEVIC, N., VUKOTIC, P., J. Radioanalytical Nuclear Chemistry, 218 (1997) 13.
[5]   MIHALJEVIĆ, N., et al., J. Radioanalytical Nuclear Chemistry ,169 (1993) 209.
[6]   MOENS, L., DEBERTIN, K., Nuclear Instruments and Methods in Physics Research, A238 (1985) 180.

[7]   DEBERTIN, K., HELMER, G.R., Gamma- and X-Ray Spectrometry with Semiconductor Detectors, Elsevir Science Publishers B.V., Amsterdam (1988).

[8]   JOVANOVIC, S., DE CORTE, F., MOENS, L., SIMONITS, A., HOSTE, J., J. Radioanalytical Nuclear Chemistry, 82/2 (1984) 379.

[9]   DE CORTE, F., JOVANOVIC S., SIMONITS, A., MOENS, L., HOSTE, J., Atomkernenergie - Kerntechnic, 44 (1984) 641.

[10]   JOVANOVIC, S., DE CORTE, F., SIMONITS, A., HOSTE, J., J. Radioanalytical Nuclear Chemistry, 92/2 (1985) 399.

[11]   DE CORTE, F., MOENS, L., JOVANOVIC, S., SIMONITS, A., DE WISPELAERE, A., J. Radioanalytical Nuclear Chemistry, Articles, 113 (1987) 177.

[12]   JOVANOVIC, S., et al, J. Radioanalytical Nuclear Chemistry, Articles, 113 (1987) 353.

[13]   JOVANOVIC, S., et al, J. Radioanalytical Nuclear Chemistry, Articles, 129 (1989) 343.

[14]   JOVANOVIC, S., et al, J. Radioanalytical Nuclear Chemistry, Letters, 135 (1989) 59.

[15]   DE CORTE, F., et al, J. Radioanalytical Nuclear Chemistry, Articles, 169 (1993) 125.

[16]   PEROVIC, S.M., JOVANOVIC, S., Proceedings of the International Conference COMCONEL-91, Part II, Cairo, Egypt (1991) 572.

[17]   VUKOTIC, P., MULDER, R.U., JOVANOVIC, S., Proceedings of the International k_O Users Workshop - Gent, Astene, Belgium (1992) 149.

Chapter 8

APPLICATION OF DIGITAL MARKER EXTENOMETRY TO DETERMINE THE TRUE STRESS-STRAIN BEHAVIOUR OF IRRADIATED METALS AND ALLOYS

O.P. MAKSIMKIN[1], M.N. GUSEV[1], I.S. OSIPOV[1], F.A. GARNER[2]
[1]Institute of Nuclear Physics, Almaty, Kazakhstan,
[2]Pacific Northwest National Laboratory, Richland WA, USA
Email: gusev.maxim@inp.kz

Abstract: To study the peculiarities of deformation hardening and flow localization of radioactive materials a non-contact "digital marker extensometry" technique has been developed. It allows us to easily define plasticity parameters and true stresses in experiments where miniature highly radioactive specimens are used. The engineering and true stress-strain relationships under plastic flow and hardening of irradiated metal polycrystals have been investigated experimentally after irradiation in two reactors in Kazakhstan. The true curves were obtained for nickel, iron, molybdenum, as well as for the Russian stainless steels $08Cr_{16}Ni_{11}Mo_3$ and $12Cr_{18}Ni_{10}Ti$. Describing these curves using the $\sigma_i = \sigma_0 + k\sqrt{\varepsilon_i}$ equation demonstrates that the concept of ultimate stress is an artifact arising from flow localization and is not fully informative of the hardening mechanisms operating in highly irradiated materials.

8.1. Introduction

To describe the plastic deformation behavior of polycrystalline metals, it is necessary to utilize dislocation theory [1, 2] combined with elements of thermodynamics [3] and mesomechanics [4]. In some cases material-specific physical processes involved in plastic flow need to be taken into account. Examples of such processes are interrupted deformation (dynamic strain aging) [5], microscopic or macroscopic localization [1,2], arising from defect-dislocation interactions [6], particularly defects induced by displacive radiation.

In such cases the "true" curves of deformation hardening expressed in true stress-true strain coordinates are used to build a physical picture of the processes operating to produce the deformation. These curves are usually obtained by conducting experiments involving various extensometry techniques [7], but in most ordinary cases researchers derive the true curves from the measurement of load vs. elongation, often referred to as an "engineering" curve.

In the case of highly irradiated metals, however, the experimentally recorded "engineering" curves cannot always be converted into true curves. This problem arises from the fact that the local flow stress in irradiated metals often has very specific peculiarities. As a result of irradiation, the metal loses its ability to deform uniformly under tension. A large portion of the highly irradiated specimen does not develop any significant deformation, while the local deformation in the neck area can be very high. In such cases, the engineering curve is inapplicable for studying the kinetics of the deformation processes and, in particular, for defining the character of the relationship between the true stress and strain values.

To obtain an understanding of the events happening in a deforming specimen and, in particular, to study the relationship between the true stresses and strains, one can use special extensometer techniques during mechanical testing, such as: optical and electron extensometry [8, 9], coordinate network techniques [10], speckle-interferometry technique [11] among others.

When radioactive materials are being tested, the use of these extensometry techniques become much more difficult, often limiting their applicability. For very small or "miniature" specimens used to reduce the level of radioactivity, any technique involving physical or near contact of either measurement probes or persons to the specimens becomes rather impractical.

To overcome such problems we have developed a "marker-extensometry" technique that is uniquely suited to examining very small, highly radioactive specimens that are prone to flow localization on a very small scale.

8.2. Materials studied

The study was performed on four pure metals – copper, nickel, molybdenum and Armco-iron. Also were examined Russian industrial alloys 12Cr18Ni10Ti and 08Cr16Ni11Mo3, which are widely used in nuclear reactors in the countries of the former Soviet Union. The compositions of these Fe-base alloys are Cr:18%, Ni:10.6%, Mn:1.7%, C:0.1% and Cr:16%, Ni:11.4%, Mn:1.6%, Mo:1.8% C<0.021%, respectively.

Two types of specimens were used in this study. Flat specimens with dimensions of $10\times3.5\times0.3$ mm were punched from strips of pure nickel, iron or molybdenum, then annealed and then irradiated over a range of doses in the core of the WWR-K reactor (located in Almaty, Kazakhstan Republic) to a maximum fluence of 6×10^{20} n/cm^2 (E > 0.1 MeV). Round tensile specimens of pure copper and $12Cr_{18}Ni_{10}Ti$ with gauge section 10 mm long and 1.7 mm diameter were also irradiated in WWR-K. All irradiations proceeded over a rather narrow range of temperature but never exceeded 353K.

Additionally, flat specimens of $08Cr_{16}Ni_{11}Mo3$ steel with dimensions of $10\times2\times0.3$ mm were sliced from various axial positions of the faces of the spent fuel assembly wrapper designated H-214 (II) that was irradiated in the BN-350 fast reactor in Aktau, Kazakhstan Republic. The damage dose rate and the accumulated dose in this assembly varied along its height. At its centerline a maximum of 15.6 dpa was reached. Unlike the WWR-K data the irradiation temperature varied relatively strongly, ranging from 553 to 600K.

The thermal treatment of the investigated materials and their irradiation conditions are given in Table 1.

Uniaxial tensile tests of both non-irradiated and irradiated specimens were performed using the "Instron-1195" facility at 293K with a deformation rate of $8.4\cdot10^{-4}$ s^{-1}. Pneumatic grippers were used for gripping of the specimens.

TABLE 1. THERMAL TREATMENT AND IRRADIATION PARAMETERS OF THE MATERIALS UNDER STUDY

Material	Thermal treatment	Irradiation temperature (K), reactor	Fluence (n/cm^2), (E>0.1 MeV) or dose (dpa)
Nickel	Annealing 1223 K, 30 min.	<353, WWR-K	1.4×10^{19} - 1.3×10^{20}
Armco-iron	Annealing 1223 K, 30 min.	<353, WWR-K	5×1018 - 1.4×1019
Molybdenum	Annealing 1473 K, 2 hours	<353, WWR-K	1.1×10^{19} - 6×10^{20}
Copper	Annealing 1023 K, 1 hour	<353, WWR-K	2×1020
Steel $12Cr_{18}Ni_{10}Ti$	Annealing 1323 K, 30 min.	<353, WWR-K	1.4×10^{19} - 1.3×10^{20}
Steel $08Cr_{16}Ni_{11}Mo_3$	Cold-work 15-20 % + annealing 1073 K, 1 hour.	553-600, BN-350	1.27 - 15.6 dpa

8.3. The details of the marker-extensometry technique

To study the kinetics of non-homogeneous deformation of highly irradiated miniature specimens, a new "digital marker extensometry" technique was developed. Small drops of dye material from a marking pen were manually applied to the polished specimen surface. The dye was chosen because it demonstrated good adhesive properties and because it deformed easily without de-bonding. The shape changes of the specimen, as well as the shape change and shift in position of the markers were recorded by digital camera with high resolution (2048×1536 pixels with the resolution of 10 micron/pixels), as shown in Fig.1.
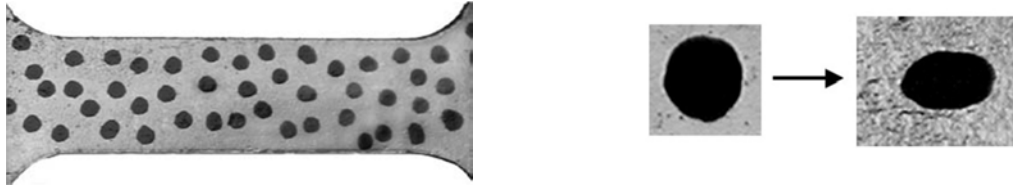
FIG.1. Gauge area of specimen before deformation (left) and change of the shape of a single marker as a result of deformation (right).

The easily reproducible and relatively large size markers used in the first cycle of the experiments were chosen as the first stage of development. Later when more specific algorithms to process the digital images have been established and a stronger optics system has been developed, it will be possible for any image element (smaller dots, small scratches, etc) to serve as markers.

In the current marker extensometry technique, which is similar to the "network technique" [10], the specimen is covered with a spot network with steps of 1-1.5 mm. This allows us to calculate the values of local deformation and stress with an error not higher than 5 and 10% respectively for any section of the specimen based on a sequence of pictures, using specially developed computer codes that calculate the distance L between the centers of the markers, Fig.2. The value of the local deformation of some chosen local section of the specimen for the *i-th* picture may be defined as $\varepsilon_i = ln(L_0/L_i)$, where L_0 is the initial distance between the markers (defined from the first picture taken before the deformation started), L_i is the current distance calculated based upon the *i-th* picture.

FIG.2. The parameters that are being measured using the marker extensometry technique.

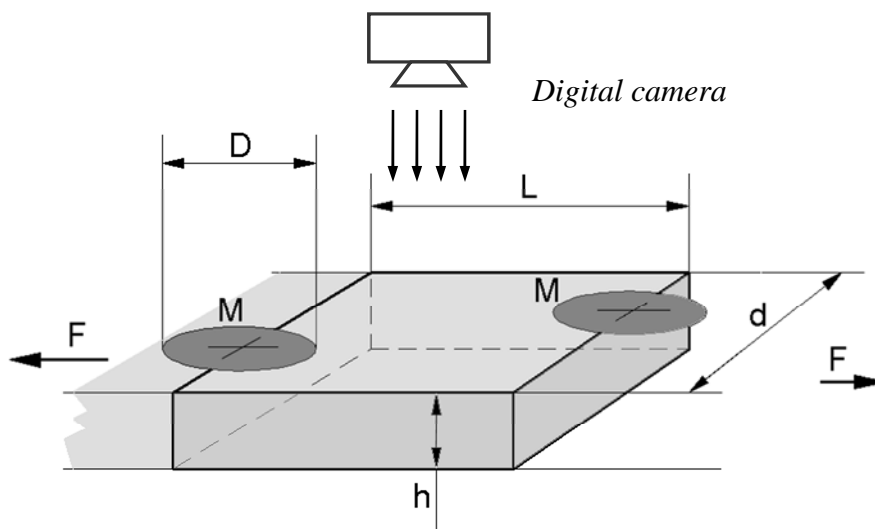The specimen is loaded by the force F, M are the marker areas; D is the marker's dimension towards the tensile axis; L is the distance between the centers of the markers; d is the width of the specimen; h is the thickness of the specimen (d and h values are defined before the deformation).

It is a well known fact that the material density ρ does not change much in the process of deformation ($\Delta\rho < 1\%$). This fact allows us to say that the volume of the specimen V might be considered as constant during the course of a tensile experiment.

Thus, the operating stress σ_i may be obtained based on the constant volume criterion V ($V=S_0 \cdot L_0 = S_i \cdot L_i =$const, where $S=h \cdot d$) as follows:

$$\sigma_i = \frac{F_i}{S_0 \cdot \left(\dfrac{L_0}{L_i}\right)}, \tag{1}$$

where F_i is the force acting at *i-th* moment of time and is defined from the engineering diagram, S_0 is initial cross section. The marker dimension along the D axis might be used instead of the L value in the calculations.

This approach allows us to define the stress value acting along the deformation axis but it does not provide an opportunity to define tangential stresses. This paper does not address the analysis of the complex stress state that takes place in the neck region as it develops.

Using the experimental values of the true stresses σ_i and the local deformation ε_i, one can construct the distribution curve along the operating length of the specimen for various moments of the deformation until its failure or to observe the "$\sigma_i - \varepsilon_i$" relationship for some section of the specimen, Fig. 3.

It is worth noting that the experimental "$\sigma_i - \varepsilon_i$" relationships for the irradiated materials [12] are rarely mentioned in the literature. In particular this is true for specimens with a large level of radiation embrittlement. At the same time, the curves "$\sigma_i - \varepsilon_i$" have a great practical value and, in particular, in the course of the simulation processes of the plastic deformation and in calculations using the ANSYS, ABAQUS or LS-DYNA codes.

8.4. Experimental results that were obtained using this technique

08Cr$_{16}$Ni$_{11}$Mo$_3$ Steel irradiated in BN-350

Fig. 2 shows typical engineering curves obtained through deformation of neutron irradiated 08Cr$_{16}$Ni$_{11}$Mo$_3$ steel. The general features of the curves are similar to that of an earlier study [13]. The yield and ultimate stress values and the plasticity obtained from these diagrams, agree well with the results of other authors [13-15]. As follows from Figure 3, the uniform deformation value is very small (2-4%), and immediately after the yield strength one can observe the development of a macroscopic neck and the engineering curve becomes non-informative concerning the work hardening processes within the neck area. From the scientific point of view it is informative to study the "$\sigma_i - \varepsilon_i$" relationship in the developing neck, Fig. 3 (curves 3 and 3′). The true curve (3′) was calculated for the developing neck based on experimental results using the optical extensometer method.

Fig. 4 shows the deformation hardening curves for the 08Cr$_{16}$Ni$_{11}$Mo$_3$ steel in the "true stresses σ_i – true deformations $(\varepsilon_i)^{0.5}$ " coordinates, which were calculated based on the digital marker extensometry data. The square root of deformation is used, which according to the suggestion of reference [16] results in linearization of the curves.
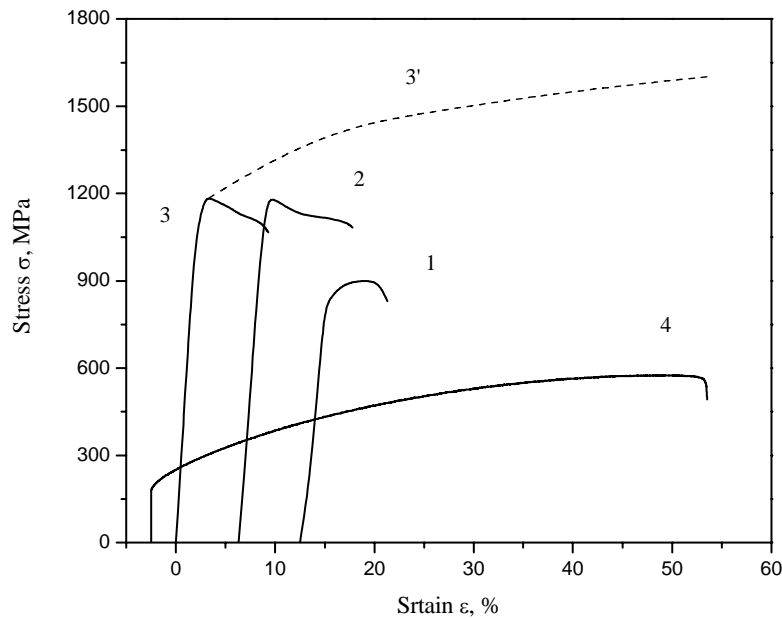
FIG.3. Engineering curves for 08Cr$_{16}$Ni$_{11}$Mo$_3$ steel presented in conventional coordinates: 1 – irradiated to 1.27 dpa at 280°C; 2 –10.8 dpa at 300°C; 3 –11.9 dpa at 354°C; 3′ – the true curve of the plastic flow for curve 3; 4 – non-irradiated steel. The curves are shifted along the strain axis to provide a better view.

As one can see by comparing Figures 3 and 4, the transition from conventional to real deformation and stress values qualitatively changes the view of the flow curves. Thus, the development of the local deformations in the neck is accompanied by continual deformation hardening of the material and by increase of the operating stresses up to the moment of failure, despite the seeming loss of hardening which is registered by the engineering curve immediately after the yield point. According to [17], here it is seen the "quasi-embrittlement" case, i.e. the suppression of the uniform deformation, and, this case should be differentiated from that of real embrittlement [18], i.e. the complete suppression of the material's capability for plastic deformation.
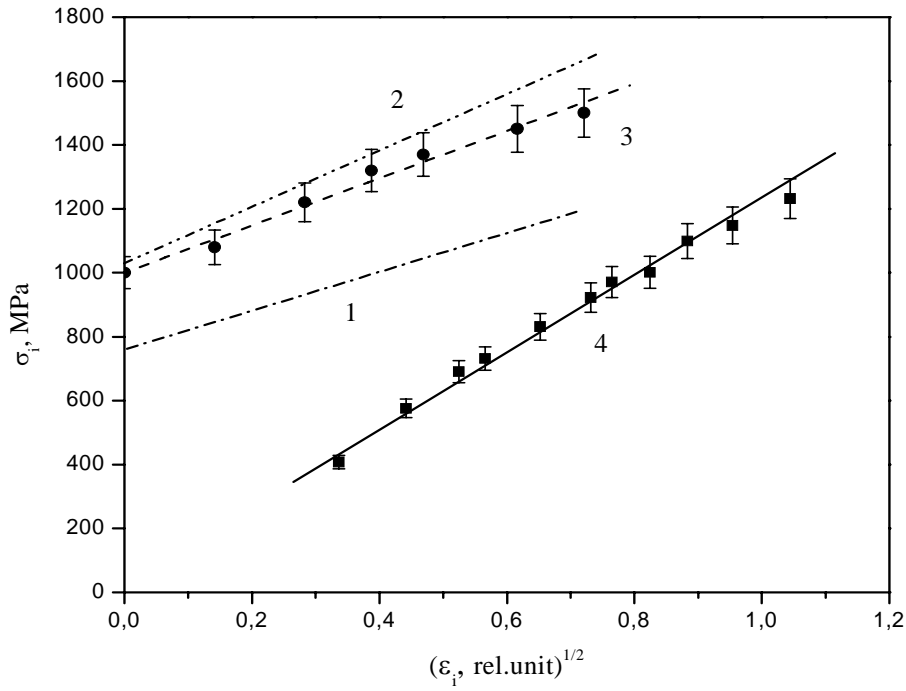
FIG.4. The "true stress σ_i – deformation $(\varepsilon_i)^{0.5}$" relationship for $08Cr_{16}Ni_{11}Mo_3$ steel.

Curves 1-4 correspond to the specimen numbers shown in Figure 3. The experimental data points are not shown for curves 1 and 2.

Analysis of the experimentally obtained $\sigma_i(\varepsilon_i)$ relationships showed that they may be described by the following equation:

$$\sigma_i = k \cdot \varepsilon_i^{0.5} + \sigma_0, \tag{2}$$

where k is the coefficient of the deformation hardening and σ_0 is a value close to the yield strength. In "$\sigma - \varepsilon^{0.5}$" coordinates these curves appear to be linear.

In this steel it is observed the monotonic growth of the σ_0 value with increasing dose, while the k value in general decreases but not monotonically. To explain this non-monotonic behavior we speculate that in addition to the dose level, factors such as differences in irradiation temperature and dose rate in this data set affect the material's structure and its deformation behavior [19].

FIG.5. Changes in yield strength (a) and plasticity (b) versus fluence: 1 – α-Fe, 2 – Mo, 3 – Ni, 4 –08Cr$_{16}$Ni$_{11}$Mo$_3$ steel. 1-4 –total and 1´-4´ – uniform deformation for the indicated materials.

Pure metals (Cu, Fe, Ni, Mo) and 12Cr₁₈Ni₁₀Ti stainless steel irradiated in WWR-K

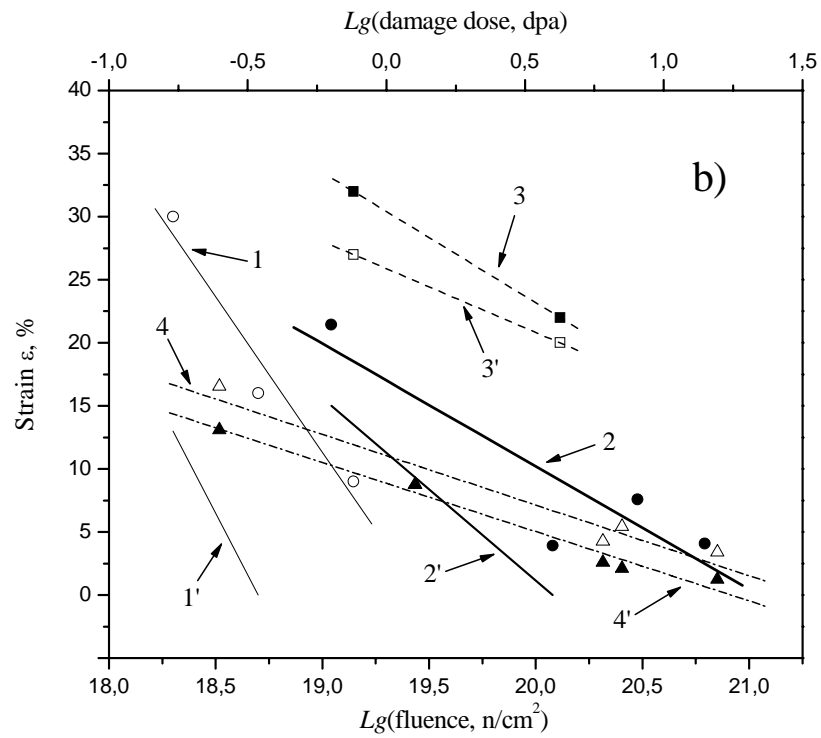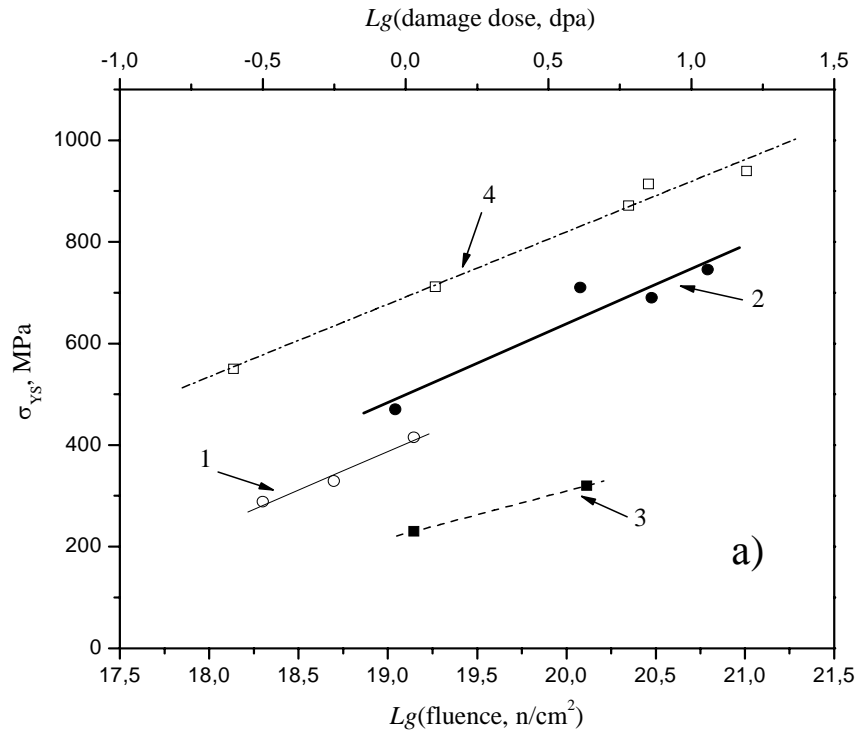Fig.5 shows strength and plastic engineering properties of the pure metals versus neutron fluence. In this figure one can see that the yield strength of these metals is steadily increasing, while the plasticity is decreasing. The data agree well with data from other studies [20].

The decrease in plasticity demonstrates itself most vividly in the bcc metals, for which the uniform deformation values plunges toward zero when the fluence reaches 1.2×10^{20} n/cm^2 for molybdenum and 1.4×10^{19} n/cm^2 for iron. Similar to the case of the steel irradiated to > 10 dpa, the uniform deformation value defined from the engineering diagrams does not exceed 4-6%, in agreement with data in [20-22]. These specimens lose their ability to deform uniformly and plastic flow becomes concentrated in a very narrow area, Fig. 6, which is usually located in the vicinity of one of the grippers. There are only a few cases when two areas of localized deformation show up. It is quite clear that in this situation the engineering diagrams are of little value to study the plastic flow of the irradiated material.
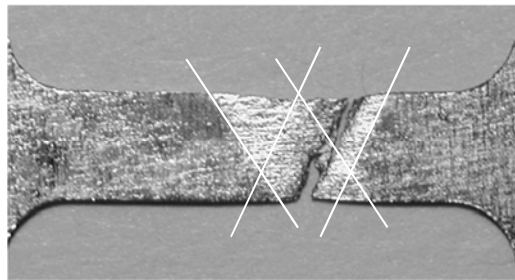

FIG.6. Localized deformation on several slip systems in molybdenum at 3×10^{20} n/cm^2.

Figures 7-9 show the engineering and true tensile curves obtained for the various metals tested. Following [16] and also for convenience it was continued to use the square root of the true deformation value of the "$\sigma_i – \varepsilon_i$" curves. Once again linearization of the "$\sigma_i – \varepsilon_i$" curves occur and can be described by the equation $\sigma_i = \sigma_0 + k\sqrt{\varepsilon_i}$.

Comparing the two types of pictures, one can see that the transition from the engineering to the true curves highlights a qualitative change in the nature of the curves. The concept of ultimate strength does not appear to be applicable since hardening continues in the deforming area up to the failure of the specimen. The local deformation may reach values that exceed values obtained from the engineering diagrams by at least 1.5-2 times.

Analyzing these experimental data one may assume that the "$\sigma_i – \varepsilon_i$" curves allow obtain more reliable information on the kinetics of the deformation processes and on some peculiarities of interactions of dislocations and radiation defects compared to that obtained from the engineering curves. Table 2 presents the values of K and σ_0 obtained from these studies. In particular, from the true curves it is seen that the σ_0 value continually increases with increasing fluence while the hardening coefficient does not change significantly.

As one can see, the *k* value for irradiated nickel is smaller than for non-irradiated nickel and at the same time *k* does not change when the fluence increases from 1.4×10^{19} to 1.3×10^{20} n/cm^2.
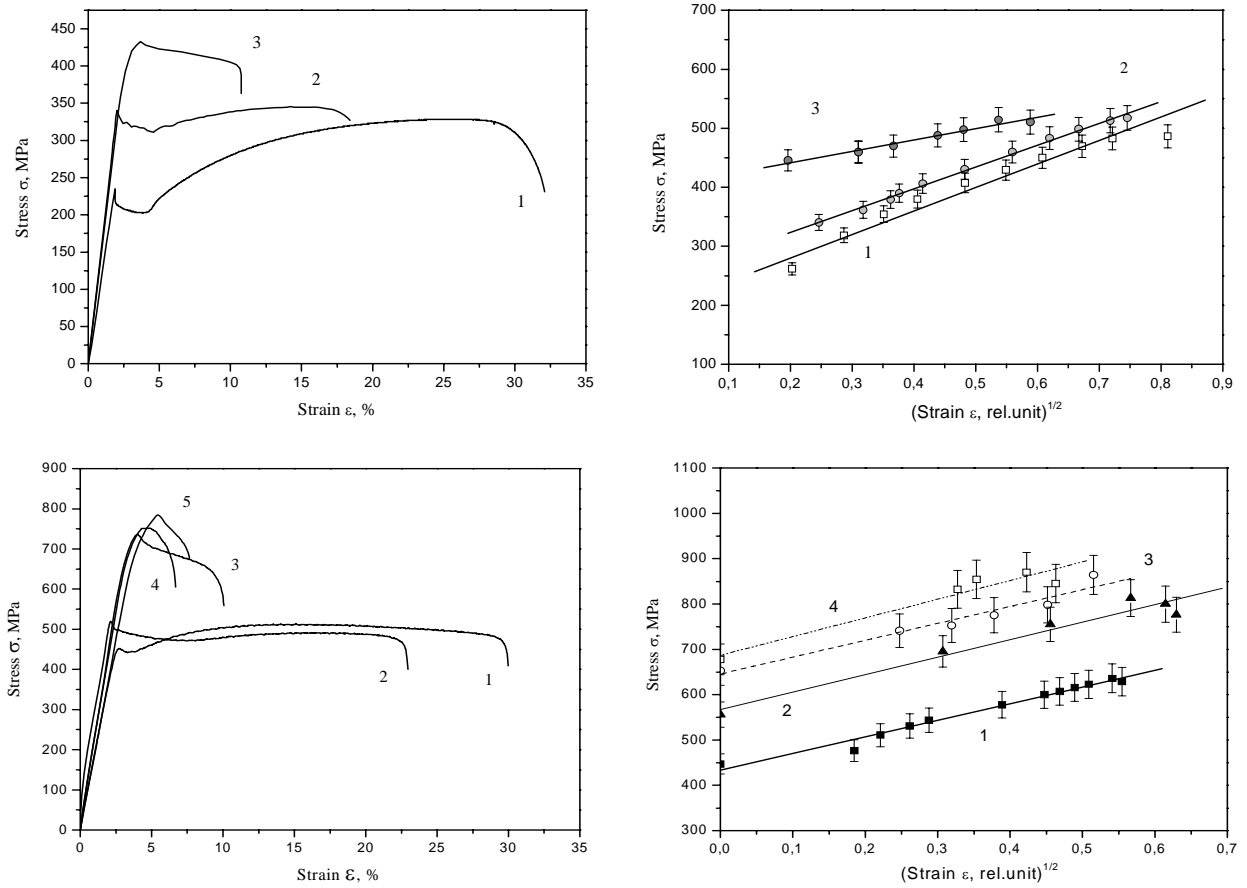
FIG.7. Engineering "stress – deformation" curves and "$\sigma_i – \varepsilon_i$" relationships for the non-irradiated and neutron irradiated bcc-materials. On the top: Armco-iron, 1 – non-irradiated specimen, 2 – 5×10^{18} n/cm^2, 3 – 1.4×10^{19} n/cm^2. On the bottom: molybdenum, 1 – non-irradiated; 2 – 1.1×10^{19} n/cm^2; 3 – 1.2×10^{20} n/cm^{20}; 4 – 3×10^{20} n/cm^2; 5 – 6.2×10^{20} n/cm^2.
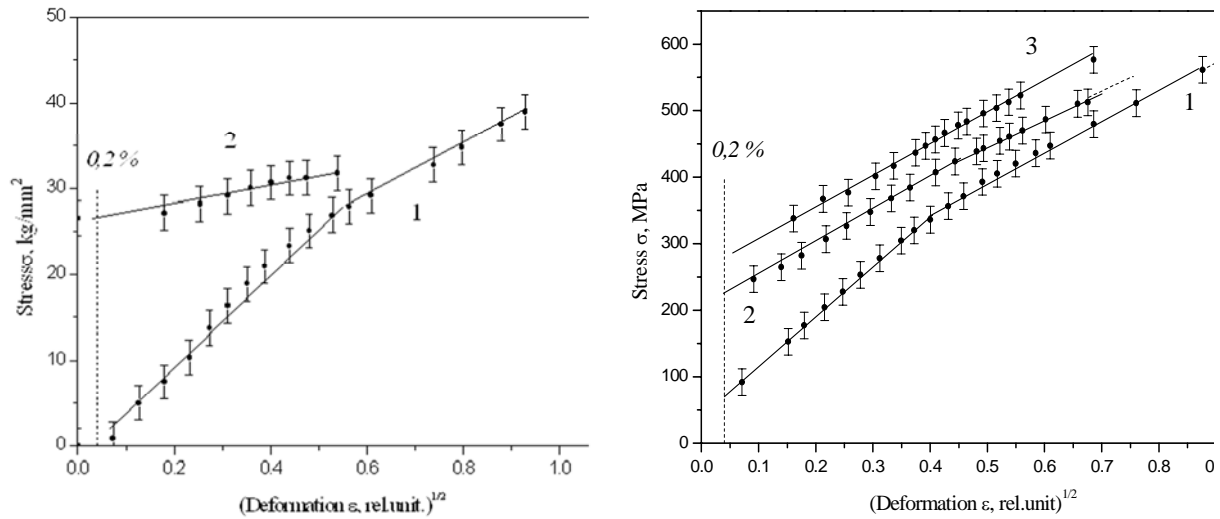
FIG.8. "$\sigma_i – \varepsilon_i$" relationships for non-irradiated and neutron irradiated copper (at the left, 1 –non-irradiated specimen, 2 – 2×10^{20} n/cm^2) and nickel (at the right, 1 –non-irradiated specimen, 2 – 1.4×10^{19} n/cm^2; 3 – 1.3×10^{20} n/cm^2)
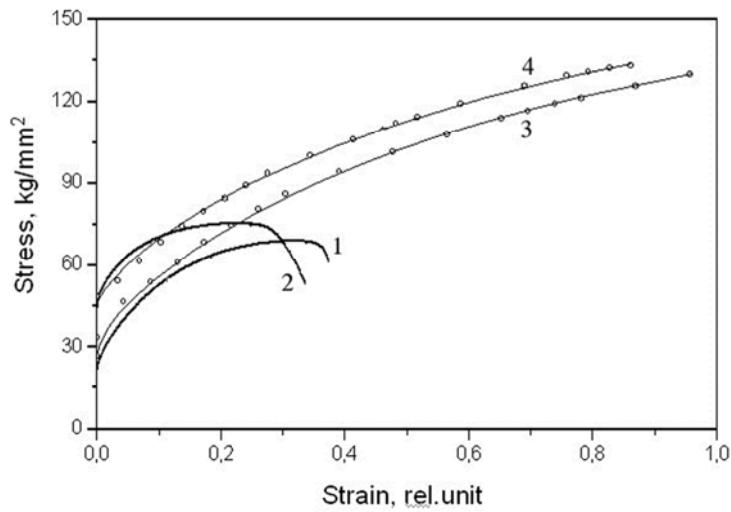
FIG.9. Engineering curves (1,2) and "$\sigma_i - \varepsilon_i$" relationships (3,4) for the non-irradiated (1,3) and irradiated (2,4) $12Cr_{18}Ni_{10}Ti$ steel in WWR-K after $1.4x10^{19}$ n/cm^2.

TABLE 2. VALUES K AND σ_0 FOR UN-IRRADIATED AND IRRADIATED MATERIALS

Material	Fluence (n/cm^2)or damage dose (dpa)	Yield stress σ_{02} (MPa)	σ_0 (MPa)	k (MPa)
Steel $12Cr_{18}Ni_{10}Ti$	0	200	180	830
Steel $12Cr_{18}Ni_{10}Ti$	$1.4x10^{19}$	510	480	790
Steel $08Cr_{16}Ni_{11}Mo_3$	15.6 dpa	920	1100	690
Ni	–	59	85	587
Ni	$1.4x10^{19}$	236	205	470
Ni	$1.4x10^{19}$	316	265	448
Fe	–	202	215	369
Fe	$5x10^{18}$	311	250	369
Fe	$1.4x10^{19}$	399	405	192
Cu	–	50	13	438
Cu	$5x10^{20}$	350	259	110

Another aspect of the marker extensometry method is that it allows the visualization of the distribution of strain along the specimen axis. This is particularly useful when the material is just beginning to harden but appears still to be in the uniform elongation regime. Note in Fig. 10 that the strain is not uniform along the length of the specimen but appears to indicate

70

some periodicity. This specimen was $12Cr_{18}Ni_{10}Ti$ irradiated in WWR-K to 1.4×10^{19} n/cm^2 or ~0.01 dpa. This indicates that some areas initiate plastic deformation before others although subsequent strain rates appear to keep pace at all positions. So the term "uniform" elongation is not a completely correct description of the deformation process. Stress concentrations near the two grips might account for two of the initiation sites but not for the other three sites.
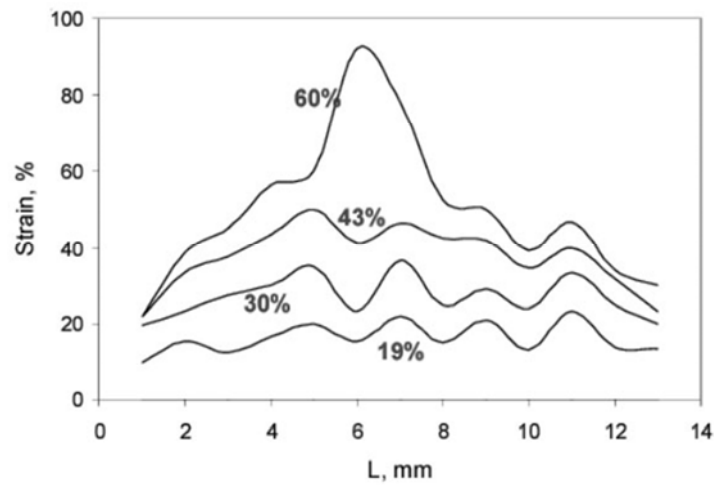
Fig.10. Distribution of strains along the length of $12Cr_{18}Ni_{10}Ti$ specimen irradiated in WWR-K to 1.4×10^{19} n/cm^2, taken at equal time intervals during the tensile test. The percentages shown are the elongation observed in the engineering curve.

Fig.11 demonstrates that until necking begins to occur the various regions exhibit identical true strain behavior, following the same true strain curve. When the ultimate stress is reached, however, necking occurs and the non-necking areas drop out of the deformation process. The true stress decreases and plastic flow stops in these bypassed areas.
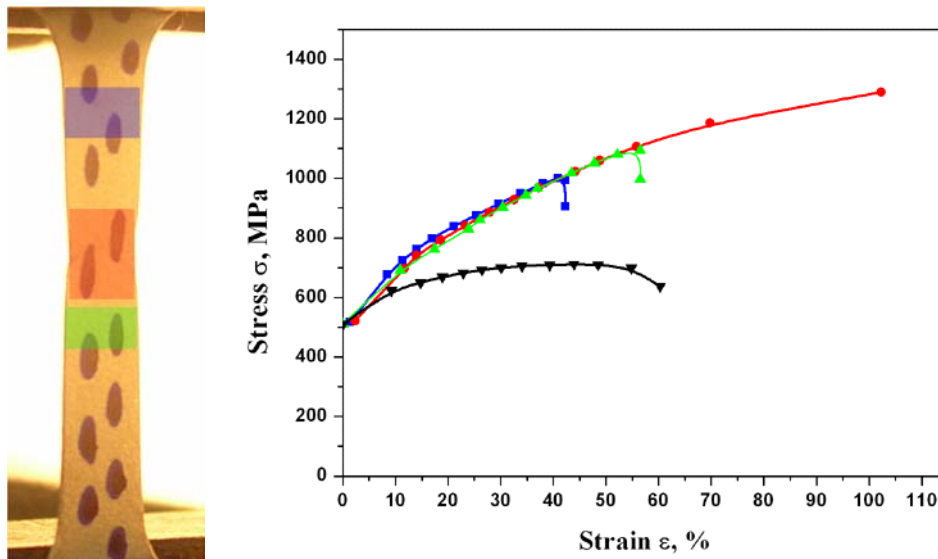
FIG.11. Comparison of engineering (black) and true strain curves (designated by color) for three areas, showing that all three follow the same true curve but as necking develops the other areas drop out of the deformation process.

8.5. Conclusions

To study the peculiarities of the deformation hardening and flow localization of radioactive materials a non-contact "digital marker extensometry" technique has been developed. It

allows to easily define the plasticity parameters and true stresses in experiments where miniature highly radioactive specimens are used.

The "σ_i – ε_i" relationship under the plastic flow and hardening of the irradiated metal polycrystals has been investigated experimentally. The true curves have been obtained for nickel, iron, molybdenum, as well as for the $08Cr_{16}Ni_{11}Mo_3$ and $12Cr_{18}Ni_{10}Ti$ steels. Describing these curves using the $\sigma_i = \sigma_0 + k\sqrt{\varepsilon_i}$ equation demonstrates that the concept of ultimate stress is an artifact arising from flow localization and is not fully informative of the hardening mechanisms operating in highly irradiated materials
.

ACKNOWLEDGEMENTS

REFERENCES

[1] MALYGIN, G.A., Structural factors which affect the stability of the plastic deformation under a tensile test of the bcc metals, Solid state physics, 47 No.5 (2005) 870.

[2] MALYGIN, G.A., Analysis of the structural factors responsible for the formation of the bottle neck area under a tensile test of the fcc metals and alloys, Solid state physics, 47 No.2 (2005) 236.

[3] IVANOVA, V.S., Synergetics: Strength and failure of the metal materials, Moscow, (1992).

[4] PANIN, V.E., KOROTAYEV, A.D., MAKAROV, P.V., KUZNETSOV, V.M., Physical mezomechanics of the materials, Institute Newsletter, Physics No.9 (1998) 8.

[5] KRISHTALL, M.M., The instability/mesoscopic non-uniformity interaction of the plastic deformation. Part 2, The non-linear model of the plastic deformation stability: the build-up, analysis, numerical simulation and quantitative estimates, Physics of Metals and Material Science, 92 No.3 (2001) 96.

[6] MALYGIN, G.A., Analysis of the factors causing the instability of deformation and the loss of the plasticity for the neutron irradiated copper, Solid State Physics, 47 (2005) 632.

[7] MAKSIMKIN, O.P., GUSEV, M.N., OSIPOV, I.S., The deformation extensometry under the mechanical tests of the highly radioactive metal and alloy specimens, Information News of the National Nuclear Center of the Republic of Kazakhstan, No.1 (2005) 46.

[8] BABUSHKIN, A.A., MAKSIMKIN, O.P., CHELNOKOV, S.Y., Optical-electron extensometer. Publications of the Academy of Sciences of Kazakhstan, Physics / Mathematics Series No 2 (1986).

[9] BRILLAUD, C., MEYLOGAN, T., SALATHE, P., Use of Laser Extensometer for Mechanical Tests on Irradiated Materials, Effect of Radiation on Materials: 17th International Symposium, ASTM STP 1270 (1996) 1144.

[10] MIGACHEV, B.A., VOLKOV, V.P., Enhancement of the measuring precision technique of the deformation state using the coordinate networks, Factory Laboratory, 54 No 5 (1988) 77.

[11] GORBATENKO, V.V., POLYAKOV, S.N., ZUEV, L.B., Visualization of the local deformation areas, using the calculational de-correlation of the video images with a

speckle-structure. (For example, the Chernov-Luders bands), Factory Laboratory. Material Diagnostics, 67 No.7 (2001) 29.

[12] BYUN, T.S., FARRELL, K., Plastic instability in polycrystalline metals after low temperature irradiation, Acta Materialia, 52 No.6 (2004) 1597.

[13] HORSTEN, MARC, G., DE VRIES, M.I., Irradiation Hardening and Loss of Ductility of Type 316L(N) Stainless Steel Plate Material Due to Neutron-Irradiation, Effect of radiation on Materials: 17th International Symposium, ASTM STP 1270 (1996) 919.

[14] HAMILTON, M.L., Other Neutron-Induced Evolution of Mechanical Properties of 20% Cold-Worked 316 Stainless Steel as Observed in both Miniature Tensile and TEM Shear Punch Specimens, Effects of Radiation on Materials, 19th International Symposium, STP 1366, 1003.

[15] GORYNIN, I.V., et al., A comparative evaluation of the operational characteristics of the austenitic class steels with respect to the operational conditions of the ITER discharge chamber, A Collection of works "Radiation Effect on the Fusion Reactor Materials", (1992) 90.

[16] TREFILOV, V.I., et al., Deformation hardening and failure of the polycrystal metals, (1989) 256.

[17] MALYGIN, G.A., Analysis of the structural factors causing the formation of the necking at tensile tests of metals and fcc-alloys, Solid State Physics, 47 No.2 (2005) 236.

[18] GARNER, F.A., Irradiation Performance of Cladding and Structural Steels in Liquid Metal Reactors, V.10A of Materials Science and Technology: A Comprehensive Treatment, VCH Publishers, (1994) 419.

[19] GARNER, F.A., Demonstration of the Separate Temperature and dpa Rate Dependencies of Void Swelling in 300 Series Stainless Steels, 12th International Conference of Fusion Reactor Materials, Santa-Barbara, December 4-9, (2005), 334.

[20] PARSHIN, A.M., Structure, strength and radiation damage of the corrosion resistant steels and alloys, Chelyabinsk, Metallurgy", Chelyabinsk branch, (1988) 656.

[21] NEUSTROEV, V.S., BOEV E.V., GARNER, F.A., Low temperature Embitterment of Austenitic Steel Examined using Ring-Pull Tensile Tests and Microhardness Measurements, 12th International Conference of Fusion Reactor Materials, Santa-Barbara, (2005) 332.

[22] MAKSIMKIN, O.P., Phase-structure processes and their role in hardening and embrittlement of the irradiated metal materials, Doctor's of Physics and Mathematic Scientific Thesis, Almaty, (1996).

ANOMALOUSLY LARGE DEFORMATION OF 12CR$_{18}$NI$_{10}$TI AUSTENITIC STEEL IRRADIATED TO 55 DPA AT 310ºC IN THE BN-350 REACTOR

M.N, GUSEV[1], O.P. MAKSIMKIN [1], I.S. OSIPOV [1], F.A GARNER[2]
[1]Institute of Nuclear Physics, Almaty, Kazakhstan
[2]Pacific Northwest National Laboratory, Richland USA
Email: gusev.maxim@inp.kz

Abstract: Whereas most previous irradiation studies conducted at lower neutron exposures in the range 100-400 ºC have consistently produced strengthening and strongly reduced ductility in stainless steels, it now appears possible that higher exposures may lead to a reversal in ductility loss for some steels. A new radiation-induced phenomenon has been observed in 12Cr$_{18}$Ni$_{10}$Ti stainless steel irradiated to 55 dpa. It involves a "moving wave of plastic deformation" at 20ºC that produces "anomalously" high values of engineering ductility, especially when compared to deformation occurring at lower neutron exposures. Using the technique of digital optical extensometry the "true stress σ –true strain ε" curves were obtained. It was shown that a moving wave of plastic deformation occurs as a result of an increase in the intensity of strain hardening, $d\sigma/d\varepsilon(\varepsilon)$. The increase in strain hardening is thought to arise from an irradiation-induced increase in the propensity of the $\gamma \rightarrow \alpha$ martensitic transformation.

9.1. Introduction

It is generally accepted that irradiation of stainless steels at temperatures of 100-400ºC leads to a rapid increase in strength and a concurrent reduction in both uniform and total elongation during deformation, a behavior that is clearly seen in "engineering" stress-strain curves and that is almost always associated with early flow localization leading to necking.

Using a technique called "digital marker extensometry", however, we have shown recently that the stress-strain deformation characteristics (true stress-true deformation) continue unchanged in the necking region even though the remainder of the specimen no longer participates in the deformation process [1, 2]. Figures 1 and 2 demonstrate this behavior for stainless steels irradiated in two different reactors. These results signal that a distinction should be made between "true embrittlement" involving suppression of material capability for plastic deformation and "quasi-embrittlement" involving a reduction of uniform and total deformation as a result of development of a macroscopic neck.

Another well-accepted perception is that continued neutron exposure quickly leads to a saturation in mechanical properties that remains unchanged until significant void swelling is attained [3-7]. It now appears that this perception must be at least partially modified for relatively low irradiation temperature and very high fluence exposure, especially for steels prone to austenite-to-martensite instability. In this paper we demonstrate that the trend toward reduced elongation with increasing exposure can be reversed at very high dose.
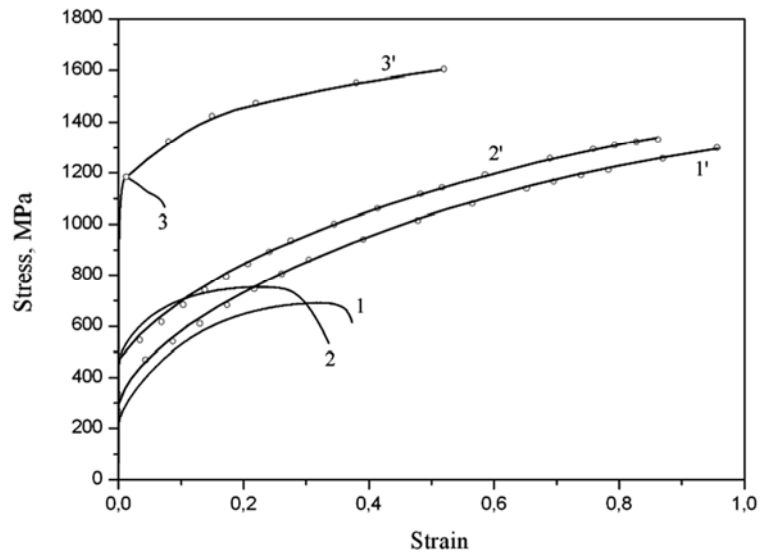
FIG.1. Engineering stress-strain curves (1, 2, 3) and "$\sigma_i - \varepsilon_i$" relationships (1', 2', 3') for non-irradiated (1) and irradiated (2, 3) stainless steels tested at 20ºC. 2 – 12Cr$_{18}$Ni$_{10}$Ti (WWR-K, 1.4x10^{19} n/cm^2 and 80ºC), 3 – 08Cr$_{16}$Ni$_{11}$Mo$_3$ (BN-350, 15.6 dpa and 340ºC).
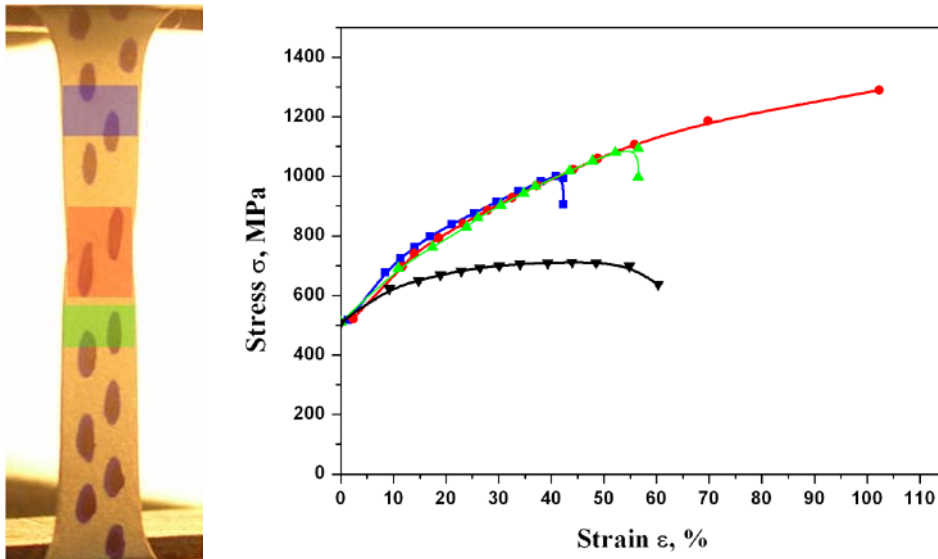
FIG.2. 12Cr$_{18}$Ni$_{10}$Ti irradiated to 1.4 x 10^{19} n/cm^2 (E>0.1) in the WWR-K reactor at 80ºC and tested at 20ºC. Comparison of engineering (black) and true strain curves (designated by colors) for three areas, showing that all three areas follow the same true curve initially, but as necking develops the other areas drop out of the deformation process.

9.2. Experimental details

A hexagonal wrapper constructed from 12Cr$_{18}$Ni$_{10}$Ti steel was removed from a spent fuel assembly designated CC-19 after irradiation in the reflector region of the BN 350 fast reactor core. The wrapper walls were 2 mm thick with face-to-face distance of 96 mm. Prior to irradiation the wrapper was formed with a final cold deformation of 15 to 20%, followed by annealing at 800°C for an hour. During irradiation the wrapper reached a maximum dose and temperature of 55 dpa and 310°C. The inlet temperature of 280ºC defines the lowest temperature of the wrapper.

76

Hexagonal cross sections of 10 mm height were cut at various elevations between +160 mm and –160 mm measured relative to the core center-plane. From these sections flat rectangular specimens of size 20x2x0.3 mm were mechanically produced. Subsequently, mini-tensile specimens with gauge length of 10x2x0.3 mm were produced by mechanical grinding and electrolytic polishing to achieve the desired dimensions and surface quality.

Pneumatic grips were used for holding the specimen in an Instron-1195 tensile machine. Uniaxial tensile tests on both unirradiated and irradiated specimens were performed at 20ºC at a strain rate of 8.3×10^{-4} s^{-1}.

A technique called "digital marker extensometry" was used which incorporates digital photo or video recording of the specimen during deformation. The surface of the specimen was marked with small (~0.3 mm) dots of dye in order to track the deformation on a local level. This technique was described in an earlier report and is especially useful in observing highly-irradiated miniature specimens subject to intense flow-localization [1,2]. Application of this technique makes it possible to obtain the "true stress–true strain" behavior for a miniature specimen, as well as to identify the localized deformation region and to trace its evolving geometry during continuous deformation.

9.3. Results

In Fig. 3 the engineering diagrams of both irradiated and unirradiated specimens are shown. As expected the unirradiated steel is characterized by high ductility and high ability to strain harden. Following irradiation to ~15 dpa at 340ºC the yield strength of similar steel strongly increases and a neck develops just after reaching the yield point. The uniform elongation is very small and total ductility falls to 3.7%.

Based on current perceptions of saturation, one would expect that steel irradiated up to 55 dpa would achieve deformations <7.5%, even in the absence of void swelling. However, a ductility of 20 to 25% was achieved in this specimen. This result was confirmed by ten other tests to be typical and not an anomaly. Note that after a small decrease in strength following yielding there is an extended plateau without significant increase in load.

As shown in Fig. 4, a series of freeze-frame video images taken during tensile testing shows that localized deformation initially forms near the upper grip position, most likely due to stress concentration by the grip. However, in contrast to irradiation to lower doses, a neck did not develop at 55 dpa. The localized deformation band instead progressively extended its lower boundary, producing a moving deformation front or deformation wave that moved down the specimen. The wave moved along ~2/3 of the specimen length. All of the deformation at a given instant appeared to occur at the wave front with material behind or in front of the wave being very weak or nonexistent.

Fig. 5 shows the distribution of local deformation over the specimen length as the test progresses. An abrupt increase in local deformation from zero up to 30 to 35% is observed at the moment the front passes that point. Failure with local deformation exceeding 60% occurred very near to the original place where the deformation wave appeared. It appears that the original wave might have continued its downward progress if failure had not occurred near the top of the specimen. Otherwise, formation of this second front had no effect on the progress of the original wave.
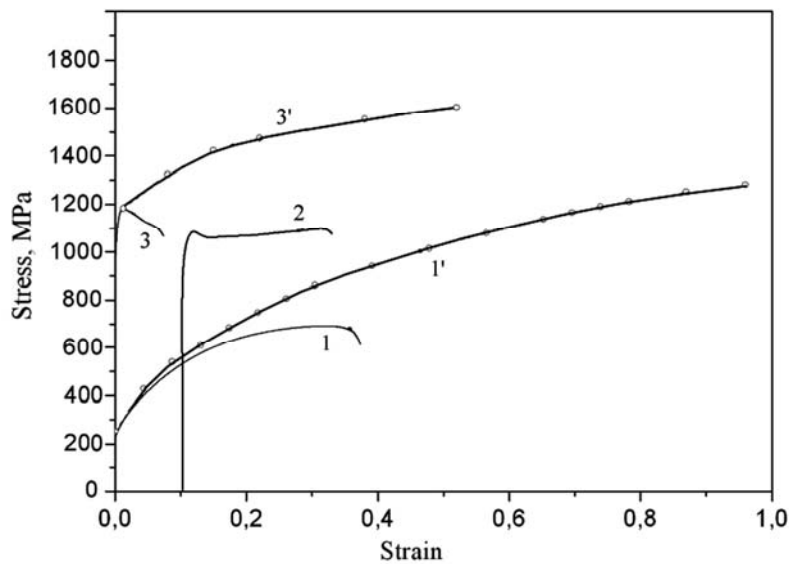
FIG.3. Engineering stress-strain diagrams (curves 1, 2, 3) at 20ºC for $12Cr_{18}Ni_{10}Ti$ (1 and 2) and $08Cr_{16}Ni_{11}Mo_3$ irradiated in BN-350 (3) along with the corresponding "true" curves (1' and 3'): 1 –unirradiated steel; 2 –irradiated to 55 dpa; 3 –irradiated to 15.6 . Curve 2 is shifted to the right to make visualization easier.
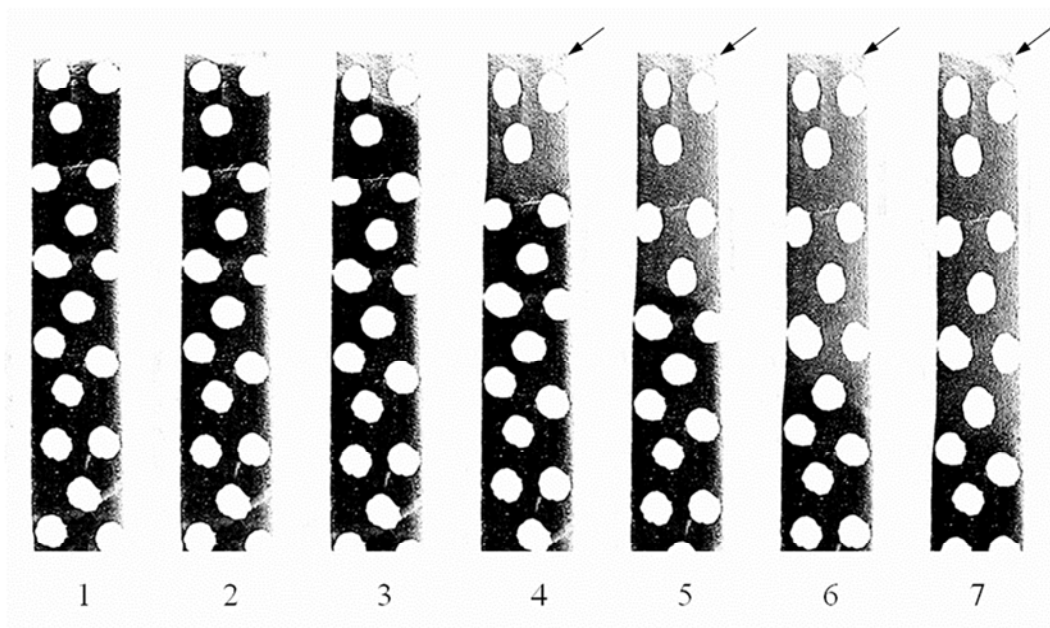
FIG.4. Freeze frames taken during deformation at 20ºC of the specimen irradiated to 55 dpa. Photographs have been digitally processed to increase the contrast. The boundary between the lighter distorted and darker undistorted areas moves downward with time. Distorted dots behind the boundary also show the local distortion. Arrows on photos 4 through 7 show the second later-developing and immobile neck.

Failure arose via development of a second late-developing deformation band that was immobile. This band is marked by arrows on frames 4 through 7 in Fig. 4. The immobility of the second deformation band was probably a result of the constraints imposed on the band by both the upper gripper and the upper boundary of the original wave. This suggests that deformation within the deformed band is terminal and will not allow the second band to propagate through already deformed material.
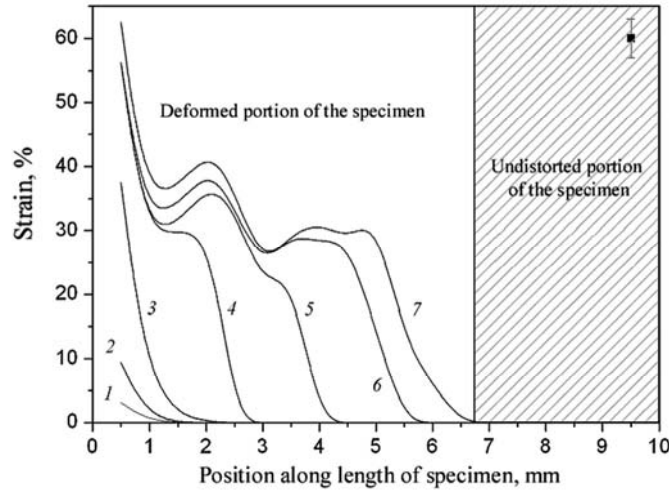
FIG.5. Distribution of local deformation along the length of the specimen irradiated to 55 dpa at various stages of the experiment. Label 1 through 7 correspond to numbers of photographs in FIG.4.

9.4. Discussion

The condition for occurrence and development of localized deformation of the neck [8, 9] is:

$$d\sigma/d\varepsilon \leq \sigma, \tag{1}$$

which can be rewritten in more convenient form:

$$d\sigma/d\varepsilon - \sigma \leq 0 \tag{2}$$

One may show that localization of deformation in compliance with a given condition starts at the moment when local strain hardening can no longer compensate for geometrical "softening" which occurs as a result of a decrease in the specimen cross section.

It is clear that for stopping local neck formation and displacement of the deformation into neighboring, less deformed space, the law which governs hardening must be changed, i.e., it is necessary that relation (2), on achieving a certain extent of deformation, becomes invalid. As a rule this does not happen in either unirradiated or neutron-irradiated pure metals, where $d\sigma/d\varepsilon$ always decreases as ε grows (see for example curve 1 on Fig. 6).

Fig.6 presents "stress-deformation" curves obtained using the marker extensometry technique. One may observe (curve 3', Fig.1 and curve 2, Fig.6) that in $12Cr_{18}Ni_{10}Ti$ at 55 dpa the initial stage of deformation is close to that of $08Cr_{16}Ni_{11}Mo_3$ at ~15 dpa. Almost immediately on reaching the yield point, $d\sigma/d\varepsilon$-σ reduces to negative values, and the neck develops. However, in contrast to other materials we have studied, at local deformations of ~25 to 30% a smooth upward trend is observed in the "σ-ε" curve. As $d\sigma/d\varepsilon$ increases the value of "$d\sigma/d\varepsilon$-σ" becomes positive, indicating that strain hardening is increasing strongly.

Apparently it is the increase in $d\sigma/d\varepsilon$ that leads to suppression of development of a local neck, thereby displacing the deformation source to neighboring, undeformed space, thus generating the deformation wave. We consider it to be very significant that the second late-forming deformation band could not move through the previously deformed region.
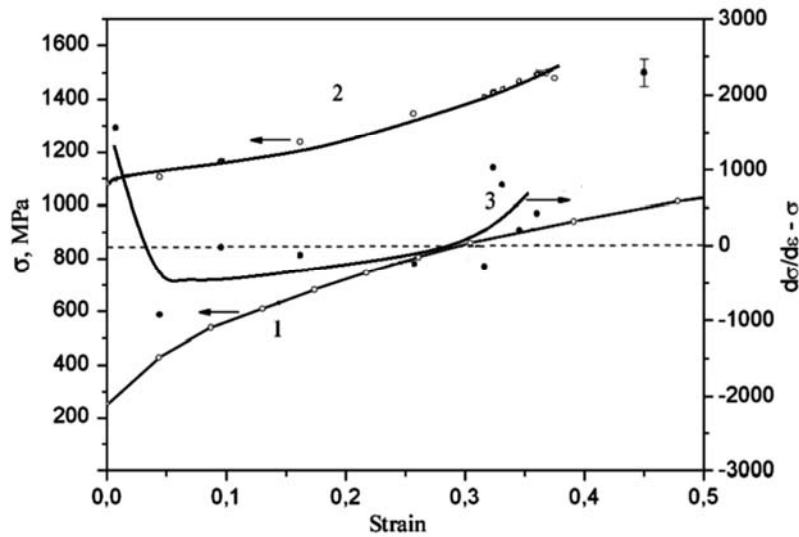
FIG.6. Curves of "true stress–true strain" for unirradiated $12Cr_{18}Ni_{10}Ti$ specimen (1) and 55 dpa specimen (2). The dependence of ($d\sigma/d\varepsilon$ - σ) versus ε (for 55 dpa-sample) is shown in curve(3).

One potential source of the wave phenomenon is the $\gamma\rightarrow\alpha$ martensitic transformation and this possibility is now being investigated. This low-nickel steel is known to be very sensitive to martensite formation, especially during low temperature deformation, and to increase in propensity toward martensite with radiation-induced hardening and radiation-induced segregation [10]. The fact that this behavior occurs at higher exposures but not at lower doses where saturation of strength had already occurred was first thought to reflect some second-order effect such as the progressive transmutation-induced loss of Mn, one of the γ-stabilizing elements. However, calculations showed only 2-3% loss of Mn had occurred by 55 dpa. Therefore other mechanisms such as radiation-induced segregation are being investigated.

Similar deformation behavior involving an increase in intensity of strain hardening has been observed in this same steel in the unirradiated condition during deformation at cryogenic temperatures [11]. Intense martensitic transformation was cited as the cause, but the marker extensometry technique wasn't used in this experiment so it is not certain whether a deformation wave was associated with this behavior.

9.5. Conclusions

A new radiation-induced phenomenon has been observed in steel $12Cr_{18}Ni_{10}Ti$ irradiated to 55 dpa. It involves "a moving wave of plastic deformation" at 20ºC that produces "anomalously" high values of engineering ductility, especially when compared to deformation occurring at lower neutron exposures or for more stable steels. Using the technique of digital optical extensometry the "true stress σ –true strain ε" curves were obtained. It was shown that a moving wave of plastic deformation occurs as a result of an increase in the strain hardening, $d\sigma/d\varepsilon(\varepsilon)$. The increase in strain hardening is thought to arise from an irradiation-induced increase in the propensity of the $\gamma\rightarrow\alpha$ martensitic transformation.

REFERENCES

[1]   MAKSIMKIN, O.P., GUSEV, M.N., OSIPOV, I.S., Deformation extensometry during mechanical tests of highly radioactive metal and alloy specimens, Information News of the National Nuclear Centre of the Republic of Kazakhstan, 1 (2005) 46.

[2]   GUSEV, M.N., MAKSIMKIN, O.P., OSIPOV, I.S., GARNER, F.A., Application of Digital Marker Extensometry to Determine the True Stress-Strain Behavior of Irradiated Metals and Alloys, Proceedings of 5th International Symposium on Small Specimen Test Technology", paper 016803JAI, Journal of ASTM International (in preparation).

[3]   GARNER, F.A., HAMILTON, M.L., PANAYOTOU, N.F., JOHNSON, G.D., The Microstructural Origins of Yield Strength Changes in AISI 316 during Fission or Fusion Irradiation, J. Nuclear Materials, 103-104 (1981) 803.

[4]   GARNER, F.A., Chapter 6: Irradiation Performance of Cladding and Structural Steels in Liquid Metal Reactors, Vol. 10A of Materials Science and Technology: A Comprehensive Treatment, VCH Publishers, (1994) 419.

[5]   HAMILTON, M.L., HUANG, F.H., YANG, W.J.S., GARNER, F.A., Mechanical Properties and Fracture Behavior of 20% Cold-Worked 316 Stainless Steel Irradiated to Very High Exposures, Effects of Radiation on Materials: Thirteenth International Symposium (Part II) Influence of Radiation on Material Properties, ASTM STP 956, F. GARNER, A., IGATA, N. C., HENAGER, H., Jr., Eds., ASTM Philadelphia, PA, (1987) 245.

[6]   PARSHIN, A.M., Structure Resistibility and Radiation Damage in Corrosion-resistant Steels and Alloys, Chelyabinsk, Metallurgy", Chelyabinsk Department, (1988) 656.

[7]   BARABASH, V., et al., Materials Challenges for ITER – Current Status and Future Activities, J. Nuclear Materials. 367-370 (2007) 21.

[8]   MALYGIN, G.A., Analysis of structural factors responsible for formation of the bottle neck area during tensile tests of fcc metals and alloys, Solid State Physics 47, No.2 (2005) 236.

[9]   TREFILOV, V.I., et al., Deformation hardening and failure of polycrystal metals, Kiev, "Naukova Dumka", (1989) 256.

[10]   WAS, G.S., Fundamentals of Radiation Materials Science, Springer, (2007).

[11]   NAGY, E, MERTINGER, V., TRANTA, F., SÓLYOM, J., Deformation induced martensitic transformation in stainless steels, Materials Science and Engineering, A378 (2004) 308.

UNIQUE IRRADIATION RIGS DEVELOPED FOR THE HFR PETTEN AT THE JRC-IE: LYRA, QUATTRO AND FUEL IRRADIATION FACILITIES

L. DEBARBERIS, B. ACOSTA, J. DEGMOVA, A. ZEMAN, M. FUETTERER,
E. D'AGATA, P. HAEHNER
JRC-IE, Institute for Energy of European Commission
Petten, Netherlands
Email: Luigi.DEBARBERIS@ec.europa.eu

Abstract: The HFR Petten is a key research reactor in Europe and in the course of the last decades several dedicated irradiation facilities have been developed and successfully operated. For example, as regards materials irradiation, in the frame of the European Network AMES (Ageing Materials and Evaluation Studies), the irradiation behaviour of reactor pressure vessel (RPV) steels, and thermal annealing efficiency and sensibility to re-irradiation damage are being investigated. Today the rig is a very promising tool for GIF research on materials. Similarly the QUATTRO rig has been tailored to GIF research. Dedicated irradiation rigs are also designed and operated by the IE to test advanced fuels; e.g. HTR fuel. An overview of the developed facilities is given in the following paper as well as examples of achieved results.

10.1. High flux reactor

The High Flux Reactor (HFR) in Petten, The Netherlands, is one of the few high power multi-purpose research reactors still in operation in Europe; see Fig. 1. It is a 45 MW water-cooled tank reactor of the Oak Ridge Research Reactor (ORR) design. The reactor is property of the European Union (EU), and belongs to the Institute for Energy (IE) of the Joint Research Centre (JRC) of the EU. Program management and users support is task of the IE. Reactor operation is contracted to the Dutch national research organisation NRG [1].

The exploitation program of the HFR is highly diversified. It encompasses not only materials and fuel research for fission and fusion reactors, but also fundamental research with neutrons, large scale radioisotope production, boron neutron capture therapy (BNCT), neutron-radiography, activation analysis and processing with neutrons [2].

Within a cylindrical containment shell, internal diameter 28 m, a thick walled concrete pool structure is arranged, comprising the reactor pool and additional pools for handling experiments and storing spent fuel elements, partly covered by a large dismantling and handling cell. The reactor core is housed in the vessel which forms part of the closed primary circuit, in which the light water coolant and moderator is circulated.

The tank is immersed in the 8.7 m deep reactor pool. At the beginning of the 1980's the reactor vessel had to be replaced because of suspected degradation of the vessel materials properties. A fully redesign and adaptation to present experimental requirements took place.
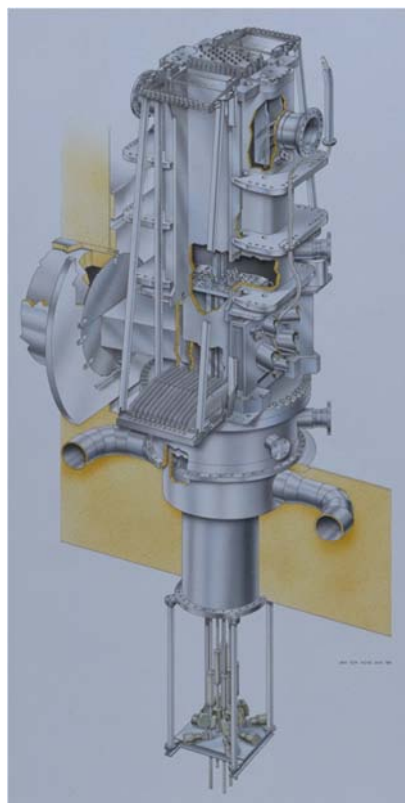
FIG.1. HFR view.

Replacement was executed in 1984.The new vessel is composed of a lower cylindrical part embedded in the concrete floor of the pool and an upper pool part with rectangular cross-section, which provides easy access to the pool side facility. Direct vertical experiment access to the in-vessel positions is through holes of the reactor top lid, which also supports the experimental tubes. The High Flux Reactor (HFR) at Petten is a multi-purpose research reactor which uses light water as coolant and moderator. The normal operating power is 45 MW. The core lattice array is a 9x9 array (729 mm x 750.4 mm) containing 33 fuel assemblies, 6 control assemblies, 19 experimental positions and 23 beryllium reflector elements. The fuel assemblies (horizontal section 81 mm x 77 mm, height 924 mm) contain 23 vertically arranged parallel, curved, fuel plates with a height of 625 mm. Each plate consists of a layer of Al + U alloy meat with a thickness of 0.51 mm, clad with Al of 0.38 mm thickness for the inner plates and 0.57 mm for the outer fuel plates. The length of the fuel inside the plate is 600 mm. The uranium is about 93% enriched in ^{235}U. The uranium content of the fresh fuel assemblies is 450 g ^{235}U. The two flat side plates of each fresh fuel assembly contain together 1000 mg ^{10}B. There are six control rod assemblies, each of them consists of a cadmium section on top of a fuel section. Their drive mechanism is situated below the reactor vessel [3].

The HFR has a regular operation schedule. One operation cycle consists of 24.7 days of reactor operation followed by a 3.3 days reactor shut-down period which is used for installation and reloading of irradiation rigs, maintenance to the reactor and experimental facilities, and for refuelling.

The locations to install irradiation capsules or rigs are as follows:

– 9 central in-core positions (in-vessel).

– 10 in-core positions (in-vessel).

– 12 positions in the West pool side facility (PSF West).

– 10 positions in the East pool side facility (PSF East).

Twelve horizontal beam tubes are also available. Irradiation experiments of interest for ageing can be places, depending on the required fluence either In-Core or in PSF (Pool Side Facility). In-Core positions deliver much higher doses and are mainly of interest for non RPV components; e.g. internals. In the PSF, fluence rates are lower than In-Core, but sufficiently high for RPV testing (EOL conditions can be achieved in ~6-8 weeks irradiation). The Irradiation device for AMES, called LYRA has been developed for the PSF. The main HFR historical milestones are given in Table 1.

TABLE 1. MAIN MILESTONES OF THE HFR PETTEN

1957	Beginning of the construction of the HFR.
1961	Provisional licence - first criticality.
1962	Definitive licence for 20 MW operation Issued by municipal authorities - transfer the ownership of the reactor over to the European Commission.
1966	Licence adaptation for operation at max. 30 MW.
1968	The EC becomes the licence holder -formal operator operation by ECN under contract.
1970	Entrance in force of the Nuclear Energy Act: Nuclear licences to be issued by National Authorities: Hindrance Act $\Rightarrow$ Nuclear Energy Act.
1970	Licence adaptation for operation at max. 50 MW.
1984	Replacement of the reactor vessel of the HFR: The vessel renewal allows operation at least until 2015.
1999	The HFR is operated by NRG under contract and responsibility of JRC-IE.
2003	Request for new HFR license.
2005	New license granted to NRG – EC retains ownership and responsibility for final decommissioning.

10.2. Irradiation rigs

In order to fulfil the various irradiation programmes a large number of standard and non standard irradiation rigs have been designed the past few decades, see for example the most commonly used rigs in Fig. 2. Several dedicated rigs have been developed to serve specific irradiation needs, high temperature, fuel irradiation, cryogenic irradiation, fuel ramp testing, tritium production, etc [4–6].
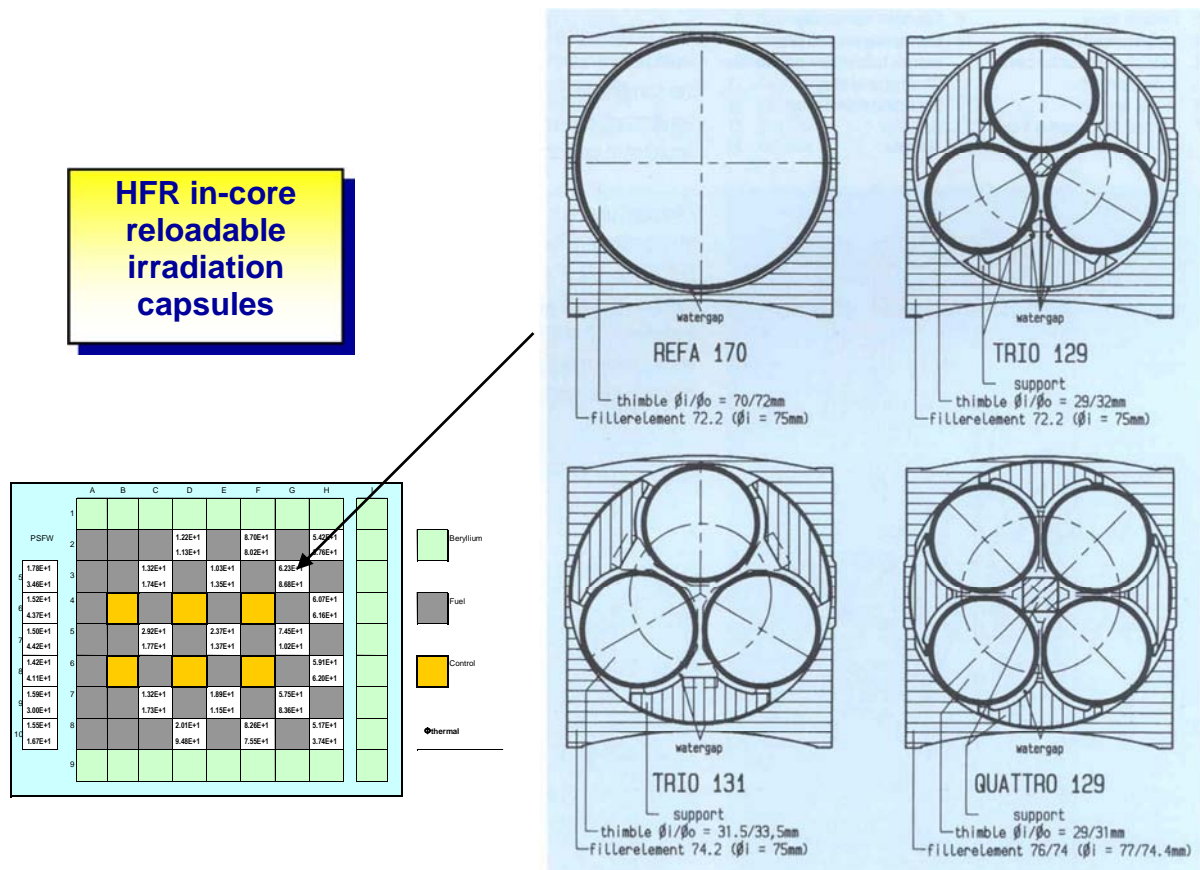
FIG.2. Standard rigs for in-core irradiation.

A few examples of dedicated rig are discussed in the following:

LYRA irradiation facility

A dedicated re-loadable irradiation facility has been designed and developed in order to carry out the necessary RPV irradiation work and reference work for AMES at the High Flux Reactor Petten, (HFR). The irradiation facility is located at the Pool Side Facility, (PSF), of the HFR. A γ-heating shield is designed in order to minimize the thermal gradients and the samples target temperature is maintained by means of a complex system of heating plates.

The required fluence levels for EOL of LWR pressure vessels can be obtained in the PSF in reasonable irradiation times, with parametric variation of irradiation time of the orders of 6-8 weeks. The γ-heating can be conveniently shielded in order to cope with the required temperature gradients. Suitable heater and temperature control units are needed to keep the samples at the required temperature during irradiation. Due to the existing natural fluence rate gradient in the PSF special provision needs to be taken in order to cope with the required fluence gradients required; i.e. periodical 180° rotation of the sample holder.

A space of up to 59x64 mm is available to accommodate sample holders with different loadings for a maximum length of sample column of up to 400 mm. As many as 200 Charpy V-notched samples (10x10x55 mm), or 12 FTT specimens (25.4x61x63.5 mm) can be accommodated in the available space. The irradiation facility can be unloaded and reloaded with a new sample holder, eventually containing pre-irradiated samples, in the dismantling cell (DM) inside the reactor building.

The use of standard capsules available for HFR in-core experiments has been considered and rejected for short precision irradiation due to a number of related disadvantages:

- Limited dimension of in-core channel.
- Difficulty in controlling and correcting the fluence and temperature gradients.
- Very high core γ-heating and no possibility to shield it.
- Limited freedom in fluence rate choice (in-core HFR positions.
- Less flexibility in irradiation time variation (fixed HFR cycle duration of 24.7 days).
- Impossibility of avoiding doses at low temperatures (reactor start-up).
- Limited space for electrical heaters.
- Difficulty regarding the optional use of cadmium shielding.
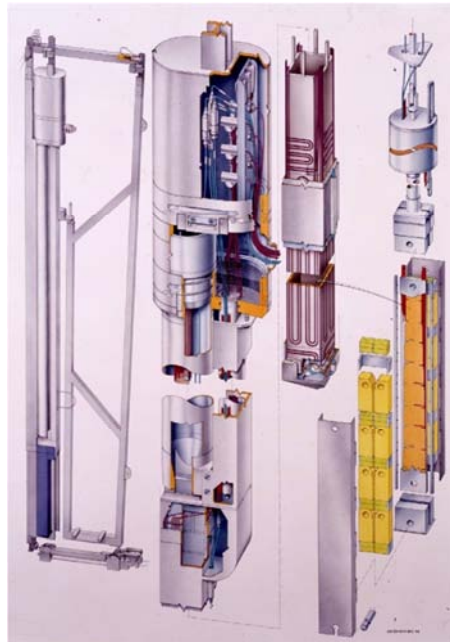
FIG.3. LYRA rig 3D view.

The use of in-core HFR positions and of standard capsules is reserved for high fluence irradiations or reactor internals ageing studies (up to several dpa).

The typical irradiation target consists mainly of a set of 40 Charpy V-notch (CVN), and 8 ASTM standard fracture toughness (FTT) specimens (25.4x61x63.5 mm). Tensile specimens can be obtained also from the CVN specimen parts. Additionally very small disks for surface analysis -about 10- and small wires (that can be put into the notch of the CVN specimens) might also be irradiated [6].

Typical PSF fluence values are dependent on the chosen position and core box wall distance; the required fluence can be built up in a different number of reactor cycles. A γ -shield has been designed in order to reduce the g-heating values to <0.15 W/g when required.

The necessary instrumentation is provided in order to demonstrate the achievement of the irradiation requirements; including:

- Sufficient number of calibrated thermocouples distributed between the samples.
- A sufficient number of flux detectors distributed between samples.
- Temperature detectors in order to verify the thermocouples recording (option).

- Self Power Neutron (SPN) Detectors (one in front and one on the back) holder) in order to verify the fluence rate gradients and to be used, after calibration against the flux detectors, as fluence indicator for the following irradiation experiments.
- Optional γ -scanning wires to verify the axial and along CVN sample axis fluence distribution; A γ-shield is mounted between the capsule and the core box wall in order to reduce the γ-heating to ~0.15W/g. The γ-shield has a separate trolley that allows the shield to be mounted in/out as the capsule is moving in/out.

10.3. HTR fuel irradiation rig

Another dedicated irradiation rig is developed to irradiate HTR fuel with the possibility to in-situ fission gas analysis also in case of simulated accidental conditions. The rig is used for fuel qualification, together with out-of-pile facilities, see Fig. 4 [5].
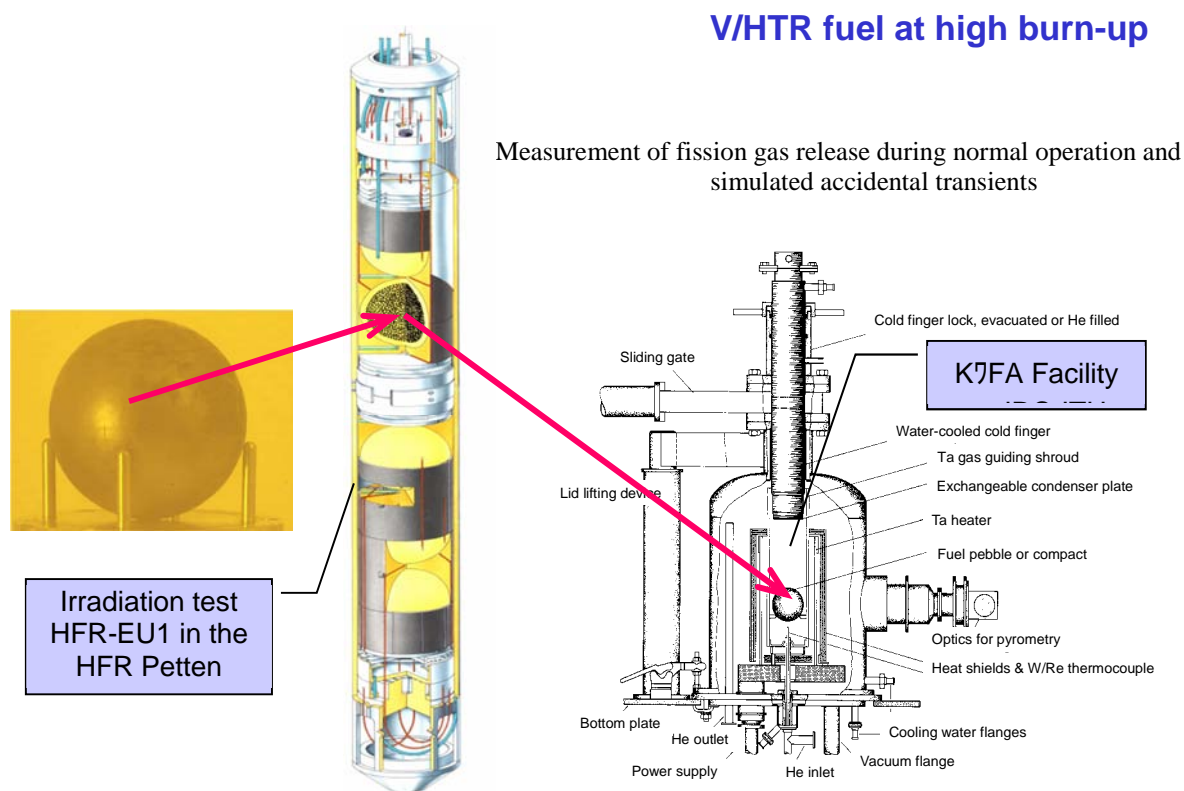
FIG.4. HTR fuel irradiation rig.

10.4. Example of results

Considering that besides standard and dedicated irradiation facility, neutron beams application are also developed at the HFR a wide variety of results are available and it will be too difficult to describe most of them. A few examples of results obtained recently in the field of RPV embrittlement are shown in the following graphs. In fact, with recent results obtained at the HFR, the semi-mechanistic model for radiation embrittlement prediction could be further developed. The model based on three additional contributions works very well on model alloys for which it was developed in first instance. After deep analysis, the model resulted also very suitable for modelling WWER-440 materials with low Nickel, see Fig. 5.
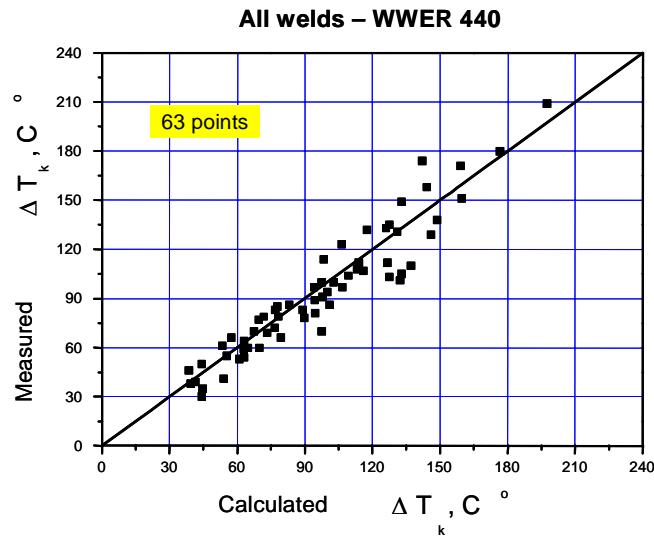
FIG.5. Results of semi-mechanistic model.

The effect of Nickel is that it can significantly enhance radiation embrittlement in model alloys and RPV materials, see Fig.6. Recent efforts to include the effect of Nickel into the semi-mechanistic model have been carried out and the results are very good. A further step, after temperature and fluence rate corrections, is to include the effect of Manganese. This is done in co-operation with IAEA (CRP-10) and with JRC initiative: model steel and realistic welds programmes.
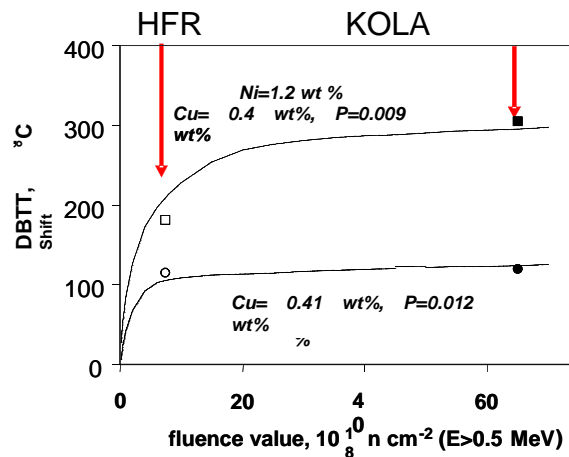
FIG.6. Typical nickel effect observed on model alloys.

As an example of a well established co-operation with the IAEA, a WWER-1000 reference steels action is recently being jointly undertaken by JRC-IAEA and the component is being stored and characterized at the moment at JRC-IE premises for future IAEA actions [7, 8].

10.5. Conclusions

Nuclear energy has to play a role as the largest single source of carbon free and base-load electricity in Europe. Sustainability, safety and security concerns, in particular nuclear safety and nuclear waste management issues, which influence the public acceptance of nuclear energy, need to be fully addressed. The JRC with the frame work programme activities is supporting the EU nuclear safety policy in EU institutional context, identifying the various customers, and providing reference results and scientific works inherent to nuclear safety.

The HFR Petten is a key research reactor in Europe and in the course of the last decades several dedicated irradiation facilities have been developed and successfully operated.

For example, as regards materials irradiation, in the frame of the European Network AMES (Ageing Materials and Evaluation Studies), the irradiation behaviour of reactor pressure vessel (RPV) steels, and thermal annealing efficiency and sensibility to re-irradiation damage is being investigated. Today the rig is a very promising tool for GIF research on materials. Dedicated irradiation rigs are also designed and operated by the IE to test advanced fuels; e.g. HTR fuel.

Important scientific results have been obtained in particular in the area of materials characterization, irradiation behaviour, high temperature behaviour and more recently on stress corrosion cracking also to support SCW applications. An overview of the developed facilities is given in this paper as well as examples of achieved results.

REFERENCES

[1]   IE-JRC-EC http://ie.jrc.ec.europa.eu/publications/annual_reports.php, Report (2008).
[2]   MOSS, R.L., et al., Procedural and practical applications of radiation measurements for BNCT at the HFR Petten Nuclear Instruments and Methods in Physics Research Section B: Beam Interactions with Materials and Atoms, 213 (2004) 633.
[3]   AHLF, J., SCHINKEL, J., Upgrading and modernization of the High Flux Reactor Petten Nuclear Engineering and Design, 137, No.1 (1992) 49.
[4]   MARKGRAF, J.F.W., TARTAGLIA, G.P., TSOTRIDIS, G., Irradiation devices and irradiation programmes at the high flux reactor (HFR) Petten for the investigation of the irradiation behaviour of stainless steels Nuclear Engineering and Design, 159 No.1 (1995) 81
[5]   FÜTTERER M.A., et al., Results of AVR fuel pebble irradiation at increased temperature and burn-up in the HFR Petten Nuclear Engineering and Design, 238 No.11 (2008) 2877.
[6]   AMES Report No 20 Project PISA - Phosphorus Influence on Steel Ageing EUR 23450 EN, ISSN 1018-5593 (2008)
[7]   DEBARBERIS, L., SEVINI, F., ACOSTA, B., KRYUKOV, A., ERAK, D., Fluence rate effects on irradiation embrittlement of model alloys International Journal of Pressure Vessels and Piping, 82 No.5 (2005) 373.
[8]   DEBARBERIS, L., et al., Effect of Irradiation Temperature in PWR RPV Materials and its Inclusion in Semi-mechanistic Model, Scripta Materialia, 53 No.6 (2005) 769.

<div align="center">**Chapter 11**</div>

USE OF THE WWR-M RESEARCH REACTOR FOR IN SITU INVESTIGATION OF THE PHYSICS AND MECHANICAL PROPERTIES OF METAL AND ALLOYS

E. GRYNIK, V. REVKA, L. CHYRKO
Institute for Nuclear Research, Kiev, Ukraine
Email: grynik@kinr.kiev.ua

Abstract: A key issue of material science related to nuclear industry is a sensitivity of structural materials to neutron irradiation. In nuclear reactors the structural materials are exposed to a neutron irradiation in addition to the mechanical and thermal impact. The irradiation causes considerable changes in the physics and mechanical material properties. These changes arise due to the formation of radiation defects and their interaction with lattice imperfections. A study of radiation effects facilitates understanding this phenomenon and allows us to predict a material behaviour under specified irradiation conditions.

Most of material characterization is based on the test of irradiated specimens after neutron irradiation but not at the time of irradiation. At the same time it is known the physical and mechanical properties of metal and alloys during neutron irradiation differ from the characteristics of irradiated materials due to much higher concentration of radiation-induced interstitials and vacancies in materials at the time of irradiation. Hence a determination of physical mechanisms of material properties changes at the time of neutron irradiation has an applied importance for the application of structural material in the nuclear industry.

One of the topical objectives of radiation materials science is a study of relaxation process in materials since relaxation characteristics describe ability of material to maintain specified stress level during a long time under different conditions including neutron irradiation. The relaxation spectrum in solids is determined quickly and accurately using the method of internal friction. A determination of internal friction at the different frequency, amplitude and temperature allows us to get info about defect properties, their location in material and interaction between each other under irradiation. The temperature dependence of internal friction for polycrystalline metals has maximum related to the grain boundaries behaviour. The study of grain boundaries relaxation can explain the radiation effect on materials.

In this paper an overview of the application of the internal friction method for in-situ investigation of the physics and mechanical properties of metal and alloys using the WWR-M research reactor is presented

11.1. The experimental method for determination of relaxation characteristics

In order to investigate the influence of neutron irradiation on relaxation properties of materials the torsion pendulum system was developed and integrated with a test channel of WWR-M research reactor in Kiev Institute for Nuclear Research (Ukraine) [1]. WWR-M is a pool-type reactor with the power 10 MWt and the maximum neutron flux (E > 0.1 MeV) in the core up to $1.2 \cdot 10^{14}$ n/cm$^2 \cdot$s. There are 27 vertical and 10 horizontal technological channels for performing scientific and applied research. A diameter of the vertical test channel is 33 mm.

The relaxation characteristics are determined using a method of internal friction. There are several test devices to measure the internal friction in materials. One of them is a torsion pendulum system which is applied for the determination of energy dissipation and elastic modulus at low frequencies of 1 – 20 Hz. In this frequency range the diffusion processes, grain boundary and interstitial atom moving and so on can be studied.

The torsion pendulum operation is based on undamped torsion oscillations. For the determination of the internal friction it is necessary to measure energy required to maintain undamped oscillations with constant strain amplitude.
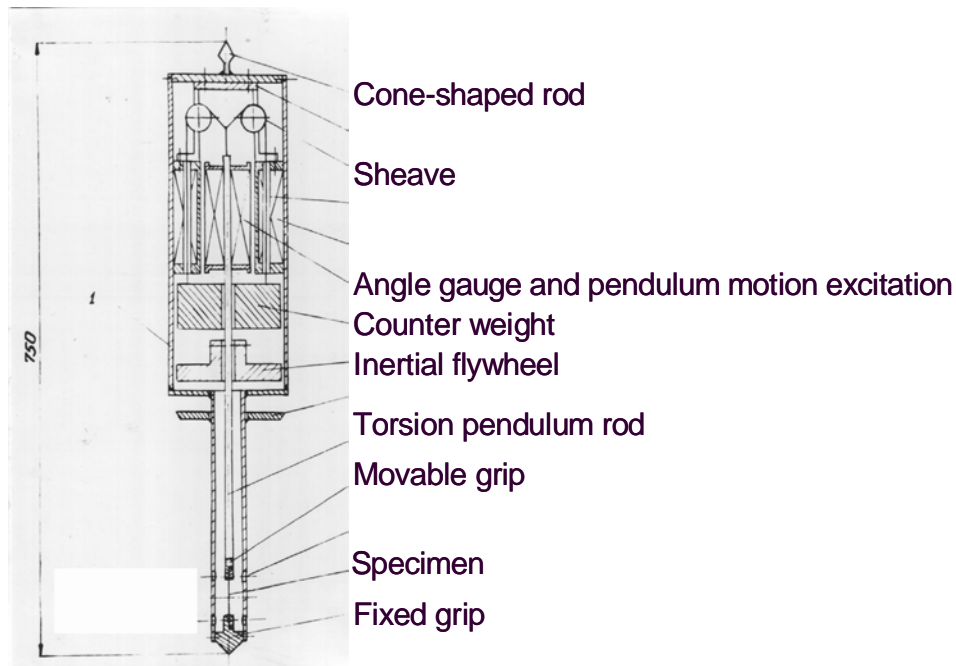
FIG.1. Torsion pendulum device.

The torsion pendulum device is designed as a removable ampoule with a fixed grip in the lower part, Fig. 1. A movable grip is fastened to a torsion pendulum rod. The test specimen is installed in these grips. An inertial flywheel and the angle gauge are fixed on the torsion pendulum rod. A movable part of the torsion pendulum is balanced with a counter weight. At the top of ampoule there is a cone-shaped rod to put the device in a technological channel of the reactor and pull out. Some ampoules are equipped with an electric heater.

It is well known that irradiation temperature has a significant influence on material radiation damage level. Hence the tests in the technological channel of a reactor should be performed at specified temperature which is well controlled. In order to maintain the specified irradiation temperature, the He pressure was being changed using a gas and vacuum system connected via communication pipes to the sealed technological channels. The He pressure range was (0.01-1) bars giving a possibility to control the temperature within 300 - 400°C.

This equipment enables to measure the internal friction and shear modulus in the temperature range of +20 to +1500°C for materials irradiated up to the fluence of $5 \cdot 10^{21}$ n/cm^2. The strain amplitude can be changed in the range of 5×10^{-4} to 5×10^{-7}, where the amplitude-independent internal friction is observed. The test specimen was a wire with a diameter of 1 mm and a length of 50 to 100 mm.

Internal friction Q^{-1} is calculated using the following expression:

$$Q^{-1} = \frac{1}{2\pi} \cdot \frac{\Delta W}{W},$$

(1)

where ΔW – a loss of energy per cycle, W – total energy of forced oscillations. After the simple conversions (taking into account the excitation parameters and specimen stiffness) we can derive a formula for the determination of internal friction from the test:

$$Q^{-1} = \frac{4 \cdot i_b \cdot C_2}{\pi \cdot C_1 \cdot e_0},$$

(2)

where C_1 and C_2 – device constants, e_o – a parameter which correspond to specified strain amplitude and i_b – an excitation current is only parameter which is recorded. As a result the internal friction values are plotted against the test temperature in the temperature range of grain boundary relaxation. The height and location of grain boundary peak of internal friction are considered.

The shear modulus is defined using the following formula:

$$G = k \cdot f^2 ,$$
(3)

where k – constant related to a type and size of specimen and parameters of an oscillation system, f – frequency of mechanical oscillations.

11.2. Investigation of He diffusion on grain boundaries for pure Fe and structural steel

An operating regime of the WWR-M reactor with a week cycle enables to get the temperature dependencies of internal friction and shear modulus for materials irradiated to a specified fluence both at the time of irradiation and when a reactor is shutdown. In this report the neutron irradiation influence on the relaxation characteristics of pure Fe and structural chromium-nickel-molybdenum steels $Cr_{16}Ni_{15}Mo_3B$ and $Cr_{16}Ni_{15}Mo_3B$ with 0.005% B is considered. The B atoms were mainly situated on the grain boundaries. The irradiation temperature for tested specimens was 350°C. The specimens were irradiated to the neutron fluence of $2.5x10^{20}$ n/cm^2 and $4.4x10^{20}$ n/cm^2 for the pure Fe and steel accordingly.

The changes of temperature and height of internal friction peak due to neutron irradiation is shown in Fig. 2 for pure Fe. The internal friction peak is related to grain boundary relaxation. The temperature and height of the peak decrease as the neutron fluence increases and become constant at the fluence of $2x10^{20}$ n/cm^2.
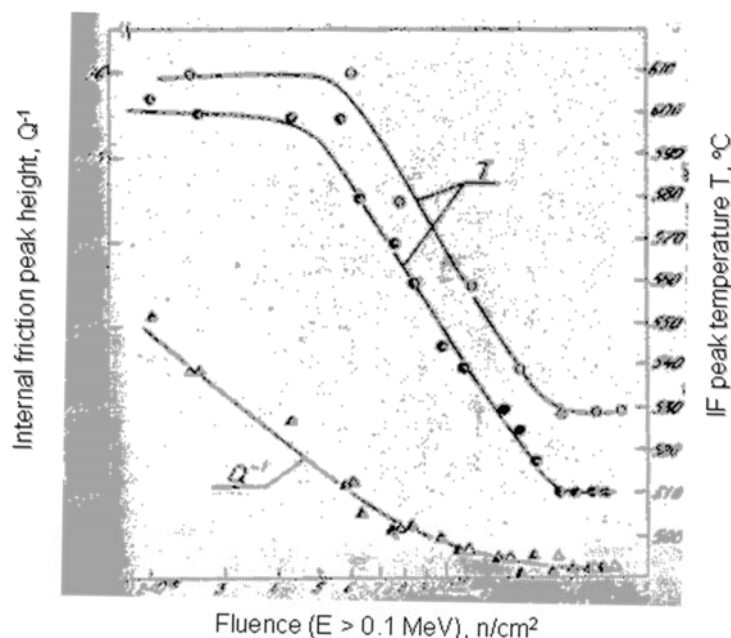

FIG.2. Effect of neutron fluence on the height (Q^{-1}) and temperature (T) of internal friction peak for pure Fe (closed symbols – at the time of irradiation; open symbols – reactor shutdown).

Fig. 2 demonstrates that a neutron fluence dependence of the temperature of internal friction peak depends on neutron fluence rate. At the time of irradiation the temperature of internal

friction peak is lower than under reactor shutdown condition in the whole range of neutron fluence. This effect is related to radiation vacancy flux towards the grain boundaries.

As usual the changes of temperature and height of internal friction peak are related to changes of a concentration of impurity atom on the grain boundaries and the saturation of internal friction peak parameters is typical for an absorption saturation of the grain boundaries with impurities. A revealed effect can be explained by the saturation of the grain boundaries with He which is originated from (n, α) – reaction under the neutron irradiation. For the confirmation of this conclusion the platinum specimens were tested. For platinum the (n,α) – reaction and He formation do not occur. In this case the changes of internal friction peak parameters have not been revealed.

For the $Cr_{16}Ni_{15}Mo_3B$ steel other type of the neutron fluence dependence of internal friction is observed [2]. It was found that a grain boundary peak of internal friction reaches a maximum at fluence of 2 x·10^{20} n/cm^2 for $Cr_{16}Ni_{15}Mo_3B$ steel and 8.7x10^{20} n/cm^2 for $Cr_{16}Ni_{15}Mo_3B$ steel with 0.005 mass % B and then decreases, Fig. 3. The temperature of internal friction peak does not change considerably.

In order to explain an observed effect, three mechanisms were considered: radiation-induced precipitation on the grain boundaries, a diffusion of alloyed elements and impurities on the grain boundaries and a diffusion of formed by (n, α) – reaction He atoms on the grain boundaries. Among these processes, only the last one resulted in the observed changes of internal friction parameters. According to Fig. 3 the micro doping $Cr_{16}Ni_{15}Mo_3B$ steel with B increase significantly the neutron fluence at which the saturation of grain boundaries with He occurs. It is possible that a presence of Boron atoms on the grain boundaries produces additional sites for He atoms. In turn this result in a saturation of grain boundaries with He for the $Cr_{16}Ni_{15}Mo_3B$ steel with B occurs at the significant higher concentration of He in comparison to $Cr_{16}Ni_{15}Mo_3B$ steel. So the conducted tests have shown that the internal friction method can be successfully used to estimate relaxation stability of grain boundaries in the relation to the helium embrittlement.
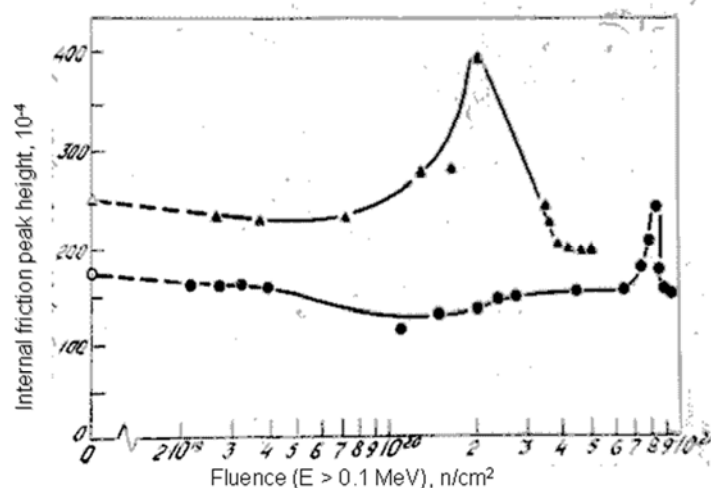

FIG.3. Change of the height of internal friction peak with neutron fluence increase for Cr16Ni15Mo3B steel (triangle) and $Cr_{16}Ni_{15}Mo_3B$ steel with 0.005 mass % B (round).

11.3. Application of the internal friction method for the investigation of radiation swelling

One of the key issues for the radiation materials science is a radiation swelling of structural materials. In this work for the estimation of radiation swelling was applied the internal friction method. Studying the influence of neutron irradiation on the temperature dependency of internal friction for Fe – ^{11}B alloy a large increase of a grain boundary peak after the neutron fluence of 5 x 10^{20} n/cm^2 was revealed. In Fig. 4 the change of the height of internal friction peak with neutron fluence increase for Fe – ^{11}B alloy is shown.
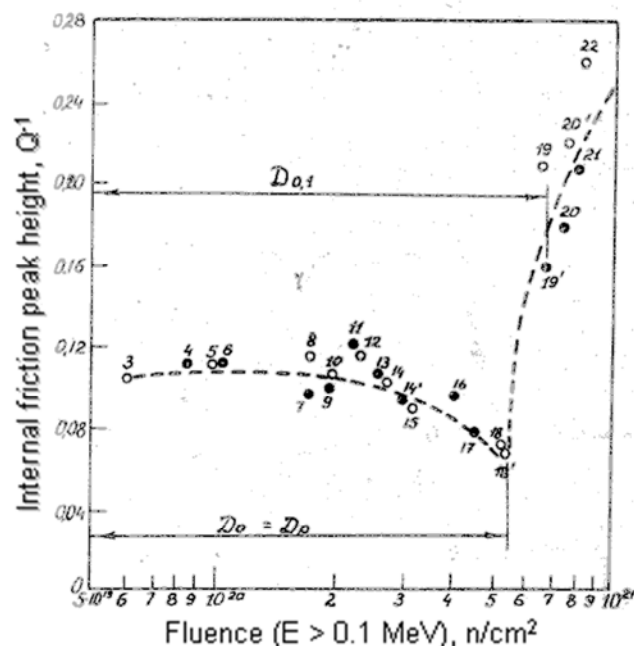
FIG.4. Change of the height of internal friction peak with neutron fluence increase for Fe – ^{11}B alloy (closed symbols – at the time of irradiation; open symbols – reactor shutdown).

Test results demonstrate a typical for metal decrease of the internal friction peak with a neutron fluence increase caused by radiations defects. Further increase of the neutron fluence leads to an anomalous growth of internal friction that indicates to a nucleation of new dumping sites. It is known [3] that in materials the effects related to a formation of vacancy voids and interstitial dislocation loops occur at the neutron fluence of $\sim 10^{21}$ n/cm^2. In this case the mechanism of internal friction which is responsible for the appearance of a high grain boundary peak might be a vacancy void nucleation and migration. Thus an anomalous growth of internal friction after a neutron fluence of 5.2x10^{20} n/cm^2 can be explained by micro void nucleation in the Fe – ^{11}B alloy. Since the micro void nucleation leads to a swelling the method of internal friction allows estimating a radiation swelling rate.

11.4. Influence of neutron radiation on dislocation mobility

In order to estimate an effect of neutron radiation on dislocation mobility of metal and alloys the method of internal friction was used and a change of shear modulus due to irradiation was investigated. In this paper the test data for pure Fe, structural and reactor pressure vessel steel are presented. Specimens were irradiated to a fast neutron (E > 0x1 MeV) fluence of $\sim 10^{21}$ n/cm^2. A frequency of torsion oscillations was 5 - 11 Hz, a specimen strain amplitude was maintained at the level of 3x10^{-5}.

For a pure Fe it was found out [4] that the shear modulus is much lower at the time of irradiation then when a reactor is shutdown at the same neutron fluence, Fig. 5. The maximum decrease in shear modulus is 10%. This modulus decrease is fully reversible and observed only at the time of irradiation. Authors [4] suppose this effect is not related to the grain boundaries and can be explained by the interaction between interstitial atoms and mobile dislocations.
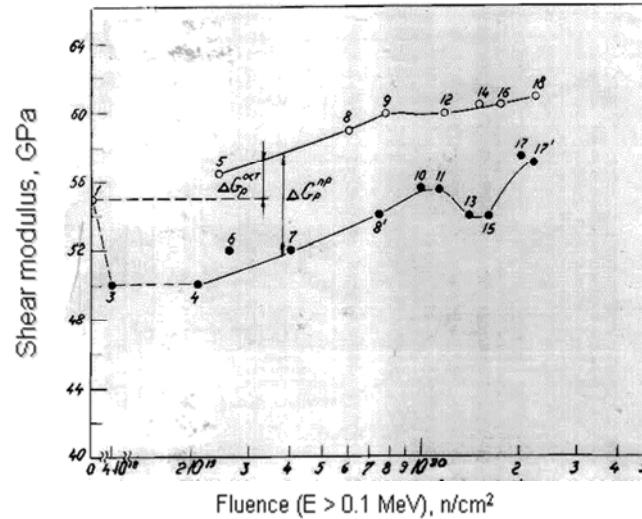
FIG.5. Dependence of shear modulus on neutron fluence for Fe at the temperature of 580 °C (closed symbols – at the time of irradiation; open symbols – reactor shutdown).

For a structural steel $Cr_{16}Ni_{15}Mo_3B$ [5, 6] the decrease of shear modulus at the time of irradiation is less then 1% and observed only in the initial period of irradiation, Fig. 6. The small effect is explained by pinning of dislocations with alloying elements. This effect disappears after a neutron fluence of 2×10^{20} n/m^2 that is related to additional pinning of dislocations with radiation defects and the radiation-induced diffusion of impurities to the dislocations.
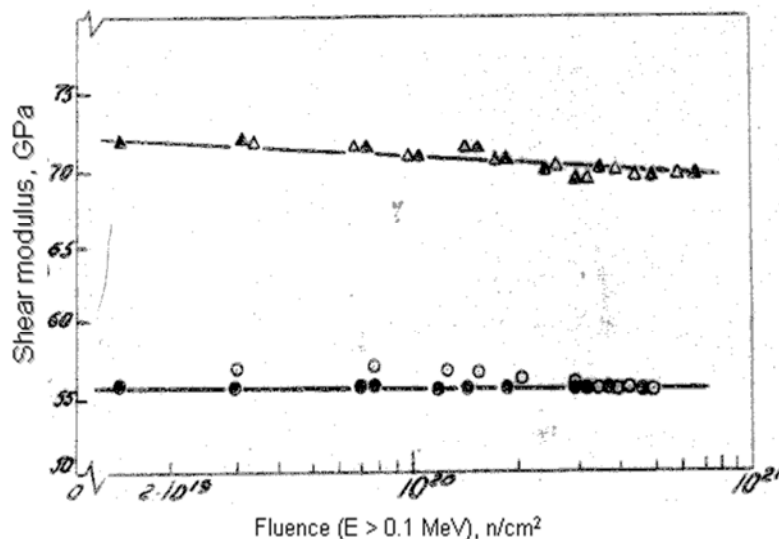
FIG.6. Dependence of shear modulus on neutron fluence for $Cr_{16}Ni_{15}Mo_3B$ steel (○) and 12CrMnNiMo (Δ) at the temperature of 500 °C (closed symbols – at the time of irradiation, open symbols – reactor shutdown).

11.5. Conclusions

In Kiev Institute for Nuclear Research (Ukraine) a remote internal friction device integrated with a test channel of the research reactor was successfully applied to study the changes of grain boundary relaxation parameters in metals and alloys at the time of and after irradiation. Using an internal friction method it was shown the Boron micro alloying of the structural steel considerably increases a neutron fluence at which the saturation of grain boundaries with He occurs. In addition the internal friction method allows us to estimate parameters of void swelling at the early stage and predict a susceptibility of materials to the radiation swelling. A reversible decrease of shear modulus was revealed for pure Fe at the time of irradiation that is related to the interaction between interstitial atoms and mobile dislocations. This effect was not observed for the structural and RPV steels that can be explained by a strong pinning of dislocations with alloying elements and precipitates.

REFERENCES

[1]   GRYNIK, E., KARASEV, V., PALIOKHA, M., Problems of Atomic Science and Engineering. Series, Atomic Material Science, 1 (1978) 25.
[2]   GRYNIK, E., Evaluation of Helium inter crystalline adsorption in 0X16H15M3Б and 0X16H15M3БP steels, Atomnaja Energija, 61 (1986) 263.
[3]   ZELENSKIY, V., NEKLUDOV, I., CHERNYAEVA, T., Radiation defects and material swelling., Kiev: Naukova dumka., (1988) 296.
[4]   GRYNIK, E., KARASEV, V., Reversible decrease of modulus shear for iron and Fe alloys at the time of irradiation. Atomnaja Energija, 54 (1983) 177.
[5]   KARASEV, V., GRYNIK, E., PALIOKHA, M., Influence of neutron irradiation on a shear modulus of reactor structural materials, Problems of Atomic Science and Engineering. Series: Radiation Damage Physics and Radiation Material Science, 1 (1987) 26.

Chapter 12

IMPROVEMENT OF IRRADIATION CAPABILITY IN THE EXPERIMENTAL FAST REACTOR JOYO

T. SOGA, T. AOYAMA, S. SOJU
Experimental Fast Reactor Department, Oarai Research and Development Center
Japan Atomic Energy Agency, 4002 Narita, Oarai, Ibaraki, 311-1393, Japan
E-Mail: Soga.Tomonori@Jaea.Go.Jp

Abstract: Japan's experimental fast reactor Joyo started the rated power operation of the "MK-III" upgraded core in 2004. This core provides a high fast neutron flux of 4.0×10^{15} n/cm^{2}s. Several important irradiation tests of fuel and material for fast reactors were successfully conducted such as mixed oxide fuel containing minor actinide (MA-MOX) and oxide dispersion strengthened (ODS) steel. In order to utilize the prominent high neutron flux and the potential for intense neutron beam, the enhancement of irradiation capabilities of Joyo is being considered not only for fast reactor development but also for the following multipurpose utilization: Neutron spectrum tailoring for creating versatile irradiation field, expansion of temperature range for various irradiation purposes, flexible transient experiment and fast neutron beam hole for multi purpose utilization.
These concepts will promote Joyo's contribution to the research and nuclear industry for future energy systems and basic and applied science.

12.1. Introduction

The experimental fast reactor Joyo of the Japan Atomic Energy Agency (JAEA) is the first sodium-cooled fast reactor (SFR) in Japan. Joyo attained initial criticality as a breeder core (MK-I core) in 1977. The basic characteristic of plutonium (Pu) and uranium (U) mixed oxide (MOX) fuel core, sodium cooling system and breeding performance were investigated in the MK-I operation that consisted of two 50 MW$_t$ and six 75 MW$_t$ duty cycles. In 1983, the reactor increased its output to 100 MW$_t$ to start the irradiation tests for the fast breeder reactor (FBR) development. Thirty-five duty cycle operations and many irradiation tests were conducted using the MK-II core by 2000.

Joyo was then modified to accelerate the fuels and materials development for the FBR in Japan [1,2]. In order to obtain the higher fast neutron flux, reactor power increased to 140 MWt with a renewal of intermediate heat exchanger (IHX) and dump heat exchanger (DHX). The core and cooling system modification for this purpose was called the "MK-III project" and it was completed in 2003. The rated power operation of the MK-III core was started in 2004. The MK-III core is used for irradiation tests of future FBRs including prototype FBR Monju and other R&D fields as well. This powerful neutron irradiation flux has an advantage especially to irradiate high burn-up fuel and to irradiate materials to high neutron dose or high dpa (displacement per atom). Recently a new upgrading program of the Joyo is in progress to further enhance the irradiation test capability.

This paper describes the fundamental irradiation capability and the upgrading program in the irradiation test reactor Joyo.

12.2. Plant description and the irradiation field characteristic

Core

The main reactor parameters of the MK-II and MK-III irradiation cores are shown in Table 1. Fig.1 shows the core configuration of the MK-III 3rd operational cycles. The MOX fuel region is divided into two radial fuel composition zones in the MK-III core to flatten the neutron flux distribution. The fissile plutonium (Pu) content (^{239}Pu + ^{241}Pu) / (U + Pu)) is about 16 wt% in the inner core fuel and about 21 wt% in the outer core fuel. And both the inner core and outer core have the same uranium enrichment of 18 wt%.

TABLE 1. MAIN JOYO CORE AND PLANT PARAMETERS

Items		MK-II	MK-III
Reactor thermal output	(MWt)	100	140
Max. No. of irradiation test S/A		9	21
Core diameter	(cm)	73	80
Core height	(cm)	55	50
^{235}U enrichment	(wt%)	18	18
Pu content	(wt%)	～30	～30
Pu fissile content (inner/outer core)	(wt%)	～20	～16/21
Neutron flux total	(n/cm^{2}s)	4.9×10^{15}	5.7×10^{15}
Fast neutron flux (E > 0.1MeV)	(n/cm^{2}s)	3.2×10^{15}	4.0×10^{15}
Primary coolant temp. (Inlet/Outlet)	(deg-C)	370/500	350/500
Operation period	(days/cycl.)	70	60
Reflector/shielding		SUS/SUS	SUS/B$_4$C
Max. excess reactivity (at 100 deg-C)	%Δk/kk'	5.5	4.5
Control rod worth	%Δk/kk'	～9	～7.6

Inner Fuel		23
Outer Fuel		59
Reflector		124
Control Rod		6
Neutron Source		1
Fuel or material irradiattion		1
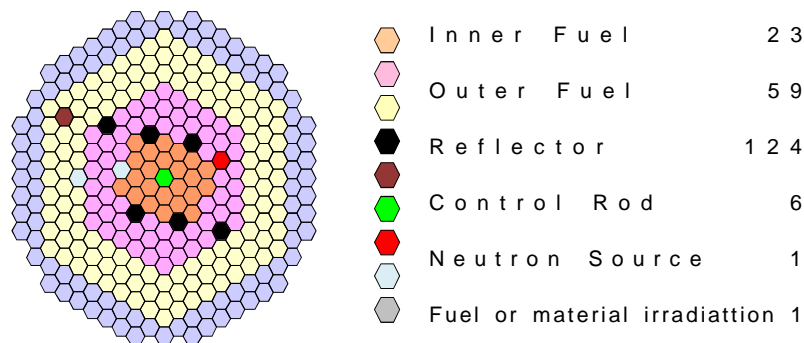
FIG.1. Core configuration of Joyo MK-III 3rd operational cycle.

The active core is cylindrical and about 80 cm in equivalent diameter and 50 cm in height. There is a radial reflector region of stainless steel surrounding the core which is about 25 cm thick. Shielding subassemblies with B$_4$C are loaded in the outer two rows of the reactor grid, replacing radial reflector subassemblies. Two of six control rods were shifted from the 3rd row to the 5th row to provide the positions for loading instrumented type irradiation test subassemblies in the high flux region of the fast neutron field. All six of the control rods have the same poison-type design. The poison section contains B$_4$C enriched to 90 wt% in ^{10}B, and there is a stainless steel follower section below it.

Cooling System

Joyo has two primary sodium loops, two secondary loops and an auxiliary cooling system as shown in Fig. 2. In the MK-III core, the sodium enters the core at 350°C at a flow rate of 1350 ton/hour per loop and exits the reactor vessel at 500°C. The maximum outlet temperature of a fuel subassembly is about 570°C.
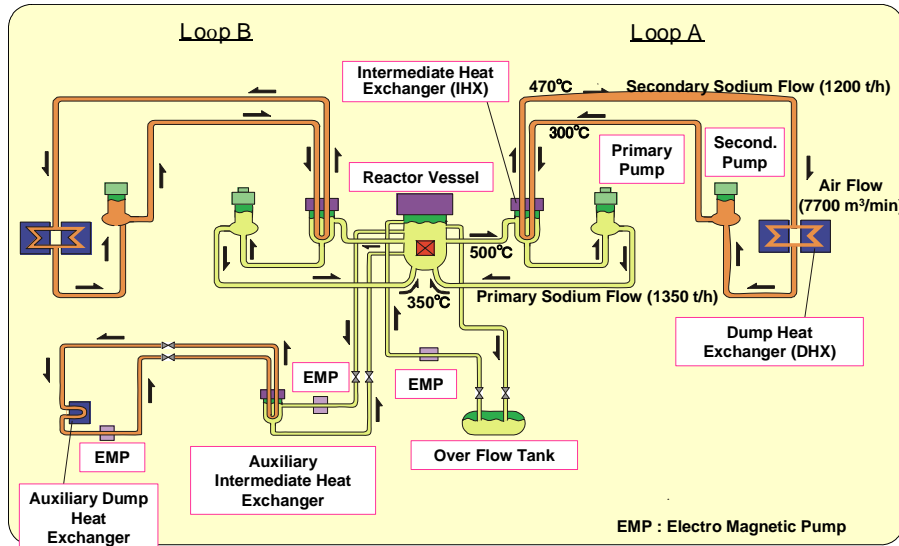
FIG.2. Joyo Mk-III heat transport system.

IHX separates radioactive sodium in the primary system from non-radioactive sodium in the secondary system. The secondary sodium loops transport the reactor heat from the IHXs to the air-cooled DHXs.

12.3. Irradiation fields characteristic test in the MK-III core

The MK-III core provides the maximum fast neutron flux of 4.0×10^{15} n/cm^{2}s that is increased about 30% compared to the previous MK-II core as shown in Table 1. This is the highest fast neutron flux in the irradiation test facilities in the world. In order to accurately predict the neutron flux including energy spectrum and temperature condition in the new MK-III core, the irradiation field characterization test [3] was performed in the 1st and 2nd operational cycles.

The detailed neutron flux distributions from the core center to the reactor vessel and temperature data in the typical irradiation subassembly were experimentally obtained by neutron dosimeters and temperature monitors. The calculated reaction rates using the 2-dimensional DORT or 3-dimensional TORT deterministic transport calculation codes agreed well with the measured values in the fuel region. A relatively large discrepancy around 10% was observed in the central non-fuel irradiation test subassembly and radial reflector region mainly due to the error in processing scattering cross section matrix used for the transport calculation. In these regions, the MCNP [4] code calculation model described the 3-dimensional heterogeneous geometry and it could reduce these discrepancies to 6%.

The irradiation field in the MK-III core is better understood hrough this characterization test. This knowledge was applied to the evaluation of the MA-MOX irradiation test which was conducted in the 3rd operational cycle as described later in a next section.

12.4. Achievement of the irradiation tests using MK-III core

The irradiation tests in the MK-III core are shown in Fig.3. The main irradiation test rigs in Joyo are outlined in Fig.4. The main items are described in the following section.

Year	2003	2004	2005	2006	2007
Operation	Performance Test	1st 2nd		3rd 4th	5th 6th cy.
MARICO-2 (ODS In-pile Creep Test)				←	→
ODS Cladding Material Irradiation Test				←	→
Am, Np Bearing Oxide Fuel Irradiation Test				▼ ▼	▼
Fuel Failure Detection Testing (FFDL)		▼			
Ferritic Wrapper Tube Fuel Irradiation Test		←			→
SASS Holding Stability Test		↔			
SASS Element Irradiation Test				←	→
Material Irradiation Test (Fusion Reactor, etc)		←		→	↔

Instrumented Irradiation Equipment

Instrumented Test Assembly (INTA)
Material Testing Rig with Temperature Control (MARICO)
Upper Core Structure Irradiation Plug Rig (UPR)
Ex-vessel Irradiation Rig (EXIR)

Uninstrumented Irradiation Equipment

Uninstrumented Fuel Irradiation Subassembly Type-A (UNIS-A)
Uninstrumented Fuel Irradiation Subassembly Type-B (UNIS-B)
Uninstrumented Fuel Irradiation Subassembly Type-C (UNIS-C)
Uninstrumented Fuel Irradiation Subassembly Type-D (UNIS-D)
Core Materials Irradiation Rig (CMIR)
Absorber Materials Irradiation Rig (AMIR)
Structure Materials Irradiation Rig (SMIR)
Surveillance Uninstrumented Irradiation Rig (SVIR)

FIG.4. Outline of irradiation test rigs in Joyo.

12.5. Self-actuated shutdown system

A self-actuated shutdown system (SASS) with a Curie point electromagnet (CPEM) has been developed in order to establish passive shutdown capability for a large-scale SFR. The basic characteristics of SASS have already been investigated by various out-of-pile tests of basic components. As the demonstration of this technique, it was required to confirm the stability of SASS in the actual operational conditions of SFR with high temperature, high neutron flux, and flowing sodium. For this purpose, the following experiments were carried out using MK-III core as shown in Fig.5.

(1)   Holding stability test

The holding stability test using the reduced-scale experimental equipment of SASS was conducted in the 1st and 2nd operational cycles using a dummy control rod in the 1st and 2nd operational cycles [5]. The holding stability of the control rod by CPEM was confirmed. The results also indicate there are no fundamental impediments to the practical use of SASS that might arise from operational trouble involving the unexpected drop during reactor operation.

(2)   Element irradiation test

The element irradiation test was conducted during the 3rd to 6th operational cycles using the upper core structure plug rig. The basic magnetic characteristics data has been obtained under the irradiation environment.
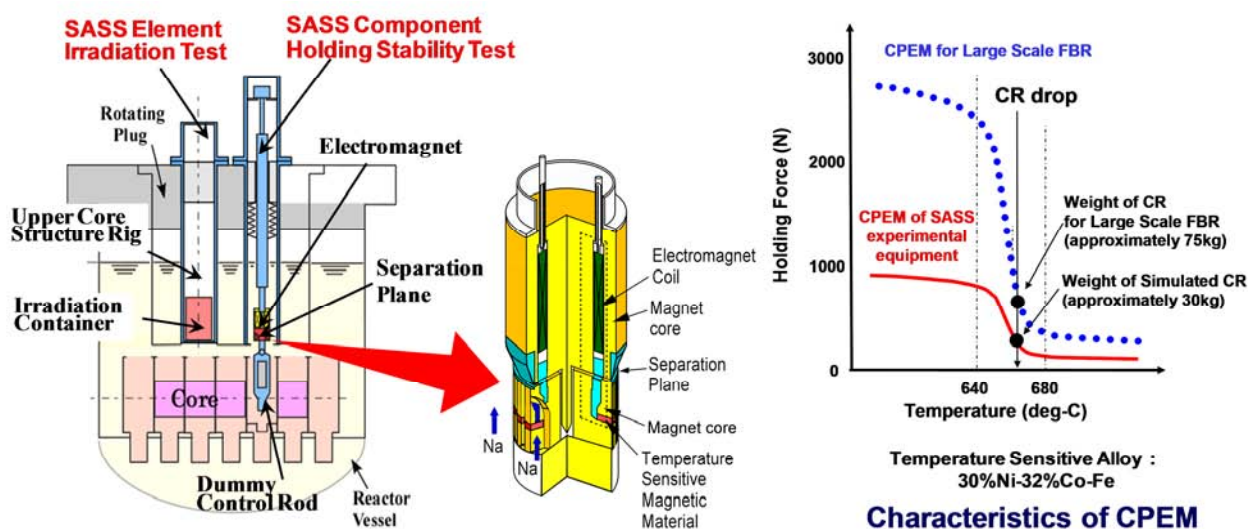
FIG.5. Irradiation test of SASS.

12.6. Short term irradiation tests for MA-MOX fuel

MA recycling and transmutation in fast reactors is being investigated as one of the promising future FBR cycle concepts. To support this investigation, Japan's first irradiation test program of MA-MOX fuel was planned. Two types of test fuel pins were prepared as shown in Fig. 6. Test pins were contained in a test subassembly where one fuel pin is installed in each of 6 stainless steel capsules. The test subassembly was designated as B11. The target linear heat rate (LHR) was determined to be approximately 430 W/cm. Two short-term irradiation tests of 10 minutes B11(1) and 24 hours B11(2) were conducted at a part of the 3rd operational cycle [6].

The B11(1) test sub-assembly containing 6 test fuel pins was loaded in the core center. The reactor power was raised continuously at a rate of 12 MWt/h from 50% to 100% of the target reactor power of 120 MWt in order to minimize the fuel restructuring before achieving the target LHR. After holding the reactor power at 120 MWt for 10 minutes, the reactor was rapidly shutdown by using the manual scram to preserve the irradiated pellet structure and to prevent additional fuel restructuring due to the fuel burn-up, Fig. 7-1. Thereafter, the B11(1) subassembly was transferred to the Fuel Monitoring Facility (FMF). Two test fuel pins were taken out of the B11 (1) subassembly to check whether or not fuel melting had occurred. The remaining 4 test fuel pins were re-loaded to Joyo as the B11(2) subassembly and then re-irradiated to investigate the MA redistribution behavior for 24 hours at 120 MWt, Fig. 7-2.

The LHRs for each pin were calculated using the MCNP code and then adjusted using E/C for ^{10}B (n, α) reaction rates measured in the MK-III core irradiation field characterization test. The evaluated LHRs after biasing by E/C are 425~434 W/cm. These predicted values agreed with the experimental values in the post irradiation examination (PIE) based on the ^{148}Nd method within 3% accuracy.
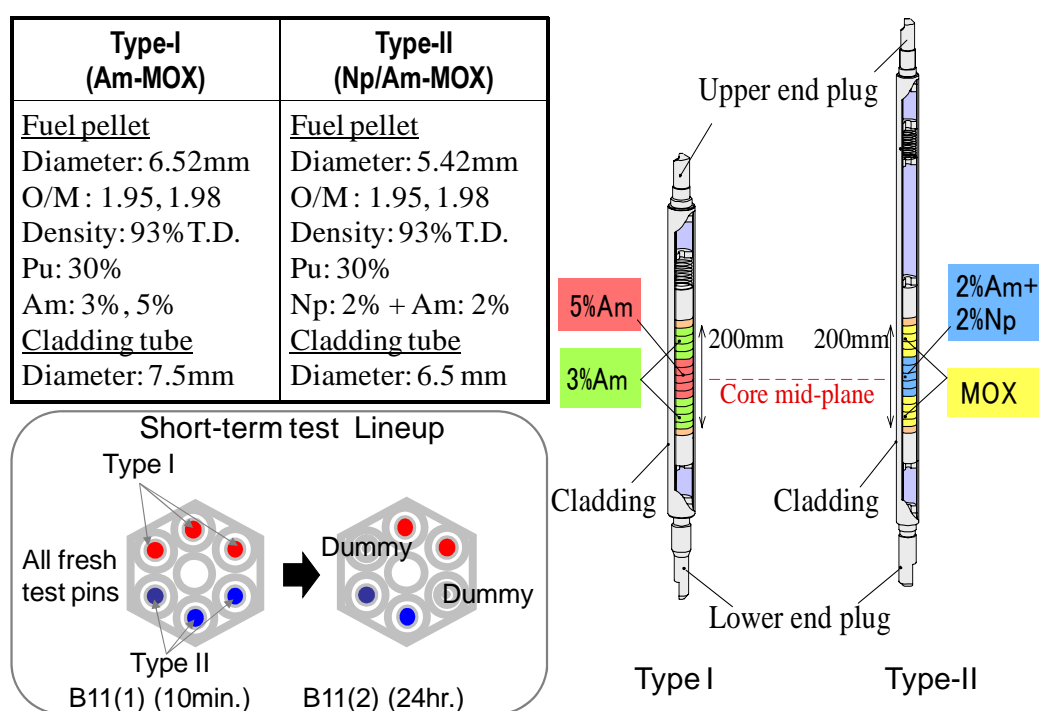
FIG.6. MA-MOX fuel pin specification.
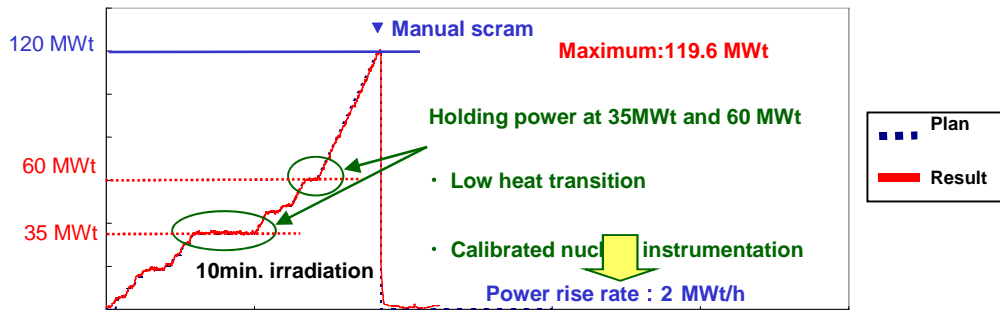
FIG.7-1. Power history of B11 (1).
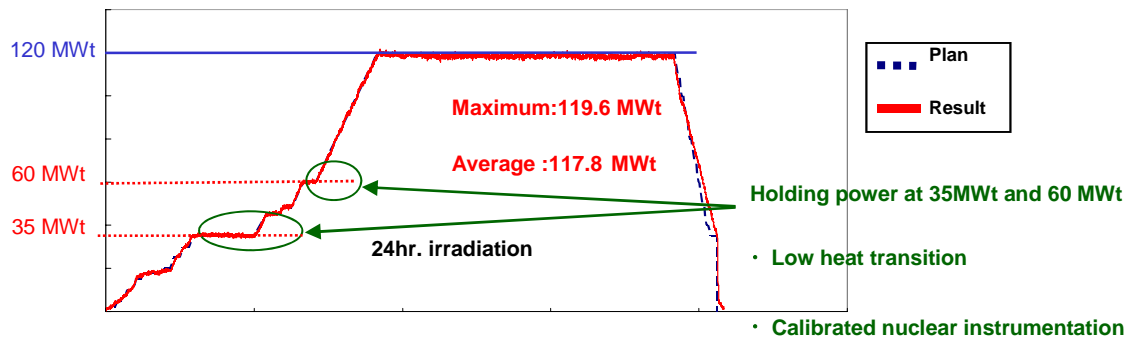
FIG.7-2. Power history of B11 (2) In-pile creep rupture test of ODS ferritic steel.

The ODS ferritic steel is the primary candidate material for the fuel cladding in the future SFR because of its low swelling properties and high strength at high temperature. Out-of-pile experiments show that ODS has higher creep rupture strength than the normal ferritic steel and it is comparable to the modified austenitic stainless steel such as the PNC1520 used as fuel cladding of Joyo and the PNC316 used as fuel cladding of Monju.

To evaluate the creep rupture strength of ODS ferritic steel under neutron irradiation, an in-pile creep rupture experiment was conducted from the 3rd to 6th operational cycles using the material irradiation rig with temperature control, named MARICO, Fig. 8 [7]. The MARICO was developed to obtain real time temperature data by thermocouples and to control the constant temperature with an accuracy of $\pm 4°C$ by changing the gas composition (mixture of He and Ar) surrounding the specimen. Twenty four ODS specimens with no fuel were prepared which were pressurized by helium gas up to 22 MPa to accelerate the creep rupture testing. During the irradiation test, the temperature of each specimen was maintained at target temperature within $\pm 4°C$ as shown in Fig. 9. From the 3rd to 6th operational cycles, ODS specimens have been tested and all were detected and identified by means of the following two methods:

− Two thermocouples were installed in each capsule to measure the temperature of the sodium in which the specimens were soaked. The temperature increase caused by change of the thermal conductivity with the released gas was detected by these thermocouples.

− A unique blend of stable xenon (Xe) and krypton (Kr) tag gas was enclosed in each specimen along with the pressurizing helium gas. The tag gas released into the argon cover gas was identified by means of gamma-ray spectrometry and RIMS (Laser Resonance Ionization Mass Spectrometry).

Drive Mechanism

Upper Core Structure

Housing

Long Bellows

Short Bellows

Latch and Cutter

Test Assembly

Capsule

Lower Guide Tube

A A

MARICO

Rotating Plug

Sodium Level

Upper Core Structure

Core

Loading Features

Cable
Gas Pipe
Irradiation Specimen

Capsule
Thermocouple

Support Structure

Section A-A

Sodium Outlet Vent Line

Basket
Gas Gap

Irradiation Specimen

Sodium Inlet Line

Thermocouple

Gas Inlet Line

Gas Exhaust Line

Capsule

FIG.8. Outline of MARICO.

Reactor power
◄- -140MWt
Periodical adjustment
Temperature
Target Temperature
Adjustment of gas composition

Temperature (deg-c)

760
755
750
745
740

0   1   2   3   4
Time (h)

FIG.9. Capsule temperature controlled by adjusting gas composition.

Improvement of irradiation capability

The upgrading programs of irradiation capability are being promoted to use Joyo for multiple R&D fields [8]. This program mainly aims at two directions. The first is an expansion of the temperature range and the neutron energy spectrum to meet irradiation needs for the existing light water reactor (LWR) or future energy system such as Generation-IV reactor and fusion reactor as illustrated in Fig. 10. The second is the additional function to be able to accept transient tests or short-term irradiation tests while achieving the high plant availability factor required for the major irradiation test to high burn-up or high dpa.
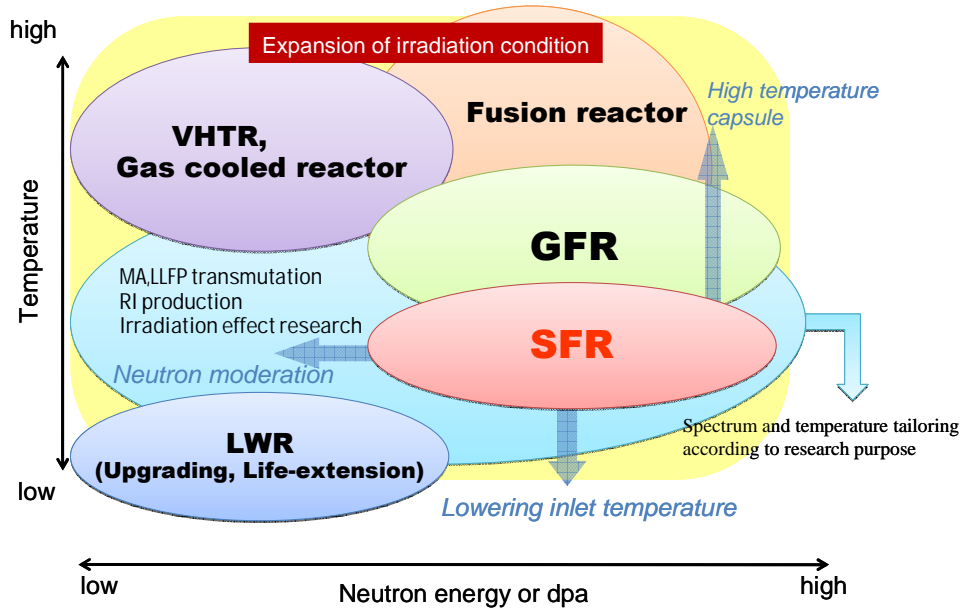
FIG.10. Expansion of irradiation condition.

Computerized reactor control system by automatic control rod operation

The reactor power of Joyo is controlled by the manual operation of control rods at present. In normal operation, the 6 control rods are regularly pulled out by operators to compensate for the reactivity loss with the fuel burn-up. This gradual decrease in reactor power and the regular control rod operations influence the irradiation temperature of the specimen. Instrumented capsules of MARICO controlled the temperature constantly as shown in Fig. 9 to compensate for the heat generation change in the core. Therefore, the automatic control rod operation can keep the reactor power constant without relying on the frequent manual operations. This function will also reduce the operator's burden in case of conducting the transient tests as precisely as planned. In Joyo, the automatic control rod operation system by computer has been newly licensed and will support the future irradiation tests.

12.7. Neutron spectrum tailoring for creating versatile irradiation field

Many nuclear reactions occurring during neutron irradiation are sensitive to the low energy neutron spectrum. The fast reactor has the potential to tailor the neutron spectrum individually by means of including equipment to moderate the neutron. This concept can contribute to the research for LWR life extension, the transmutation study of the long-lived fission product (LLFP) or MA and radio isotope (RI) production [9].

Fig. 11 shows the layout of the moderated neutron irradiation field in the current concept. Seven steel reflector subassemblies are replaced with a target subassembly surrounded by six moderator subassemblies containing Be or zirconium hydride ($ZrH_{1.65}$).

Fig. 12 shows the 70 group neutron spectrum and flux values in the target subassembly compared with those in the driver fuel and radial reflector regions. The moderator does not significantly affect the neutron flux in the fuel region due to the reflectors between the driver fuel subassembly and moderator. Table 2 compares the calculated transmutation rates at the core mid-plane. Especially note the ^{99}Tc transmutation rate was 21% using $ZrH_{1.65}$ and 27.8 % using Be as moderator and it was approximately 10 times higher than the case without moderator.

The maximum power increase of the driver fuel by the moderated neutrons leaking from the moderator subassemblies is only 7%. This power increase is not a problem because the driver fuel subassemblies in the 4th and 5th row have adequate margin to the peak power limits during the rated 140 MWt operation.
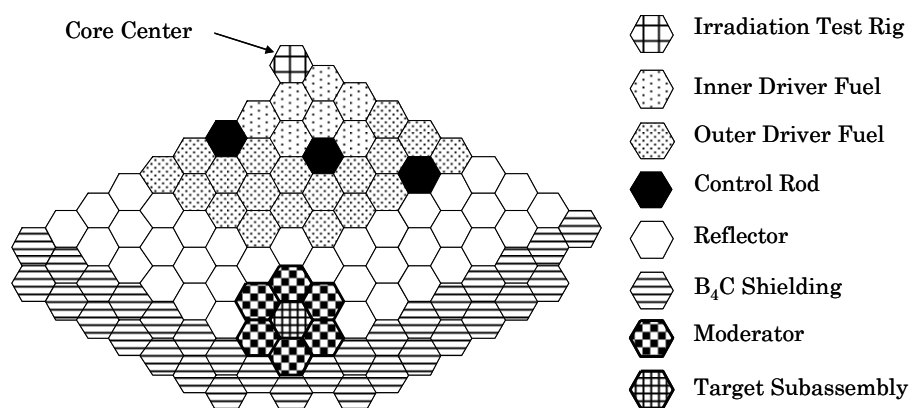
FIG.11. Slow neutron irradiation field (1/3 core model).
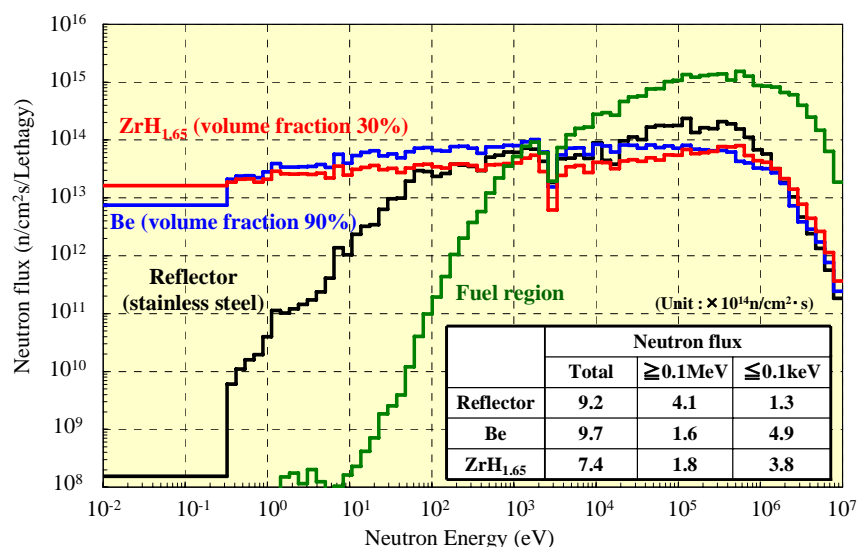
FIG.12. Comparison of neutron spectrum.

12.8. Expansion of temperature range for various irradiation purposes

(1)   Low temperature field

In the conventional MK-III operation, the temperature of irradiation specimens is higher than the core inlet temperature of 350°C. The creation of a lower irradiation temperature condition provides the opportunity to investigate the temperature dependency of the irradiation effect of the material, and it enables the irradiation test for LWR materials.

The core inlet temperature is now able to be decreased to less than 300°C with a new license, from the potential of the DHXs. Figure 13 shows the axial distribution of fast neutron flux and coolant temperature. Assuming that the inlet temperature is 290°C, a fast neutron flux of about 2x10^{15} n/cm^{2}s can be obtained in the LWR temperature range (320°C-370°C).

TABLE 2. TRANSMUTATION RATE OF ^{99}TC AND ^{129}I AT THE CORE MID-PLANE

	Fractional transmutation rate, %/year	
	^{99}Tc	^{129}I
Rad. Reflector	3.0	1.7
Be (90%)	27.8	6.6
ZrH$_{1.65}$ (30%)	21.0	6.8
ZrH$_{1.65}$ (60%)	17.1	7.7
Core region	5.4	3.4
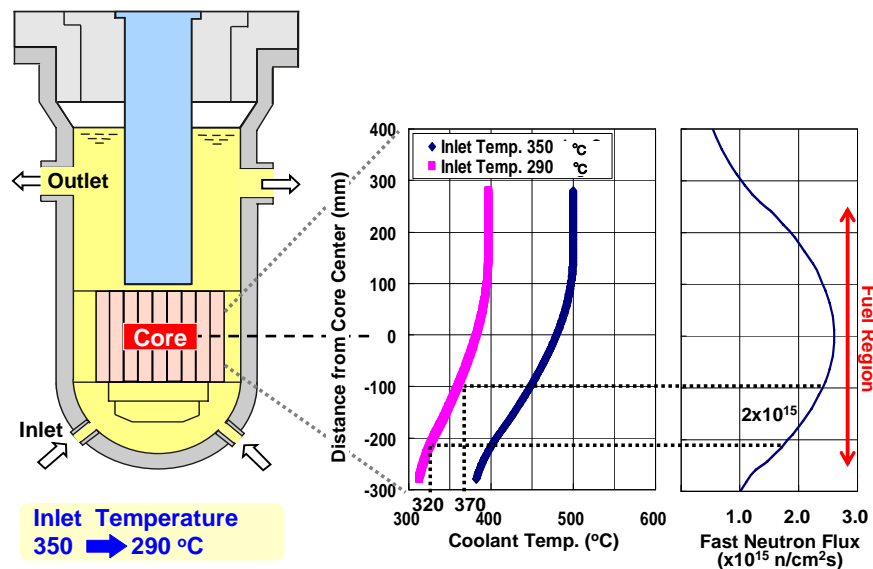
FIG.13. Irradiation condition at the lower temperature operation.

(2) High temperature field

The material development at the high temperature is required as a key technology to develop new nuclear power energy supply systems. For instance, the high reactor outlet temperatures of 800°C to 1000°C are being expected in the Generation-IV VHTR (Very High Temperature Reactor) and the GFR (Gas cooled Fast Reactor) in order to achieve high power generation efficiency. In the fusion reactor, research of materials at high dpa with high temperatures of over 1000°C is required for the advanced blanket systems.

A high temperature irradiation capsule is designed as shown in Fig.14 to conduct material irradiation tests for Generation-IV or fusion reactors. The irradiation capsule will be equipped with a tungsten (W) inner tube to obtain a higher gamma heating rate. Preliminary calculations show that the temperature of the specimen achieves over 1000°C as shown in Fig. 15.
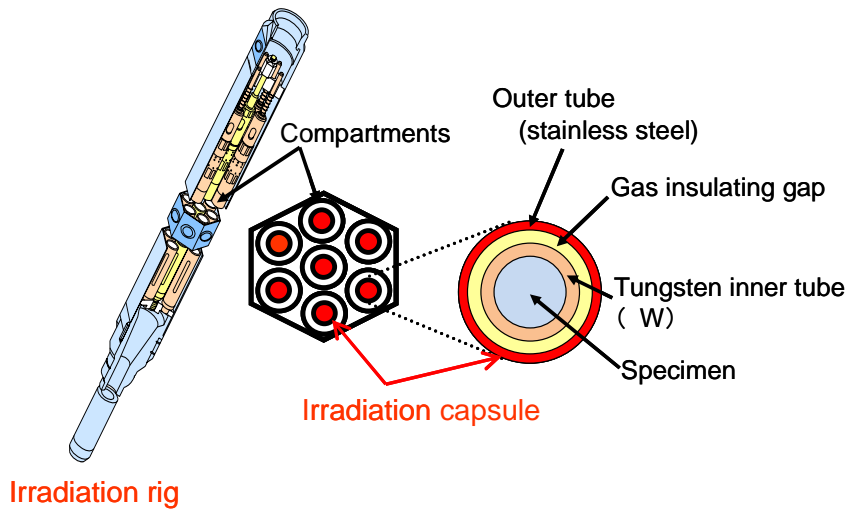
FIG.14. The irradiation rig and high temperature irradiation capsule.
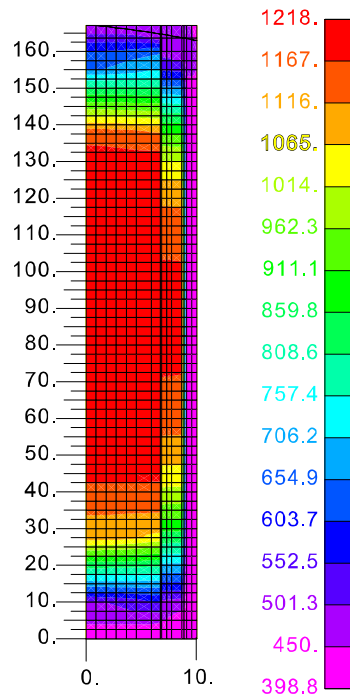
FIG.15. Temperature distribution in the high temperature irradiation capsule (RZ-model).

12.9. Flexible transient experiment

In the transient irradiation test of MA-MOX fuel, the power of the experimental fuel pin was increased by the reactor power rise. However, the rate of reactor power increase is restricted by the safety limits of the cooling system. In addition, plant availability factor is decreased when many reactor start-ups and shutdowns are required.

A sample movable device is being developed in order to simulate a transient overpower without changing the reactor power. The power is increased by using the axial gradient of the neutron flux. The technique which had been developed for the SASS test device can be applied. Figure 16 outlines the specimen movable device and axial neutron flux distribution. The current study of a specimen movable device anticipates a moving range from -25 to +9090 cm measured from the core mid-plane. Neutron flux and linear heat rate can be changed easily by a factor of approximately 100 by moving the sample up and down in a short time while keeping the reactor power constant. In the case of fuel irradiation test, the rise of LHR of approximately 40 W/cm a minute will be attained. This rate of power increase becomes 10 times larger than the present rate.

This flexible transient experiment function is supported using the automatic control rod operation system to compensate for the reactivity change due to the vertical sample movement.
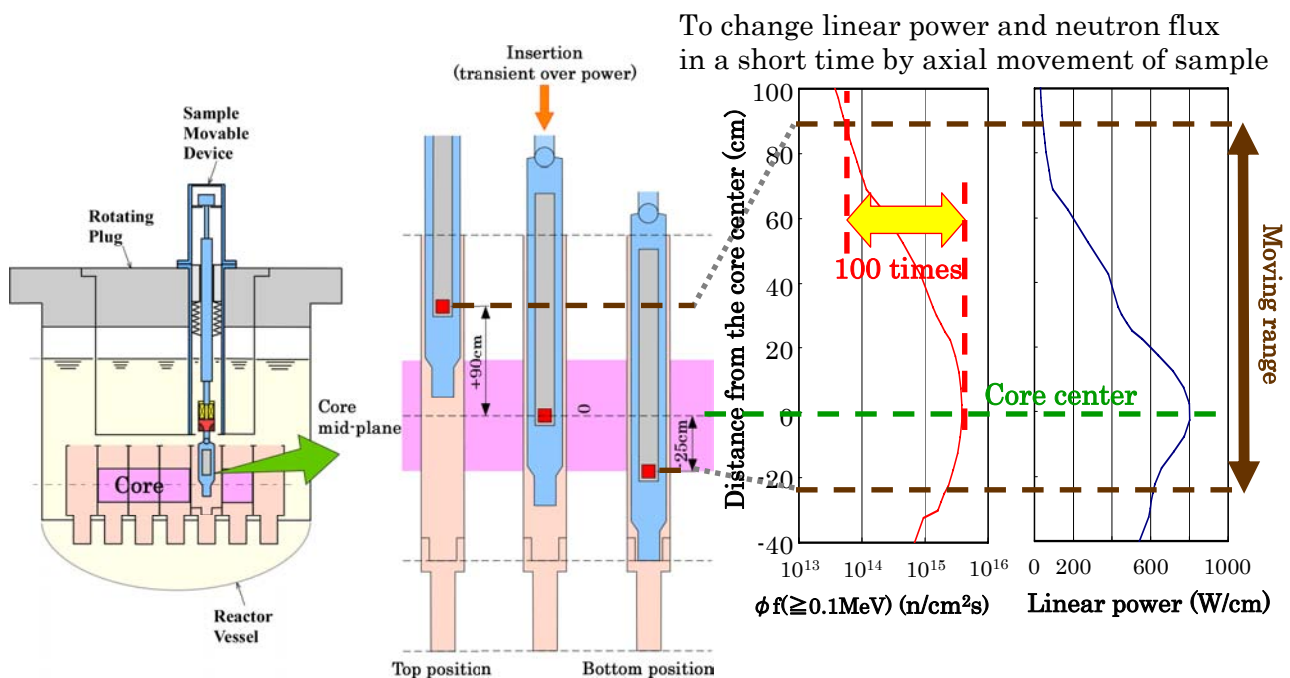
FIG.16. Outline of the sample movable device.

12.10. Fast neutron beam hole for multipurpose utilization

The installation of a fast neutron beam hole is proposed to shorten the turnaround period in the material irradiation test and to make Joyo more convenient as an irradiation test facility. Figure 17 outlines the concept of fast neutron beam hole and calculated fast neutron flux distribution. The beam hole will be set up to penetrate through the rotating plug and to reach to the core mid-plane of Joyo. This facility will be equipped with a mechanism to insert and remove sample capsules in the beam hole independent of the reactor operation. A fast neutron flux in the range from 4×10^9 to 4×10^{15} n/cm^{2}s is predicted at the irradiation hole in the core center. The calculation for the basic shielding design is under consideration to select the

adequate gamma filter to improve the neutron-gamma ratio. This facility will make Joyo available for short-term material irradiation tests and for the production of short-lived isotopes without restriction of the duty cycle operation (60 days).
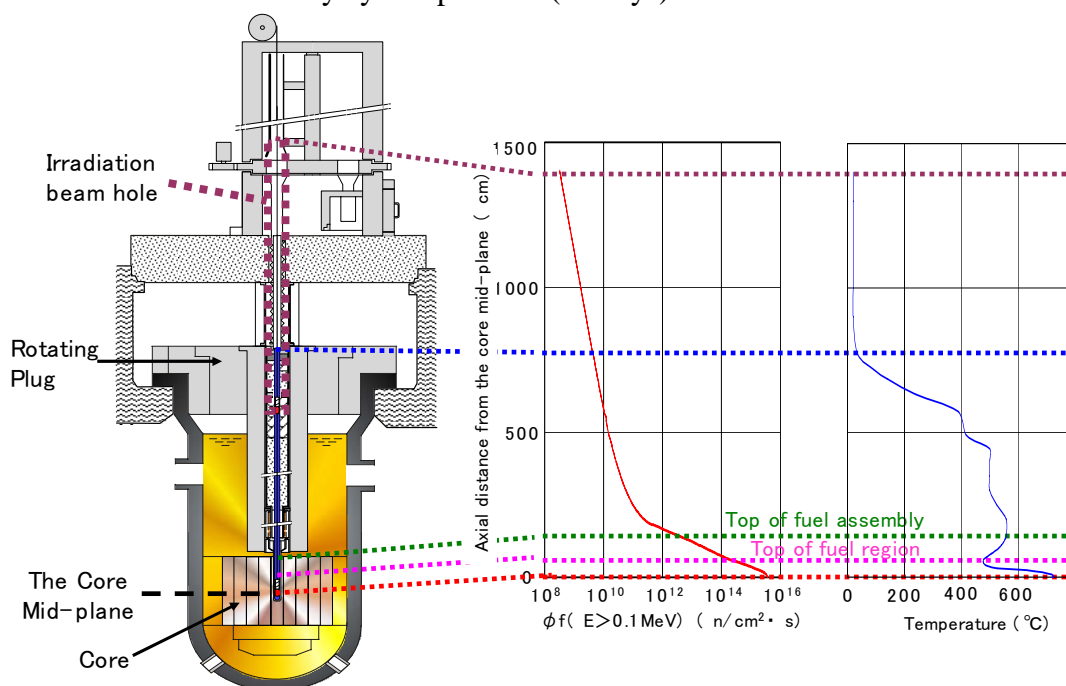
FIG.17. Outline of the fast neutron beam hole.

12.11. Conclusions

Joyo provides the highest fast neutron flux in the world. Several upgrading programs are being promoted to pioneer new irradiation testing applications. The licenses for the computerized reactor control system by automatic control rod operation, neutron spectrum tailoring and lowering coolant temperature have already been permitted, and the design work of all the concepts introduced in this paper has started. These improvements of irradiation capability are expected to promote international collaborations and utilization by external users through sharing the infrastructure for high-quality irradiation tests.

REFERENCES

[1] MAEDA, Y., et al., Nuclear Technology, 150 No.1 (2005) 16.
[2] AOYAMA, T., et al., Nuclear Engineering and Design, 237 (2007) 353.
[3] MAEDA, S., et al., Characterization of Neutron Fields in the Experimental Fast Reactor Joyo MK-III Core, 13th International Symposium on Reactor Dosimetry, the Netherlands (2008).
[4] X-5 Monte Carlo Team, MCNP - A General Monte Carlo N-Particle Transport Code, Version 5, LAUR-03-1987, Los Alamos National Laboratory (2003).
[5] TAKAMATSU, M., et al., Journal of Nuclear Science and Technology, 44 No.3 (2007) 511.
[6] SOGA, T., et al., J. of Power and Energy Systems, 2 No.2 (2008).
[7] ITO, C., et al., J. of Power and Energy Systems, 2 No.2 (2008).
[8] MAEDA, S., et al., Enhancement of irradiation capability of the Experimental Fast Reactor Joyo, 13th Int. Symp. on Reactor Dosimetry, the Netherlands (2008).
[9] AOYAMA, T., J. of Nuclear and Radiochemical Sciences, 6 No.3 (2005) 279.

IRRADIATION TESTING OF STRUCTURAL MATERIALS IN FAST BREEDER TEST REACTOR

S. MURUGAN, V.KARTHIK, K.A.GOPAL, N.G. MURALIDHARN, S.VENUGOPAL, K.V. KASIVISWANATHAN, P.V. KUMAR, B.RAJ

Indira Gandhi Centre For Atomic Research Kalpakkam - 603 102, India.
Email: Murugan@Igcar.Gov.In

Abstract: Fast Breeder Test Reactor (FBTR) at Kalpakkam, India is a sodium cooled fast reactor with neutron flux level of the order of 10^{15} n/cm^2.s and temperature of coolant in the range of 600-720 K (330-450°C), which is being used for the development of fuel and structural materials required for Indian Fast Reactor Programme. Irradiation performance testing on structural materials is being carried out by subjecting prefabricated specimens to desired experimental conditions as part of planned irradiation experiments, and by testing of material samples sourced from actual fuel clad tubes / fuel assembly wrapper tubes irradiated to various fuel burn up levels in FBTR. Pressurised capsules of Zirconium alloys and D9 alloy (modified stainless steel type 316 with controlled additions of titanium and silicon) have been developed to determine the in-reactor creep performance of indigenously developed zirconium alloys and D9 alloy. Pressurised capsules made of zirconium alloys were subjected to fluence levels up to 1.1 x 10^{21} n/cm^2 (E > 1 MeV) in FBTR at temperatures of 579 to 592 K and diameter measurements were carried out in the hot cell facility to determine the irradiation creep rate. Pressurised capsules of D9 alloy are currently undergoing irradiation at a temperature of 623 K in FBTR along with small size tensile test specimens and shear punch test specimens of D9. Non-instrumented gas-gap type irradiation capsule has been developed to achieve higher irradiation temperatures (673 to 873 K) of structural material specimens. The irradiation induced mechanical property changes in cold worked AISI Type SS316 fuel cladding of FBTR have been determined from tensile testing of portions of irradiated fuel clad tubes in the hot cells. Tests were carried out on clad tubes with dpa ranging from 13 to 83 at various test temperatures from ambient (300 K) to irradiation temperature (790 K). Shear punch tests have been used for characterizing the tensile property changes in cold worked AISI Type SS 316 wrapper material of FBTR fuel assemblies. From the results of shear punch tests on irradiated specimens, using correlation equations, the tensile properties of the wrapper material irradiated to various dpa ranging from 30 to 83 have been estimated. A considerable increase in the strength and decrease in the ductility of the wrapper material with increasing dpa was observed from the results. This paper discusses the salient features of irradiation facilities available at FBTR, irradiation experiments carried out on structural materials, and some of the important results obtained from tests on irradiated structural materials.

13.1. Introduction

Fast Breeder Test Reactor (FBTR) at Kalpakkam, India is a sodium cooled fast reactor and is an excellent facility for irradiation of structural material specimens. The flux in FBTR is of the order of 10^{15} n/cm^2.s and the fast flux (E >1 MeV) is about 26% of this. Irradiation performance testing on structural materials is being carried out in two ways: (i) by subjecting prefabricated specimens to desired conditions of temperature and neutron fluence levels as part of planned irradiation experiments in FBTR, and (ii) testing of material samples extracted from irradiated fuel clad tubes / fuel assembly wrapper that have been irradiated to various fuel burn up levels in FBTR. In this paper, the salient features of irradiation facilities available in FBTR for irradiation of structural material specimens, development of pressurised capsules for determination of irradiation creep rate on structural materials, and implementation of irradiation experiments on structural materials of interest to India's thermal and fast reactor programmes are briefly described. Some of the important results obtained from tests on structural materials irradiated are also presented in this paper.
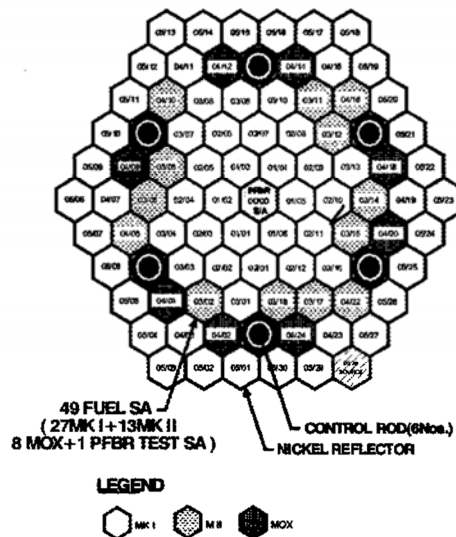
FIG.1. Core of FBTR (up to 5th).

13.2. Core of fast breeder test reactor

FBTR is a sodium cooled, mixed carbide fuelled reactor. Its main aims are to generate experience in the operation of sodium cooled fast reactor and to serve as an irradiation facility for the development of fuel and structural materials for fast reactors. FBTR achieved its first criticality with a core of 22 Mark–I fuel (70% PuC, 30% UC) subassemblies, rated for 10.6 MWt. Progressively the core was expanded by adding carbide fuel of Mark-II composition (55% PuC, 45% UC) fuel subassemblies at outer locations. Based on out of pile tests, and stage-wise post irradiation examination, the linear heat rating of Mark-I fuel has been progressively raised from the initial conservative value of 250 W/cm to 400 W/cm and initial burn up limit of 25 GWd/t to 155 GWd/t in stages [1]. The reactor has so far been operated upto a power level of 17.4 MWt by raising the linear power of Mark-I fuel to 400 W/cm. Eight numbers of high plutonium MOX subassemblies (44% PuO_2 - 56% UO_2) were inducted into the core in 2007. FBTR has completed 14 irradiation campaigns so far, for the purpose of evaluation of the performance of indigenously developed high Pu mono carbide driver fuel, irradiation of Zirconium alloys used in Indian Pressurised Heavy Water Reactors (PHWRs) for assessing their irradiation creep behavior and other physics and engineering experiments. The core of 14th irradiation campaign had 49 fuel subassemblies (27 Mark-I subassemblies, 13 Mark-II subassemblies, 8 MOX subassemblies, and one test fuel subassembly simulating power reactor MOX fuel). The core plan of present small core (upto 5th ring containing fuel subassemblies) is shown in Fig. 1. In 15th irradiation campaign reactor temperatures will approach design values [1]. During this campaign, core inlet temperature will be 380°C and core outlet temperature will be 500/510°C.

13.3. Classification of irradiation experiments/capsules

Irradiation experiments can be classified into two categories: non-instrumented and instrumented.

Non-instrumented experiments/capsules

Experiments that can be carried out in capsules without any online measurement / control facilities are non-instrumented experiments and the capsules used are non-instrumented capsules. There are many positions available in FBTR for irradiation of non-instrumented capsules. Calculations and / or post irradiation examination can give data regarding irradiation

temperature and neutron fluence of specimens irradiated in such capsules. Most of the experiments for mechanical property evaluation of structural materials can be carried out using non-instrumented capsules.

Instrumented experiments/capsules

Instrumented experiments are carried out in capsules with provision for on-line measurement/control facilities. Experimental parameters such as temperature can be monitored/controlled. The central 0-0 position of the core of FBTR can be used for instrumented irradiation experiments. Instrumented capsules are being developed for irradiation of structural materials in FBTR.

13.4. Facilities Available in FBTR for irradiation of structural material specimens

Irradiation of structural material specimens can be performed in FBTR using special fuel, and nickel / steel subassemblies.

Special fuel subassembly

This is a modified version of a standard Mark-I fuel sub assembly. Standard fuel subassembly contains 61 fuel pins with seven top and bottom axial blanket pins. In the special fuel subassembly, central pin of top and bottom axial blanket pins and central seven pins from fuel region are removed to make place for a removable capsule of OD 12 mm and ID 10 mm. The space available for loading of specimens in the special fuel subassembly is approximately 10 mm diameter x 320 mm long.

Special nickel / steel subassemblies

These special subassemblies are modified nickel and steel reflector subassemblies. Standard nickel/steel subassembly contains nickel / steel blocks arranged inside a hexagonal wrapper tube. In the special subassembly, a central bore of diameter 16 to 22 mm is made in the blocks to insert a removable irradiation capsule. The space available for irradiation in these types of capsules is limited to 12 to 18 mm in diameter x 320 mm long.

Facility to carry out instrumented experiments

A special plug called "Central Irradiation Plug For Testing And Experiments (CIPTEX)" offers a leak tight access to the central location of FBTR core (0-0 position) to carry out irradiation experiments using an instrumented device. the equipment holder well of CIPTEX will be introduced into a special fuel subassembly with a housing in the form of a channelled guide tube. CIPTEX offers the advantage of highest flux in FBTR and the possibility of online monitoring for the irradiation experiments. the space available for irradiation is approximately 18 mm diameter x 320 mm long.

13.5. Irradiation experiments on structural materials carried out in FBTR

Non-instrumented irradiation experiments have been carried out on structural material specimens in FBTR. This involves fabrication of irradiation capsules with material specimens loaded in them. Depending on the temperature required to be attained, the irradiation capsule can be of vented type (with holes in the irradiation capsule for entry and exit of reactor sodium) or gas-gap type (with gas insulation layer around the subcapsule containing specimens to attain temperatures higher than reactor sodium temperature). The irradiation capsules are locked in special subassemblies and irradiated in FBTR. Normally five / six numbers of special steel subassemblies with irradiation capsules are loaded in the reactor simultaneously and after desired irradiation they are discharged from the reactor, one by one,

at periodic intervals to attain different fluence levels in the specimens. Post irradiation examination is carried out on the discharged material specimens in the hot cells to evaluate the change in mechanical properties. A brief description of the irradiation experiment carried out on Zirconium alloys and the experiment being carried out on D9 alloy is given below.
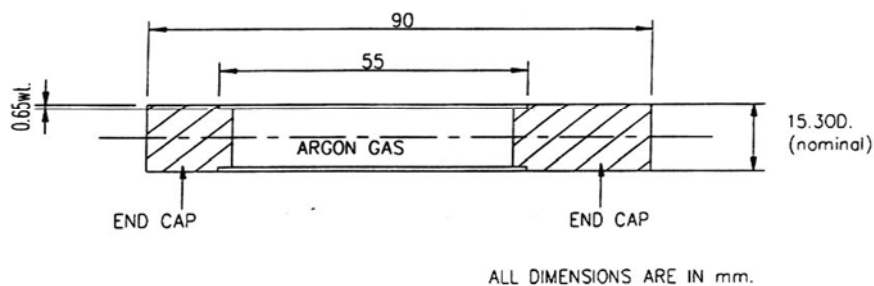
FIG.2. Sketch of zirconium alloy pressurized. Capsule.

13.6. Experiments with Zirconium alloy specimens

An irradiation experiment was carried out in FBTR to determine the irradiation creep rate of indigenously developed zirconium alloys used for fabrication of pressure tubes in PHWRs of India. Small size pressurised capsules made of Zircaloy-2 and Zr-2.5%Nb alloy filled with argon (and a small fraction of helium) at pressures between 4.7 to 6.7 MPa were utilized in this irradiation experiment. The outer diameter of the pressurised capsule was 15.3 mm and the nominal wall thickness was 0.65 mm. The overall length of pressurised capsule was 90 mm. A sketch of zirconium alloy pressurised capsule is shown in Fig.2. Technology for making the pressurised capsules was developed at Indira Gandhi Centre for Atomic Research (IGCAR). Nominal pressure during irradiation was 9.6 and 12.6 MPa (in Zircaloy-2 and Zr-2.5% Nb capsules respectively) and the nominal hoop stress intensity during irradiation was 105 and 147.5 MPa (in Zircaloy-2 and Zr-2.5%Nb capsules respectively).

The irradiation temperature desired for this experiment was around 300°C, since this is the temperature to which the pressure tubes are exposed to in PHWRs. The irradiation temperatures of the five pressurised capsules assembled in each of the irradiation capsules were calculated to be 306, 310, 314, 318, 319°C respectively. The irradiation capsule is assembled in a special steel subassembly and six such subassemblies were loaded in FBTR. The sketch of irradiation capsule with zirconium alloy pressurised capsules locked in special sub assembly is shown in Fig. 3. Duration of irradiation of the zirconium alloy pressurised capsules was 35 to 80 Equivalent Full Power Days (EFPDs) at 8 MWt power.

The special carrier subassemblies along with the irradiation capsules were taken out of FBTR sequentially. The irradiation capsules were dismantled in the hot cells of Radio Metallurgy Laboratory (RML) and pressurised capsules were retrieved from the irradiation capsules by carrying out cutting operations [2].

116
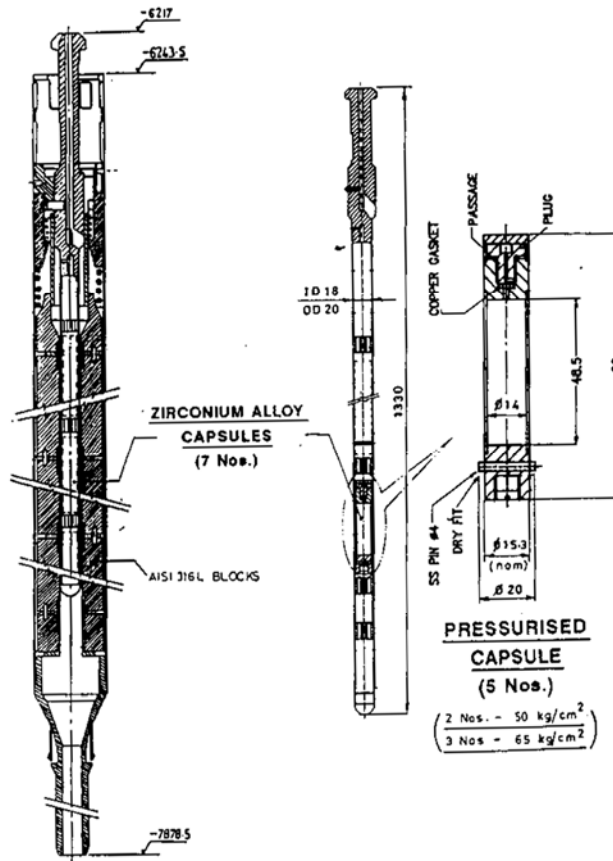
FIG.3. Irradiation capsule with zirconium alloy pressurized capsules locked in special sub assembly.

Pre-irradiation measurements like outer diameter, inner diameter, and weight of the capsule before and after pressurisation were taken for all the pressurised capsules. The diameter was measured using a fixture and digital micrometer with 1-micrometer accuracy. During post irradiation examination, the weight of each pressurised capsule was measured and it was ensured that there was no leak of gas from the capsule. The outer diameter of the each pressurised capsule was measured at 5 angular and 6 longitudinal locations. To determine the increase in diameter of the capsule due to irradiation, the average of the measurements carried out in the central portion (10 mm long) of the pressurised capsule was utilized.

A typical result obtained is shown in Fig. 4. Figs 4 (a) and (b) show the variation of creep strain with fluence (E > 1MeV) and radiation damage (dpa). Normalization of the data for thermal reactor flux conditions was carried out by taking the nominal fast flux (E > 1 MeV) value in thermal reactor as 3.2×10^{13} n/cm^2.s. The fluence values are divided by this fast flux value to obtain the exposure hours in thermal reactor environment. Fig. 4 (c) shows the creep data as a function of this effective exposure time in PHWR environment. The data exhibit a linear behaviour with respect to fluence, displacement dose, and time; thereby enabling estimation of the creep rates, at conditions used in this experiment.

TABLE1. THE STEADY STATE CREEP RATES OBTAINED ARE GIVEN BELOW [3]

Material	Temp, ºC	Average stress, kg/cm^2	Steady state creep rate (explain unites and values)		
			Fluence E>1Mev)]$^{-1}$	[dpa]$^{-1}$	[hr]$^{-1}$
Zircaloy-2	306	1062	0.4467 x 10^{-23}	1.625 x 10^{-3}	5.100 x 10^{-7}
Zircaloy-2	310	1051	0.1100 x 10^{-23}	0.500 x 10^{-3}	1.300 x 10^{-7}
Zr-2.5%Nb alloy	314	1500	0.4670 x 10^{-23}	2.450 x 10^{-3}	5.125 x 10^{-7}
Zr-2.5%Nb alloy	318	1467	0.5000 x 10^{-23}	2.600 x 10^{-3}	5.725 x 10^{-7}
Zr-2.5%Nb alloy	319	1457	1.0530 x 10^{-23}	4.050 x 10^{-3}	12.067 x 10^{-7}
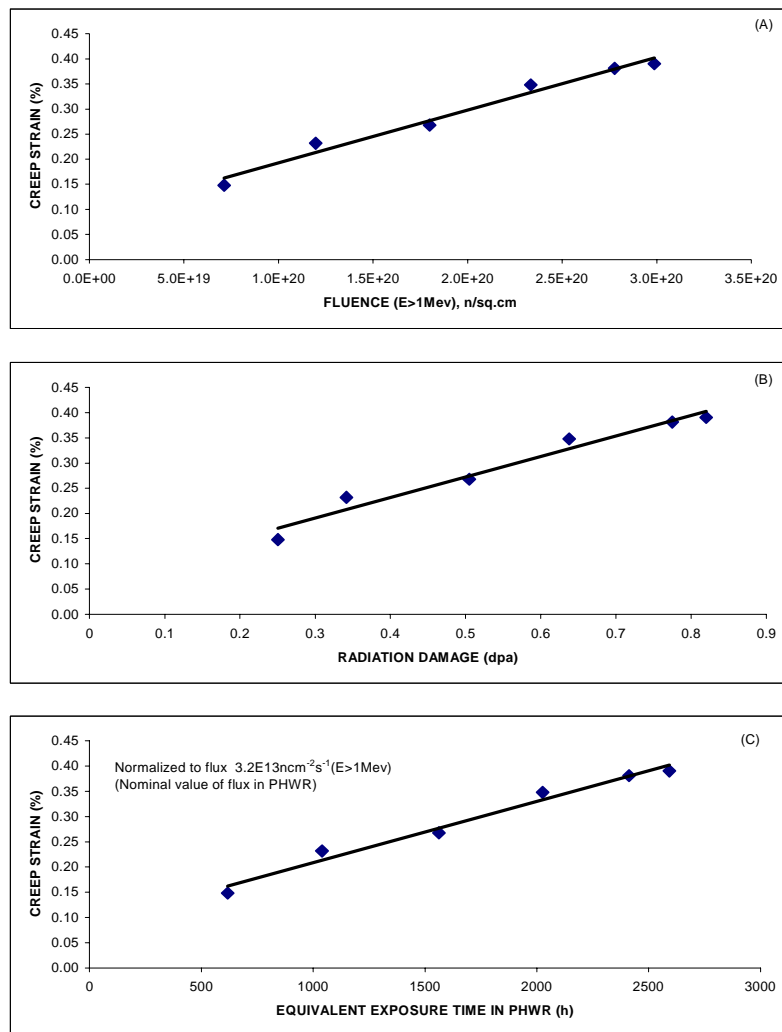
FIG.4. Creep of Zr-2.5% Nb at a temperature of 319°C and an average stress of 145.7 MPa. (a) Creep strain versus fluence (E >1 MeV), (b) Creep strain versus radiation damage (dpa), (c) Creep strain versus time.

It can be noted here, that there was variation between the texture of pressurised capsule and the texture of actual pressure tube used in PHWRs and a correction factor based on theoretical

formulation was applied to the above values of steady state creep rate to determine the steady state creep rates for pressure tubes.

13.7. Experiment with D9 alloy specimens

D9 alloy (modified stainless steel type 316 with controlled additions of titanium and silicon) is the cladding and wrapper tube material selected for Prototype Fast Breeder Reactor (PFBR) being constructed at Kalpakkam. Pressurised capsule of D9 alloy has been developed to determine the in-reactor creep performance of indigenously developed D9 alloy.

D9 pressurised capsules were fabricated from indigenously developed D9 alloy clad tube of outer diameter 6.6 mm and 0.45 mm wall thickness. D9 tube is closed by welding at one end and fitted with special end plug at the other end, which enable filling of gas at the desired pressure into the tube using a pressurising system. A gas mixture of 97% argon and 3% helium is used for the pressurisation. The length of the pressurised capsule is about 70 mm. Capsules with an internal pressure of 6.5 MPa at room temperature has been successfully developed at IGCAR. A sketch and components of D9 pressurised capsule are shown in Fig. 5.
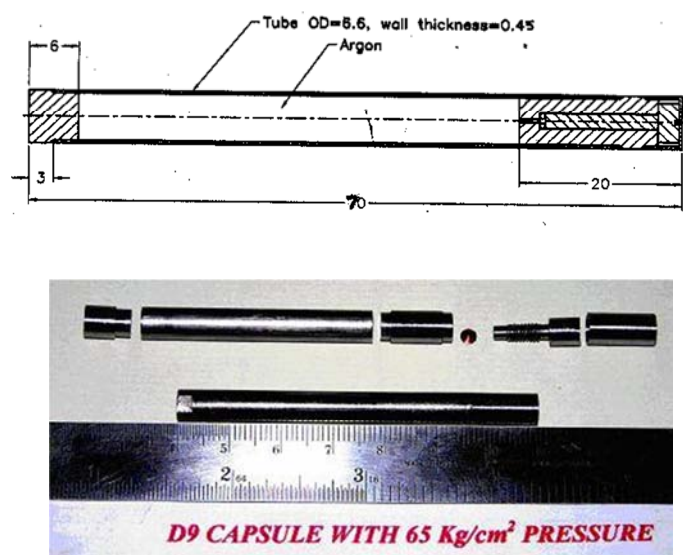
FIG.5. Sketch and components of D9 alloy pressurised capsule.

Irradiation of D9 pressurised capsules is progressing in FBTR to determine the irradiation creep behaviour at a temperature of 350°C which is the temperature of flowing sodium around the irradiation capsule. The hoop stresses that are developed in the D9 pressurised capsules at the irradiation temperature are 30, 60 and 90 MPa respectively. Desired duration of irradiation is more than one year and the maximum damage attained will be more than 24 dpa. After desired irradiation, post irradiation examination will be carried out on these pressurised capsules at hot cell facility. This experiment will provide data on indigenously developed D9 alloy at 350°C.

13.8. Development of non-instrumented gas-gap type irradiation

A non-instrumented gas-gap type irradiation capsule has been developed for irradiation structural material specimens in FBTR at temperatures higher than that of the sodium flowing around the irradiation capsule. Fig.6 shows the sketch of a non instrumented gas gap irradiation capsule.

In this type of capsule, there are five subcapsules coaxially located in the irradiation capsule and the specimens are kept in static sodium inside the subcapsules with gas gap between sub capsules and irradiation capsule. The specimen temperature will rise due to neutron and gamma heating in the reactor. Helium-argon gas mixture with selected composition will be filled in the annular gap between each subcapsule and the respective portion of irradiation capsule to attain desired higher temperatures. The annular spaces around different subcapsules are not inter-connected and due to this, the specimen irradiation temperatures of 400, 450, 500, 550 and 600ºC (temperatures of interest to fast reactor programme) will be achieved in the five subcapsules. As part of this development, a mock up irradiation capsule containing five subcapsules has been fabricated. Sodium filling in the subcapsules was carried out in an argon atmosphere glove box and an innovative sealing method was developed to seal the sodium-filling path in a leak tight manner. The subcapsules were machined in such a way that they are located coaxially within irradiation capsule one over the other and to have a separate uniform gas insulation layer around each of the subcapsules. X-radiography examination was carried out on the mock up irradiation capsule and this facilitated verification of the internal configuration of the capsule.

Six numbers of gas-gap type non-instrumented irradiation capsules are being fabricated for subjecting specimens of structural materials of interest to desired high temperatures and fluence values in FBTR.
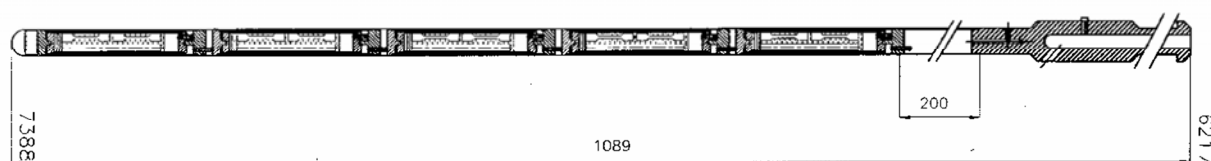
FIG.6. Sketch of non-instrumented gas-gap capsule.

13.9. Post irradiation testing of samples sourced from irradiated fuel clad tubes/fuel assembly wrapper tubes

A few results obtained from testing of material samples sourced from fuel clad tubes / fuel assembly wrapper tubes irradiated to various fuel burnup levels in FBTR are discussed in this Section.

Type 316 Stainless Steel (316 SS) in 20% cold worked condition is used as the structural material for fuel cladding and wrapper tube in FBTR. Neutron irradiation of cladding and wrapper induces changes in mechanical properties associated with micro-structural evolution. The evaluation of mechanical property changes of the irradiated cladding and wrapper is very essential for extending their use in the reactor to achieve higher burnup. The mechanical properties of irradiated cladding were determined by tensile tests in the hot cell facility using a 20 kN capacity universal tensile test machine fitted with a resistance heating furnace (Fig. 7) as per the ASTM E-8 and ASTM E-21 standards. The tests were carried out on tube specimens sectioned from various locations along the length of the fuel pin corresponding to a combination of dpa (0-83) and irradiation temperature (700-775 K). Irradiated clad tubes of approximately 70 mm length were fitted with mandrels from the ends and gripped using special type compression fittings. The tensile test was performed at various test temperatures using a programmable controller/computer at a nominal strain rate of $4x10^{-4}$ s^{-1}.

120
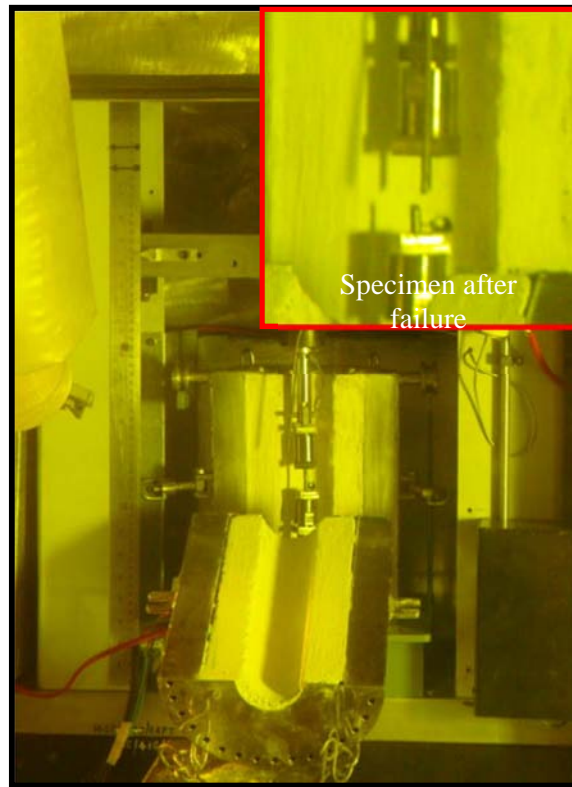
FIG.7. Remote tensile test machine in the hot cell facility.
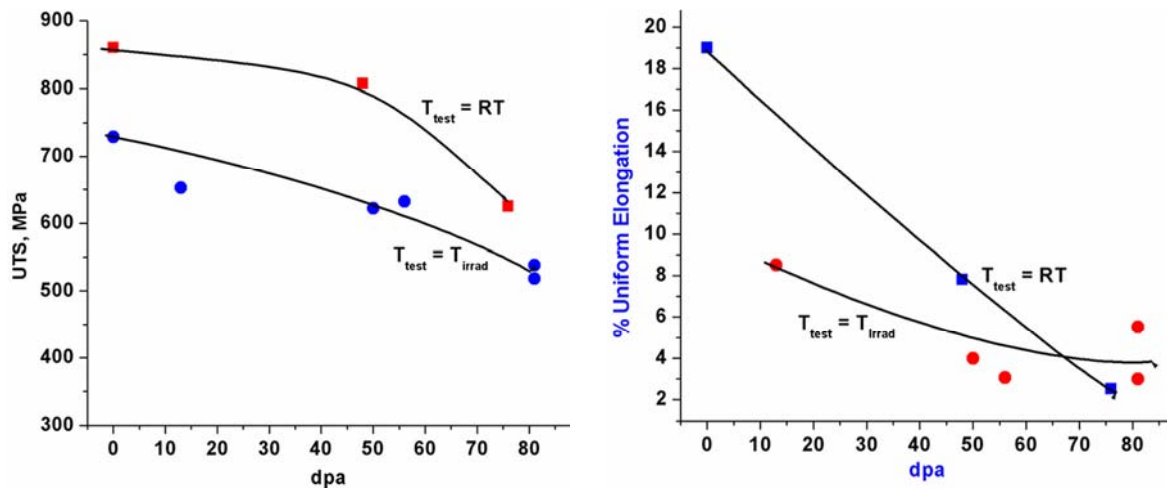
FIG.8. Trends in the UTS and % uniform elongation of SS316 cladding with dpa,
RT - Room temperature, T_{test} – Test temperature, T_{irrad}–Irradiation temperature
(703-K -773 K).

The tensile test results of irradiated cladding that was taken from fuel pin, which was irradiated to a burnup of 100 GWd/t (56 dpa), revealed that the clad tubes retained sufficient high temperature strength, while the uniform elongation reduced monotonically with increasing dpa to values as low as 3% at test temperatures corresponding to reactor operating conditions (723 K).

Tensile tests at various temperatures like the fuel handling (453 K) and ambient conditions (300 K) also indicated sufficient strength and ductility at these operating conditions. Tensile tests carried out on irradiated clad tubes that had seen 155 GWd/t burnup (81 dpa) at 485ºC indicated that the ultimate tensile strength (UTS) had reduced to about 520 MPa, while the uniform elongation was around 3-4.5%. The decreasing trend in the UTS and % elongation with dpa is depicted in Fig 8. International experience shows that austenitic alloys tend to soften in strength with the onset of nil ductility with increasing void swelling [4]. This has been interpreted as due to the effect of high stress concentration caused by high void density and heavy precipitation leading to softening, flow localization and the associated ductility losses.
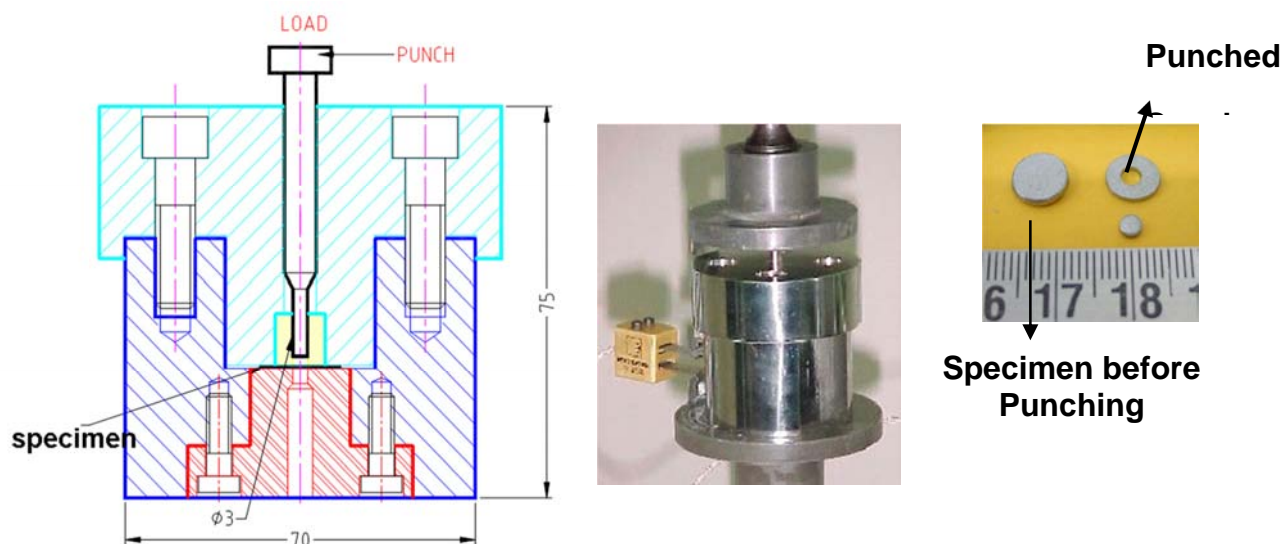
FIG.9. The shear punch test fixture, experimental setup and the miniature specimens.

For evaluating the tensile properties of the hexagonal wrapper, miniature specimen technique like shear punch tests [5] have been carried out. By using small specimens for testing irradiated materials, the radiation dose levels drastically decreases in proportion to its volume and it becomes possible to take them out of the hot cells and conduct mechanical testing in comparatively simple shielded enclosures with reduced radiological hazards. The test involves blanking a 1.0 mm thick and 8.0 mm diameter small specimen in a test fixture using a flat cylindrical punch, Fig. 9. The load-displacement plot obtained during the punching operation is analyzed and correlated with the conventional tensile test data. The test technique is standardized using specimens of SS 316 with various cold rolled and solution annealed microstructures. Tensile-to-shear punch property correlation is established from the standardization experiments. Shear punch tests are carried out on small specimens extracted at different locations along the length of the subassembly corresponding to different dpa. It is seen from the shear punch test results that there is an increase in the room temperature yield strength (YS) and UTS with increasing dpa (Fig. 10 a) and a decrease in the ductility. The tensile properties of wrapper show a hardening behaviour as its irradiation temperature is around 400-430ºC. The evaluated parameters indicate the presence of sufficient tensile strength and ductility at room temperature.

The trends in the void swelling of the cladding and wrapper as a function of dpa are shown in Fig. 10 b). The volumetric swelling after 81 dpa (peak) corresponding to the burnup of 155 GWd/t was estimated to be around 11.5% for the SS316 cladding and around 4% for wrapper. The rates of clad swelling are quite high at dpa > 60 as compared to behaviour at lower dpa. This is also evident from the higher rates of increase in the diameter of the clad

with increasing dpa. The swelling of the cladding is higher than that of wrapper which is attributed to the high temperatures of the cladding close to the peak swelling regime of SS316. The post-irradiation data on the cladding and wrapper were very useful for performance assessment of FBTR structural material and in progressively enhancing the burn-up of the FBTR to the present level of 155 GWd/t without any failure.

13.10. Future plan of irradiation experiments

Irradiation experiments on clad and wrapper tube materials such as D9 and modified D9 alloy will be carried out using vented / gas-gap non-instrumented capsules in FBTR. Instrumented structural material irradiation capsules will be developed for use in FBTR.
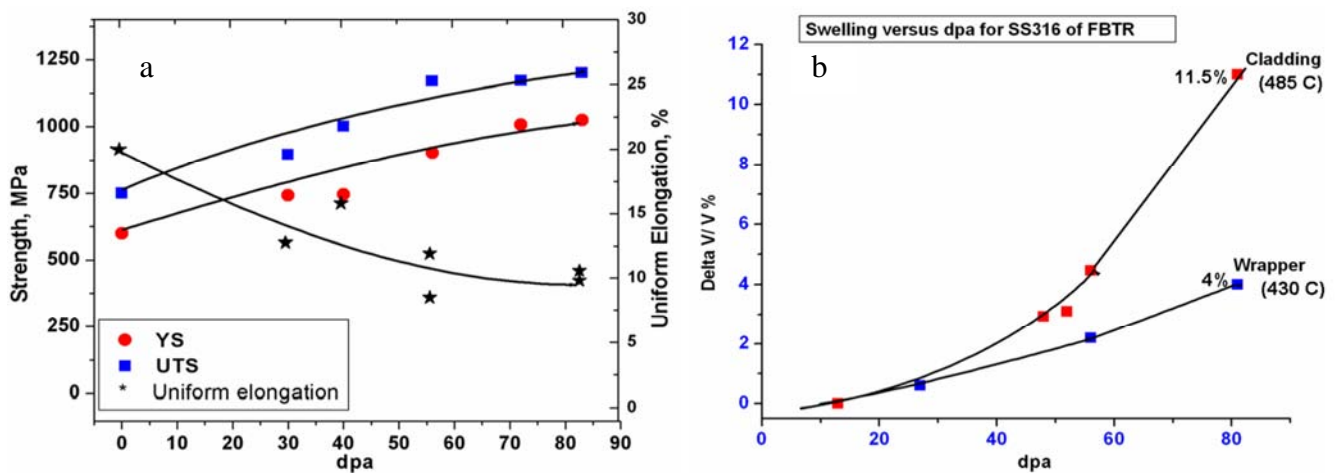
FIG.10 (a) The trends in the room temperature strength and ductility of the irradiated SS316 wrapper of FBTR as a function of dpa, (b) Volumetric swelling of the FBTR cladding and wrapper determined from immersion density measurements as a function of dpa.

13.11. Conclusions

This paper discusses briefly the facilities available in FBTR for structural material irradiation, details of pressurised capsules developed for irradiation creep experiments, irradiation experiment carried out using zirconium alloy pressurised capsules for thermal reactor programme, irradiation experiment being carried out using D9 alloy pressurised capsules for fast reactor programme and some of the important results from post irradiation examination of fuel cladding and fuel subassembly wrapper tubes of FBTR which have seen irradiation damage levels up to 83 dpa. Future plan of irradiation experiments on structural material specimens is mentioned.

REFERENCES

[1]   Indira Gandhi Centre for Atomic Research, Kalpakkam, Fast Breeder Test Reactor – Annual Report (2008).

[2]   KASIVISWANATHAN, K.V., JOJO, J., Dismantling of irradiated zirconium alloy pressurised capsules, IGC News Letter 43 (2000) 10.

[3]   MURUGAN, S., CHAURASIA, P.K., KUMAR, P.V., BALDEV, R., Creep of Zirconium Alloys - Report on Irradiation Experiment Carried out in FBTR, IGC Report No.254, Kalpakkam (2003).

[4]   FISSOLO, A., CAUVIN, R., HUGOT, J.P., LEVY, V., Effects of Radiation on Materials 14th International Symposium, Vol. II, ASTM STP 1046, (Packan, N.H., Stoller, R.E., Kumar, A.S., Eds.), American Society for Testing and Materials, Philadelphia (1990) 700.

[5]   LUCAS, G.E., ODETTE, G.R., SHECKHERD, J.W., Shear punch and micro hardness tests for strength and ductility measurements, The Use of Small-Scale Specimens for Testing Irradiated Materials, ASTM STP 888, (Corwin, W.R., Lucas, G.E., Eds.), American Society for Testing and Materials (1986) 112.

Chapter 14

NEUTRON SCATTERING STUDIES OF MATERIALS IRRADIATED AT HIGH NEUTRON FLUENCE

P. LUKÁŠ[1,2], P. MIKULA[1,2], J. ŠAROUN[1,2], P. STRUNZ[1,2], M. VRÁNA[1]
[1]Nuclear Physics Institute As Cr, V.V.I., 250 68 Řež, Czech Republic
[2]Research Centre Řež, Ltd., 250 68 Řež, Czech Republic
Email: mikula@ujf.cas.cz

Abstract: A dedicated shielding box enabling safe manipulation with highly radioactive specimens was developed in NPI Řež as an auxiliary equipment of neutron diffraction stress/strain scanners. The box was designed to provide the following functions, an easy specimen installation in the hot cells, a remote control of specimen positioning, input and output beam shutters and collimators. Employing this facility, the stress mapping experiments on radioactive components can be realized by means of the current stress/strain scanners. Similarly, the method of small-angle neutron scattering has been advantageously used for studies of evolution of microstructure changes of strongly irradiated steels, however, on a larger scale in comparison with the dimension of the crystal lattice. The results of the experimental work are presented in this paper.

14.1. Introduction

Various material properties as e.g. ductility, strength, elasticity, brittleness could be strongly influenced by a radiation damage at a high neutron fluence with a considerable effect on the functional fatigue and operational life of components under irradiation and thermo-mechanical loading. From a safety point of view, very critical items are reactor structural materials and especially the weld joints on the reactor core components. Complex information on evolution of microstructure changes and the residual stress level as a function of time and neutron fluence plays a key role for assessment of the component integrity and for an estimation of the operational live. Studies of structure defects as well as the residual stresses in as-manufactured and used components are thus of a great importance. In this way neutron scattering provides unique possibilities of nondestructive testing of such microstructural changes resulting in structure defects and/or residual stresses. The nondestructive neutron scattering methods for scanning of the internal stresses in polycrystalline materials as well as small-angle neutron scattering (SANS) for studies of inhomogeneities in surrounding homogeneous bulk material have become widely applied and the utilization of such techniques for material characterization is then very important [1]. As the measured effects are relatively small, a special sample environment should be used to avoid unacceptable detector signal coming directly from the highly radioactive samples.

Residual stresses are stresses that are locked-in within a material, and can exist without any external load. They are caused by incompatible internal permanent strains. However, they can be generated or modified at every stage in the component life cycle, from original material production to final disposal or can be formed in a material during repairs. Welding is e.g. one of the most significant causes of residual stresses and typically produces large tensile stresses whose maximum value is approximately equal to the yield strength of the materials being joined and balanced by lower compressive residual stresses elsewhere in the component. Therefore, residual stresses or their development brought about by an applied external force are difficult to predict in engineering materials and can have a strong influence on their basic mechanical properties. Residual stresses may reduce the performance parameters or cause failure of manufactured products. The large penetration depth and selective absorption of neutrons make them a powerful tool in nondestructive testing of materials in a rather high depth under the surface. Moreover, neutron diffraction is phase sensitive. Neutron diffraction studies can thus significantly help one to improve the manufacturing quality of engineering components, to optimize their design criteria in applications and to predict their operational life.

A special task represents the determination of residual stresses in highly radioactive samples, which were exposed to high neutron fluence. For this purpose a special compact shielding box, where the radioactive sample is situated, was constructed in NPI Řež. This dedicated facility enables us an easy specimen installation in the hot cells and a remote control of specimen positioning and beam shutters. Employing this shielding box, the strain/stress mapping experiments on radioactive components can be then realized by means of the current stress/strain scanner.

SANS also belongs to nondestructive experimental techniques widely used for structure investigations of condensed matter. This technique also has its unique advantages; in particular it enables the distinction of inhomogeneities from a homogeneous matrix consisting of very close elements in the periodic table. Moreover, rather bulky samples (0.1-1 cm^3) can be studied due to the low attenuation of neutrons in most materials. SANS scattering is concerned with the measurement of elastic scattering cross-sections in a range of momentum transfer values Q between 10^{-5}-10^{-1} Å^{-1}. The scattering into this momentum space range provides information on size, shape and concentration of inhomogeneities in studied materials within the space size from about 30 Å to 30 μm. However, it is practically impossible to cover this broad Q-range by the only one type of a SANS instrument. While the most common collimator facilities are used in SANS experiments with $Q>2\times10^{-3}$ Å^{-1}, double-crystal (DC) nondispersive settings have been proved to be more efficient when higher Q-resolution is required.

14.2. Residual strain/stress measurement by neutron diffraction

The stresses displace atoms from their original positions in a crystalline material, which in fact result in changes of the interatomic distances, which vary, from those in a stress-free case. The stresses are not measured directly by diffraction techniques, but one measures residual strains, which are then converted to stresses using appropriate moduli. Neutron diffraction along with X-ray diffraction, where angular positions of diffraction maxima are directly bound with the values of lattice constants through the Bragg equation, offers a unique non-destructive technique for investigation of stress fields. Thus, the elastic strains are derived from the change in the lattice spacing of the crystalline material. By translating the specimen through a neutron beam, stresses at different locations can be determined. In fact, neutron diffraction is the only non-destructive and highly accurate method which can facilitate 3-D mapping of residual stress in bulk components.
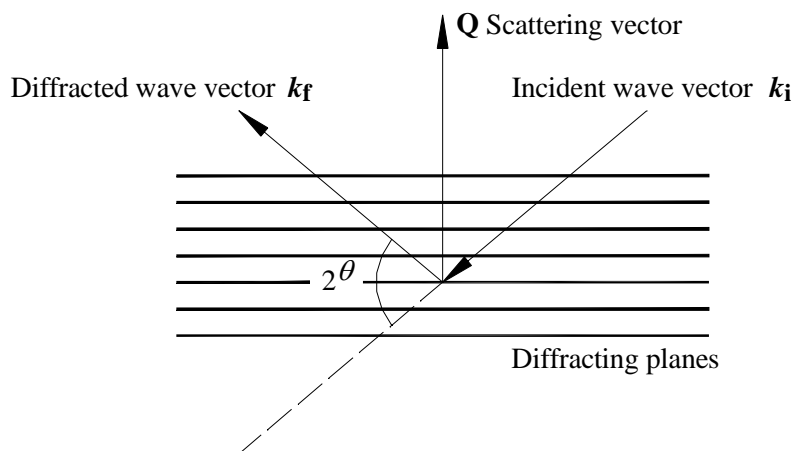

FIG.1. Schematic illustration of Bragg scattering geometry.

A crystalline material when placed in a neutron beam of the wavelength λ,, which is comparable with the lattice spacing, gives a diffraction pattern with position for a plane (*hkl*) defined by the Bragg relation

$$2d_{hkl}\, sin\, \theta_{hkl} = \lambda, \tag{1}$$

where d_{hkl} is the interplanar spacing (lattice spacing), λ the neutron wave-length and θ_{hkl} is the half of the angle between the incident and the scattered beams (see Fig.1).

As for a fixed λ the Bragg angle θ_{hkl} is sensitive only to the change of the lattice spacing d_{hkl}, the strain (the strain component) is measured in the direction of the scattering vector, $Q = k_f - k_i$, which bisects the angle between incident and diffracted beams and is perpendicular to the diffracting planes (as shown in Fig. 1). Lattice spacing can be determined from the measured angular position of the diffracted peak (Bragg reflection) by illuminating the specimen with a monochromatic collimated beam of neutrons. If the specimen contains no strain, the lattice spacing is called the strain free (stress free) value for the material and is denoted by $d_{0,hkl}$. In a stressed specimen, lattice spacing is altered and a shift in angular position of the corresponding Bragg peak reflects the elastic strains according to following equation:

$$\varepsilon_{hkl} = \frac{d_{hkl} - d_{0,hkl}}{d_{0,hkl}} = \frac{\Delta d_{hkl}}{d_{0,hkl}} = \frac{\sin \theta_{0,hkl}}{\sin \theta_{hkl}} - 1. \tag{2}$$

Stress (σ_{ij}) and strain (ε_{ij}) are tensors quantities related one to another by the elastic stiffness tensor C_{ij}, and the elastic compliance tensor S_{ij}:

$$\sigma_{ij} = \sum_{kl} C_{ijkl} \varepsilon_{kl}, \text{ and } \varepsilon_{ij} = \sum_{kl} S_{ijkl} \sigma_{kl}, \tag{3}$$

where σ_{ij} and ε_{ij} have 9 components, 6 of which are independent, and C_{ij} and S_{ij} have 81 components, 36 of them can be independent [2,3].

Essentially, most engineering calculations are based on isotropic continuum mechanics. In this case, C_{ij} can be written in terms of just two independent elastic components, such as *Young's modulus*, *E*, and *Poisson's ratio, ν*. Consequently, the relationship between stress and strain can be expressed by using the generalized *Hooke's law:*

$$\sigma_{ij} = \frac{E}{1+\nu} \left[\varepsilon_{ij} + \frac{\nu}{(1-2\nu)} (\varepsilon_{11} + \varepsilon_{22} + \varepsilon_{33}) \right], \tag{4}$$

where i, j = 1,2,3 indicate the components of main directions.

The neutron strain scanner evaluates the variations of lattice spacing within a sample with a spatial resolution of the order of few millimetres given by the dimensions of the gauge volume. The diameter of the polycrystalline grains should be about two orders of magnitude smaller than the dimensions of the chosen gauge volume, which is geometrically defined by the used optical components (slits, collimators) and scattering angle. The best geometrical choice corresponds to $2\theta=90°$. Consequently, if possible the best choice is an intense Bragg peak at 2θ in the vicinity of 90°. Beam parameters of the dedicated diffractometer should be

adjusted such that the angular position of the sample reflections could be measured with a precision of 0.01%.
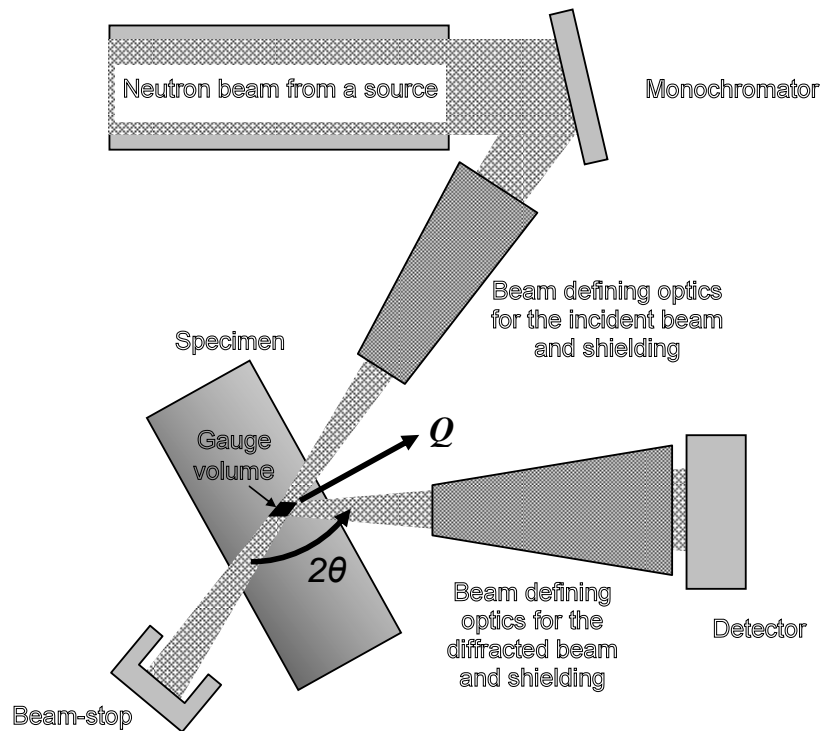
FIG.2. Schematic illustration of a conventional reactor source based diffractometer for strain measurement.

For macrostrain/macrostresses scanning the *FWHM* of the diffraction profile at a scattering angle of 90° is usually $< 1.5 \times 10^{-2}$ rad. If the resolution of the instrument is higher (*FWHM* $\leq 2 \times 10^{-3}$ rad), even mirostrains/stresses in the plastic deformation region can be investigated on the basis of the peak profile analysis, when the plastic deformation results in a change of the width and the form of the diffraction peak profile. If the strain/stress diffractometer is equipped with a tension/compression rig and a heating system for samples, then, the response of the lattice of the sample under thermo-mechanical load in elastic as well as plastic deformation region can be investigated in situ.
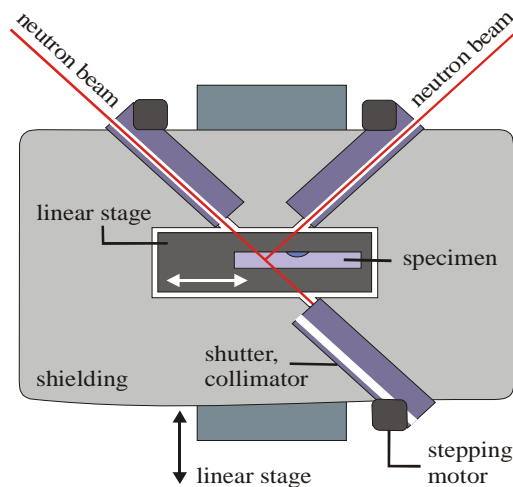
FIG.3. Schematic sketch of the experimental shielding container for strain/stress scanning of the irradiated specimens.

128

14.3. New facility for neutron diffraction studies of residual stresses in highly radioactive materials

This dedicated facility [4] enables an easy specimen installation in the hot cells and a remote control of specimen positioning and beam shutters and collimators. By using this shielding box, the stress mapping experiments on radioactive components can be realized by means of the current stress/strain diffractometers. In the case of diffraction measurements of residual strains in austenitic stainless steels, the most convenient reflection seems to be 311 reflection due to the linear response of the dependence (σ, ε_{311}) even beyond the yield point. The schematic sketch of the dedicated shielding box is shown in Fig. 1. The led container body is designed with an effective shielding layer of 16 cm. This shielding capacity would be sufficient to work with irradiated austenitic specimens up to maximum activity of 4×10^{12} Bq. The internal space of the container is equipped with a linear stage and a specimen holder. Three independent beam shutters and collimators controlled by stepping motors are used for the incident and diffracted neutron beams in transmission and reflection geometry, respectively. The rotating steel collimators provide a circular channel of the diameter of 1cm. The input and output beam were formed by Cd-masks of a size of 3×3 mm^2. The strain determined in such a diffraction experiment is then averaged over the gauge volume of $3 \times 3 \times 3$ mm^3. The irradiated specimen in a transport container was delivered into the hot cell of the LVR-15 reactor. Here, the specimen was installed into the experimental container after which it was transported directly to the reactor hall and installed at the corresponding spot of the neutron diffraction facility.

TABLE1. CHEMICAL COMPOSITION OF USED STEEL (WT.%)

C	Si	Mn	P	S	Cr	Ni	Nb	Co
0.031	0.57	1.27	0.016	0.012	17.10	9.30	0.52	0.040

The tested CT specimens were manufactured from the steel A347 weld joint sample. The material sample had been cut from the H4 circumferential weld joint of the BWR NPP core shroud. The CT specimens of notch length of 20 mm were machined to have the crack plane in heat-affected zone of the weld joint (Fig.2). At first, the CT specimen was irradiated in experimental reactor LWR-15 to 6.2×10^{20} n/cm^2, then tested inside the in-pile reactor water-loop BWR-2. It was supplied the normal BWR water environment of 150–200 ppb oxygen content and conductivity below 0.3 μS/cm for totally 2200 hours and the hydrogen BWR water environment for 230 hours in the loop. At the same time the specimen was loaded, first using cyclic and then constant load regime. The crack growth rate was measured using potential drop technique. After the tests the specimen was final fractured by fatigue at room temperature in air. The half of the CT specimen containing the base metal was further used for the neutron diffraction experiment. The total specimen activity was determined as 11 GBq.
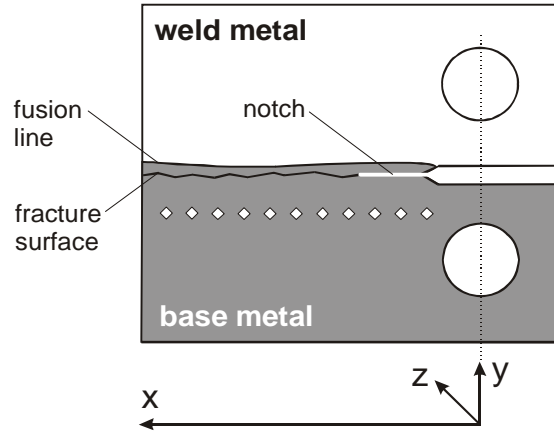
FIG. 4. Schematic drawings of the CT specimen, white squares near fracture surface indicate a location of the measuring points.

This neutron diffraction experiment mainly focused on the feasibility study of the new experimental container. The only one scan of the residual strains near the fracture surface (y = - 6mm) was realized in the radioactive CT specimen. The location of measuring points is shown in Fig. 2. The component of the strain tensor perpendicular to the fracture surface was only examined. For comparison, the reference non active CT specimen was treated in the same way except that the irradiation in reactor was examined as well. The results of diffraction mapping of residual strains are displayed in Fig. 3a,b. Despite a rather deep scan (6 mm under the fracture surface) both scans show similar peaks of tensile residual strains of the same amplitude of ε ~3×10^{-4} located in the vicinity of the crack tip.
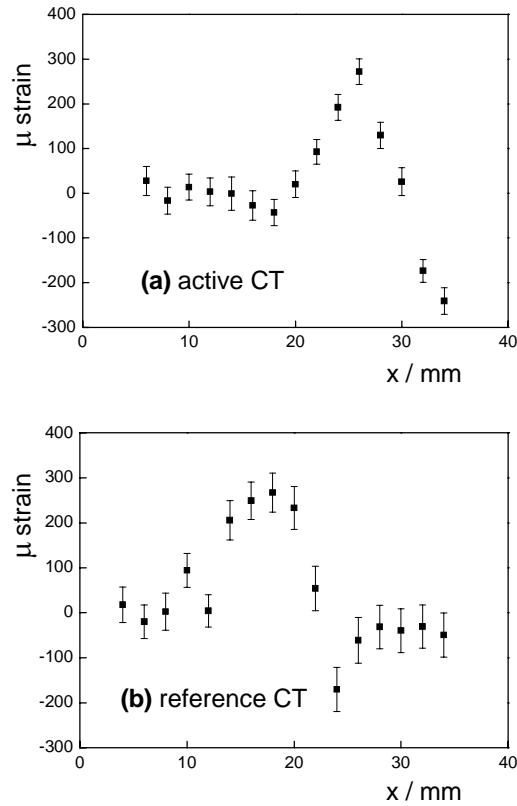
FIG.5 a,b. Scan of the residual strain component perpendicular to the fracture surface in the active specimen (a) and the reference specimen (b).

The localization of the strain maximum is slightly different in both examined specimens, but it can be caused by irregular propagation of the crack tip. Taking into account the corresponding elastic modulus of about 200 GPa, the stress level is roughly estimated as 60 MPa. In the present experiment, a relatively good precision and sensitivity of about $\sim 6\times10^{-5}$ in strain determination was achieved. Finally, it can be stated that the application of this technique in evaluation of residual stress level in reactor components in dependence on their operation time and neutron fluence can be very important for assessment of the component integrity and for a support of the operation prolongation.

14.4. Characterization of radiation-induced precipitates in reactor pressure vessel steels by SANS

Embrittlement of steels exposed to high doses of neutron irradiation essentially reduces the lifetime of reactor pressure vessels (RPV). The degradation of mechanical properties due to irradiation is closely related to the creation of ultra-fine precipitates resulting from radiation-enhanced diffusion processes in damaged crystal lattice [5]. There are significant differences in the nature of the radiation-induced precipitates (RIP) depending on the composition of RPV steels. Measurements by atom probe field ion microscopy (APFIM) and atom probe tomography (APT) show that copper-rich precipitates appear in steels with high levels of Cu after relatively low fluence [6,7]. On the other hand, rather diffuse aggregates of other solute atoms are formed if copper content is low like in the VVER-type RPV steels. These aggregates contain high amount (> 80 at%) of iron, while the content of solute atoms (typically Mn, Cr, Si, P and Ni) depends on the matrix composition. In both cases, the radiation-induced features have similar mean radius of about 1 nm and lead to similar embrittlement effects manifested as increase in yield strength, hardness or ductile-to-brittle transition temperature. While APT provides valuable data on composition and inner structure of the precipitates, their mean size or volume fraction can be measured efficiently by SANS. Although the information content of SANS data is too low to describe the complex microstructure of steels in detail, this method has substantial advantage of yielding integral characteristics of the precipitates like volume fraction, mean size or size distribution averaged over macroscopic sample volumes. These statistically representative parameters can be thus directly related to the mechanical parameters characterizing embrittlement. Moreover, magnetic interaction of neutrons with heterogeneities in ferromagnetic matrix permits to determine the ratio of total and nuclear scattering cross-sections (so called *A-ratio*) as an additional parameter, which helps to assess chemical compositions of the precipitates. In this study, we have employed the SANS method to characterize RIP in VVER type steels with varying Cu, Ni and P contents and the western-type steel A533B. From magnetic component of SANS, volume fractions and size distributions of the precipitates assuming their non-ferromagnetic character can be evaluated. Observed differences in radiation sensitivity (*i.e.* the dependence of RIP volume fraction on fluence) are discussed with the help of measured *A*-ratios and known chemical composition of the steels.

The investigated materials included the base metals of the Cr-Mo-V and Cr-Ni-Mo-V steels (used in VVER 440 and 1000 reactors), the Cr-Ni-Mo-V steel alloyed additionally with Cu and P and the IAEA reference steel A533-B. Steel compositions are listed in Tab. 1. More details on composition, sample treatment and results of TEM analysis can be found in.

TABLE 2. COMPOSITION OF MATERIALS IN WT%.

Steel	Sample	Si	Mn	P	Cr	Ni	Mo	V	Cu
15Kh2MFA	A0, A13	0.17	0.46	0.014	2.90	0.07	0.66	0.31	0.07
A533-B, Cl.1	C0, C1	0.25	1.40	0.019	0.12	0.84	0.50	0.003	0.14
15Kh2NMFA	D0-D2	0.26	0.59	0.005	2.22	1.27	0.63	0.09	0.03
15Kh2NMFA+Cu	E0, E1	0.17	0.48	0.012	2.06	1.28	0.56	0.10	0.30
15Kh2NMFA+P	F0, F1	0.20	0.34	0.021	2.14	1.27	0.58	0.10	0.08

Specimens A0 - F0 are original non-irradiated materials used for reference. The other samples were irradiated at the light-water research reactor LVR-15 in Řež at temperatures 275 -300°C. The fluxes and fluence for neutron energies E < 0.5 MeV are given in Table 3.

TABLE 3. IRRADIATION PARAMETERS.

Specimen	A13	C1	D1	D2	E1	F1
Flux [10^{16} m^{-2} s^{-1}]	57	57	29.5	34	26	26
Fuence [10^{24} m-2]	0.56	0.6	0.29	0.97	0.15	0.18

The SANS measurements were carried out at the pin hole SANS instrument in HMI Berlin for two detector distances of 1.1 m and 4 m and mean neutron wavelength of 0.6 nm, resulting in the total accessible range of scattering vector magnitudes (0.2-3) nm^{-1}. The specimen magnetization was saturated by horizontal magnetic field of 1.1 T. The size distributions for reference and irradiated samples are shown in Fig. 6. In all cases, RIP can be recognized as the peak at $R \sim 1.5$ nm. This peak is much higher for the materials containing copper (C, E) than for the low-Cu steels. Except for sample D1, the peak position remains roughly the same and the differences in peak integral should therefore correspond to differences in number density of RIP. However, changes in magnetic scattering contrast can also play role. Fig.7a showing integrated volume fractions of RIP documents the differences in radiation sensitivity of precipitation between different steels. Values of A-ratio, $A \equiv 1 + (\Delta\rho M/\Delta\rho N)^2$ fitted for the two populations of precipirares are shown in Fig. 7b.
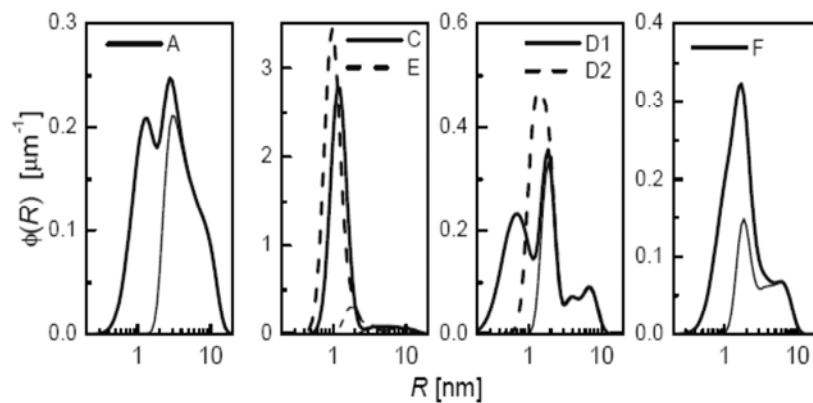

FIG.6. Size distributions of precipitates. Thin lines show corresponding non-irradiated states.

While $\Delta\rho M$ is the same for all non-magnetic precipitates, $\Delta\rho N$ depends on their chemical composition. Differences in A-ratios therefore indicate varying chemical composition of the precipitates. Although the A-ratio alone is not sufficient for determination of chemical composition, it can help in considering possible role of different solute atoms in formation of RIP. Nuclei with scattering lengths much lower than Fe like V, Mn, Cr or vacancies increase the contrast for nuclear scattering and lead thus to low values of A-ratio. On the contrary, nuclei with scattering lengths close to iron like Ni or Cu raises the A-ratios.
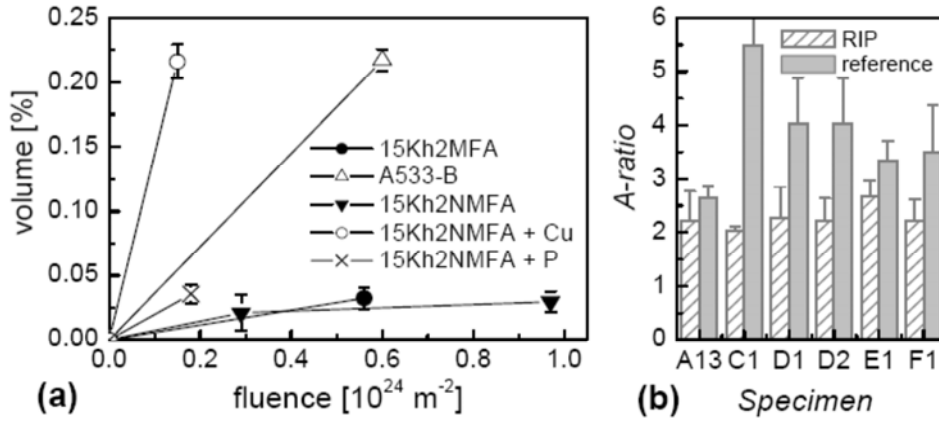
FIG.7. (a) Volume fractions of radiation-induced precipitates (RIP) for steels of different compositions (see Tab. 2). (b) A-ratios for RIP and medium-sized precipitates present already in reference material.

14.5. Conclusions

On the basis of the obtained results we can state that non-irradiated materials are characterized in our results by the population of precipitates in the range of radii between 2 and 20 nm. Obviously, there are also larger precipitates in the steels, but they are not resolved in the Q-range of our measurements and contribute only by the Porod background. In the given size-range, vanadium-carbides are known to exist in VVER type steels. Indeed, the low A-ratio observed in sample A is close to the value $A = 2.4$ resulting from the composition of VC particles measured by APFIM in [8] and to other SANS results [9]. For the other steels, A-ratios are higher and indicate the presence of precipitates with different composition. Possible candidates from those actually observed in RPV steels in this size range are VN and Mo_2C precipitates [10]. In the A533 steel, the vanadium-carbides cannot form and the average A-ratio is thus even higher.

As to the irradiated materials, we have observed much higher volume fractions of RIP in high-Cu steels (C, E) than in the low-Cu ones (A, D, F), though they were irradiated to similar fluence. This is not surprising, as copper is known to contribute to the formation of RIP with the highest enrichment factor. However, the A-ratios were much lower than we could expect for Cu precipitates ($A > 6$). Probable explanation is in high level of Mn (> 30 at.%) and/or magnetisation of these precipitates. Such high Mn content was actually observed by APT in steels with high Cu and Mn levels [11]. The volume fractions were evaluated under assumption that the precipitates are nonmagnetic. While there is persistent controversy concerning the magnetic properties of Cu-rich precipitates [6, 11], this assumption is almost certainly incorrect for RIP in low Cu-steels (samples A,D,F) with high (> 80 at.%) concentration of iron [8]. Consequently, the measured volume fractions can appear lower due to the lower than assumed magnetic contrast. As a possible scenario, let us consider a solute aggregate with composition measured in [8], Fe + 12 at.% Si + 13 at.% Mn and assume 5 %

of vacancies in the feature. This composition yields $A = 2.3$ equal to those measured for samples A, D and F provided that the average magnetic moment per Fe atom in the aggregate is by factor 0.7 lower than in the ferrite matrix. True volume fractions would then be higher by factor 4.1.

ACKNOWLEDGEMENT

REFERENCES

[1]   HUTCHINGS, M.T., KRAWITZ, A.D., (eds.), Measurement of Residual and Applied Stress Using Neutron Diffraction, NATO ASI Series, Applied Sciences 26, Kluwer Acad. Publ. (1992).

[2]   WITHERS, P.J., Residual stress: definition, in Encyclopedia of Materials: Science and Technology, IV: Structural Phenomena, K.H.J. Buschow et al., Eds., Elsevier, Oxford (2001) 8110.

[3]   TUTTLE, M.E., Review of the concepts of stress, strain, and Hooke's Law, Dept. Mechanical Engineering, University of Washington, Seattle.

[4]   LUKÁŠ, P., VRÁNA, M., MIKULA, P., BROŽOVÁ, A., ERNESTOVÁ, M., Physica B, 385-386 (2006) 670.

[5]   ŠAROUN, J., KOČÍK, J., GARCIA-MATRES, E., MURAŇSKÝ, O., STRUNZ, P.Z., Kristallogr. Suppl. 23 (2006) 393.

[6]   MILLER, M.K., RUSSEL, K.F., SOKOLOV, M.A., NANSTAD, R.K., J. Nuclear Materials 320 (2003) 177.

[7]   HYDE, J.M., ELLIS, D., ENGLISH, C.A., WILLIAMS, T.J., Effects of radiation on Materials: 20th International symposium (Philadelphia: ASTM STP 1405), 262-287 (2001).

[8]   MILLER, M.K., RUSSELL, K.F., KOČÍK J., KEILOVÁ, E., J. Nuclear Materials 282 (2000) 83.

[9]   GROSSE, M., BÖHMERT, J., GILLES, R., J. Nuclear Materials 254 (1998) 143.

[10]   MILLER, M.K., M.G., BURKE, J. Nuclear Materials 195 (1992) 68.

[11]   MILLER, M.K., WIRTH, B.D., ODETTE, G.R., Mater. Sci. Eng. A533 (2003) 133.

STUDY OF IRRADIATION EFFECTS IN MATERIALS WITH HIGH NEUTRON-FLUX FISSION REACTORS

T. SHIKAMA

Institute for Materials Research, Tohoku University

2-1-1 Katahira, Aobaku, Sendai, 980-8577, Japan

Email: Shikama@Imr.Tohoku.Ac.Jp

Abstract: History of irradiation studies utilizing fission reactors in university-related activities of Japan is briefly reviewed and the future prospect will be described. For a moment, two major materials irradiation fission reactors, JMTR and JOYO are under refurbishment, which resultantly highlights importance of international collaboration.

15.1. Introduction

Studies of irradiation effects in material with fission reactors are facing to an important turning-point after their long histories with accumulation of vast data-bases. Studies related with present-water cooled power reactors as well as with advanced nuclear power systems such as Generation-IV types and nuclear fusion reactors are strongly demanding higher neutron fluence irradiation, where the typical irradiation dose demanded will be far beyond 10 dpa for structural materials. There, needed neutron flux will exceed 10^{18}n/m^{2}s and hopefully it will be in the range of 10^{19}n/m^{2}s. In the meantime, an accumulated irradiation data-base clearly shows that acquisition of comprehensive irradiation parameters, such as temperatures, oxygen chemical potentials, neutron spectra, and gamma-ray dose rates is indispensable for establishing reliable understandings in behaviors of materials in actual nuclear systems. There, appropriate instrumentations are essential for irradiation rigs used in high-neutron-flux irradiation. Also, recent advance of understandings of irradiation effects highlights importance of in-situ type studies in fission reactors. Examples will be studies for transient behaviors of nuclear fuels and issues related with chemical compatibility of materials with their environments under irradiation, such as stress corrosion cracking studies. Study on dynamic radiation effects in functional materials will be another example. Functional materials are expected to play a more and more important role in advanced nuclear systems, where real time diagnostics of operation conditions and resultant feedback-control of the operation conditions are important.

In a water-cooled type fission reactor, a nuclear heating rate (a gamma-ray dose rate) is usually high, namely about 10 W/g (10^4 Gy/s) for 10^{18} n/m^{2}s fast neutron flux (E > 0.1MeV) for iron. There, a higher neutron-flux irradiation means a higher nuclear heating rate. It means that components composing irradiation rigs will be easily heated up to above 500ºC, if they are not appropriately cooled. Usually, the reliable instrumentations are very difficult, when the gamma-dose rate exceeds 10 W/g for iron. There, mineral insulating cables and thermocouples, if they are thermally isolated and it will easily happen, will be heated up locally above 1000ºC. Also, the temperature gradient in materials under irradiation is substantial, when materials' dimension is large.

Thus, new instrumentation techniques will be essential for the advanced irradiation studies in a high-neutron flux reactor. Also, some coupling type irradiation utilizing a mixed spectrum reactor and a fast reactor should be taken into consideration. The paper will report present status of instrumentations for reactor dosimetry and in-situ measurements in Japan for fundamental studies of nuclear materials utilizing fission reactors.

15.2. History of heavy irradiation study utilizing fission reactors in university-related activity in Japan

Materials study utilizing fission reactors in Japan started in 1960s utilizing JRR-2 (Japan Research Reactor 2) of Tokai Research Establishment of Japan Atomic Energy Research Institute (JAERI, corresponding to the present Japan Atomic Energy Agency (JAEA)). There, the materials were irradiated in a small aluminum-made capsule dipped directly into its core coolant water. There was not a temperature control system and irradiation temperature was typically around 50-100ºC. The fast neutron fluence attained was around $10^{22} - 10^{23}$ n/m^2 at the maximum.

Meeting with increasing demands for reactor irradiation, a new fission reactor, Japan Materials Testing Reactor (JMTR) was constructed and went into its criticality in 1969 in Oarai Research Establishment of JAERI. JMTR is a light water cooled and moderated tank type reactor for multipurpose uses. The Oarai Branch of Institute for Materials Research (IMR-Oarai) of Tohoku University was founded in 1971 to work as a coordinator between reactor users in universities and the JMTR. General features of the JMTR are shown in Table 1 and a role of IMR-Oarai in conjunction with JMTR and other research reactors is schematically shown in Fig. 1 [1].

Materials were accommodated in a specially designed irradiation rig and typical irradiation temperature was in the range of 100-600ºC. The fast neutron fluence attainable in a year will be at the most around 10^{25} n/m^2. Starting with non-instrumented irradiation rigs, several instrumented irradiation rigs were developed as shown in Fig. 3, meeting with demands of university researchers whose interests diverged in a wide research fields.

In the meantime, demand for a much higher fast neutron fluence was elicited in university researchers, whose major concerns were in the fields of development of a nuclear fusion reactor. For the realization of a commercially compatible nuclear fusion reactor, development of structural materials which could survive neutron fluence up to $10^{26} - 10^{27}$ n/m^2, more than 100 dpa (displacement per atom).

Thus, utilization of high neutron flux fast reactor, JOYO was started in 1978. The JOYO was an experimental sodium-cooled fast breeder reactor (the fast reactor) and its major mission at that time was development and validation of fundamental technologies for the sodium-cooled fast breeder reactor. Thus, the material irradiation for nuclear systems other than a fast reactor was recognized as a side business and the irradiation was carried out mainly with non-instrumented rigs.

By 1980s, importance of appropriately control of irradiation conditions and acquisition of irradiation parameters were well appreciated. For higher neutron fluence irradiation in more defined conditions, university researchers started utilization of FFTF-MOTA (Fast Flux Test Facility – Materials Open Test Assembly) of Pacific Northwest Laboratory of the USA in 1987, under the Monbusho (Ministry of Education of Japan) / USDOE (Department of Energy of the USA) nuclear fusion science collaborative program [2]. In FFTF-MOTA, irradiation temperature was actively controlled. Also, in JOYO, a new instrumented irradiation rig called INTA was developed to realize the active temperature control, and then, more versatile temperature control irradiation rig called MARICO and its successor MARICO-2 were developed. More sophisticated instrumented irradiation rigs were developed for JMTR irradiation as shown in Fig. 2. in 1990s, whose example is shown in Fig. 3, for multi temperature and multi neutron fluence control. Instrumented irradiation rigs for in-situ measurement of material-property changes under reactor irradiation were also developed in JMTR in 1980s-1990s.

TABLE 1. FEATURES OF JMTR (JAPAN MATERIALS TESTING REACTOR)

Reactor Power	50 MWt
Fast Neutron Flux (Max)	4×10^{18} n/m^2.s
Thermal Neutron Flux (Max)	4×10^{18} n/m^{2}s
Flow of Primary Coolant	6000 m^3.h
Coolant Temperature	49□ – 56□
Core Height	750 mm
Fuel	ETR type, 19.8% ^{235}U
Irradiation Capability (Max)	60 capsules
Fluence/y (Max)	3×10^{25} n/m^2 .y
dpa of Stainless Steel (Max)	4 dpa
Diameter of Capsule	30 – 65 mm
Temp. Control (Max)	2000 ℃
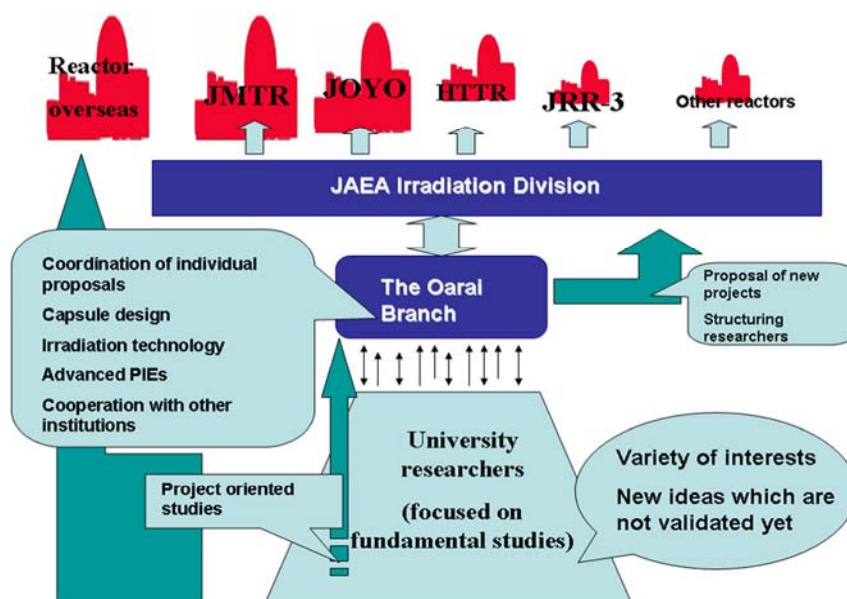
FIG.1. Role of the IMR-Oarai for utilization of fission reactors for university researches in Japan.
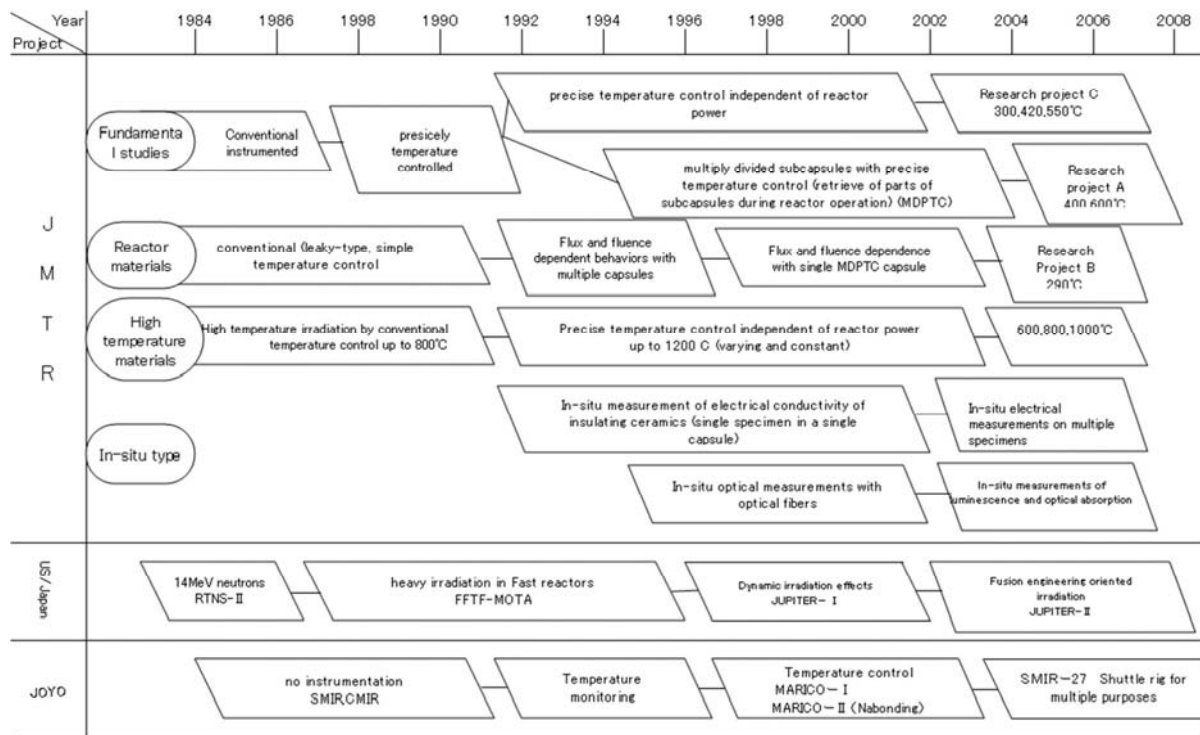
FIG.2. Development of materials irradiation rigs in the IMR-Oarai.

These efforts were extended in the Japan/USA collaboration mentioned above in the 1990s in the reactor of HFIR (High Flux Isotope Reactor) of Oak Ridge National Laboratory. Measurements of the electrical conductivity of ceramic insulators and protonic conductors, and of thermal conductivity of nuclear fusion candidate materials such as SiC/SiC composites were carried out in JMTR and HFIR. Optical measurements were also carried out in JMTR using radiation resistant silica-glass optical fibers. Optical measurements were implemented in BR-2 (Belgium Reactor 2) of SCK/CEN (Belgian Center for Nuclear Energy) under the international collaboration of the ITER – EDA (ITER-Engineering Design Activity). JMTR stopped its operation temporarily in 2006 for refurbishment, aiming for its restart in 2011. In addition, JOYO ceased its operation in 2007 due to a problem caused by instrumented irradiation with MARICO-2. The IMR-Oarai exploited the possibility of utilizing fission reactors overseas and extended its collaboration with SCK/CEN, resulting in the start of the utilization of BR-2 for materials irradiation in 2005. BR-2 is a light water cooled reactor which has many features which are similar to those of JMTR, with a slightly higher fast neutron flux.
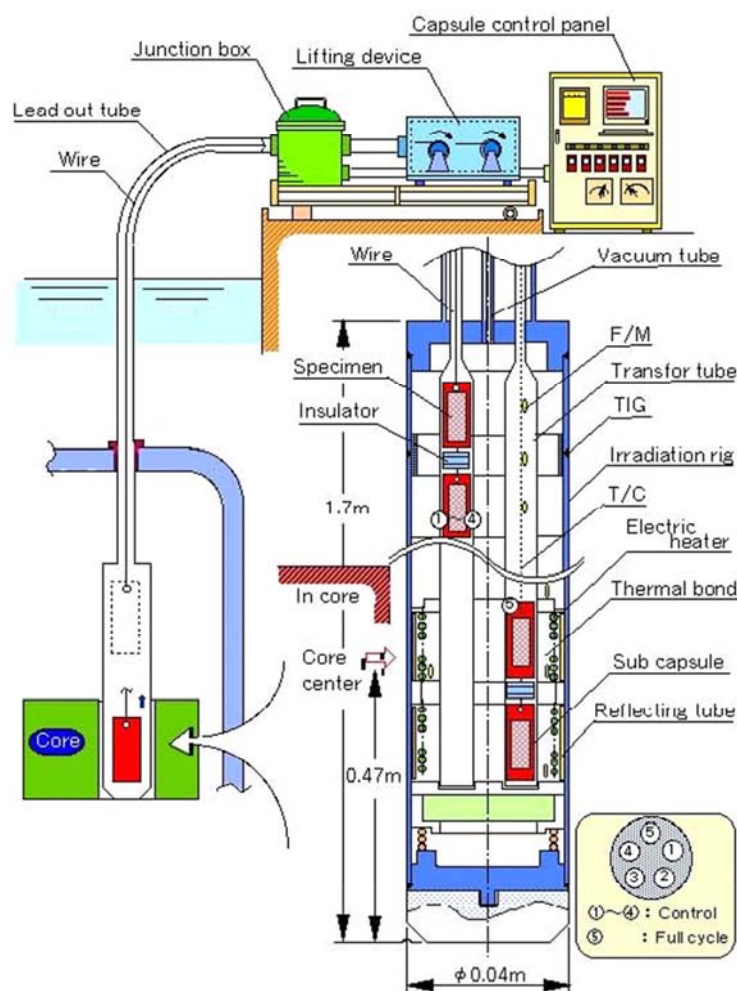
FIG.3. Multi temperature and neutron fluence control irradiation rig in JMTR.

Up to now, three programs, GAYSHA, MICADO-1 and MICADO-2 were accomplished, utilizing irradiation rigs of CALLISTO, ROBIN and BAMI. The project of MICADO-3 is under way.

15.3. Irradiation studies from a view points of university researchers

In the early stages of reactor utilization for study of radiation effects in materials, a fission reactor was regarded mainly as a high intensity neutron source. For engineering aspects, validation of wholesomeness of materials and their assembly in a specific nuclear environment was a major target. There, a fission reactor was regarded as an actual practical environment for the application of concerned materials and their assembly and necessity of active control of irradiation conditions were not strongly recognized. At this stage, vast amounts and kinds of materials were irradiated in materials testing reactors such as JMTR and JOYO. In addition, in the fields of materials science, initial concerns were that the phenomena related with interactions between energetic neutrons and materials and detailed control of irradiation parameters were beyond its scope (too sophisticated and too expensive).

In the meantime, fundamental aspects of irradiation effects were studied with more irradiation-conditions controllable tools such as ion and electron accelerators and fusion neutron sources (such as RTNS-2 (Rotating target Neutron Source 2) of Lawrence Livermore National Laboratory of the USA, and FNS (Fast Neutronics Source) of the JAEA); Advancement of studies by computer simulation techniques was remarkable. To interpret

complicated irradiation behaviours of materials in fission reactors from fundamental mechanisms of irradiation effects, irradiation in a fission reactor under more well-defined and well-controlled conditions was becoming more and more needed. A typical example will be an evolution of irradiation studies from the EBR-2 (Experimental Breeder Reactor 2 of Idaho National Laboratory) project to the FFTF-MOTA project in the USA. In Japan, the transition was much more moderate and was not deliberately done, however, in retrospect the trend clearly identified that the number of instrumented irradiation rigs increased as the time went by in JMTR as well as in JOYO. A general perspective of study of irradiation effects in fission reactors is schematically shown in Fig. 4.

Development of instrumented and irradiation-conditions controllable rigs was not difficult in general in water-cooled type materials testing reactors such as JMTR and HFIR. There, feed-through systems through a pressure boundary was preinstalled and cables needed for instrumentations were easily taken out of the reactor core regions. Some reactors do not have a pressure boundary such as JRR-3. In the meantime, realization of the instrumentations in a fast reactor is not easy in general. Incarnation of MOTA facility in FFTF was a remarkable demonstration of the advanced reactor- irradiation-technology in the USA. MARICO and MARICO-2 project in JOYO would have demonstrated advanced irradiation-technology in Japan, but resultantly, it reconfirmed difficultness of the instrumentation in fast reactors. However, in general, reactor irradiation with detailed instrumentations and in well-defined conditions is now a proven technology in many materials testing reactors.
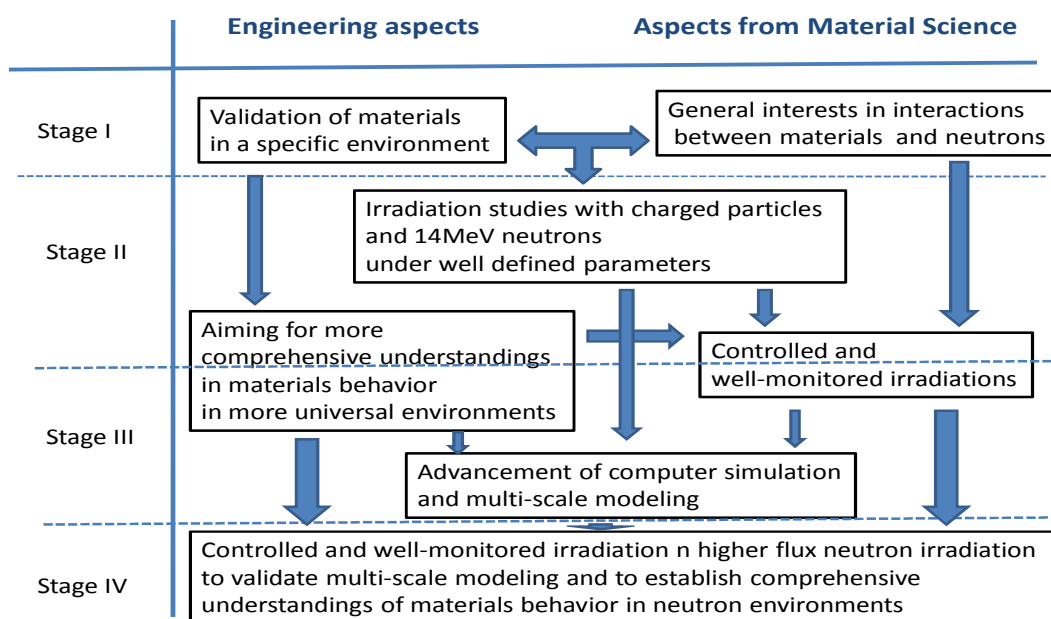
FIG. 4. Evolution of irradiation study in conjunction with fission-reactor irradiation studies.

The next step will surely be the instrumented and controlled reactor irradiation with higher fast neutron flux and fluence. For the innovation of nuclear power systems, comprehensive understandings of neutron irradiation effects with neutron fluencies higher than can be realized in a conventional materials-testing-reactors (corresponding to about several dpa). Lifetime extension and improvement of safety/efficiency of a present light water power reactor is demanding irradiation studies with neutron fluence much higher than 10^{25} n/m^2 (preferably higher than 15-20 dpa). Development of the fast breeder reactor and nuclear fusion reactor is demanding fast neutron fluence higher than 10^{26} n/m^2 (preferable in the range of 200 dpa). To achieve the high fast neutron fluence, the neutron flux higher than middle of

10^{18} n/m^2.s will be needed. In a conventional water cooled fission reactor, such as JMTR and HFIR, it means that the associated gamma-ray dose rate is higher than 10^4 Gy/s, namely a nuclear heating rate of higher than 10 W/g for iron.

The electrical conductivity measurements in the JUPITER project in HFIR mentioned above and the study of behaviour of magnetic probes for burning plasma fusion devices in JMTR clearly showed the difficulty of reliable instrumentations in the reactor core region where the gamma-ray dose rate exceeds 10^4 Gy/s. In the coming decade, instrumented irradiation in a high flux reactor core region is planned in materials testing reactors such as JMTR. However, it will be a difficult technical challenge and development of technology such as development of reliable mineral insulating cables and their termination techniques as well as long-life electric heaters will be indispensable. Probes monitoring irradiation conditions, such as oxygen chemical potential, hydrogen concentration, temperatures, gamma-ray dose rate, neutron flux, etc., are very difficult to develop in such a high gamma-ray dose rate environments, insuring their reliability and long-life. Also, materials irradiation below 300-350ºC in a gamma-ray dose rate higher than 10W/g is in general very difficult, except for installation of an active special cooling system. The irradiation below 300-350ºC is very important for studies related to a light water cooled and moderated reactors.

In the meantime, the sodium-cooled fast reactor is a definite disadvantage for the instrumented irradiation as the boundary structure surrounding its core environment is too complicated to satisfy safety regulations. The trouble associated with MARICO-2 irradiation rig in JOYO took place to demonstrate the difficulty. Also, the coolant temperature is higher than that of a light water cooled and moderated type reactors. However, the fast reactor has a definite advantage over a water cooled materials testing reactor, namely, it has a relatively low gamma-ray dose rate, referring to the same fast neutron flux. A typical gamma-ray dose rate will be less than 10^4 Gy/s with the fast neutron flux of 10^{19} n/m^{2}s, being about 10th of that in a water cooled fission reactor. Thus, a sodium-cooled fast reactor may be able to play a definite role in instrumented irradiation with a desirable high fast neutron flux, therefore, we would need to overcome technical difficulties related to the complicated boundary surrounding its reactor core.

In Japan, JRR-3 will cover the utilization stage of I and II in Fig. 4, and JMTR will cover from stage I to III. Only JOYO will have a potential to cover from stage I through IV. It will be very difficult to utilize the next fast reactor, MONJU as a material testing reactor in stage IV, as its main mission is to validate commercially available sodium-cooled fast breeder reactor, and there, complicated instrumentations and related modification of safety boundary structures will not be realistic. Another important aspect to be addressed finally will be issues related to the use of low enriched uranium fuels and a multi-purpose utilization of a reactor. The use of low enriched uranium is an inviting result compared to the non-proliferation problem. In addition, multi-purpose utilization of a materials testing reactor is also socially inevitable as a countermeasure to deal with a very high cost of a reactor operation.

However, the conversion of fuels from highly enriched uranium to low enriched uranium is making a reactor operation more restricted. It sometimes hampered scientific feasibility, though it must be accommodated. To ensure reactivity of a nuclear core for meeting sophisticated demands from advanced materials tests, adaption of more advanced nuclear fuels such as U-Mo will be strongly needed.

Also, in multi-purpose utilization of a reactor, some purposes will strongly interfere with each other. For example, from a viewpoint of radioisotope production and nuclear doping, long and steady state operation is needed. There, an interruption period of a reactor operation should be

minimized. Profiles of neutron flux should not be disturbed in each operation cycle. In the meantime, in advanced materials test, a long interruption period is needed to accommodate sophisticated instrumentation. Irradiation conditions such as neutron flux and fluence would be modified cycle-to-cycle to satisfy specific demands from each experiment. From the view point of materials science, the present "multi-purpose" sounds sometimes "too many purposes" Simplification of reactor purposes is strongly recommended through collaboration among multiple reactors internationally.

15.4. Conclusions

After its long history, the materials irradiation studies utilizing fission reactors are facing a turning-point. The major concerns in this area will be toward instrumented and controlling irradiation in a higher neutron flux. Development of new irradiation technologies, including development of new materials needed for the new technologies will be needed. In the meantime, materials irradiation studies utilizing fission reactors are becoming increasingly expensive and time consuming. Collaboration among organizations participating fission-reactor materials irradiation will be inevitable.

REFERENCES

[1]   SHIKAMA, T., Utilization of research reactors for fundamental studies in university related activities in Japan, presented at the International Conference on Research Reactors: Safe Management and Effective Utilization, Sydney, Australia (2007).

[2]   Special issue for celebrating its 50th anniversary of nuclear fusion research, History and Prospects of Fusion Research in Japan, J. Plasma and Fusion Research, 84 (2008) http://www/jspf.or.jp/ (in Japanese).

Chapter 16

STUDIES OF FAST NEUTRON ABSORBING MATERIALS FOR FAST NEUTRON FLUENCE MEASUREMENT

T. XIDING

Physics Experiment Research Laboratory, Nuclear Power Institute of China
P.O. Box 291-113, Chengdu, Sichuan, China
Email: Tangxiding@Yahoo.Cn

Abstract: For fast neutron fluence measurement, the neutron activation detectors are covered sometimes by multi-layer covering materials like Cd, B, Gd, CdO, BN, Ti, V, Al and Ni, the influence of the neutron absorbed by all elements in these materials should be considered. There are only three kinds of total cross sections of Cd, B and Cd in International Reactor Dosimetry File, so that the cross section processing code X333 can only process these three total cross sections for the neutron spectrum adjustment code STAYNL to consider the influence of the absorbed neutron. In order to consider the influence of neutrons absorbed by all elements, we calculated the total cross section of multi-layer covering materials (for example CdO + Ni-Fe) from the total cross sections of nuclides found out from nuclear data library (for example ENDF-6) and inserted them into IRDF library to form a new one. All of the absorbed neutrons can be considered by using the new library. We had reprocessed two measured data by using the new library, the new results is smaller 1.5% and 2.6% than the olds.

16.1. Introduction

For fast neutron fluence measurement, the neutron activation detectors are covered sometimes by multi-layer covers like Cd, B, Gd, CdO, BN, Ti, V, Al and Ni, the fast neutron is absorbed a little by the covers of neutron activation detector. The materials such as BN and CdO had been used for thermal neutron filters of the irradiation surveillance capsules of the Second Nuclear Power Plant of QIN SHAN (QINSHAN 2nd NPP) and DAYA Bay NPP and the LINGAO NPP, in order to decrease the second reactions and the impurity fission reactions. When the neutron spectrum is adjusted by STAYNL [1] code, the X333 code [2] can only process the total cross sections of Cd, B and Gd for STAYNL to consider the influence of the absorbed fast neutron because there is only the three elements' total cross sections in the International Reactor Dosimetry File (IRDF) [3-4], not for other elements and compounds.

The fast total cross sections of many elements are about a few barns, so the abilities of absorbing fast neutron of many elements are approximate. The neutron spectrum adjustment considered only the influence of the absorbed fast neutron by Cd or B in our fast neutron measurements. This processing method is correct for thermal neutron and epithermal neutron because the other elements' thermal neutron total cross sections are much smaller than Cd, B and Gd. For fast neutron measurement, the influence of the neutron absorbed by all elements in covering material should be considered. The paper described the processing method to consider the influence of neutron absorbed by all elements in covering material of neutron activation detectors, and reprocessed the measured reaction rates data of two irradiation surveillance capsules, the new fast neutron fluence results is smaller, approximately 1.5 - 2.6% than the old results.

16.2. Analysis of the influence of fast neutron absorbed by the covering material

The fast neutron spectrum averaged total cross section $\overline{\sigma}_{tf}$ above 0.1 MeV is calculated as follows:

$$\overline{\sigma}_{tf} = \frac{\int\limits_{0.1MeV}^{20MeV} \sigma_t(E)\phi(E)dE}{\int\limits_{0.1MeV}^{20MeV} \phi(E)dE} \qquad\qquad (1)$$

where:

$\sigma_t(E)$ total cross section, barn , and

$\phi(E)$ neutron fluence rate per unit energy, $n/(cm^2.s)$.

The fast neutron attenuation factor of material, F, is calculated as follows:

$$F = \exp(-N\overline{\sigma}_{tf}d) \qquad\qquad (2)$$

if:

$$N = \rho N_A / m,$$

Where:

N molecule/atom number of material in unit cm^3, n/cm^3,

ρ theory density of material, g/cm^3,

N_A Avogadro's number, $6.022 .10^{23} mol^{-1}$,

m molecular/ atomic weight of material, g/mol,

d thickness of covering material, cm.

The ratio between the thermal neutron total cross sections and epithermal neutron total cross sections can be in the order of 100 - 1000 times, while the fast neutron total cross sections are almost the same order of magnitude, see Fig. 1. The fast neutron spectrum averaged total cross section and the fast neutron attenuation factors of materials are in table 1. For the same thickness of the covering materials, the fast neutron attenuation factors of Fe, Cd, CdO, BN are almost equal. Not only Cd, B and Gd have to be considered but also other elements like O, N, C need to be taken into account for determination of the attenuation.

The vertical section of the cylindrical fission detector and covering parts of DAYA Bay NPP is shown in Fig. 2. We reprocessed the measured reaction data of the capsule V of DAYA Bay NPP unit 2 from neutron spectrum adjustment to calculate the fast neutron fluence rates for several Cd thicknesses, the ratios of the fast neutron fluence rates are given in table 2.

The weighted fast neutron fluence rate with covering material is smaller than that without covering material, and the thicker covering material is, the smaller weighted fast neutron fluence rate is.
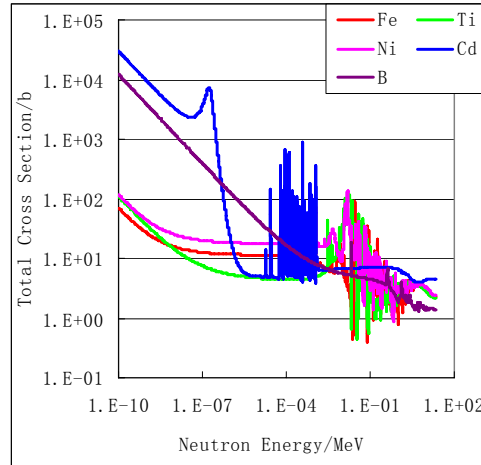
FIG.1. Total cross sections of Fe, Ti, Ni, Cd and B.
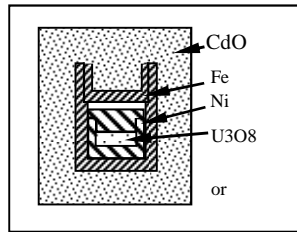
FIG.2. vertical section of the cylindrical fission detectors of DAYA Bay NPP.

TABLE 1. THE FAST NEUTRON SPECTRUM AVERAGED TOTAL CROSS SECTION
AND THE FAST NEUTRON ATTENUATION FACTORS OF MATERIALS IS THE FAST
NEUTRON ATTENUATION FACTORS OF THE 6MM THICKNESS MATERIAL

Element	N (n/cm^3)	σ (barn)	F_{2mm}	F_{6mm}
Ti	5.71E+22	3.11	0.965	0.899
Ni	9.13E+22	3.78	0.933	0.813
B	1.30E+23	2.69	0.932	0.810
Cd	4.63E+22	5.9	0.947	0.849
Fe	8.47E+22	3.22	0.947	0.849
Gd	3.02E+22	6.85	0.959	0.883
Cd0	3.26E+22	8.92	0.944	0.845
BN	5.51E+22	4.89	0.948	0.851
B$_4$C	2.75E+22	13.38	0.929	0.802

Note: F_{2mm} is the fast neutron attenuation factors of the 2mm thickness material

There are two methods suited to calculate the fast neutron attenuation of oxygen of CdO, N or BN. The first is to modify measured reaction rate of neutron detector, the second is to calculate the total cross sections of CdO and BN, and put them into IRDF. The following describe the second method.

TABLE 2. THE RATIOS OF FAST NEUTRON FLUENCE RATES (E>1.0MEV)

Reaction	Reaction rates (s^{-1})	$\dfrac{\phi_{f2.2}}{\phi_{f0}}$	$\dfrac{\phi_{f3.175}}{\phi_{f0}}$
^{54}Fe (n,p) ^{54}Mn	1.058E-14	1.020	1.039
^{58}Ni (n,p) ^{58}Co	1.509E-14	1.017	1.034
^{63}Cu (n,a) ^{60}Co	1.062E-16	1.025	1.050
^{93}Nb (n,n') ^{93m}Nb	4.095E-14	1.001	1.003
^{237}Np (n,f) F.P.	5.783E-13	1.066	1.138
^{238}U (n,f) F.P.	5.894E-14	1.060	1.125
Weighted fast neutron fluence rate		1.031	1.064

Note: ϕ_{f0} fast neutron fluence rate without covering material, n/cm^2.s,

$\phi_{f2.2}$ fast neutron fluence rate with 2.2 mm thickness covering material, n/cm^2.s, 2.2 mm is calculated by $3.175mm \times \rho_{Cd}/\rho_{Cdo}$, ρ_{Cd} (where ρ are the densities),

$\phi_{f3.175}$ fast neutron fluence rate with 3.175 mm thickness covering material n/cm^2.s.

16.3. Total Cross Section Calculation of Material for X333 Code

In order to process nuclide cross section into element cross section, or into compound cross section, the all total cross section obtained from nuclear data Library was changed into the same 9372 group energy structure, the calculation equation is follows:

$$\sigma_i^9 = \begin{cases} \sigma_j & E_i^9 = E_j \\ \dfrac{(\sigma_{j+1} - \sigma)(E_i^9 - E_j)}{E_{j+1} - E_j} + \sigma_j^e & E_j < E_i^9 < E_{j+1} \end{cases}$$

(3)

where:

σ_i^9 total cross section in the ith energy group of the 9372 group energy structure, cm^2,

σ_j total cross section in the jth energy group with discretionary energy structure, cm^2,

When some element's total cross section could not be found it was was calculated from it's stable nuclides' total cross sections found from nuclear data library such as ENDF-B6, the calculation equation is follow:

$$\sigma_{ei}^9 = \frac{\sum_k \left(a_k \sigma_{k,i}^9\right)}{\sum_k a_k} \tag{4}$$

where:

σ_{ei}^9 total cross section of element in the ith energy group in 9372 group energy structure, cm^2,

a_k isotope abundance of the kth kind stable isotope of element,

$\sigma_{k,i}^9$ total cross section in the ith energy group of the kth kind of stable isotope in 9372 groups energy structure.

The compound total cross section is calculated as:

$$\sigma_{ci}^9 = \sum_l \left(n_l \sigma_{ei}^9\right) \tag{5}$$

where:

σ_{ci}^9 total cross section of compound in the ith energy group in the 9372 group energy structure, cm^2,

n_l atom number of the lth element in compound molecule.

For example, the ith energy group total cross section of B$_4$C equals $4 \times \sigma_{Bi}^9 + \sigma_{Ci}^9$.

If the neutron detector is covered by multilayer covers the total cross section of the multilayer covers is calculated as:

$$\sigma_{ti}^9 = \frac{\left(\sum_t Z_t \sigma_{cti}^9\right) - Z_{Fe} \sigma_{Fei}^9}{\sum_t Z_t} \tag{6}$$

where:

σ_{ti}^9 total cross section of covers in the ith energy group in 9372 group energy structure, cm^2,

Z_t molecule/atom number of the tth layer cover in one square centimeter area, n/cm^2,

σ_{cti}^9 total cross section of the tth layer cover in the ith energy group in 9372 group energy structure, cm^2,

atom number of iron in one square centimeter area when the location of multilayer covers is replaced by iron supposedly, n/cm^2,

$\sigma^9_{Fe\,i}$ total cross section of iron in the ith energy group in 9372 group energy structure,cm^2.

The total cross sections of multilayer covers must be calculated into the 640 group SAND-II energy structure before inserting them into IRDF Library as:

$$\sigma^6_m = \frac{\sum_i \sigma^9_{ti} \phi^9_i}{\sum_i \phi^9_i} \qquad E_m \le E_i \le E_{m+1}$$

(7)

where:

σ^6_m total cross section in the mth energy group in the 640 group SAND-II energy structure, cm^2,

ϕ^9_j neutron fluence rate in the ith energy group in the 9372 group energy structure, structured with the Maxwell spectrum, the 1/E spectrum and the fission spectrum.

3.5   The thickness of multilayer covers must be modified in order to be used by X333 code because this code can only process the element cover. The calculation equation is :

$$d^{'} = \frac{m_{Cd}}{\rho_{Cd}} \sum_t \left(\frac{d_t \cdot \rho_t}{m_t} \right)$$

(8)

where:

$d^{'}$ Cadmium's equivalent thickness of multilayer covers, cm,

m_{Cd} atomic weight of Cadmium, g/mol,

ρ_{Cd} density of Cadmium, g/cm^3,

d_t thickness of the tth layer cover, cm,

ρ_t density of the tth layer cover, g/cm^3,

m_t molecular/atomic weight of the tth layer cover , g/mol.

Specifically total cross section and Cadmium's equivalent thickness must be processed for each type of covering case before neutron spectrum is adjusted by STAYNL, and the name of cover must is Cd. Of course, boron and gadolinium can be used for equivalent.

The weighted fast neutron fluence rate with covering material is smaller than the one without covering material, and the thicker the covering material is, the smaller weighted fast neutron fluence rate is.

Two methods exist which are suitable for calculating fast neutron attenuation of oxygen of CdO, N or BN. The first is to modify measured reaction rate of neutron detector, the second is

to calculate the total cross sections of CdO and BN, and put them into IRDF. The following describes the second method:

TABLE 3. THE FAST NEUTRON SPECTRUM AVERAGED TOTAL CROSS SECTION AND THE FAST NEUTRON ATTENUATION FACTORS OF MATERIALS IS THE FAST NEUTRON ATTENUATION FACTORS OF THE 6MM THICKNESS MATERIAL

	N (n/cm^3)	σ(barn)	F_{2mm}	F_{6mm}
Ti	5.71E+22	3.11	0.965	0.899
Ni	9.13E+22	3.78	0.933	0.813
B	1.30E+23	2.69	0.932	0.810
Cd	4.63E+22	5.9	0.947	0.849
Fe	8.47E+22	3.22	0.947	0.849
Gd	3.02E+22	6.85	0.959	0.883
Cd0	3.26E+22	8.92	0.944	0.845
BN	5.51E+22	4.89	0.948	0.851
B$_4$C	2.75E+22	13.38	0.929	0.802

TABLE 4. THE RATIOS OF FAST NEUTRON FLUENCE RATES (E>1.0MeV)

Reaction	Reaction rates (s-1)	$\dfrac{\phi_{f2.2}}{\phi_{f0}}$	$\dfrac{\phi_{f3.175}}{\phi_{f0}}$
54Fe (n,p) 54Mn	1.058E-14	1.020	1.039
58Ni (n,p) 58Co	1.509E-14	1.017	1.034
63Cu (n,a) 60Co	1.062E-16	1.025	1.050
93Nb (n,n') 93m Nb	4.095E-14	1.001	1.003
237Np (n,f) F.P.	5.783E-13	1.066	1.138
238U (n,f) F.P.	5.894E-14	1.060	1.125
Weighted fast neutron fluence rate		1.031	1.064

Note: ϕ_{f0} fast neutron fluence rate without covering material, n/cm^2.s,

$\phi_{f2.2}$ fast neutron fluence rate with 2.2 mm thickness covering material, n/cm^2.s, 2.2 mm is calculated by $3.175mm \times \rho_{Cd}/\rho_{Cao}$, ρ_{Cd} (where ρ are the densities),

$\phi_{f3.175}$ fast neutron fluence rate with 3.175 mm thickness covering material n/cm^2.s.

16.4. Total Cross Section Calculation of Material for X333 Code

In order to process nuclide cross section into element cross section, or into compound cross section, the all total cross section obtained from nuclear data Library was changed into a same 9372 groups energy structure, the calculation equation is follows:

$$\sigma_i^9 = \begin{cases} \sigma_j & E_i^9 = E_j \\ \dfrac{(\sigma_{j+1} - \sigma)(E_i^9 - E_j)}{E_{j+1} - E_j} + \sigma_j^e & E_j < E_i^9 < E_{j+1} \end{cases}$$

$$(9)$$

where:

σ_i^9 total cross section in the ith energy group of the 9372 group energy structure, cm^2,

σ_j total cross section in the jth energy group with discretionary energy structure, cm^2,

When some element's total cross section can not be find it was calculated from it's stable nuclides' total cross sections found from nuclear data library such as ENDF-B6, the calculation equation is follow:

$$\sigma_{ei}^9 = \frac{\sum_k (a_k \sigma_{k,i}^9)}{\sum_k a_k}$$

$$(10)$$

where:

σ_{ei}^9 total cross section of element in the ith energy group in 9372 group energy structure, cm^2,

a_k isotope abundance of the kth kind stable isotope of element,

$\sigma_{k,i}^9$ total cross section in the ith energy group of the kth kind of stable isotope in 9372 groups energy structure.

The compound total cross section is calculated as:

$$\sigma_{ci}^9 = \sum_l (n_l \sigma_{ei}^9)$$

$$(11)$$

where:

σ_{ci}^9 total cross section of compound in the ith energy group in the 9372 group energy structure, cm^2,

n_l atom number of the lth element in compound molecule.

For example, the ith energy group total cross section of B_4C equals $4 \times \sigma_{Bi}^9 + \sigma_{Ci}^9$.

If the neutron detector is covered by multilayer covers the total cross section of the multilayer covers is calculated as:

$$\sigma_{ti}^{9} = \frac{\left(\sum_t Z_t \sigma_{cti}^{9} \right) - Z_{Fe} \sigma_{Fei}^{9}}{\sum_t Z_t}$$

(12)

where:

σ_{ti}^{9} total cross section of covers in the ith energy group in 9372 group energy structure, cm^2,

Z_t molecule/atom number of the tth layer cover in one square centimeter area, n/cm^2,

σ_{cti}^{9} total cross section of the tth layer cover in the ith energy group in 9372 group energy structure, cm^2,

Z_{Fe} atom number of iron in one square centimeter area when the location of multilayer covers is replaced by iron supposedly, n/cm^2

σ_{Fei}^{9} total cross section of iron in the ith energy group in 9372 group energy structure, cm^2.

The total cross sections of multilayer covers must be calculated into the 640 group SAND-II energy structure before inserting them into IRDF Library as:

$$\sigma_m^{6} = \frac{\sum_i \sigma_{ti}^{9} \phi_i^{9}}{\sum_i \phi_i^{9}} \qquad E_m \le E_i \le E_{m+1}$$

(13)

where:

σ_m^{6} total cross section in the mth energy group in the 640 group SAND-II energy structure, cm^2,

ϕ_j^{9} neutron fluence rate in the ith energy group in the 9372 group energy structure, structured with the Maxwell spectrum, the 1/E spectrum and the fission spectrum.

3.5   The thicknesses of multilayer covers must be modified in order to be used by X333 code because this code can only process the element cover. The calculation equation is :

$$d^{'} = \frac{m_{Cd}}{\rho_{Cd}} \sum_t \left(\frac{d_t \cdot \rho_t}{m_t} \right)$$

(14)

where:

$d^{'}$ Cadmium's equivalent thickness of multilayer covers, cm,

m_{Cd} atomic weight of Cadmium, g/mol,

ρ_{Cd} density of Cadmium, g/cm^3,

d_t thickness of the tth layer cover, cm,

ρ_t density of the tth layer cover, g/cm^3,

m_t molecular/atomic weight of the tth layer cover , g/mol.

Specifically total cross section and Cadmium's equivalent thickness must be processed for each type of covering case before neutron spectrum is adjusted by STAYNL, and the name of cover must is Cd. Of course, boron and gadolinium can be used for equivalent.

16.5. Reprocessing the measured data

The calculation neutron fluence rate spectrum of the capsule V of DAYA Bay NPP Unit **2** was adjusted again by STAYNL code through using the same input data except the total cross section of the covers of the fission detector, and same processing method was applied for the capsule A of the QIN SHAN 2nd NPP Unit 1. The total cross sections of covers are calculated for Ni+CdO-Fe and Ti+BN-Fe by the equation (6), respectively. The cover name is Cd if its thickness is calculated according to equation (8). The new weighed fast neutron fluence rates were calculated after neutron spectrum adjustment. The ratio of the new results to the old results of DAYA Bay NPP are in table 3, the ratio of the new results to the old results of the QIN SHAN 2nd NPP are in table 4. The new results are 1.5 - 2.6% smaller than the previous one due to the fact that the new total cross section of the cover in IRDF is obtained by subtracting the iron's.

TABLE 5. RATIOS OF THE NEW FAST NEUTRON FLUENCE RATE RESULT TO THE PREVIOUS FOR CAPSULE V OF DAYA BAY NPP UNIT 2

	Before spectrum adjustment	After spectrum adjustment
^{54}Fe (n,p) ^{54}Mn	1.000	0.990
^{58}Ni (n,p) ^{58}Co	1.000	0.991
^{63}Cu (n,a) ^{60}Co	1.000	0.987
^{93}Nb (n,n') ^{93m}Nb	1.000	0.999
^{237}Np (n,f) F.P.	0.977	0.978
^{238}U (n,f) F.P.	0.965	0.963
Weighted	0.991	0.985

TABLE 6. RATIOS OF THE NEW FAST NEUTRON FLUENCE RATE RESULT TO THE PREVIOUS FOR CAPSULE A OF THE QIN SHAN 2ND NPP UNIT 1

	Before spectrum adjustment	After spectrum adjustment
$Fe^{54}(n,p)$ Mn^{54}	1.000	0.976
$Ni^{58}(n,p)$ Co^{58}	1.000	0.978
$Cu^{63}(n,a)$ Co^{60}	1.000	0.977
$Nb^{93}(n,n')$ $Nb^{93}m$	1.000	0.999
$Np^{237}(n,f)$F.P.	0.960	0.964
$U^{238}(n,f)$F.P.	0.968	0.961
Weighted	0.988	0.974

16.6. Conclusions

For fast neutron fluence rate measurement by radioactivation techniques, when the fast detector is covered by some materials for filtering thermal neutron or other aims, the influence of fast neutron absorbed by the element in cover needs to consider not only these element such as Cd, B, and Gd, but also to consider other elements, for example N, C, O, Ni, Ti, V and Al, and ought to subtract the influence of the replaced material from them because the space of the replaced material in the activation detector is not covered.

REFERENCES

[1] SZONDI, E.J., NOLTHENIUS, H.J., ZSDNAY, E.M., User's Guide to the Neutron Spectrum Adjustment Code STAYNL, BME-NTI 223/95 (1995).
[2] SZONDI, E.J., NOLTHENIUS, H.J., User's Guide to the Cross Section Processing Code X333, BME-NTI 222/95 (1995).
[3] International Reactor Dosimetry File (IRDF-90 version 2), IAEA-NDS-141 (1993).
[4] International Reactor Dosimetry File 2002 (IDRF-2002) (2006).

STUDYING OF INFLUENCE OF A NEUTRON IRRADIATION ON ELEMENT CONTENTS AND STRUCTURES OF ALUMINUM ALLOYS SAV-1 AND AMG-2

U.S. SALIKHBAEV, S.A. BAYTELESOV, F.R. KUNGUROV, A.S. SAIDOV
Institute of Nuclear Physics, U.Gulomov Street, Pos Ulugbek,
Tashkent 100214, Uzbekistan
Email: Baytel@Inp.Uz

Abstract: One of the fundamental problems in the area of the study of structural materials is to create a radiation-resistant material fit for long-term operation under high-dose neutron radiation conditions. At present, SAV-1 and AMG-2 aluminum alloys are used at the WWR-M reactors as fuel elements which are different from other alloys, especially from the physical and mechanical properties point of view, like super-durability, corrosion resistance and high creep performance.
This work is devoted to a study on the influence of neutron radiation on the elemental composition and structure of the SAV-1 and AMG-2 alloys. With this aim in view, the samples of these alloys were exposed to neutron flux at the WWR-SM reactor at the Institute of Nuclear of Physics of the AS of the RUz, using the fluencies of $\sim 10^{19}$ n/cm^2.

17.1. Measurement of neutron flux spectrum

Au, Co, Ni, Ti, Fe monitors were made of thin roll flat metal foil, where Y and Mg are taken in the form of MgO and Y_2O_3. Two sets of monitors have been weighed, packed into polyethylene packages, wrapped in aluminum foil and soldered in quartz ampoules. One of ampoules has been soldered in Cd glass for cut-off of the thermal flux component during the irradiation process. Irradiation of both containers was carried out for 2 hours in the second channel of the reactor general neutrons flux [1-3]. Measurement of samples' gamma activity was carried out in 3-10 days after irradiation. Registration of samples gamma spectrum was carried out on HP Ge detector with multichannel analyzer DSA1000 of Canberra firm, the processing of gamma spectrum was carried out by means of standard software package Genie 2000.

TABLE 1. DESCRIPTION OF MONITORS

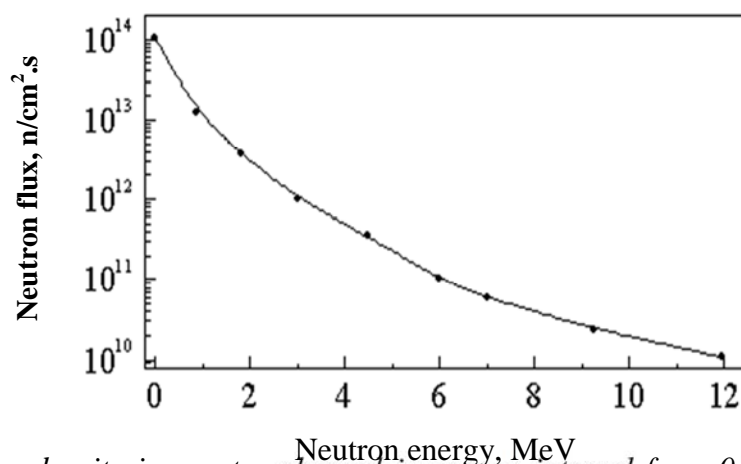| Reaction	%	E, MeV	T1/2	E, keV	Mass, mg
$^{197}Au(n,\gamma)^{198}Au$	100		2.7d		5
$^{58}Ni(n,p)^{58}Co$	67.88	2,6	71,3d	810.8 (99)	12.25
$^{24}Mg(n,p)^{24}Na$	78.7	6,3	15,05h	1368.5 (100)	1.1457
$^{48}Ti(n,p)^{48}Sc$	73.94	7	1,83d	1312.1 (100)	15.15
				1037.4 (100)	
				983.5 (100)	
$^{46}Ti (n,p) ^{46}Sc$	7.93	4.5	83,89d	889.2 (100)	15.15
				1120.5 (100)	
$^{54}Fe (n,p) ^{54}Mn$	5.84	3	312,6d	834.8 (100)	9.05
$^{89}Y(n,2n)^{88}Y$	100	12	108,1d	898 (92)	5.9842
				1836.1 (100)	
$^{60}Ni (n, p) ^{60}Co$	26.23	6	5,26y	1173.2 (100)	12.25
				1332.5 (100)	

FIG.1. Neutron flux density in reactor channel in energy interval from 0.025 eV up to 12 MeV.

TABLE 2. EXPERIMENT RESULTS OF FAST NEUTRON FLUX IN THE REACTOR (^{58}NI, OPTICAL ABSORPTION)

Measurement	Channel	^{58}Ni, 10^{-12}	optical absorption
1	7-1	1.89	0.4
2	4-1	4.78	0.65
3	5-1	6.39	0.9
4	6-1	4.15	0.96
5	3-7	10.12	1.18
6	7-3	10.02	1.15
7	2-4	4.98	1.52
8	4-2	17.52	1.44
9	6-2	12.03	1.57
10	6-7	10.36	1.65

TABLE 3. SHOWS THE RESULTS OF CALCULATION FOR NEUTRON FLUX SPECTRUM BY MCNP4C CODE:

Channel	Energy, MeV	Flux, n/cm2.s
1-4	0 - 6.2500E-07	1.33244E+14
	6.2500E-07 – 8.0000E-01	3.95490E+13
	8.0000E-01 – 3.0000E+00	7.47058E+12
	3.0000E+00 – 2.0000E+01	1.81057E+12
	Total	1.82074E+14
2-5	0 - 6.2500E-07	1.97076E+14
	6.2500E-07 – 8.0000E-01	1.36796E+14
	8.0000E-01 - 3,0000E+00	3.20508E+13
	3.0000E+00 - 2,0000E+01	8.09698E+12
	Total	3.74019E+14
6-2	0 – 6.2500E-07	1.54672E+14
	6.2500E-07 - 8,0000E-01	1.33735E+14
	8.0000E-01 - 3,0000E+00	3.31201E+13
	3.0000E+00 - 2,0000E+01	8.57388E+12
	Total	3.30102E+14

The definition of the crystal structure and parameters of a lattice (l = 0.15418 nanometers) of alloys was determined by X-ray diffraction measurement (DRON-3M). According to the radiographic analysis, as expected, initial alloys SAV-1 and AMG-2 have face-centered cubic (fcc) arrangement with lattice parameter, a = 4.066 ± 0.003 Å and a = 4.0726±0.003 Å, respectively. Small increase of alloys' lattice parameter in comparison with the reference aluminum sample of (4.0414 Å) is the result of the presence of impurities.

To determine the elemental composition and structure of the samples, the latter were studied with the help of the micro analyzer "Jeol" JSM 5910 IV- Japan. Tables 4 and 5 summarize the contents (%) of the elements Mg, Al, Fe, Si and Cu for the alloys SAV-1 and AMG-2, correspondingly, before and after the samples were subjected to 10^{19} neutron/cm^2 fluence. It is

worth noting that data in Table 4 coincides with published data for the SAV-1 and AMG-2 samples. In addition, the tables contain the measurement data only for those points which fail to appear in the area of local formations of insoluble intermetal phases. Tables 4 and 5 present screened illustration of the samples SAV-1 for elements Mg, Al, Fe and Si before and after irradiation with the fluence of 10^{19} neutron/cm^2. Fig.2 shows local formations in form of as white stains of insoluble inter-metal Al-Mg-Si-Fe phases with the size of (1-10) μm (for example, Fig. 2 for Si). The measurement of the element content at these two points has given the following result:

(i) Al – 66.72%; Mg – 11.06%; Si – 15.80%; Fe –5.96%.

(ii) Al – 69.70%; Mg – 4.88%; Si – 13.37%; Fe –11. 63%.

After irradiation, Fig.3, the surface of the sample appears oxidized and the local insoluble inter-metallic Al-Mg-Si-Fe phases which are broken up and scattered over a large volume of the sample becoming actually evenly distributed over all the volume [4,5]. It is especially well-seen on the bitmap pictures (Fig. 3.) for Fe and Mg. Such a breaking up of the local insoluble inter-metallic phases in the final analysis has caused a considerable change in the elemental composition in the three points measured which is seen in Table 5. It seems that a considerable change in the size of the local insoluble intermetal phases causes a change in the thermal conductivity, specific resistance, as well as microhardness of the samples when the latter have been subjected to irradiation. The further investigations will be devoted to determination of the above-mentioned characteristics of the samples.

TABLE 4. ELEMENTAL COMPOSITION (%) OF THE SAV-1 AND AMG-2 SAMPLES BEFORE IRRADIATION

Sample	#	Mg	Al	Si	Mn	Fe	Cu	Total
SAV-1	1	1.00	98.42	0.45	0.00	0.14	0.00	100.00
SAV-1	2	1.04	98.24	0.54	0.00	0.13	0.06	100.00
SAV-1	3	1.15	98.12	0.51	0.02	0.14	0.06	100.00
Average		1.06	98.26	0.50	0.01	0.14	0.04	100.00
AMG-2	4	2.81	96.72	0.00	0.21	0.27	0.00	100.00
AMG-2	5	2.77	96.65	0.00	0.27	0.25	0.07	100.00
AMG-2	6	2.82	96.72	0.00	0.24	0.23	0.00	100.00
Average		2.80	96.70	0.00	0.24	0.25	0.02	100.00

TABLE 5. ELEMENTAL COMPOSITION (%) OF THE SAV-1 SAMPLE AFTER IRRADIATION AT 1019 N/CM2

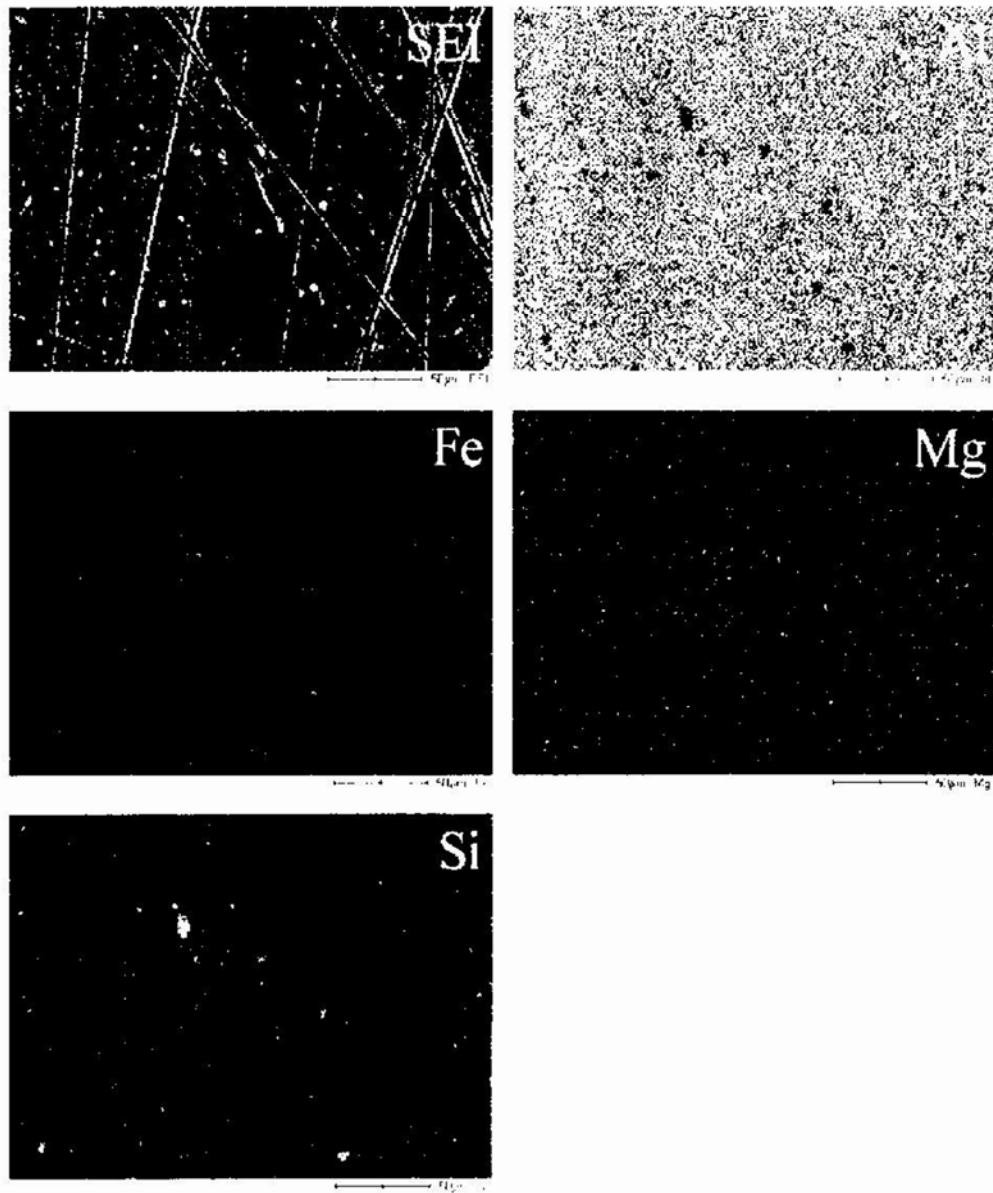| Sample	#	Mg	A1	Si	Fe	Cu	Total
SAV-1	1	0.48	96.33	2.72	0.44	0.04	100.00
SAV-1	2	0.57	97.42	1.77	0.25	0.00	100.00
SAV-1	3	0.55	97.054	1.66	0.27	0.00	100.00
Average		0.53	97.09	2.05	0.32	0.01	100.00
AMG-2	4	1.23	97.51	0.58	0.68	0.00	100.00
AMG-2	5	1.56	97.204	0.56	0.68	0.00	100.00
AMG-2	6	1.71	97.32	0.57	0.31	0.09	100.00
Average		1.50	97.34	0.57	0.56	0.03	100.00

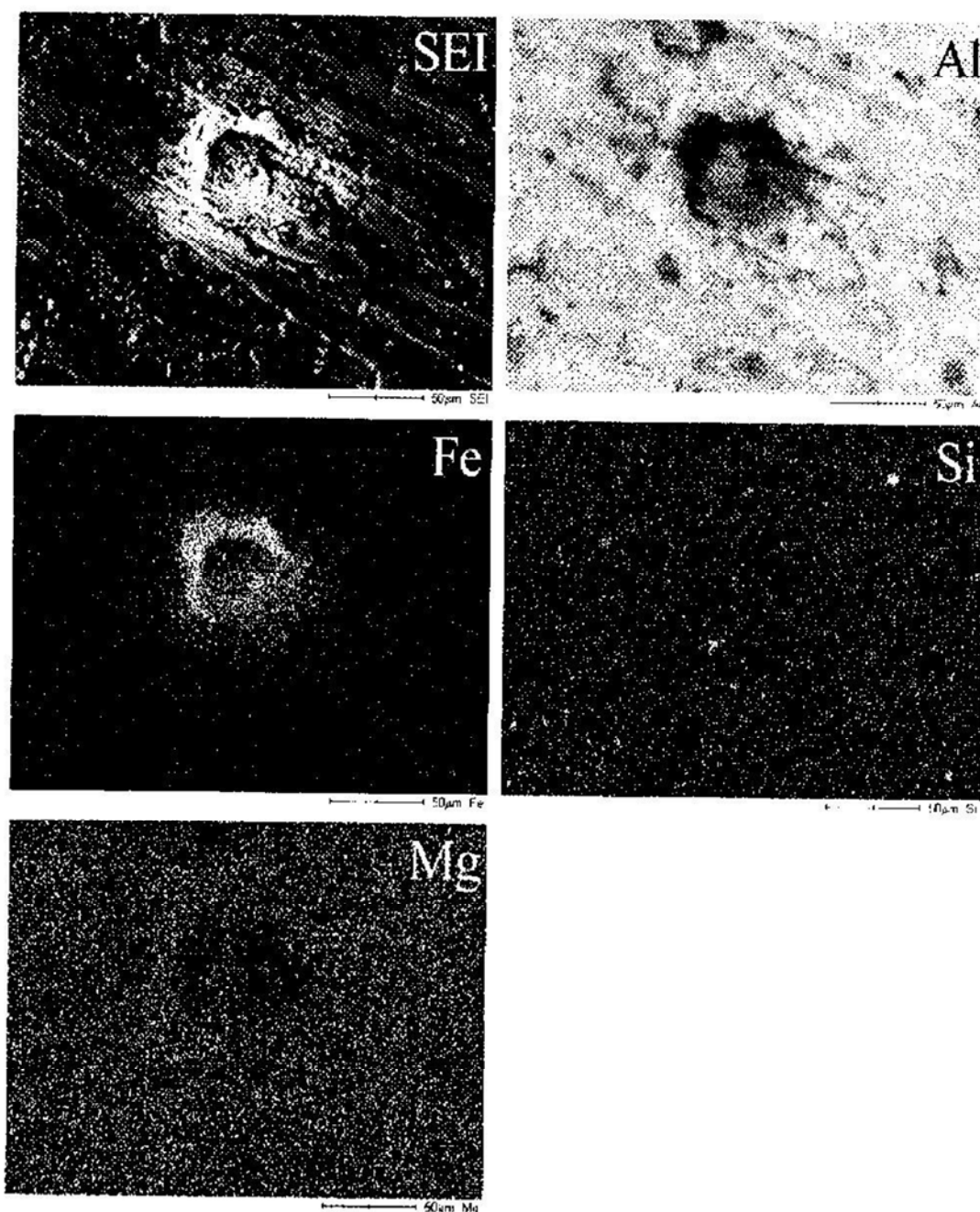*FIG.2. Microstructure of SAV-1 initial alloy (before irradiation).*

FIG.3. Microstructure of SAV-1 alloy after irradiation at 10^{19} n/cm.^{2}.

The results of microhardness measurement shows that there is a strong dependence of Hμ and indenter weight (F ≈ 3 N). For higher weights (F > 3 N) microhardness practically does not depend on weight. As the depth of penetration of the diamond pyramid depends on weight, it is possible to draw a conclusion that in the surface layer of samples at microhardness scale, apparently plays essential role

Essential increase of Hμ after irradiation at fluence above 10^{17} n/cm^2 and rather poorly linearly growth at the further increases of the fluence. Microhardness essentially increases at the first irradiation level. Essential reduction of the defects size (smashing) and dispersion of local insoluble intermetallic phases of alloys after irradiations appears.
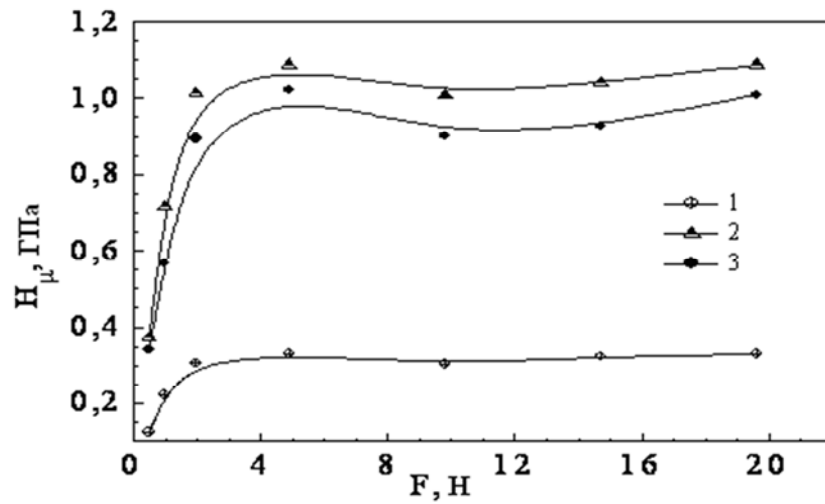
161

FIG.4. Neutron irradiated SAV-1 alloy samples' microhardness dependence from loading on indentor: not irradiated (1); irradiated by fluences 1018 n/cm2 (3) and 1019 n/cm2 (2).

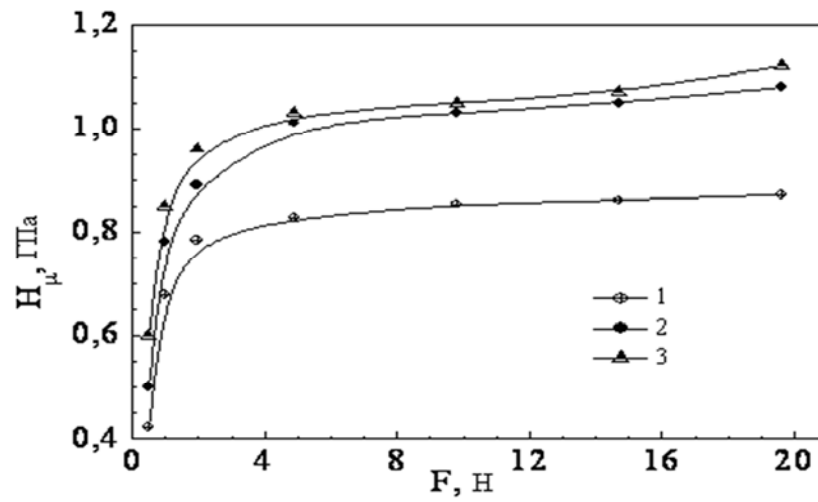*FIG.5. Neutron irradiated AMG-2 alloy samples' microhardness dependence from loading on indenter: not irradiated (2); irradiated by fluences 10^{18} n/cm^2 (2) and 10^{19} n/cm^2 (3).*

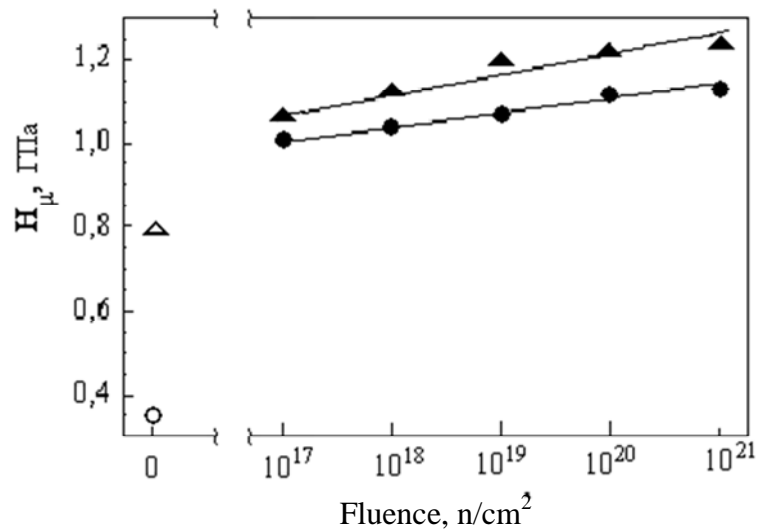*FIG.6. AMG-2 (▲) and SAV-1 (●) alloys microhardness dependence form neutron fluence. Points marked for comparison corresponding to Hµ values of not irradiated AMG-2 (△) and SAV-1 (○).*

162

17.2. Conclusions

Influence of reactor irradiation at various fluences (10^{17} - 10^{21} n/cm^2) on a microstructure and microhardness of alloys SAV-1 and AMG-2 was studied. It is revealed, that reactor irradiation leads to practically uniform redistribution of the impurities in all samples, before irradiation there was non-uniform distribution.

It was found that swelling is insignificant in the investigated fluence range. It is established, that under the influence of irradiation microhardness of alloys essentially increases at primary irradiation starting at 10^{17} n/cm^2 and linearly grows with the fluence up to 10^{21} n/cm^2. The microhardness increases as result of smashing and dispersion of local insoluble Al-Mg-Si-Fe inter-metallic phases on great volume of alloy, and growth with the concentration of radiation defects.

BIBLIOGRAPHY

[1]   YULDASHEV, B.S., et al., Exploitation and utilization of the reactor WWR-SM INP AS Uzbekistan with fuel UO$_2$ 36% enrichment. Journal Atom Energy, 2 No.8б V.99, (2005) 147.

[2]   BAYTELESOV, S.A., et al., About some characteristics of WWR-SM reactor at work with the low enriched nuclear fuel, Journal of Nuclear and Radiation Physics, ISSN: 1687-420X, 1 No.2 (2006) 119.

[3]   BAYTELESOV, S.A., et al., Influence of the reactor irradiation on the microstructure and microhardness of aluminium alloys SAV-1 and AMG. Journal alternative energy and ecology, No 9 (2008).

[4]   BAYTELESOV, S.A., DOSIMBAEV, A.A., KUNGUROV, F.R., SALIKHBAEV, U.S., Neutron-Physical and Thermohydraulic Calculations of VVR-SM with High- And Low-Enrichment Uranium Fuel Assemblies, Journal Atomic Energy, 104 No. 5 (2008) 349.

[5]   BAYTELESOV, S.A., DOSIMBAEV, A.A., KUNGUROV, F.R., SALIKHBAEV, U.S., Calculation of Emergency Situations occurring during the conversion of the Research Reactor at the Institute of Nuclear Physics of the Academy of Sciences of The Republic of Uzbekistan, Journal Atomic Energy, 104 No.6 (2008) 444.

STRUCTURAL MATERIAL INVESTIGATIONS IN THE HIGH TEMPERATURE IRRADIATION FACILITY OF THE BUDAPEST RESEARCH REACTOR

F. GILLEMOT, M. HORVÁTH, G. URI, L. TATÁR, T. FEKETE, Á. HORVÁTH,
Materials Department, Hungarian Academy of Sciences Kfki Atomic Energy Research Institute (Aeki), H-1525 Budapest, Po. Box 49, Hungary
Email: Akos.Horvath@Aeki.Kfki.Hu

Abstract: The Budapest Research Reactor is operated by the KFKI Atomic Energy Research Institute in Hungary. After full reconstruction it was started again in 1993, and a new irradiation rig called BAGIRA-1 (Budapest Advanced Gas-cooled Irradiation Rig Assembly) was installed in close co-operation with the Paul Scherer Institute (Switzerland). The rig is operational since 1998 and it is used to irradiate nuclear reactor vessel and fusion equipment materials in order to study and evaluate the irradiation ageing. The average fast neutron flux at the position of the rig is about $6 \times 10^{13} n/cm^2 s$ (>1 MeV). This paper is a review of the material testing studies completed so far and the recent improvements of the rig.

18.1. Introduction

The nuclear and/or fusion energy are the sustainable energy sources for the future. The present fleet of nuclear reactors are operating well, but to reduce the use of fossil fuel, to produce economical and safe energy, further development is necessary. Either the „Generation Four" fission reactors or the fusion reactors should be operated at higher temperature than the present PWR-s (Pressurized Water Reactor), and the design lifetime should be increased to 60 years. These requirements put higher thermal and irradiation load on the structural materials. The higher temperature operation and the higher EOL (End-of-Life) neutron fluence require new structural materials or at least to determine the high temperature radiation toughness of the available ones. These tasks require high capacity neutron sources.

The irradiation damage consist three main mechanisms: precipitations (Cu, Ni, Mn precipitations are the most typical), segregations (Phosphorus segregations are the most typical), and matrix damage. The precipitations occur generally shortly after the start of the irradiation, segregations request higher fluence and matrix damage is slow, Fig.1. For studying or modelling the irradiation damage is necessary to know the effects of these three components [1]. The first two should be studied in middle power research reactors, where the flux effect is small or negligible. The matrix damage study requires the end of life fluence which mostly can be reached only in high flux reactors or in spallation sources. Spallation sources have a serious limitation on the specimen size, and in small size specimens no valid fracture toughness can be measured. These facts show, that in the development of the materials of future fission and fusion reactors, both the research reactors (including middle and high flux reactors) and spallation sources will play important role.

FIG.1. Theoretical view of the three main irradiation damage mechanisms.

18.2. Irradiation rigs in the Budapest Research Reactor

The Budapest research reactor - after full reconstruction - was started again during 1993. The reconstructed reactor successfully passed the 1 year test period, and since January 1994 is in normal operation. Radiation embrittlement research is available since then.

Due to the increased power (now the reactor is operating with 10 MW, and the design power is 20 MW) a new irradiation rig was necessary for material testing. In close co-operation with the Paul Scherer Institute (Switzerland) we built the new rig called BAGIRA 1 (Budapest Advanced Gas-cooled Irradiation Rig with Aluminum structure). The irradiation volume of the rig is 360x20x40 mm. The designed operation temperature range was between 250-350ºC. The heating is gamma heating, the temperature measurement is performed by 6 thermocouples, the temperature controlled by a helium-nitrogen gas mix flow. Electric resistance heating is used for adjust the temperature differences among the different sections of the rig. The maximum fast fluence within the rig is 3- $6x10^{13}$ n/cm^{2}s.

FIG.2. The location of the irradiation rigs in the core of the Budapest Research Reactor.

Detailed description of the irradiation rig is given elsewhere [2,3]. Presently the rig has been redesigned, and the aluminium parts of the target holder have been changed for titanium alloy. The upgraded design is used recently for irradiation at 450°C, and can be operated up to 500 C.
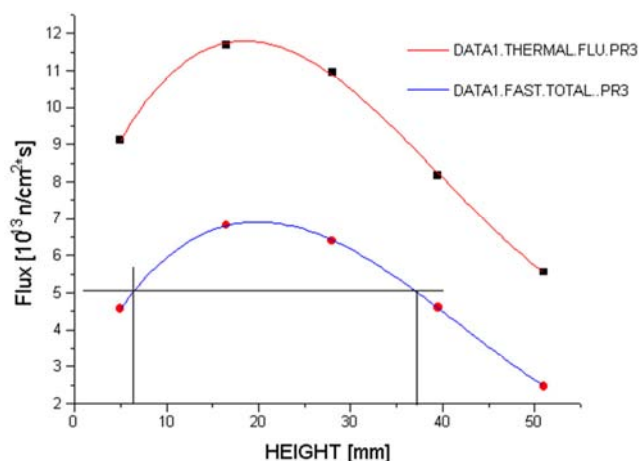

FIG.3. The vertical flux distribution at the core position of the BAGIRA 1 irradiation rig.

The Budapest Research Reactor used many other materials for testing too i.e: Irradiation of tungsten, ceramics, zirconium glass and plastic samples can be performed in different irradiation capsules and boxes within or without the core. The neutron beams (including cold neutron source) are also used for neutron radiography, neutron backscattering, small angle neutron scattering, time of flight spectroscopy, etc.

After irradiation, the target holder with the irradiated specimens is transported into the hot cells of the Institute. The target holder will be opened in the hot cell and the specimens will be stored in separated groups in canisters until testing, or transport to another laboratory.

There is a semi-hot laboratory, where tensile, impact, hardness and fracture mechanical tests can be performed on irradiated specimens. Low and high cycle fatigue testing has recently been introduced. From the remnants of the specimens, so called reconstituted specimens are produced and machined. Metallography and scanning electron microscope, neutron radiography, small angle scattering test, magnetic measurements also can be performed on irradiated materials.

18.3. Material study for future nuclear facilities at the Budapest Research Reactor

The Budapest Research Reactor and the BAGIRA 1 and 2 rigs are widely used to study the irradiation effects on the structural materials in order to evaluate the safety and lifetime of the presently operating and future nuclear energy sources. The Institute participated/participates in the International Atomic Energy Agency's (IAEA) co-ordinated research programmes (CRP-3 to CRP-9) mostly with irradiated material testing. Also contributed with irradiated material testing to many EU framework programs (FRAME, GRETE, COBRA, ATHENE, PERFECT, COVERS, NULIFE) and to the European Fusion programme. Below, are some examples from the recently completed studies.

*Ti-alloys***:** Ti alloys has been irradiated and tested for ITER fusion device. In the tokamak type fusion devices the first wall and the vessel is connected with elastic connation elements. The high strengths and low Young modulus of the Ti-alloys allow using them as elastic elements. This part of the device suffers about 0.5 dpa irradiation. Ti-6l-4V alloy has been irradiated and the mechanical properties tested.

*RPV cladding***:** most of the Reactor Pressure Vessels (RPV) of the PWRs are clad inside with a welded stainless steel layer. It is generally made by welding and 3-10 mm thick. This cladding was neglected at earlier Pressurized Thermal Schock (PTS) analysis. However if the cladding is ductile and free from defects, at PTS calculation does not necessitate the use of hypotethical surface cracks. If so, the calculations result in 20-30% longer lifetime, which is very important at lifetime extension of the power plant [4]. The irradiation damage of cladding is different from the ferritic and austenitic steels too. Tensile curves obtained on cladding are shown in Fig. 4.
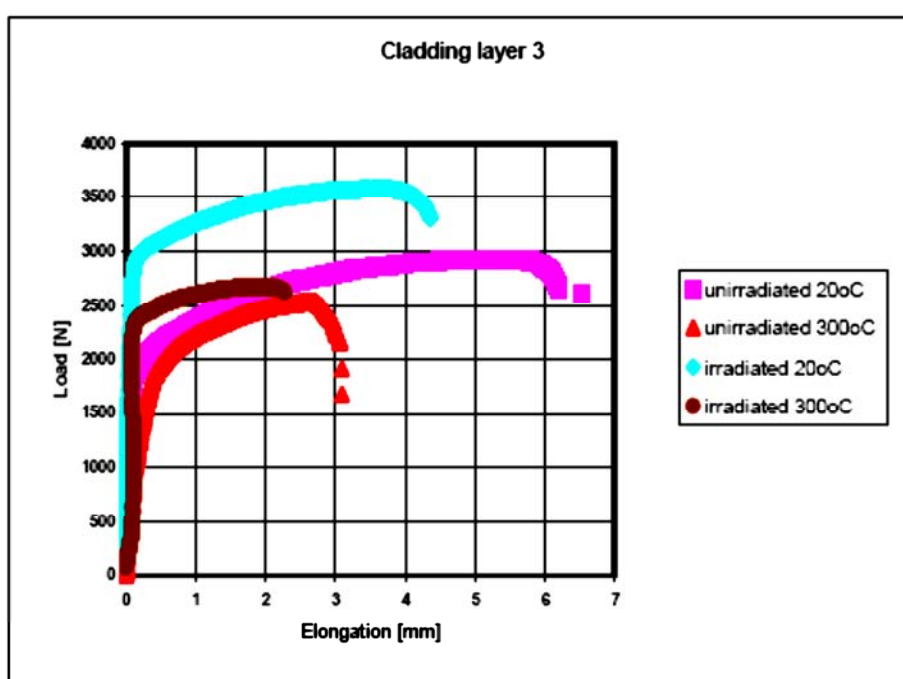

FIG.4. Tensile results obtained on RPV cladding.

Tungsten: tungsten is resistant against high temperature. Diverters and other first wall elements of the fusion devices and some parts of the high temperature gas-cooled rectors are planned to produced from tungsten alloys. The radiation embrittlement of tungsten alloys studied on samples irradiated in the BAGIRA rig. Load-deflection curve obtained on three point bend test of irradiated tungsten bars is shown in Fig. 5.
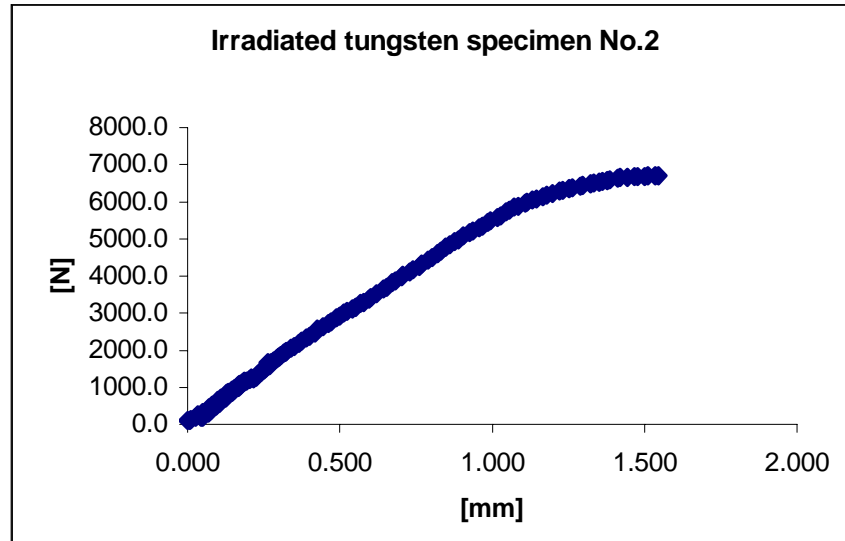
168

FIG.5. Load-deflection curve obtained on three point bending testof irradiated tungsten rod.

9% Cr steels: the 9% Cr ferrit-martensitic steels have high strengths at high temperature, resistant against creep at the 650-900°C temperature range. They consist of alloying elements which produce short half time isotopes during operation. After significantly shorter time than the others they can be treated as low activity waste, and can be reused after 100 years. In the power industry similar steels are regularly used, the production and machining technology is well known. The purpose of our study was to evaluate the fracture toughness on small size irradiated Eurofer specimens, and determine the limitations of the use of reconstituted specimens and the so called Master Curve method [5]. Master Curve obtained on unirradiated 9% Cr steel is shown in Fig. 6.
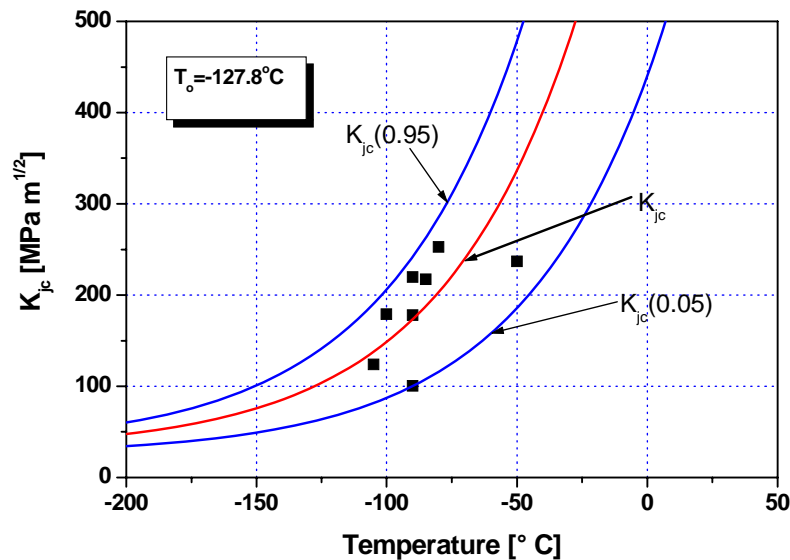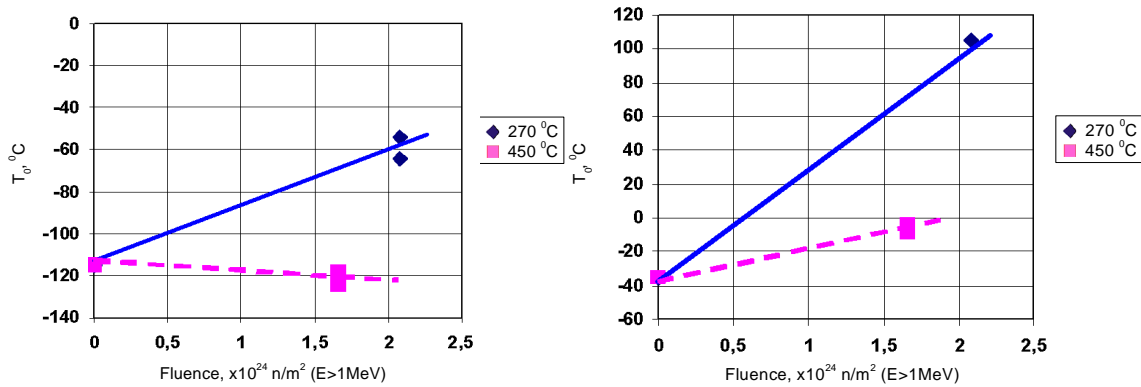

FIG.6. Master curve toughness testing result on unirradiated 9%Cr steel.

Application Cr-Mo-V steel on high temperature: the End of Life (EOL) fluence of the WWER-440 reactors are one of the highest among the operating light water reactors. It can reach the $2x10^{24}$ n/m^2 value. The reactor pressure vessel is made from a forged Russian Cr-Mo-V steel (called 15H2MFA, see Table 1. for composition). It is a very good toughness against radiation embrittlement. The efficiency of the future reactors can be higher at higher operating temperature (350-560°C) range. The fossil plants which operate at this temperature are built from Cr-Mo and Cr-Mo-V steels. These materials are widely used by the industry, thus the nuclear application do not need extensive technology development, even long term creep and thermal ageing properties are well known. They are candidate materials for the future fourth generation supercritical water reactors. Samples made of this steel and its welds have been irradiated in the Budapest Research Reactor at 270°C and at 450°C. The fracture toughness, tensile, hardness and fractography tests have been performed on the irradiated samples. The results show that after the irradiation at 270°C (the operating temperature for the WWER-440 reactors) the Master Curve T_0 shift was in the range of 100°C (still acceptable value for the present operating reactors) however the irradiation caused shift after 450°C irradiation with the same fluence was nearly zero, Fig.7. Similar results obtained using tensile or hardness testing. Metallography and fractography also have shown that the steel and its welds remained ductile after high fluence neutron irradiation at 450°C.

TABLE 1. CHEMICAL COMPOSITION OF THE WWER-440 RPV STEEL AND ITS WELDS

Composition, %	15H2MFA (Greifswald NPP Unit 8.)	15H2MFA weld Nr.502
C	0.16	0.03
Si	0.29	0.50
Mn	0.54	1.23
P	0.014	0.037
S	0.013	0.013
Cr	2.70	1.41
Mo	0.68	0.48
V	0.28	0.18
Ni	0.07	0.13
Cu	0.09	0.14

(a) base metal   *(b) weld*

FIG.7. Radiation embrittlement of 15H2MFA and its weld as a function of the fluence and irradiation temperature

18.4. Conclusions

Present and future research reactors can play an important role in the testing of the irradiation toughness of the structural materials of the future energetic fission and fusion plants. The Budapest Research Reactor operates two controlled temperature dry irradiation rigs for radiation embrittlement studies on reactor pressure vessel materials. One of the irradiation rigs is recently upgraded to use for higher temperature tests for the next generation fusion and fission reactors.

REFERENCES

[1] DEBARBERIS, L., et al., Effect of Irradiation Temperature in PWR RPV Materials and its Iinclusion in Semi Mechanistic Model, Scripta Materiala, 53 (2005) 769.

[2] GILLEMOT, F., URI, G., FEKETE, T., GAJDOS, F., FRANKL, L., The New High Temperature Irradiation Rig of the Budapest Research Reactor. Specialist Meeting, Irradiation Embrittlement and Mitigation Espoo, Finland (1995).

[3] GILLEMOT, F., URI, G., Development of the BAGIA irradiation rig, Progress report of the Budapest Neutron Centre, KFKI Atomic Energy Research Institute (2000).

[4] GILLEMOT, F., HORVÁTH, M., VIEHRIG, H.W., DEBARBERIS, L., Behaviour of Irradiated RPV Cladding, 23rd Symposium on Effect of Radiation on Materials, ASTM, San Jose, California (2006).

[5] GILLEMOT, F., HORVÁTH, M., HOUNDEFFO, E., Uri, G., Reconstitution Technology of EUROFER 97, Progress report of the Atomic Energy Research Institute, Hungary, Budapest (2005).

[6] GILLEMOT, F., et al., Radiation Stability of WWER RPV Cladding Materials, Int. Journal of Pressure Vessels and Piping, 84 (2007) 469.

Chapter 19

OVERVIEW OF MEMBER STATES' ACTIVITIES

19.1. Working group's summary

Extensive discussions among meeting participants revealed a broad range of possibilities for irradiation and material testing. Participants described technical characteristics of their respective irradiation facilities and testing methods. Taking into account present activities and plans for the future, it turned out that many facilities are complementary, which is an invitation for closer collaboration.

Czech Republic: Nuclear Physics Institute, AS CR, v.v.i. Rez is interested in investigations of changes of material characteristics of steels, silicon based ceramics as well as phase transformation effects brought about by a high fluence neutron irradiation. For such investigations, NPI AS CR, v.v.i. Rez offers for the CRP project, the use of nondestructive neutron scattering methods as powder diffractometry for crystalline structure studies, scanning of the internal macro- and microstresses in polycrystalline materials as well as small-angle neutron scattering for studies of inhomogeneities in surrounding homogeneous bulk material. All these methods for material characterization are routinely used in NPI and carried out at a high level of standard. The knowledge of structure changes cannot be avoided in order to understand the material mechanical properties of their behavior as well as for their prediction in the course of irradiation by high neutron fluence. The cooperation in development of the HTR and SCWR loops is offered by Nuclear Research Institute Rez, p.l.c.

Brazil: Due to the low power research reactor in use in Brazil, but with possibility of having a new research reactor with higher power, country is interested in: (i) keeping the exchange of knowledge on rigs for testing materials at medium and high fluence; (ii) to motivate the use and development of new materials for medium and high fluence dosimetry; (iii) to continue the exchange of knowledge on developments of new out-of-pile and in-pile techniques for irradiated materials testing.

Uzbekistan: Following point have been highlighted: (i) willingness for collaboration with other countries in RR application for materials under high neutron fluence, (ii) the need and expectation of financial support from IAEA for exchange of visitors/experts, (iii) the need for financial support from the IAEA to continue the project "Studying of influence of a neutron irradiation on element contents and structures of aluminum alloys". up to 2×10^{22} n/cm^2 fluence and (iv) possibility for participation in other projects in the area of radiation performance testing of advanced materials.

Bangladesh: The information presented during the meeting can help to establish future collaboration between Member States in some common issues. Some of the interested Member States have no irradiation facilities with high neutron fluence, but they may have some interesting test techniques which may be applied to investigate the un-irradiated- and irradiated materials. For instance, in Bangladesh the irradiation of materials with high neutron fluence is not possible. However, some test techniques like neutron activation analysis (NAA), neutron radiography (NR), small-angle neutron scattering (SANS) and high-resolution powder diffractometry (HRPD) can be applied. To date, no hot cell laboratory exists for handling and testing highly radioactive materials.

To transport un-irradiated samples from one member state to another, is not a difficult task, however, the question is how to transport the irradiated materials. This is an issue that still needs to be resolved.

Ukraine: It is pointed out that participation in this IAEA Technical Meeting provides a good opportunity to gain knowledge about what has been done in the research reactor application in member states. It was suggested to share the experience of research reactors where a state-of-the-art technology and instrumented capsules are applied in the frame of Material Radiation Program. It is reasonable to develop the recommendations and basic requirements for Material Radiation Program to get correct test data.

China: The NAPC Physics Section of the IAEA is carrying out very important and helpful work for new material research. New advanced theoretical calculation technology is needed for a better design and control in advanced material research area and new advanced test measurement technology is also needed for testing and validating the calculated results.

Korea: It would be useful if the IAEA could provide an information channel (periodic newspaper or meeting), especially related to the progress of irradiation test and technology of new materials for NGNP (Next Generation Nuclear Plant). It is also recommended that the IAEA could provide a communication channel to discuss and solve each country's technical problems on the irradiation technologies and facilities. The IAEA should also provide a reasonable method to evaluate efforts of each country's contribution.

European Commission: the EC would like to co-operate in any materials initiative related to the support of the following GIF future reactors of type: HTR/VHTR, SCWR and LFR. This will be in-line with the current development at JRS:

- Pb-loop to support the development of LFR in particular.
- Gas loops for erosion-corrosion studies (GIF - GFR).
- SCC loops, also in-pile up to SCW conditions.
- Embrittlement and irradiation creep of structural materials.

In particular, the testing of such materials in research reactor and or accelerated methods like accelerators, etc. Moreover, the techniques related to such materials are of crucial interest; including: development of neutron monitors compatible with the different environmental conditions. Irradiation technology and development of complex rigs is also an area were co-operation is welcomed. The development of neutron methods like e.g. SANS is also important.

Practical suggestions:

- IAEA CRP on materials for future reactors.
- IAEA CRP on dosimetry and monitors for advance applications like GI, INPRO, etc.
- Knowledge transfer in the field of irradiation technology (workshops, visit to assembly sites, etc.) to train new people.
- Provision via IAEA/JRC of reference materials (e.g. ODS steels) for educational purposed and round-robin.

Japan: As a result of discussions held, the diversity of interest among Member States was made apparent. However, several focal points could be identified, assuming that utilization of research reactors can be categorized into several stages. Comprehensive discussions could be effectively organized by appropriate setups of small working groups designated for each specific focused topic. One example will be a study of heavy irradiation damages for development of materials for advanced nuclear systems. Here, the related research reactors are expected to have a high neutron flux, larger than middle of 10^{18}n/m^{2}s(E>0.1MeV). Another topic could be effective utilization of medium sized research reactors with thermal

power in the range of 1-10MW. Utilization of small research reactors has much more well-defined prospects, such as regional inspiration of science, welfare, education, training and etc.

Kazakhstan: The Institute of Nuclear Physics (INP, Kazakhstan, Almaty) offers the use of irradiation facilities (mainly – WWR-K research reactor) and research equipment for sample/material irradiation, radioisotope production, investigation of radiation effects in structural materials. Methods of tensile test, combined with optical extensometry and deformation calorimetry are routinely used in INP.INP is open for collaboration in area of radiation material science (irradiation program, joint research etc). Materials interesting for INP include: advanced stainless steels, ODS-steels, nano-structured materials, alloys with fine-grain structure. One of the most interesting aspects of joint research can be the investigation of deformation induced martensitic transformation in irradiated chromium-nickel steels (model alloys) for practical use of "deformation wave" effect. This effect (spontaneous delocalization of deformation die to martensite transformation) leads to high plasticity value after irradiation to high damage doses (a few dpa or more). The first step of such a project may be the manufacturing of 4-5 metastable Cr-Ni alloys with different parameters of stability (tendency to $\gamma \rightarrow \alpha$ transformation). Samples of selected materials can be irradiated in the participant's research reactors (different temperatures, damage doses, etc.). Non-irradiated and irradiated samples can be examined (tensile test, magnitometry or other methods of marten site content measurement) and influence of irradiation on stability of Cr-Ni alloys can be defined. It is expected that parameters of irradiation may be enough for appearance of "deformation wave".

India: A main interest of our research centre (IGCAR, Kalpakkam, India) is the development of fuel cladding and wrapper tube materials for fast reactors which can withstand a temperature range of 400-700°C and a fluence level of about 200 dpa. Extensive irradiation experiments are required to be carried out towards evaluating the irradiation performance of these materials (which are under development).

IGCAR is interested in strengthening the capability to carry out instrumented capsule irradiation experiments in FBTR and also the strengthening of designing different types of non-instrumented irradiation capsules for structural material testing. Knowledge exchange and collaboration in this regard is very much anticipated. The possibility of irradiation testing of some materials of common interest in FBTR or other international high flux facilities can be examined.

Egypt: Some RR institutes start research in material irradiation and characterization. Building on such research and cooperation between RR institutes could be useful especially for RRs which have no or poor material irradiation activities. For instance to develop research and testing capabilities in irradiated material characterization and surveillance of their reactor structures and internals. Other benefits are to exchange experience and share services. The IAEA could support a CRP in mechanical testing and characterization of materials used in RR structures and internals (Al alloys, SS, Zr).

Hungary: AEKI operates a medium size (10MW power) research reactor, and is interested in either fundamental or applied research in the field of irradiation ageing of structural materials. There is experience in the VVER-440 type NPP reactor vessel steel and Eurofer, Tungsten, Titanium alloys. AEKI is interested in cooperation on investigation of alloys related to GenIV materials, ODS, ceramics, developing non-destructive testing in order to better characterize irradiation ageing and developing new alloys for dosimetry purposes. For the applicability of ODS type of steels, joining is an issue. AEKI participated in several European research

programs so far, and has experience in collaborative work, transportation of radioactive materials, round robin type tests, etc.

The development of new reactor materials and the design of experiments should be supported by modeling of the relevant physical phenomena. A Research team is open for any cooperation on meso- and macro-scale modelling of the influence of radiation on mechanical properties. Model development requires micro-scale characterization of radiation damage, using among others neutron based techniques. As handling of radioactive material needs extra care, progress in the use of small samples for mechanical tests is important.

Israel: It is suggested that the IAEA supports cooperation between Member States in a way that countries with small RR (with low fluence) could contribute to material testing by using their post-irradiation devices (e.g. powder diffractometer) to test samples that have been irradiated in high flux reactors.

Appendix

MEETING AGENDA

Technical Meeting (TM-34779)

Research Reactor Application for Materials Under High Fluence

17 – 21 November 2008, Meeting Room F0811
IAEA, Vienna, Austria

Monday, 17 November

09:00 – 09:30	Registration at Gate 1
09:30 – 10:00	Welcome and opening remarks:
	Mr N. Ramamoorthy, Director-NAPC
	Mr G. Mank, Head, Physics Section
	Mr A. Zeman, Scientific Secretary
10:00 – 10:45	Mr S..M. Hossain:
	Current Status and Perspectives of Nuclear Reactor Based Research in Bangladesh
10:45 – 11:15	Break
11:15 – 12:00	Mr J.A. Perrotta: Status of Research Reactor Utilization in Brazil
12:00 – 13:00	Lunch
13:00 – 13:45	Mr T. Xiding: Fast Neutron Shielding Research of the Shielding Material for Fast Neutron Fluence Measurement
13:45 – 14:30	Mr P. Mikula: Neutron scattering structure studies of materials loaded by a high neutron fluence
14:30 – 15:00	Break
15:00 – 16:30	WORKING GROUP: RR irradiation facilities recent status and new challenges
16:30 – 17:00	Session Summary

Tuesday, 18 November

09:00 – 09:45	Mr J.Burian:
	LVR-15 Reactor Application for Material Testing
9:45 – 10:30	Mr M.A. Gaheen: Utilization of Egyptian Research Reactor and Modes of Collaborations
10:30 – 11:00	Break
11:00 – 11:45	Mr A. Horvath: Structural material investigations in the high temperature irradiation facility of the Budapest Research Reactor
11:45 – 13:00	Lunch
13:00 – 13:45	Mr S. Murugan: Irradiation Testing on Structural Materials in Fast Breeder Test Reactor
13:45 – 14:30	Mr T. Shikama: Study of irradiation effects in materials with high-neutron-flux fission reactors
14:30 – 15:00	Break
15:00 – 16:30	WORKING GROUP On-going and new irradiation programmes in R&D of advanced materials
16:30 – 17:00	Session summary

Wednesday, 19 November

09:00 – 09:45	Mr T. Soga: Improvement of irradiation capability in the Experimental Fast Reactor Joyo
09:45 – 10:30	Mr N.M. Gusev: The Experience of Material Science Research at WWR-K reactor
10:30 – 11:00	Break
11:00 – 11:45	Mr. K.N. Choo: Material Irradiation at HANARO, Korea
11:45 – 12:30	Mr S. Jovanovic: Applicability of ANGLE Software for Semiconductor Detector Gamma-Efficiency Calculations to Research Reactor Neutron Flux Characterization
12:30 – 13:30	Lunch
13:30 – 15:00	Technical Report – drafting
15:00 – 15:30	Break
15:30 – 16:30	Technical Report – drafting (continuous)
16:30 – 17:00	Session summary
18:00 –	Hospitality

Thursday, 20 November

09:00 – 09:45   Mr L. Debarberis:
                  Unique Irradiation Rigs developed for the HFR Petten at the JRC-IE;
                  details of LYRA, QUATTRO and Fuel Irradiation facilities

09:45 – 10:30   Mr V. Revka:
                  A use of the VVR-M research reactor for in situ investigation of the physics
                  and mechanical properties of metal and alloys

10:30 – 11:00   Break

11:00 – 11:45   Mr S. A. Baytelesov:
                  Studying of influence of a neutron irradiation on element contents and
                  structures of aluminum alloys SAV-1 and AMG-2

11:45 – 12:30   Closing of the presentations – panel discussions

12:30 – 13:00   Lunch

13:00 – 15:00   Coordinated Research Activities - proposals

15:00 – 15:30   Break / Group photo

15:30 – 16:30   Coordinated Research Activities - proposals (continuous)

16:30 – 17:00   Session summary

Friday, 21 November

09:00 – 11:00   Technical Report – finalization of document

11:00 – 11:30   Break

11:30 – 12:30   Presentation of outputs

12:30 – 13:00   Closure / Departure

ABBREVIATIONS

3D-AP	3-Dimensional Atom Probe
APFIM	Atom Probe Field Ion Microscopy
APT	Atom Probe Tomograpy
BNCT	Boron Neutron Capture Therapy
CPEM	Curie Point Electro Magnet
DCT	Dry Central Thimble
dpa	Displacement per atom
ECP	Electro Chemical Potential
EPMA	Electron Probe Micro Analysis
EOL	End Of Life
FA	Fuel Assembly
FBTR	Fast Breeder Test Reactor
FM	Ferritic-Martensitic steel
FTL	Fuel Test Loop
HEU	High Enriched Uranium
HFETR	High Flux Engineering Test Reactor
HFR	High Flux Reactor
HLWSF	High Level Waste and Spent Fuel
HRPD	High Resolution Powder Diffractometer
HTS	Hydraulic Transfer System
HTR	High Temperature Reactor
IP	Ion Position
IMEF	Irradiation Materials Examination Facility
IPT	In-Pile Test
IRDF	International Reactor Dosimetry File
ITER	International Thermonuclear Experimental Reactor
LEU	Low Enriched Uranium
LH	Large Hole
LFR	Lead cooled Fast Reactor
MJTR	Min Jiang Test Reactor
MOX	Mixed Oxide Fuel
MTR	Material Test Reactor
NAA	Neutron Activation Analzsis
NTD	Neutron Transmutation Doping
NDT	Non-Destructive Testing
NP	Nuclear Program
NPP	Nuclear Power Plant
NR	Neutron Radiography

ODS	Oxide Dispersion Strengthened steel
OPT	Out-Pile Test
PAS	Positron Annihilation Spectroscopy
PFW	Primary First Wall
PHWR	Pressurised Heavy Water Reactor
PIGE	Proton Induced Gamma Emission
PIXE	Proton Induced X-ray Emission
PSD	Position Sensitive Detector
PSF	Pool Side Facility
PTS	Pressurized Thermal Schock
PWR	Pressurised Water cooled Reactor
QA/QC	Quality Assurance / Quality Control
R&D	Research and Development
RAFM	Reduced Activation Ferritic-Martensitic steels
RBS	Rutherford Back Scattering
RIP	Radiation Induced Precipitates
RML	Radio Metallurgy Laboratory
RPV	Reactor Pressure Vessel
RR	Research Reactor
RRRFR	Russian Research Reactor Fuel Return
RROUC	Research Reactor Operation and Utilisation Committee
RSCC	Radiation Safety and Control Committeee
SANS	Small Angle Neutron Scattering
SASS	Self Actuated Shutdown System
SCC	Stress Corrosion Cracking
SCWR	Super Critical Water Reactor
SEM	Scanning Electron Microscopy
SFR	Sodium cooled Fast Reactor
SiC	Silicon-Carbide
SNF	Spent Nuclear Fuel
SS	Stainless Steel
SSRT	Slow Strain Rate Test
TAS	Triple Axis neutron Spectrometer
TEM	Transmission Electron Microscopy
VHTR	Very Hight Temperature Reactor
VVER	Vodo-vodnij Energitecski Reaktor
XRD	X-Ray Diffraction
XRF	X-Ray Fluorescence

CONTRIBUTORS TO DRAFTING AND REVIEW

Baytelesov, S.	Institute of Nuclear Physics, U.Gulomov street, Pos Ulugbek, Tashkent 100214, Uzbekistan Tel: +998712893508 Fax: +998711503088 Email: baytel@inp.uz
Burian, J.	Nuclear Research Institute Rez, plc., Husinec-Rez 130, Rez near Prague CZ 25068, Czech Republic Tel: +420266172455 Fax: 00420 266 172045 Email: bri@ujv.cz
Choo, Kee Nam	Korea Atomic Energy Research Institute 150 Deokjin-dong, Yuseong-gu Daejeon 305-353 Korea, Republic of Tel: 0082428682381 Fax: 0082428636522 Email: knchoo@kaeri.re.kr
Debarberis, L.	JRC-EC, Project Officer, Head of Unit, Nuclear Design Safety, European Commission Joint Research Centre P.O. Box 2 NL-1755ZG Petten Tel: 0031 224 565130 Fax: 0031 224 565109 Email: Luigi.DEBARBERIS@ec.europa.eu
Gaheen Mohamed, Abd El-Monem	Egyptian Atomic Energy Authority (EAEA), ETRR-2 Research Reactor 13759, Abou Zabal, Egypt Abou Zabal 13759 Egypt Tel: +20244691755 Fax: 20244691754 Email: magaheen@yahoo.com
Gusev, M.,N.	Institute of Nuclear Physics Ibragimov St., 1 Almaty 050082 Kazakhstan Tel: +7(727)386-52-62 Fax: +7(727)386-52-60 Email: gusev.maxim@inp.kz

Hirshfeld, H.	Soreq Nuclear Research Center Yavne 81800 ISRAEL Tel: 00972 89434464 Fax: 00972 8 9434133 Email: hirshfel@soreq.gov.il
Horvath, A. L.	HAS KFKI Atomic Energy Research Institute Konkoly Thege 29-33 Budapest 1121 Hungary Tel: +3613922222/3628 Fax: +3613959162 Email: akos.horvath@aeki.kfki.hu
Hossain, Syed Mohammod	Bangladesh Atomic Energy Commission (BAEC); Atomic Energy Research Establishment, (AERE); Institute of Nuclear Science and Technology (INST), Ganakbari, Savar, P.O. Box 3787, Dhaka 1000, BANGLADESH Tel: 00880 2 7788249 Fax: 00880 2-7701337 Email: syed9495@yahoo.com
Jovanovic, S.	Centre for Eco-toxicological Research of Montenegro Put Radomira Ivanovica 2 P.O. Box: 374 Podgorica MNE-81000 Montenegro Tel: 00382-67-546968/264-551 Fax: 00382-81-244608 Email: bobo_jovanovic@yahoo.co.uk
Mikula, P.	Nuclear Physics Institute CAS, v.v.i. Husinec- Rez Rez near Prague 25068 Czech Republic Tel: +420 266173553 Fax: +420 220940141 Email: mikula@ujf.cas.cz
Murugan, S.	Indira Gandhi Centre for Atomic Research IDEAS / Metallurgy and Materials Group Kalpakkam - 603 102 India Tel: +91 44 27480500 Ext. 23356 ; +91 44 27480138 Fax: +91 44 27480138 Email: murugan@igcar.gov.in

Perrotta, J.A.	Comissão Nacional de Energia Nuclear (CNEN); Instituto de Pesquisas Energeticas e Nucleares (IPEN) Av. Prof. Lineu Prestes, 2242 Cidade Universitaria, 05508-000 Sao Paulo, BRAZIL Tel: 0055 11 31338942; 0055 11 3133 8942 Fax: 0055 11 38123546 Email: perrotta@ipen.br
Revka, V.	Institute for Nuclear Research National Academy of Science Nauki ave. 47 Kiev 03680 Ukraine Tel: +380445254820 Fax: 380445254463 Email: grynik@kinr.kiev.ua
Shikama, T.T.	Institute for Materials Research, Tohoku University 2-1-1 Katahira, Aobaku, Seidai, 980-8577 Japan Sendai 980-8577 Japan Tel: +81222152060 Fax: +8122215-2061 Email: shikama@imr.tohoku.ac.jp
Tang, Xiding	NUCLEAR POWER INSTITUTE OF CHINA Box291-113,Chengdu,Sichuan,China P.R. Chengdu 610005 China Tel: 0086 2885904485 Fax: 0086 2885904130 Email: tangxiding@yahoo.com
Soga, T.	Experimental Fast Reactor Department O-arai Research and Development Center Japan Atomic Energy Agency (JAEA) 4002 Narita-cho, Oarai, Ibaraki ,311-1393 Japan Tel: +81-29-267-4141 Fax: + 81 29 267 7109 Email: soga.tomonori@jaea.go.jp

IAEA
International Atomic Energy Agency

Where to order IAEA publications

In the following countries IAEA publications may be purchased from the sources listed below, or from major local booksellers. Payment may be made in local currency or with UNESCO coupons.

AUSTRALIA
DA Information Services, 648 Whitehorse Road, MITCHAM 3132
Telephone: +61 3 9210 7777 • Fax: +61 3 9210 7788
Email: service@dadirect.com.au • Web site: http://www.dadirect.com.au

BELGIUM
Jean de Lannoy, avenue du Roi 202, B-1190 Brussels
Telephone: +32 2 538 43 08 • Fax: +32 2 538 08 41
Email: jean.de.lannoy@infoboard.be • Web site: http://www.jean-de-lannoy.be

CANADA
Bernan Associates, 4501 Forbes Blvd, Suite 200, Lanham, MD 20706-4346, USA
Telephone: 1-800-865-3457 • Fax: 1-800-865-3450
Email: customercare@bernan.com • Web site: http://www.bernan.com

Renouf Publishing Company Ltd., 1-5369 Canotek Rd., Ottawa, Ontario, K1J 9J3
Telephone: +613 745 2665 • Fax: +613 745 7660
Email: order.dept@renoufbooks.com • Web site: http://www.renoufbooks.com

CHINA
IAEA Publications in Chinese: China Nuclear Energy Industry Corporation, Translation Section, P.O. Box 2103, Beijing

CZECH REPUBLIC
Suweco CZ, S.R.O., Klecakova 347, 180 21 Praha 9
Telephone: +420 26603 5364 • Fax: +420 28482 1646
Email: nakup@suweco.cz • Web site: http://www.suweco.cz

FINLAND
Akateeminen Kirjakauppa, PO BOX 128 (Keskuskatu 1), FIN-00101 Helsinki
Telephone: +358 9 121 41 • Fax: +358 9 121 4450
Email: akatilaus@akateeminen.com • Web site: http://www.akateeminen.com

FRANCE
Form-Edit, 5, rue Janssen, P.O. Box 25, F-75921 Paris Cedex 19
Telephone: +33 1 42 01 49 49 • Fax: +33 1 42 01 90 90
Email: formedit@formedit.fr • Web site: http://www. formedit.fr

Lavoisier SAS, 145 rue de Provigny, 94236 Cachan Cedex
Telephone: + 33 1 47 40 67 02 • Fax +33 1 47 40 67 02
Email: romuald.verrier@lavoisier.fr • Web site: http://www.lavoisier.fr

GERMANY
UNO-Verlag, Vertriebs- und Verlags GmbH, Am Hofgarten 10, D-53113 Bonn
Telephone: + 49 228 94 90 20 • Fax: +49 228 94 90 20 or +49 228 94 90 222
Email: bestellung@uno-verlag.de • Web site: http://www.uno-verlag.de

HUNGARY
Librotrade Ltd., Book Import, P.O. Box 126, H-1656 Budapest
Telephone: +36 1 257 7777 • Fax: +36 1 257 7472 • Email: books@librotrade.hu

INDIA
Allied Publishers Group, 1st Floor, Dubash House, 15, J. N. Heredia Marg, Ballard Estate, Mumbai 400 001,
Telephone: +91 22 22617926/27 • Fax: +91 22 22617928
Email: alliedpl@vsnl.com • Web site: http://www.alliedpublishers.com

Bookwell, 2/72, Nirankari Colony, Delhi 110009
Telephone: +91 11 23268786, +91 11 23257264 • Fax: +91 11 23281315
Email: bookwell@vsnl.net

ITALY
Libreria Scientifica Dott. Lucio di Biasio "AEIOU", Via Coronelli 6, I-20146 Milan
Telephone: +39 02 48 95 45 52 or 48 95 45 62 • Fax: +39 02 48 95 45 48
Email: info@libreriaaeiou.eu • Website: www.libreriaaeiou.eu